

**Role of the nitrate/potassium
transporter NRT1.5/NPF7.3 in the
regulatory network of ion homeostasis
in *Arabidopsis thaliana***

Dissertation

to obtain the academic degree
Doctor rerum naturalium (Dr. rer. nat.)

Submitted to the Department of Biology, Chemistry, Pharmacy
of Freie Universität Berlin

by

Maria Florencia Sena Falero

2021

Berlin, Germany

Printed with the support of the German Academic Exchange Service (DAAD)

Die vorliegende Arbeit wurde in der Zeit von Oktober 2016 bis Dezember 2020 unter der Leitung von Prof. Dr. Reinhard Kunze am Institut für Biologie - Angewandte Genetik angefertigt.

1. Gutachter: Prof. Dr. Reinhard Kunze. Freie Universität Berlin, Institut für Biologie - Angewandte Genetik.

2. Gutachterin: Prof. Dr. Margarete Baier. Freie Universität Berlin, Institut für Biologie- Pflanzenphysiologie.

Disputation am: 8.07.2021

Declaration of Authorship

I hereby declare that this thesis and the work presented in it are my own and has been generated by me as the result of my own original research. All direct or indirect sources used are acknowledged as references.

14.07.2021 María Florencia Sena Falero

Date, name

Contents

I. Summary.....	10
II. Zusammenfassung (German summary).....	11
1. Introduction	
1.1. Potassium (K^+) and nitrate (NO_3^-) in higher plants.....	13
1.2. Nitrate transporters and channels in higher plants.....	14
1.2.1. NO_3^- transport in roots: uptake, storage into vacuoles, and efflux.....	16
1.2.2. Long-distance transport of NO_3^-	18
1.3. Potassium transporters and channels in higher plants.....	19
1.3.1. K^+ transport in roots: uptake, storage into vacuoles, and efflux.....	24
1.3.2. Long-distance transport of K^+	25
1.4. Regulation of K^+ and NO_3^- transport in plants.....	25
1.4.1. Plasma membrane potential.....	26
1.4.2. Cellular pH.....	27
1.4.3. Secretory pathway.....	29
1.4.4. Transcriptional regulation.....	31
1.4.5. Calcium-regulated phosphorylation.....	31
1.5. Crosstalk between K^+ and NO_3^- transport in <i>Arabidopsis thaliana</i> : The nitrate/potassium- H^+ antiporter NRT1.5.....	33
1.6. Aim of the thesis.....	35
2. Materials and Methods	
2.1. Materials	
2.1.1. Enzymes and kits.....	36
2.1.2. Oligonucleotides.....	36
2.1.3. Plasmids.....	41
2.1.4. Bacteria and yeast strains.....	43
2.1.5. Plant material.....	44
2.1.6. Database and Software.....	45
2.1.7. Sequencing.....	46
2.1.8. Medium and selection.....	46

2.1.8.1. Medium for cultivating bacteria.....	46
2.1.8.2. Medium for cultivating <i>S. cerevisiae</i>	47
2.1.8.3. Medium for cultivating <i>Arabidopsis thaliana</i>	48
2.2. Methods	
2.2.1. Transformation into bacteria, yeast and plants.....	48
2.2.1.1. Chemical transformation of <i>Escherichia coli</i>	48
2.2.1.2. Transformation of <i>Agrobacterium tumefaciens</i> by electroporation	49
2.2.1.3. Chemical transformation of <i>Saccharomyces cerevisiae</i>	49
2.2.1.4. <i>Agrobacterium tumefaciens</i> -mediated transformation of <i>Arabidopsis thaliana</i>	50
2.2.1.5. <i>Agrobacterium tumefaciens</i> -mediated transformation of <i>Nicotiana benthamiana</i> ...	50
2.2.2. Molecular biology methods.....	50
2.2.2.1. Classical cloning of constructs for yeast complementation.....	50
2.2.2.2. Gibson cloning of constructs for plant complementation.....	51
2.2.2.3. Gibson cloning of constructs for protein localization.....	51
2.2.2.4. Gateway cloning of constructs for split-ubiquitin assay.....	52
2.2.2.5. Gateway cloning of constructs for the pBiFC-2in1 assay.....	52
2.2.3. Genomic DNA isolation.....	52
2.2.4. <i>Arabidopsis thaliana</i> RNA isolation.....	53
2.2.5. cDNA synthesis.....	53
2.2.6. Quantitative real time PCR.....	54
2.2.7. Elemental analysis.....	54
2.2.8. Nitrate measurement.....	54
2.2.9. Histochemical detection of GUS.....	55
2.2.10. Extracellular acidification assay.....	55
2.2.11. Split root assay.....	55
2.2.12. Confocal microscopy.....	56
3. Results	
3.1. Protein sequence analysis of NRT1.5 transporter in <i>Arabidopsis thaliana</i>.....	57
3.1.1. NRT1.5 protein alignment unveils low conservation of motifs involved in NO ₃ ⁻ /H ⁺ transport within NTR1 transporter family.....	57
3.2. Phenotypical analysis of the <i>nrt1.5</i> knockout mutant.....	59

3.2.1. Ion homeostasis-associated genes are differential regulated in <i>nrt1.5</i> at low nutrition supply.....	59
3.2.2. <i>NRT1.5</i> promoter activity in roots depends on K ⁺ uptake.....	62
3.2.3. NRT1.5 is not required for the perception of external K ⁺ contents.....	63
3.2.4. NRT1.5 modulates the root architecture in dependency of extracellular potassium, nitrate, and pH.....	65
3.2.5. The NRT1.5 ^{G209E} expression does not phenotypically complement the <i>nrt1.5</i> mutant.....	66
3.3. Identification of novel regulatory components involved in nutrient translocation in plants.....	67
3.3.1. NRT1.5 interacts with AHA2, CBL3, CIPK23, PEP12, SLAH1, SLAH3 and VAMP722 in the bimolecular fluorescence assay (BiFC) in <i>N. benthamiana</i>	70
3.3.2. Gene expression of <i>AHA2</i> , <i>CBL3</i> , <i>PEP12</i> , <i>SLAH1</i> , <i>SLAH3</i> , and <i>VAMP722</i> is affected by low nutrition supply in the <i>nrt1.5</i> mutant.....	72
3.3.3. Identification of homozygote lines and transcript levels of <i>aha2</i> , <i>cbl3</i> , <i>pep12</i> , <i>slah1</i> , <i>slah3</i> and <i>vamp722</i> mutants.....	73
3.3.4. Shoot phenotypes of <i>aha2</i> , <i>cbl3</i> , <i>pep12</i> , <i>slah1</i> , <i>slah3</i> and <i>vamp722</i> mutants are not phenocopies of <i>nrt1.5</i> at low nutrition supply.....	75
3.4. Elucidation of the physiological significance of the interaction between NRT1.5 and the proton pump, AHA2.....	76
3.4.1. AHA2 contributes in K ⁺ root-to-shoot translocation under low nutrition supply.....	76
3.4.2. NRT1.5 and AHA2 are involved in the modulation of root architecture under low nutrition supply.....	81
3.4.3. NRT1.5 and AHA2 are not functional as a K ⁺ sensors.....	83
3.4.4. NRT1.5 and AHA2 are ion transporters involved in plasma membrane depolarization in <i>Arabidopsis thaliana</i> and <i>Saccharomyces cerevisiae</i>	86
3.4.5. NRT1.5 and AHA2 mediate changes in extracellular pH at low nutrition supply in <i>Arabidopsis thaliana</i>	88
3.4.6. NRT1.5 and AHA2 expression in <i>Saccharomyces cerevisiae</i> is not directly correlated with K ⁺ export function under acidic conditions.....	90
3.4.7. NRT1.5 and AHA2 protein-protein interaction depends on the K ⁺ and H ⁺ transport activity respectively.....	92

3.4.8. NRT1.5, NRT1.5 ^{G209E} , AHA2, and AHA2 ^{D684V} proteins localize in cellular membranes of <i>Saccharomyces cerevisiae</i> and <i>Nicotiana benthamiana</i>	97
3.4.9. Plasma membrane H ⁺ -ATPase family members are transcriptionally regulated by low nutrition.....	101
3.4.10. AHA2 interaction with other NRT1 family members.....	102
3.5. Elucidation of the physiological significance of the interaction between NRT1.5 and the anion channels SLAH1 and SLAH3.....	103
3.5.1. <i>slah1/nrt1.5</i> and <i>slah3/nrt1.5</i> mutants do not show phenotypes at low nutrition supply	106
3.5.2. Overexpression of SLAH1 and SLAH3 in <i>Arabidopsis</i> do not show shoot phenotypes at low nutrition supply.....	107
3.5.3. SLAH1, SLAH3 and NRT1.5 contribute to with the maintenance of plasma membrane potential	109
3.6. Elucidation of the physiological significance of the interaction between NRT1.5 with CBL3, PEP12, and VAMP722.....	110
3.6.1. The lack of CBL3, VAMP722, and PEP12 genes do not show a link with NRT1.5 under low nutrition supply in <i>Arabidopsis thaliana</i>	111
3.6.2. Co-expression of CBL3 and CIPK23 or PEP12 and VAMP722 do not influence the K ⁺ export activity and localization of NRT1.5 in yeast.....	113
4. Discussion	
4.1. AtNRT1.5 protein sequence analysis unveils different characteristic features of the NRT1 family proteins	116
4.2. NRT1.5 is a significant component correlated with the molecular regulation of potassium and nitrate transport in <i>Arabidopsis</i> roots.....	118
4.2.1. Transcriptional analysis of <i>nrt1.5</i> at low nutrition supply suggests changes in the ion contents in shoots	118
4.2.2. <i>NRT1.5</i> promoter is regulated by nutrient availability and uptake.....	120
4.3. NRT1.5 has an important role in root architecture and plant development.....	120
4.3.1. NRT1.5 is not involved in root K ⁺ perception.....	120
4.3.2. NRT1.5 modulates the root architecture in dependency of external nitrate, potassium, and pH.....	122

4.4. Identification of interaction partners of NRT1.5 uncovers mechanisms of posttranslational regulation.....	123
4.5. NRT1.5 and AHA2 are correlated with the maintenance of the plasma membrane potential and cellular pH.....	125
4.6. NRT1.5 requires the conserved Gly²⁰⁹ in TM5 to interact with AHA2 at the plasma membrane	126
4.7. NRT1.5 and AHA2 protein localization is independent of G209E and E684V mutations respectively.....	128
4.8. Different H⁺-ATPases family proton pumps are correlated with K⁺ and NO₃ homeostasis	130
4.9. K⁺ export activity of NRT1.5 is not detected in <i>Saccharomyces cerevisiae</i>	131
4.10. Interaction between NRT1.5 the with anion channels SLAH1 and SLAH3.....	132
4.11. Potential posttranslational regulation of NRT1.5 by CBL3 and CIPK23.....	133
4.12. Interaction between NRT1.5 and the vesicle trafficking proteins PEP12 and VAMP722....	134
4.13. Conclusions and perspectives.....	137
5. References.....	138
6. Acknowledgements.....	163
7. Appendix.....	166

I. Summary

Nitrate (NO_3^-) and potassium (K^+) absorbed by plant cells are carried throughout the plant via short-distance distribution (cytoplasm to vacuole) and long-distance transportation (root to shoot). These two pathways jointly regulate the content of NO_3^- and K^+ in all higher plants. The *Arabidopsis thaliana* transporter NRT1.5 is responsible for the loading of NO_3^- and K^+ from the root cytoplasm of pericycle cells into the xylem vessels, facilitating the long-distance transport of NO_3^- and K^+ through the roots to the shoots. In this work, the amino acid sequence analysis of NRT1.5 unveiled a low conservation between the NRT1 family members in motifs and residues involved in nitrate and proton transport, suggesting and supporting the diverse substrate specificity of the transporter. Phenotypical analysis of *nrt1.5* knockout mutant demonstrated that NRT1.5 is important for the root growth in dependency on external potassium, nitrate, and pH availability. How NRT1.5 is involved in the control of the root architecture in nutrient availability- and pH-dependent manner is discussed as a direct or indirect influence of interaction with other cellular components. The bimolecular fluorescent complementation in tobacco plants was used to verify the NRT1.5 interactions at the plasma membrane. Proteins related to pH homeostasis (AHA2), vesicle traffic (PEP12 and VAMP722), calcium-regulated phosphorylation (CBL3 and CIPK23), and anion homeostasis (SLAH1 and SLAH3) were identified. Gene expression of *AHA2*, *CBL3*, *PEP12*, *SLAH1*, *SLAH3*, and *VAMP722* were affected by low nutrition supply in the *nrt1.5* mutant, evidencing a molecular correlation between NRT1.5 and the interaction partners. The *nrt1.5* knockout mutant showed several phenotypes under K^+ and NO_3^- deficiencies regarding leaf senescence and alteration of the root architecture. The *cbl3*, *pep12*, *slah1*, *slah3*, and *vamp722* knockout mutants and the double mutants with *nrt1.5* did not show phenotypes evidencing any biological interaction with NRT1.5. The understanding of the physiological roles of the interaction partners of NRT1.5 in potassium and nitrate homeostasis has been challenging due to the high redundancy of all candidates in their pathways. However, the H^+ -ATPase AHA2 together with NRT1.5 were capable to affect K^+ loading to shoots, modulate the root architecture, alter the extracellular pH, and plasma membrane potential. Also, from the 11 members of H^+ ATPase, the *AHA4* and *AHA6* were up-regulated under K^+ and NO_3^- deficiencies. However, the lack of both *NRT1.5* and *AHA2* play a critical impact in the expression of all 11 members, leading to an alteration in the control of extracellular pH at K^+ and NO_3^- deficiency conditions. A cellular role of NRT1.5 and AHA2 interaction is hypothesized, where NRT1.5 activity by its H^+ antiporter function

might generate a ΔpH in the cytosol that AHA2 may restore at the plasma membrane of root cells. Investigation about the binding sites of NRT1.5-AHA2 interaction demonstrated that a conserved glycine residue in the transmembrane domain 5 of NTR1.5, overlapping in a potential LRR motif, is crucial for the protein-protein interaction. A substitution in this glycine at position 209 into a charged amino acid affected the K^+ transport function of NRT1.5 and avoided the interaction with AHA2.

Overall, this study unravels that the joint activity and function of NRT1.5 and AHA2 take place in the maintenance of potassium and nitrate homeostasis in plants.

II. Zusammenfassung

Nitrat (NO_3^-) und Kalium (K^+), die von Pflanzenzellen aufgenommen werden, werden über Kurzstreckenverteilung (Zytoplasma zur Vakuole) und Langstreckentransport (Wurzel zum Spross) durch die Pflanze transportiert. Beide Wege regulieren gemeinsam den Gehalt an NO_3^- und K^+ in allen höheren Pflanzen. Der Transporter NRT1.5 aus *Arabidopsis thaliana* ist für die Beladung von NO_3^- und K^+ aus dem Wurzelzytoplasma der Perizykelzellen in die Xylemgefäße verantwortlich und ermöglicht so den Langstreckentransport von NO_3^- und K^+ durch die Wurzeln zu den Sprossen. In dieser Arbeit enthüllte die Aminosäuresequenzanalyse von NRT1.5 eine geringe Konservierung zwischen den NRT1-Familienmitgliedern hinsichtlich der Motive und Aminosäurereste, die am Nitrat- und Protonentransport beteiligt sind, was die vielfältige Substratspezifität des Transporters nahelegt und unterstützt.

Die phänotypische Analyse der *nrt1.5* knockout Mutante zeigte, dass NRT1.5 wichtig für das Wurzelwachstum in Abhängigkeit der externen Kalium-, Nitrat- und pH-Verfügbarkeit ist. Wie NRT1.5 an der Kontrolle der Wurzelarchitektur in Abhängigkeit der Nährstoff- und pH-Verfügbarkeit beteiligt ist, wird im Zusammenhang mit dem direkten oder indirekten Einfluss der Interaktion mit anderen zellulären Komponenten diskutiert. der bimolekularen Fluoreszenzkomplementierung in Tabak wurde verwendet, um die NRT1.5-Interaktionen an der Plasmamembran zu verifizieren. Es wurden Proteine identifiziert, die mit der pH-Homöostase (AHA2), dem Vesikelverkehr (PEP12 und VAMP722), der Kalzium-regulierten Phosphorylierung (CBL3 und CIPK23) und der Anionen-Homöostase (SLAH1 und SLAH3) in Verbindung stehen. Die Genexpression von AHA2, CBL3, PEP12, SLAH1, SLAH3 und VAMP722 wurde durch die geringe Nährstoffversorgung in der *nrt1.5*-Mutante beeinträchtigt, was eine molekulare Korrelation

zwischen NRT1.5 und den Interaktionspartnern belegt. Die *nrt1.5* knockout Mutante zeigte unter K^+ - und NO_3^- -Mangel verschiedene Phänotypen hinsichtlich Blattseneszenz und Veränderung der Wurzelarchitektur. Die knockout Mutanten *cbl3*, *pep12*, *slah1*, *slah3* und *vamp722* sowie deren Doppelmutanten mit *nrt1.5* zeigten keine Phänotypen, die auf eine biologische Interaktion mit NRT1.5 hinweisen. Das Verständnis der physiologischen Rollen der NRT1.5 Interaktionspartner in der Kalium- und Nitrat-Homöostase war aufgrund der hohen Redundanz aller Kandidaten in ihren Stoffwechselwegen eine Herausforderung. Jedoch war die H^+ -ATPase AHA2 zusammen mit NRT1.5 in der Lage, die K^+ -Beladung der Sprossen zu beeinflussen, die Wurzelarchitektur zu modulieren, sowie den extrazellulären pH-Wert und das Plasmamembranpotential zu verändern. Von den 11 Mitgliedern der H^+ ATPase wurden *AHA4* und *AHA6* unter K^+ und NO_3^- Mangel induziert. Das Fehlen von *NRT1.5* und *AHA2* hatte allerdings einen kritischen Einfluss auf die Genexpression aller 11 Mitglieder, was zu einer Veränderung der Kontrolle des extrazellulären pH-Wertes unter K^+ und NO_3^- Mangel Bedingungen führte. Es wird eine zelluläre Rolle der Interaktion zwischen NRT1.5 und AHA2 vermutet, wobei NRT1.5 durch dessen H^+ -Antiporterfunktion einen ΔpH im Cytosol erzeugen könnte, den AHA2 an der Plasmamembran der Wurzelzellen wiederherstellen kann. Untersuchungen der Bindungsstellen der NRT1.5-AHA2-Interaktion zeigten, dass ein konservierter Glycinrest in der Transmembrandomäne 5 von NTR1.5, welcher sich mit einem potentiellen LRR-Motiv überschneidet, für die Protein-Protein-Interaktion entscheidend ist. Die Substitution dieses Glycins an Position 209 durch eine geladene Aminosäure beeinträchtigte die K^+ -Transportfunktion von NRT1.5 und verhinderte die Interaktion mit AHA2. Insgesamt entschlüsselt diese Studie, dass die gemeinsame Aktivität und Funktion von NRT1.5 und AHA2 an der Aufrechterhaltung der Kalium- und Nitrat-Homöostase in Pflanzen beteiligt ist.

1. Introduction

1.1. Potassium (K^+) and nitrate (NO_3^-) in higher plants

Potassium (K^+) and nitrogen (N) are essential macronutrients influencing the growth and development of higher plants. Acquisition of these nutrients is essential for plant performance, but limitation or excess of these nutrients in most agricultural soils limit the productivity. While K^+ is generally available to plants only as a simple monoatomic cation, N is available in soils in the form of diverse compounds, for example, nitrate (NO_3^-), ammonium (NH_4^+), and amino acids (Xu et al., 2012). Another distinction is that K^+ is not metabolized to an organic form, it remains as a soluble ion inside plants, where it has crucial functions in many physiological processes, such as enzyme activation, cation-anion balance regulation, osmoregulation, turgor generation, cell expansion, pH homeostasis, and control of membrane potentials (Taiz and Zeiger, 1991). NO_3^- is the most prevalent N form in soils and it is required for optimal plant growth and development, but in contrast to K^+ , N is covalently bound in many organic compounds, including proteins, nucleic acids, chlorophyll, co-enzymes, and phytohormones. To be assimilated, NO_3^- is taken up from the soil and converted into ammonium by nitrate and nitrite reductases, and then incorporated into amino acids via the glutamine-synthetase and glutamate synthase (GS-GOGAT) pathway (Xu et al., 2012).

NH_4^+ is another N form and it is preferred over nitrate by most plants, but ammonium uptake through roots is tightly controlled because an elevated ammonium concentration in the cytosol becomes toxic to the plant (Gazzarrini et al., 1999).

The intersections between K and N physiology are explored at several levels, from molecular-genetic processes to compartmentation, to whole plant physiology, and discussed in the context of both N-K cooperation and antagonism (reviewed by Coskun et al., 2017). For example, K^+ plays an essential role as a counter ion of NO_3^- , facilitating the uptake, translocation, and distribution of these ions between roots and shoots (Ródenas et al., 2017). In contrast to the cooperative relationship between K^+ and NO_3^- nutrition, the uptake and translocation of K^+ and NH_4^+ are often found to be antagonists, likely because of the similarities between the two ions in terms of their hydrated diameters, charge, and influence on membrane potentials (ten Hoopen et al., 2010). However, the mechanistic basis for the mutual influences in plant nutrition exerted by these nutrients is poorly understood.

1.2. Nitrate transporters and channels in higher plants

The first step of the NO_3^- transport in higher plants from soil is the uptake into root cells where NO_3^- can be redirected out of the root cell either by extrusion in the external medium or loaded into the xylem vessel to reach the aerial organs. The third possible fate for NO_3^- either in roots or leaves, is its uptake by the vacuole where it participates in the osmoregulation or serves as a reservoir to sustain the growth process when the external nitrogen supply becomes limiting (Forde, 2000). All this traffic requires the coordinated transport of nitrate through different cellular membranes, subcellular compartments, and organs. To do so, higher plants have evolved a combination of transporters and channels with diverse ranges of affinity and specificity.

NO_3^- transporters and channels in higher plants are encoded by four gene groups, (1) *NRT1/PTR* (nitrate transporter 1/peptide transporter, renamed as NPF), (2) *NRT2/NNP* (nitrate transporter 2/nitrate-nitrite porter), (3) *CLC* (chloride channels), and (4) *SLAC1/SLAHs* (slow-type anion channel-associated 1/homologues) (**Figure 1**).

The *NRT1/PTR* or *NPF* family, part of the large major facilitator superfamily (MFS) proteins, is the biggest nitrate transporter family with 53 members in *Arabidopsis thaliana* and more than 80 in *Oryza sativa* (Zhao et al., 2010). Not all members can transport NO_3^- since NRT1s and PTRs belong to the same family, but only NRT1s have been described as NO_3^- transporters, whereas PTRs or POTs (Proton-dependent oligopeptide transporter) have been described as a di/tripeptide transporters. All family members consist of two sets of six transmembrane helices, and both are connected by a long hydrophilic cytosolic loop, highly conserved in plants (Steiner et al., 1995; Tsay et al., 2007).

Besides NO_3^- and peptide transport activities other *NRT1/PTR* substrates were identified in the last years, e.g. nitrite (Pike et al., 2014), chloride (Li et al., 2016), and hormones like auxin, abscisic acid, gibberellins, and jasmonates (Chiba et al., 2015; Wulff et al., 2019), suggesting multi-specificity of the *NRT1* family.

The *NRT2* family was identified in a wide range of higher plant species, including barley, soybean, and *Arabidopsis* (Forde, 2000). The *NRT2* is a highly conserved family with seven members (*NRT2.1-NRT2.7*) in *Arabidopsis*, and similarly to the *NRT1/PTR* family, these membrane proteins contain 12 predicted α -helical transmembrane domains, a central cytoplasmic loop, and cytosolic and hydrophilic N and C termini (Forde, 2000). All characterized *NRT2* members belong to the high-affinity transport systems and they are classified into inducible (iHATS) or constitutive

(cHATS) (Tsay et al., 2007). NO_3^- is their unique substrate identified and they are generally unable to transport NO_3^- on their own since almost all NRT2 proteins, except NRT2.7, need to specifically interact with the partner protein NAR2 (Nitrate Assimilation Related protein, also known as NRT3.1) to be active (Okamoto et al., 2006).

The chloride channel (CLC) family is present ubiquitously in all domains of life and in Arabidopsis, seven members were identified. Initially, CLC have been described specifically in chloride (Cl^-) transport, and later most of them have been defined in NO_3^- vacuolar homeostasis (De Angeli et al., 2006; Von Der Fecht-Bartenbach et al., 2010). CLCa and CLCb are the major members driving nitrate into the vacuoles (Monachello et al., 2009; Von Der Fecht-Bartenbach et al., 2010) and CLCc is involved in the regulation of stomatal movements and contributes to salt tolerance (Jossier et al., 2010). CLCg is expressed in mesophyll cells and participates in salt tolerance (Nguyen et al., 2016), and CLCd and CLCf proteins are localized to Golgi membranes, where CLCd plays a crucial role in the regulation of luminal pH in the trans-Golgi network by transporting Cl^- or NO_3^- (Fecht-Bartenbach et al., 2007). The function of CLCf remains elusive (Marmagne et al., 2007) and CLCe is situated in the thylakoid membrane of chloroplasts and participates in the regulation of photosynthetic electron transport (Herdean et al., 2016).

The SLow-type Anion Channel Associated/SLAC1 Homologues (SLAC/SLAH) is the smallest family with NO_3^- transport function with five members in angiosperms, the SLAC1 (S-type anion channel), and four homologs, SLAH1 to SLAH4 (Dreyer et al., 2012). All of them display a common predicted structure of 10 transmembrane α -helices, where the transmembrane domain 5 contains the pore with a central and highly conserved phenylalanine residue, that potentially represents the anion gate (Chen et al., 2010). These family members have in common their plasma membrane localization, but they show distinct tissue-specific expression patterns. *SLAC1* is exclusively expressed in guard cells, *SLAH4* in the root vascular system, *SLAH2* in lateral root primordia and root tips, and *SLAH3* in all plant tissues (Negi et al., 2008; Geiger et al., 2011; Zheng et al., 2015).

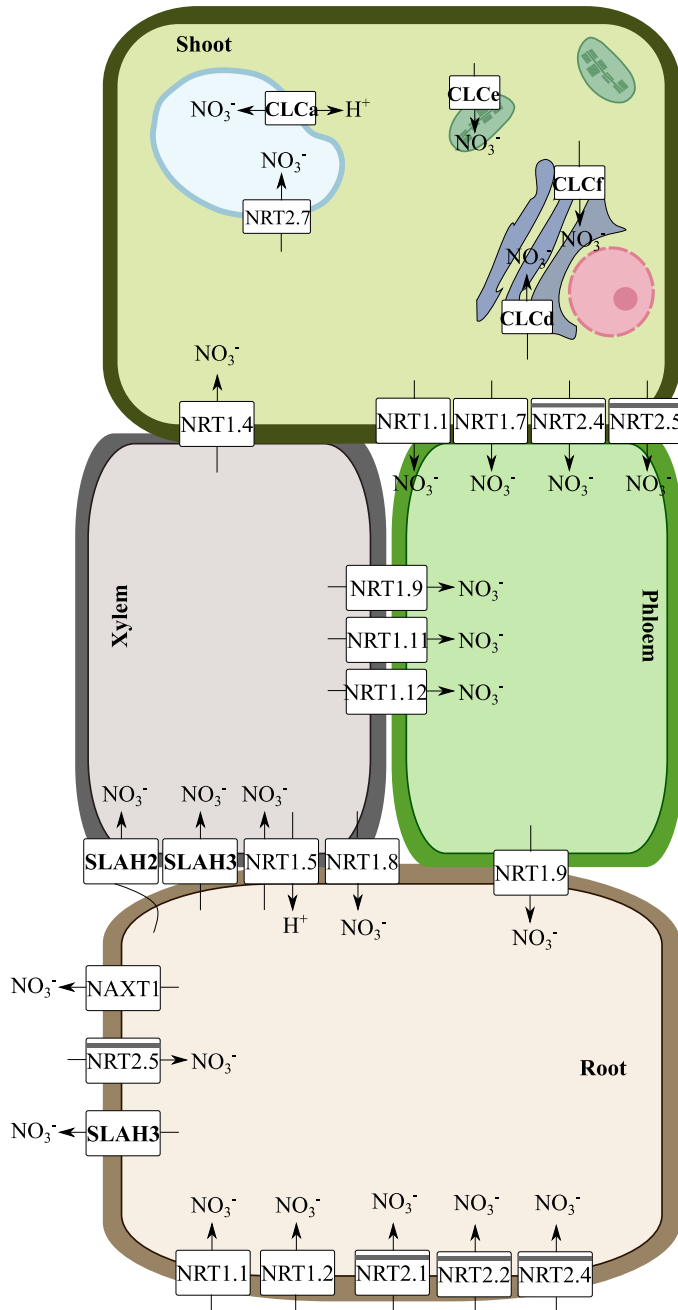


Figure 1: Nitrate transport in *Arabidopsis thaliana*. Simplified overview of NO_3^- transport in *A. thaliana* from root uptake to the shoot distribution connected by xylem and phloem. Most of NRT1/PTR, NRT2, CLC, and SLAC/SLAHs families are represented. The transporter and channel (bold cases) functions represented are root uptake, root efflux, loading/unloading of the xylem, and loading/unloading of the phloem. At the cellular level, the proteins represented here are localized at the plasma membrane, vacuoles, chloroplast, and Golgi. Except for NRT2.7, all NRT2 proteins interact with NAR2.1 to be functional (represented as grey line in each NRT2 transporter). NRT1 and NRT2 are membrane NO_3^- transporters functioning as an H^+/NO_3^- symporter or antiporter (function not represented in the figure with the exception of NRT1.5). Figure created and adapted from Wang et al., 2012; O'Brien et al., 2016; Guan, 2017.

1.2.1. NO_3^- transport in roots: uptake, storage into vacuoles, and efflux

As a result of fluctuations of NO_3^- concentrations in soils, plants have evolved two uptake systems with different kinetic properties: low-affinity transport system (LATS) for high external nitrate concentrations ($>0.5\text{mM}$) and high-affinity transport system (HATS) for low nitrate concentration ($<0.5\text{mM}$), into which most nitrate transporters can be categorized. With few exceptions, the NRT1/PTR transporters are LATS, and the NRT2/NNP family members are HATS (Forde, 2000).

NRT1.1/NPF6.3, NRT1.2/NPF4.6, NRT2.1, and NRT2.2 transporters have been shown to participate in root NO_3^- uptake. NRT1.1 is the most extensively studied NRT1 transporter in *Arabidopsis thaliana* involved in root uptake. NRT1.1 is the exception in the family since it can conditionally function as nitrate LATS or HATS. The transporter switches between the two modes of action and is regulated by phosphorylation at threonine residue 101; when phosphorylated, NRT1.1 functions as a high-affinity nitrate transporter, whereas, when dephosphorylated, it functions as a low-affinity nitrate transporter. This regulatory mechanism allows plants to change rapidly between high- and low-affinity nitrate uptake, which may be critical when competing for limited nitrogen (Liu and Tsay, 2003). The NRT1.1 expression is mainly in the plasma membrane of epidermis, cortical and endodermal root cells, where it can work also as a NO_3^- sensor, perceiving different levels of external NO_3^- (Ho et al., 2009). Another LATS member also involved in nitrate uptake is the NRT1.2 transporter and its activity is restricted to low-affinity nitrate transport in the root epidermis and root hairs (Huang et al., 1999). One more NRT1 family member involved in nitrate transport in roots is the nitrate excretion transporter 1 (NAXT1). NAXT1 is mainly expressed at the plasma membrane of the cortex of mature roots in *Arabidopsis* and is responsible for nitrate excretion. Although the physiological role of nitrate efflux remains unclear, it is known that the net root nitrate uptake is the balance between nitrate influx and efflux and is affected by nutrient availability (Wang et al., 2012).

From the NRT2 family, NRT2.1 is the best-characterized HATS with localization at the plasma membrane of cell roots, and expression in epidermal and cortical root cells (Chopin et al., 2007). The *NRT2.1* gene requires simultaneous expression of *NAR2* to express the high-affinity nitrate transport activity in *Arabidopsis* (Okamoto et al., 2006), and the two-component nitrate uptake system of NRT2 and NAR2 is present in other plant species such as barley and rice (Ishikawa et al., 2009; Feng et al., 2011). In addition, NRT2.2 and NRT2.4 also participate in high-affinity nitrate uptake in roots whereas NRT2.4 is having a very high-affinity range. The relative contribution of these transporters to nitrate uptake is dependent on the developmental stages of the root, and the nitrate status of the plant (Wang et al., 2012).

CLC channel members are also involved in nitrate transport in roots. For example, CLCa can accumulate specifically nitrate in the vacuoles in roots of *Arabidopsis thaliana* (Geelen et al., 2000; De Angeli et al., 2006), and CLCb was described as a NO_3^-/H^+ channel in the tonoplast, but the expression of *CLCb* is much lower than *CLCa* (Von Der Fecht-Bartenbach et al., 2010).

1.2.2. Long-distance transport of NO_3^-

Nitrate can be assimilated into the root, however, the percentage of root assimilation vs shoot assimilation depends on the plant species. At high concentration of nitrate in soils, nitrate assimilation occurs mainly in the shoot in most plants, probably because the shoot is more energy-efficient (Taiz and Zeiger, 1991). The first step of nitrate assimilation in shoots is the translocation out of the roots via xylem loading into the xylem vessels and deliver to the aerial parts of the plants. NRT1.5 was reported to be a major transporter in loading nitrate into the xylem sap (Lin et al., 2008). In addition, SLAH1/SLAH3 heteromerization was reported to facilitate SLAH3-mediated anion efflux from pericycle cells into the root xylem vessels. The SLAH3 anion channel is not active per se but requires extracellular nitrate and phosphorylation by calcium-dependent kinases (Cubero-Font et al., 2016). SLAH2, the closest homolog of SLAH3 is expressed in the root stele and the hypocotyl. Although the physiological role of SLAH2 in the root stele has not yet been explored in detail, it is tempting to speculate that SLAH2 is responsible for nitrate specific loading of xylem vessels (Hedrich and Geiger, 2017).

Two low-affinity nitrate transporters, NRT1.8 and NRT1.9, expressed predominantly in xylem parenchyma cells and root companion cells (phloem) respectively, negatively impact the root-to-shoot nitrate transport. NRT1.9 mediates nitrate transport back to roots via phloem, and NRT1.8 removes the nitrate via xylem vessels back to roots. This mechanisms prevents excess amounts of nitrate from being accumulated in shoots (Li et al., 2010; Wang and Tsay, 2011).

In mature leaves, NRT1.7 is involved in nitrate remobilization from older leaves to younger leaves by loading nitrate into minor veins (Fan et al., 2009). NRT1.12 and NRT1.11 are involved in the transfer of xylem-borne nitrate to the phloem in the petiole (Hsu and Tsay, 2013).

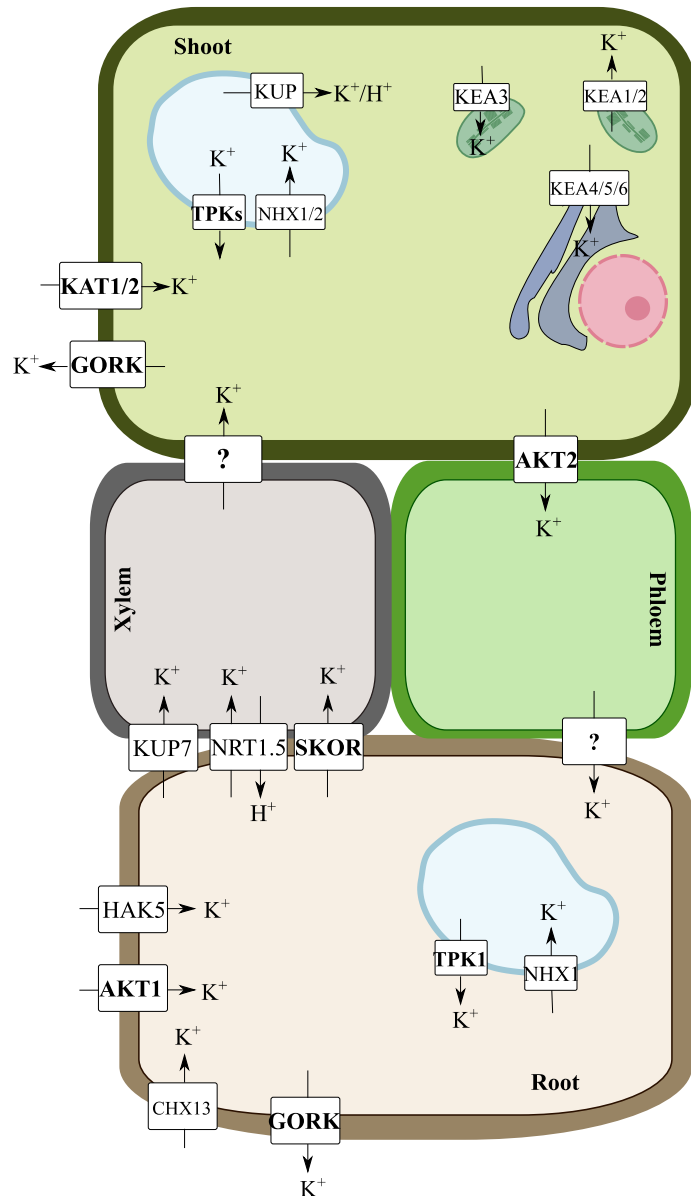
At the destination organs, nitrate is either stored inside vacuoles using K^+ as a counter ion, where both ions contribute to osmotic adjustment (Martinoia et al., 2012), or reduced to nitrite and then partitioned into the plastids to be assimilated to organic nitrogen (Wang et al., 2012). The high-affinity nitrate transporter NRT2.7 and the channel-like NO_3^-/H^+ exchanger CLCa and CLCb were identified as responsible for nitrate translocation into vacuoles in seeds and leaves respectively (De Angeli et al., 2006; Von Der Fecht-Bartenbach et al., 2010). Concerning seeds, the ultimate sink tissue, NRT1.6, another low-affinity plasma membrane-localized nitrate transporter, is expressed in the vascular tissue of siliques and the funiculus, ensuring nitrate supply to developing seeds (Almagro et al., 2008).

1.3. Potassium transporters and channels in higher plants

K^+ is taken up from the soil by root epidermal and cortical cells and enters into the root symplast where it may be stored in vacuoles to fulfill osmotic functions, or it is transported to the shoot via the xylem (Taiz and Zeiger, 1991).

Subsequently, shoot cells may also supply stored K^+ for redistribution via the phloem. In this transit from the soil to the different plant cellular compartments and organs, K^+ crosses various cell membranes and tissues through different K^+ specific transport systems. More than 70 K^+ channels and transporters have been identified and characterized in *Arabidopsis thaliana* and they are widely diverse in their energetic coupling, activity, affinity, structure, cellular/tissue localization (Very and Sentenac, 2003) (Figure 2).

Figure 2: Potassium transport in *Arabidopsis thaliana*. Simplified overview of K^+ transport in *A. thaliana* from root uptake to shoot distribution connected by xylem and phloem by K^+ channels (in bold cases) and transporters. Adapted from Wang and Wu, 2017; Ragel et al., 2019; Raddatz et al., 2020.



K^+ transporters and channels have been categorized into six different gene families in higher plants, comprising of three channel families, (1) *Shaker*, (2) *TPK* (tandem-pore K^+), and (3) *Kir-like* (K^+ inward rectifier) (Very and Sentenac, 2003) and three transporter families (1) *KUP/HAK/KT*, (2) the high-affinity K^+ transporters (*HKT*), and (3) the big family of cation-proton antiporters (*CPA*)

(include, CHX: cation/H⁺ antiporters, NHX: Na⁺/H⁺ exchanger and KEA: K⁺ exchanger antiporter subfamilies) (Gierth and Mäser, 2007; Chanroj et al., 2012).

Arabidopsis thaliana contains 15 genes encoding potassium channels and they have been classified into two channel classes depending on the voltage sensibility: non-voltage-gated and voltage-gated K⁺ channels (**Table 1**). The group of voltage-gated K⁺ channels consists of four α -subunits surrounding a central aqueous pore for K⁺ permeation at the plasma membrane. Each subunit contains six transmembrane segments, which can be divided into two different modules: the first four α -helices form a voltage-sensor domain that contains multiple positively charged residues that move within the membrane in response to voltage and directly control the opening or closing of the channel. The transmembrane segments 5, 6, and the pore loop, form the pore domain (P), involved in the permeation pathway. The loop segment comprises the universal and conserved TxxTxGYG motif which is a hallmark for most potassium selective channels in plant and animal cells (Doyle et al., 1998). Moreover, plant α -subunits have a long C-terminal region including several functional domains: a linker region (C-linker), a cyclic nucleotide-binding homology domain (cNBD), an ankyrin domain, and a KT/KHA domain (Daram et al., 1997).

The non-voltage-gated channels have weak sensitivity to membrane potentials, and consist of six members, five tandem-pore channels (TPK1–TPK5), and a single subunit (KCO3) that resulted from gene duplication of a tandem-pore channel gene and subsequent partial deletion (Voelker et al., 2010). TPK channels possess four transmembrane segments and two pore-loop domains in tandem containing the highly conserved motif domain TXGYGD (Czempinski et al., 1997). The cytosolic C-terminal tail contains two EF hand domains (putative Ca²⁺-binding sites) suggesting their sensitivity to Ca²⁺. The cytosolic N-terminal tail contains a binding site for 14-3-3 proteins (Latz et al., 2007).

Table 1: K⁺ channels in *Arabidopsis thaliana* classified as voltage and non-voltage-gated K⁺ channels. The 3 family members of K⁺ channels, TPK (tandem pore K⁺), K_{ir}-like, and Shaker channels are represented. Abbreviations: PM, plasma membrane. VM, vacuolar membrane. ER, endoplasmic reticulum. Extra, extracellular space. Intra, intracellular space. P, P1 and P2, pore domains. EF, EF hand domain. +, positively charged amino acids. cNBD, cyclic nucleotide binding domain. anky, ankyrin repeat domain. K_{(T)/HA}, acidic domain.

Channel class	Name	Locus ¹	Localization ²	Channel structure ³		
Non-voltage gated K⁺ channel	Tandem pore K⁺			TPK		
		TPK1	At5g55630	VM		
		TPK2	At5g46370	VM		
		TPK3	At4g18160	Thylakoid		
		TPK4	At1g02510	PM and ER		
TPK5	At4g0840	VM				
Voltage gated K⁺ channel	K_{ir}-like	KCO3	At5g46360	VM	K_{ir}-like	
	Shaker	KAT1	At5g46240	PM		
		Inward-rectifying	KAT2	At4g18290	PM	
		rectifying	AKT1	At2g26650	PM	
			AKT5	At4g32500	PM	
			SPIK	At2g25600	PM and cytosol	
			KC1	At4g32650	Chloroplast, PM and ER	
		Weakly rectifying	KT2	At4g22200	PM, plasmodesma and ER	
		Outward-rectifying	SKOR	At3g02850	PM	
	GORK	At5g37500	PM	Shaker		

¹ Gene designation from TAIR10 (www.arabidopsis.org). ² Prediction of protein subcellular localization from SUBA4 database (www.suba.live). ³ Protein topology predictions for channels were adapted from Jegla et al., 2018; Ragel et al., 2019.

Membrane transport of potassium can be mediated either by potassium channels as described before (**Table 1**), utilizing mainly the membrane potential to facilitate the transport of potassium against the electrochemical gradient, or by transporters. Several K⁺ transporters have been identified and classified in three different families. The KT/HAK/KUP family members mediate K⁺ transport through a K⁺/H⁺ symport mechanism (Grabov, 2007). The high-affinity K⁺ transporters (HKT) were initially studied regarding K⁺ transport but subsequently received more attention due to their roles in Na⁺ transport (Almeida et al., 2013; Benito et al., 2014). The cation

proton antiporter (CPA) family is big and diverse, including CPA1 (NHX) and CPA2 (KEA and CHX) subfamilies. They were originally described as Na⁺/H⁺ transporters, but several CPAs were recently shown to also transport K⁺ (Bassil et al., 2019; Tsujii et al., 2019) (**Table 2**).

In *Arabidopsis thaliana* 13 members of the KT/HAK/KUP family have been identified (Mäser et al., 2001), and 26 in *Oryza sativa* (Amrutha et al., 2007). Transporters belonging to this family are also found in fungi, bacteria, and even in virus genomes (Greiner et al., 2011; Santa María et al., 2018). The structural topology showed the presence of common attributes among all of them: (1) a hydrophobic core containing 10–14 transmembrane segments, (2) three well-described cytosolic domains, the N- and C-termini, and (3) a region containing approximately 70 residues situated between the second and third transmembrane domains.

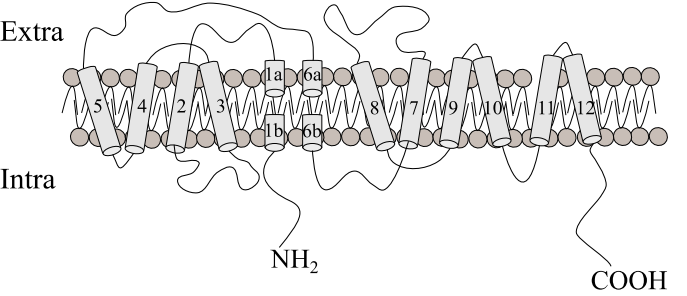
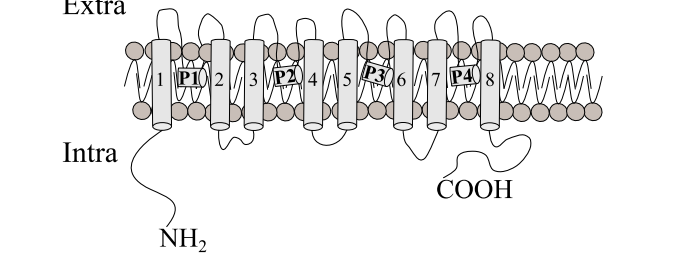
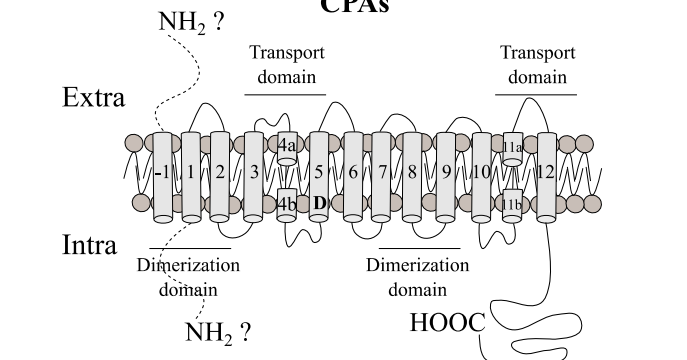
The members of the high-affinity K⁺ transporter (HKT) family facilitate Na⁺ selective uniport or Na⁺/K⁺ symport with a channel-like activity in plants (Benito et al., 2014). In *Arabidopsis thaliana* only one member was described and identified, AtHKT1, with preference for Na⁺ (Davenport et al., 2007). HKT genes have also been identified in other higher plants, e.g. *TaHKT1* in wheat (Schachtman and Schroeder, 1994), *OsHKT1-OsHKT9* in rice (Garcia-deblás et al., 2003) or *HvHKT1.5* in barley (Huang et al., 2020). Plant HKT transporters display similarity in their core structure with the K⁺ transporter TrkH from *Vibrio parahaemolyticus*, comprising eight transmembrane domains (TM) and four pore-forming (P) domains successively arranged in four TM1-P-TM2 motifs in a single polypeptide chain, forming a central permeation pathway similar to that of tetrameric *Shaker*-like K⁺ channels (Cao et al., 2011).

The cation-proton antiporters (CPA) are the third and also largest K⁺ transporter family, including the Na⁺/H⁺ exchangers (NHX), K⁺ efflux antiporters (KEA), and cation/ H⁺ exchangers (CHX). They are cation/H⁺ antiporters that modulate the pH, electrical, and cation balance locally (Sze and Chanroj, 2018). In *Arabidopsis thaliana* more than 50 genes code for CPA proteins (**Table 2**), and in the last years many of them have been associated to K⁺ transport and pH homeostasis, for example, NHXs involved in K⁺/H⁺ vacuolar transport (Bassil et al., 2019), KEAs associated to K⁺ efflux transport in chloroplasts (Tsujii et al., 2019), and K⁺ transport by CPXs in plasma and endomembrane systems (Zhao et al., 2008; Sze and Chanroj, 2018).

Table 2: K⁺ transporters in *Arabidopsis thaliana*. The members of the three families KT/HAK/KUP, HKT, and CPA are represented. Abbreviations: PM, plasma membrane. VM, vacuolar membrane. ER, endoplasmic reticulum. Extra, extracellular space. Intra, intracellular space. P₁₋₄, P-loops involved in ion

1. Introduction

selectivity. D, a conserved Asp. Transporter structures are a general and simplified representation topology due to the diversity of structures and conserved domains. For CPA transporters the structure is a representation mainly from AtCHX17 and AtNHX1.

Transporter names and classes	Cellular localization ¹	Transporter structure ²
<p>Low/ high-affinity K⁺ uptake:</p> <p>KT/HAK/ KUP</p> <p>HAK5</p> <p>KUP1-KUP12</p> <p>High-affinity K⁺:</p> <p>HKT</p> <p>HKT1</p>	<p>PM</p> <p>PM, VM, ER, thylakoid</p> <p>PM, mitochondria</p>	<p>KT/HAK/KUP</p> 
<p>Na⁺/H⁺ exchanger:</p> <p>CPA1</p> <p>NHX1-NHX8</p> <p>K⁺ efflux antiporter :</p> <p>CPA2</p> <p>KEA1-KEA6</p>	<p>PM, VM, Golgi</p> <p>Thylakoid, Golgi</p>	<p>HKT</p> 
<p>Cation/ H⁺ exchanger:</p> <p>CHX1-CH28</p>	<p>PM, VM, ER, Endosome, Golgi</p>	<p>CPAs</p> 

¹ Prediction of protein subcellular localization from SUBA4 database (www.suba.live). ² Protein topology predictions for KT/HAK/KUP are adapted from Very and Sentenac, 2003; Ragel et al., 2019, for HKT from Almeida et al., 2013; Ragel et al., 2019 and for CPAs from Gierth and Mäser, 2007; Czerny et al., 2016; Sze and Chanroj, 2018.

1.3.1. K⁺ transport in roots: uptake, storage into vacuoles, and efflux

The uptake of K⁺ by roots exhibits biphasic kinetics in response to an increase in external concentrations corresponding to high and low-affinity transport systems, which work at low (<1 mM) and high (>1 mM) external K⁺ concentrations respectively (Gierth and Mäser, 2007). The current model for root K⁺ uptake postulates that at high concentrations in the soil, K⁺ crosses the membranes mostly through channels, which allow ions to move down the concentration gradient. In contrast, at low K⁺ concentration, active transporter systems are needed in order to pull K⁺ inside the cell against its electrochemical gradient. Root uptake of K⁺ in *Arabidopsis thaliana* is conducted by the voltage-gated K⁺ channel AKT1, and the high-affinity K⁺ transporter HAK5 (Rubio et al., 2010; Nieves-Cordones et al., 2014).

The activity of AKT1 and HAK5 mediate almost all K⁺ absorption in roots and both are critical for plant K⁺ nutrition (Nieves-Cordones et al., 2016). Among the K⁺ uptake channels of *Arabidopsis*, only AKT1 and KC1 are abundantly expressed in root tissues (Reintanz et al., 2002). If KC1 is expressed alone it remains in the endoplasmic reticulum, but it can be recruited to the plasma membrane to regulate AKT1 activity under K⁺ limitation, where AKT1/KC1 complex renders the channel more efficient (Geiger et al., 2009; Wang et al., 2010).

Other K⁺ channels and transporters contribute to a minor degree to K⁺ uptake. For example, CHX13, a plasma membrane cation/H⁺ antiporter promotes relatively high-affinity K⁺ uptake by K⁺-starvation (Zhao et al., 2008). The transporter KUP7 is involved in K⁺ acquisition under K⁺-limited conditions (Han et al., 2016). In addition, the voltage-gated channel GORK (guard cell outward-rectifying K⁺), which is expressed mainly in guard cells and also in root outer cell layers (epidermal, root hairs, and cortex), is supposed to be a major pathway for stress-induced K⁺ leakage from root cells, e.g. by exposure of roots to high salt (Demidchik et al., 2014).

Several KT/HAK/KUP transporters have been localized to the tonoplast, storing K⁺ into the vacuole. The vacuolar K⁺ pool, the main reservoir for K⁺ in the cell, plays biophysical functions, e.g. lowering the osmotic potential, generating turgor, and driving cell expansion (Wang and Wu, 2013). Vacuolar NHX-type exchangers have been shown to serve this critical function in plant cells. Recently the tonoplast-localized NHX1, NHX2, and NHX4 are described as the main transporters involved in the uptake of K⁺ into vacuoles (Bassil et al., 2019). The two-pore K⁺ (TPK) channels are K⁺ selective vacuolar cation channels, where TPK1 is involved in the regulation of vacuolar K⁺ release mainly during stomatal closure but also radicle growth (Gobert et al., 2007).

1.3.2. Long-distance transport of K^+

Potassium absorbed by peripheral root cells and not compartmentalized in vacuoles must be transported to the upper parts of the plant through the xylem. This step is critical in the long-distance distribution of K^+ from roots to the upper parts of the plant and is driven by specialized transport systems. Some of them are described here. Potassium channels SKOR and AKT2 play an important role in K^+ translocation via xylem and phloem. SKOR (Stelar K^+ Outward Rectifier) is expressed in root stele cells (pericycle and xylem parenchyma cells) of *Arabidopsis*, where it mediates K^+ secretion by xylem parenchyma cells of roots and toward the xylem vessels (Gaymard et al., 1998). Large quantities of K^+ recirculate from roots to shoots via the xylem and subsequently return to the roots via the phloem. The magnitude of the K^+ flux recirculated from the shoots to the roots would constitute a signal by which the growing shoots could communicate to roots their K^+ requirement and regulate K^+ secretion into the xylem sap (and eventually root K^+ uptake). The AKT2 channel protein plays a dual role by loading K^+ in source tissues and unloading K^+ in sink organs (Lacombe et al., 2000).

Members of the KT/HAK/KUP family, e.g. AtKUP7 and OsHAK5, have been proposed to facilitate long-distance K^+ transport from root to shoot, presumably by mediating K^+ uptake into the xylem parenchyma cells (Yang et al., 2014; Han et al., 2016). And NRT1.5, a member of the NRT1 family, also is described to contribute in the long-distance transport of K^+ . NRT1.5 releases K^+ from *Xenopus* oocytes and yeast in a pH-dependent manner and has been proposed to function as a K^+/H^+ antiporter (Li et al., 2017a).

1.4. Regulation of K^+ and NO_3^- transport in plants

Plants have evolved a large ensemble of K^+ and NO_3^- transport systems with defined functions in nutrient uptake by roots, storage into vacuoles, and ion translocation between subcellular compartments, tissues, and organs as it was described in sections 1.2 and 1.3. This new section describes critical cellular components and pathways which regulate, coordinate, and govern the K^+ and NO_3^- nutrition in plants. Conversely, some cellular pathways are directly affected or regulated by K^+ and NO_3^- transport in plants and these are also described in section 1.4.

1.4.1. Plasma membrane potential

In higher plants, the cellular membrane potential ($\Delta\Psi$) in physiological conditions is defined as being negative in the cytoplasm relative to the extracellular space due to an asymmetric distribution of charges (-150 to -250 mV). Ion movements through the plasma membrane can displace locally the $\Delta\Psi$ to membrane depolarization (electropositive in intracellular space) or hyperpolarization (highly electronegative in intracellular space). For example, an immediate physiological response to the root NO_3^- uptake coupled with H^+ commonly leads to $\Delta\Psi$ depolarization of the cells (Meharg and Blatt, 1995; Britto and Kronzucker, 2005). A regulatory mechanism to prevent NO_3^- uptake-associated acidification of the cytoplasm is an increase in the plasma membrane (PM)-ATPases activity. The increase of cytoplasmic H^+ is a signal triggering the PM-ATPase to pump H^+ out of the cytosol to repolarize and maintain $\Delta\Psi$ (Espen et al., 2004). Cellular depolarization is also caused by the K^+ uptake in cotransport with H^+ . The entry of K^+ with H^+ electrically balance the extrusion of two H^+ per ATP hydrolyzed by plasma membrane H^+ -ATPase (Rodriguez-Navarro et al., 1986). Inevitably, nutrient limitations induce changes in plasma membrane potential, however, plants have evolved mechanisms to trigger specific transport systems using the changes in the $\Delta\Psi$. For example, K^+ limitation induces hyperpolarization of the plasma membrane of root cells and enhances transcription of the high-affinity K^+ uptake transporter, *HAK5*, (Rubio et al., 2014), or plant voltage-gated K^+ channels can open at hyperpolarized membrane potentials allowing and enhancing the uptake of K^+ (Gambale and Uozumi, 2006; Dreyer and Uozumi, 2011). In line with this, *SKOR*, being an outward-rectifying channel, opens upon membrane depolarization to allow cytosolic K^+ efflux. The gating of *SKOR* is sensitive to extracellular K^+ concentration, with a maximum activity around 10mM K^+ . In the presence of ample external K^+ , the channel opens at less negative membrane voltages, thereby minimizing the risk to serve as an undesirable K^+ -influx pathway (Gaymard et al., 1998).

Potassium availability is not the only way to trigger plasma membrane potential changes in root cells. When plants face a reduction in anion availability such as nitrate or chloride, an alteration in the plasma membrane potential occurs. To activate slow-type anion channels like *SLAC1* in the guard cell plasma membrane, an initial depolarization phase is required, but upon more hyperpolarized potentials a slow gate deactivation occurs (Hedrich and Geiger, 2017).

1.4.2. Cellular pH

Cellular pH homeostasis is regulated through the activities of nitrate and potassium transport systems, and proton-pumps affecting proton production or consumption during root uptake, short and long-distance transport, and assimilation of nutrients (Sze and Chanroj, 2018; Feng et al., 2020). Plants have several cellular and tissue compartments with different pH values, for example, the cytosol has pH values at 7.2-7.4 (Shen et al., 2013), while the vacuole and apoplast maintain more acidic pH levels at 5-5.5 (Felle, 2001). The maintenance of optimal pH in plant cells has to be tightly regulated and is established by two main cellular approaches, (1) active H⁺ pumping complexes, such as the plasma membrane H⁺-ATPase (PM-H⁺-ATPase), vacuolar H⁺-ATPase (V-ATPase) and the vacuolar H⁺-pyrophosphatase (V-PPase) (Gaxiola et al., 2007), and (2) by root uptake of nutrients since nutrient transporters are involved in the co-transport of H⁺ and their activity have been linked with cellular pH homeostasis (Gerendás and Schurr, 1999; Reguera et al., 2015).

H⁺-ATPases mediate the extrusion of protons by ATP hydrolysis from the cells and establish a proton gradient, which energizes the secondary uptake of nutrients and facilitates many cellular processes by acidification of extracellular space (Palmgren, 2001). Reports about the physiological roles of H⁺-ATPase are sparse in the literature, due to three main reasons. (1) The expression levels of H⁺-ATPases are surprisingly constant in response to abiotic stimuli, including light (Kinoshita and Hayashi, 2011), salinity (Gévaudant et al., 2007) and nutrient limitation (Maathuis et al., 2003; Haruta et al., 2010). (2) Plants have a multigene family of H⁺-ATPases, for example in *Arabidopsis thaliana* 11 genes have been identified (*AHA1-AHA11*) and each cell type can express several different isoforms (Baxter et al., 2003). Transcription analyses of the 11 *AHA* genes indicate that *AHA1* and *AHA2* are the most highly expressed members of this family throughout plant life (Haruta et al., 2010) (**Table 3**). (3) Ectopic overexpression of unmodified H⁺-ATPase typically has no effect on plant growth (Gévaudant et al., 2007).

Table 3: The proton pumps in *Arabidopsis thaliana*. AHA (Arabidopsis H⁺-ATPase) family members.

Name	Locus ¹	Expression% ²	Organ localization of H ⁺ -ATPase in plants ³
AHA1	At2g18960	98.1	
AHA2	At4g30190	96.0	
AHA3	At5g57350	82.1	
AHA4	At3g47950	29.7	
AHA5	At2g24520	47.3	
AHA6	At2g07560	14.5	
AHA7	At3g60330	37.6	
AHA8	At3g42640	46.6	
AHA9	At1g80660	14.7	
AHA10	At1g17260	29.0	
AHA11	At5g62670	84.5	

¹Gene model for the locus from TAIR10 (www.arabidopsis.org). ² Signal percentile in expression arrays from transcriptional profiling with microarrays (Haruta et al., 2010) ³ The image and the main tissue specificity of each proton pump were generated using the eFP browser 2.0 at bar.utoronto.ca.

Plant PM H⁺-ATPases contain five cytosolic domains, including the N terminus, actuator domain, nucleotide-binding domain, phosphorylation domain, and a regulation (R) domain (Palmgren, 2001). The C-terminal or R domain contains two critical autoinhibitory regions and several functionally important phosphorylation sites, the status of which modulates the enzyme activity (Palmgren, 1991). Regulation of PM H⁺-ATPases involves the phosphorylation/ dephosphorylation of specific amino acid residues within the R domain and modulation of the AHA interaction with other proteins. A Ser/Thr protein kinase (PKS5) phosphorylates the PM H⁺-ATPase AHA2 at a Ser⁹³¹ in the C-terminal regulatory domain. This phosphorylation abolishes the interaction with an activating 14-3-3 protein (Fuglsang et al., 2007). Moreover, a peptide hormone receptor, PSY1R (Plant peptide containing Sulfated Tyrosine Receptor), interacts and phosphorylates AHA2 at a residue in its autoinhibitory C-terminal domain and demonstrate that modification of this residue activates proton pumping of AHA2 (Fuglsang et al., 2014).

The activity of membrane H⁺-ATPases and H⁺-coupled transporters establishes and regulates cytoplasmic pH homeostasis. Both NO₃⁻ and K⁺ can be imported into root cells by H⁺-coupled mechanisms across the plasma membrane through energetically uphill processes (Rodríguez-Navarro, 2000; Fan et al., 2017).

1.4.3. Secretory pathway

Membrane proteins, such as nutrient transporters and channels, are usually translated into the endoplasmic reticulum and traffic via the Golgi to the plasma membrane, tonoplast, or other target membranes. In all eukaryotes, secretory traffic to the plasma membrane is mediated by SNARE proteins (soluble N-ethylmaleimide-sensitive factor attachment protein receptor), which drive the traffic of membrane proteins and soluble cargo between various endomembrane compartments to cellular membranes (Bassham et al., 2008) (**Figure 3**). Eukaryotic SNAREs can be classified either by their subcellular localization (functional classification) or according to the occurrence of conserved amino acid residues in the center of the SNARE motif (structural classification). Functional classification divides SNAREs into vesicle-associated and target membrane-associated SNAREs (v- and t-SNAREs, respectively) (Söllner et al., 1993). Alternatively, under the structural classification, SNAREs can be grouped as Q and R-SNAREs owing to the occurrence of either a conserved glutamine or arginine residue in the center of the SNARE domain (Fasshauer et al., 1998). The three types of target membrane-localized Q-SNAREs that contribute to the formation of a SNARE complex can be further subdivided into Qa, Qb, and Qc-SNAREs (Bock et al., 2001). Qa-SNAREs are also frequently referred to as syntaxins (Bennett et al., 1992), and R-SNAREs (so-called longins) are often designated as vesicle-associated membrane proteins (VAMP) (Baumert et al., 1989).

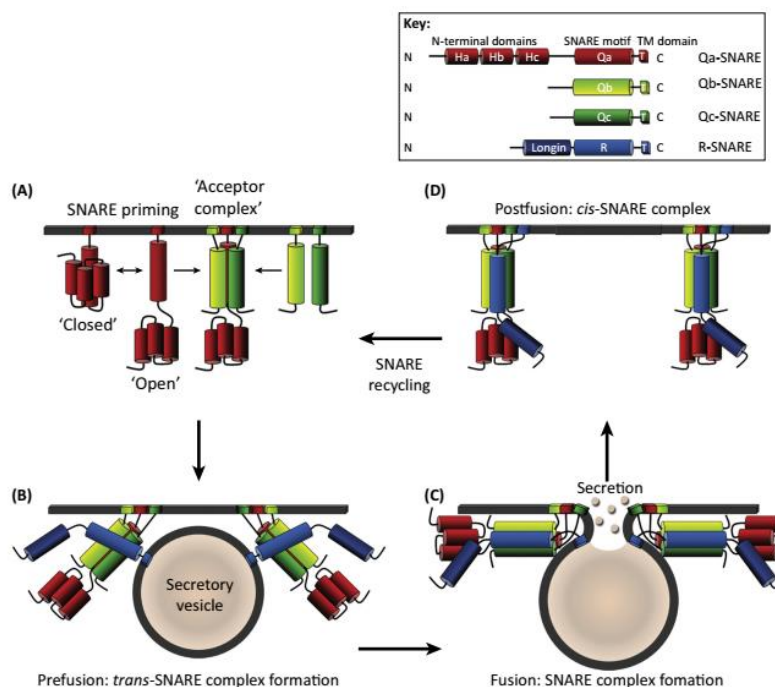


Figure 3: The SNAREs cycle in vesicle trafficking. (A) Binding of the membrane- and vesicle-localized SNAREs in a cognate SNARE core complex involves priming of the Qa-SNARE at the target membrane. The Qa-SNARE transits from its ‘closed’ to ‘open’ conformation, which exposes the Qa-SNARE domain for binding with the Qb- and Qc-SNAREs. The Qa, Qb, and Qc-SNAREs when bound together form the ‘acceptor’ complex, which is available for binding to the R-SNARE. (B) Formation of the trans-SNARE complex following interactions between the R-SNARE on the vesicle and the ‘acceptor’ complex at the target membrane draws the secretory vesicle to the target membrane for fusion. (C) Formation of a stabilized Qa, Qb, Qc, and R-SNARE core complex leads to the fusion of the secretory vesicle with the target membrane and release of the vesicle cargo. (D) Following vesicle fusion, cis SNARE complex disassembly allows for the recycling of the SNARE proteins and sustains further secretory traffic. Figure adapted from Karnik et al., 2017.

In *A. thaliana* Qa-SNARE (SYPs) and VAMPs (subfamilies, VAMP71, VAMP72, YKT6, and SEC22) are the major contributors to secretory vesicle trafficking and have been implicated in a range of biological processes including control of transporters and/or channels involved in plant nutrition. For example, trafficking and localization to the plasma membrane of the K⁺ channel KAT1 is dependent on the Qa-SNARE SYP121 (Sutter et al., 2006). SYP121 also interacts with the K⁺ channels KC1 and AKT1. This tripartite SNARE-K⁺ channel complex regulates gating for the K⁺ channels, a suggested function for SNARE in the context of coordination of vesicle traffic with transmembrane ion transport (Honsbein et al., 2009; Grefen et al., 2010). Intriguingly, R-SNARE VAMP721, which is localized to the vesicle membrane before fusion, also binds and modulates the activity of the K⁺ channels, such as KC1 and KAT1 (Zhang et al., 2015). KC1 also binds another R-SNARE, SEC11, at the plasma membrane together with SYP121 which triggers the assembly of the secretory machinery for exocytosis (Waghmare et al., 2019).

Trafficking of nitrate transporters to the plasma membrane is not well described and characterized in the literature in the context of SNAREs and the secretory pathway. Nevertheless, nitrate uptake through NRT2.1 depends on interaction with NAR2 protein, which carries an N-terminal ‘secretory pathway signal’ (Orsel et al., 2006), and SYP122 exhibits increased phosphorylation after nitrate deprivation (Menz et al., 2016).

1.4.4. Transcriptional regulation

Many K^+ and NO_3^- transporter and channel genes are transcriptionally up-regulated under K^+ or NO_3^- deprivation respectively (Wang and Wu, 2013; Zhao et al., 2018a). *HAK5* is considered the most prominent gene induced by low K^+ (Gierth et al., 2005), and multiple transcription factors regulating *HAK5* expression have been described (Hong et al., 2013). K^+ deficiency also results in upregulation of *KEA5* (Shin and Schachtman, 2004), *CHX17* (Cellier et al., 2004), *NHX3* (Liu et al., 2010), or the downregulation of *SKOR*, or *AKT2* (Maathuis et al., 2003).

Transcriptional regulation of genes participating in the low-affinity transport of NO_3^- showed that *NRT1.1* and *NRT1.5* are induced by NO_3^- deprivation (Tsay et al., 1993; Lin et al., 2008), however, *NRT1.2* expression is not altered by this condition (Huang et al., 1999). The NRT2, high-affinity transport members are also responsive to NO_3^- deprivation conditions, *NRT2.1* and *NRT2.2* are induced under nitrate deficient conditions (Cerezo et al., 2001; Scheible et al., 2004), and the transcription factors NLP7, TGA1, bZIP1, and TCP20 have been described to regulate *NRT1.1*, *NRT2.1*, and *NRT2.2* transcription (O'Brien et al., 2016).

Complex transcriptional regulation cross-talk occurs in K^+ and NO_3^- transport (see section 1.5). K^+ deficiency induces the expression of K^+ transporter genes as a mechanism to enhance the K^+ uptake and translocation but also alters the transcription of NO_3^- transporter genes. Several high-affinity nitrate transporter genes are downregulated under K^+ deficient conditions including *NRT2.1*, *NRT2.3*, and *NRT2.6* (Armengaud et al., 2004; Armengaud et al., 2009) in Arabidopsis, in tomato (Zhao et al., 2018b), and in rice (Ma et al., 2012). Also NO_3^- deficiency alters the expression of K^+ transporters and channels as a compensatory response due to nutrient deficiency. For example, K^+ channels *AKT1* and *SKOR* involved in K^+ uptake and translocation to shoot, are downregulated under deficiency of nitrate in Arabidopsis (Ródenas et al., 2017), whereas the K^+ transporter *HAK5* is upregulated under nitrate deprivation (Rubio et al., 2014; Meng et al., 2016).

1.4.5. Calcium-regulated phosphorylation

Calcium-regulated proteins play a key role in the posttranslational phosphorylation process. They can be divided into three major groups: calcium-dependent protein kinases (CPK), CPK related protein kinases (CRK), and calcineurin-B like proteins (CBL). CBLs differ from the other two groups because they are Ca^{2+} sensor proteins without kinase activity. However, Ca^{2+} -bound and -

activated CBLs interact with a group of kinases called CBL-interacting protein kinases (CIPK), thereby enhancing CIPK autophosphorylation and recruitment to their target proteins (Batistič and Kudla, 2009). In *A. thaliana*, 10 members of CBLs and 26 members of CIPKs constitute a diverse and specific interacting network for the plant Ca^{2+} signaling system, regulating genes and ion channels with a unique expression and subcellular localization (Saito and Uozumi, 2020).

The main K^+ uptake systems, AKT1 and HAK5 are regulated positively by CIPK23 and CBL1 and CBL9 (Ragel et al., 2015; Sánchez-Barrena et al., 2020) (**Figure 4**). HAK5 activation produced an increase in the affinity of K^+ transport, ensuring the entry of K^+ into the cell (Nieves-Cordones et al., 2014; Ragel et al., 2015), and phosphorylation of AKT1 results in channel activation that maximizes K^+ influx (Geiger et al., 2009). CIPK9, most likely paired with CBL2 or CBL3, also regulates K^+ homeostasis under low K^+ conditions via phosphorylation of a yet unknown target (Pandey et al., 2007). Another CBL member, CBL10, is capable of CIPK-independent negative regulation of AKT1 activity, suggesting a role in maintaining the balance of K^+ uptake (Liu et al., 2013).

The CIPK23/CBL1-9 module not only phosphorylates and activates K^+ uptake systems but also mediates high and low-affinity transition of the nitrate transporter and sensor NRT1.1 (Ho et al., 2009; Lérán et al., 2015). NRT1.1 is a unique transporter switching between low-affinity to high-affinity by dimerization, which is controlled by phosphorylation of Thr¹⁰¹ by CBL1/9-CIPK23 (Sun et al., 2014). The CBL1/9-CIPK23 complex also is capable of eliciting anion efflux through SLAC1 and SLAH3 (Maierhofer et al., 2014) and CBL5-CIPK11 can also activate SLAC1 (Saito et al., 2018). CIPK8 plays a role in the nitrate response by influencing the expression level of several nitrate-responsive genes including NRT1.1 and NRT2.1 (Hu et al., 2009), and CBL7 was shown to regulate the expression levels of NRT2.4 and NRT2.5 (Ma et al., 2015).

GORK is involved in stomatal closure, either directly or indirectly, and is activated by CPK21 (van Kleeff et al., 2018), CPK33 (Corratgé-Faillie et al., 2017) and CBL1-CIPK5 (Förster et al., 2019). In addition, Ca^{2+} also triggers the attenuation of stomatal opening. CPK13 controls the K^+ influx of the K^+ channels KAT1 and KAT2 (Ronzier et al., 2014). Additionally, CBL2/3 and CIPK9/17 were reported to regulate stomatal movement via control of vacuolar morphology (Song et al., 2018), possibly achieved by phosphorylation of the vacuolar localized transporters like K^+/H^+ antiporter NHX (Barragán et al., 2012) and the K^+ channel TPK1 (Gobert et al., 2007).

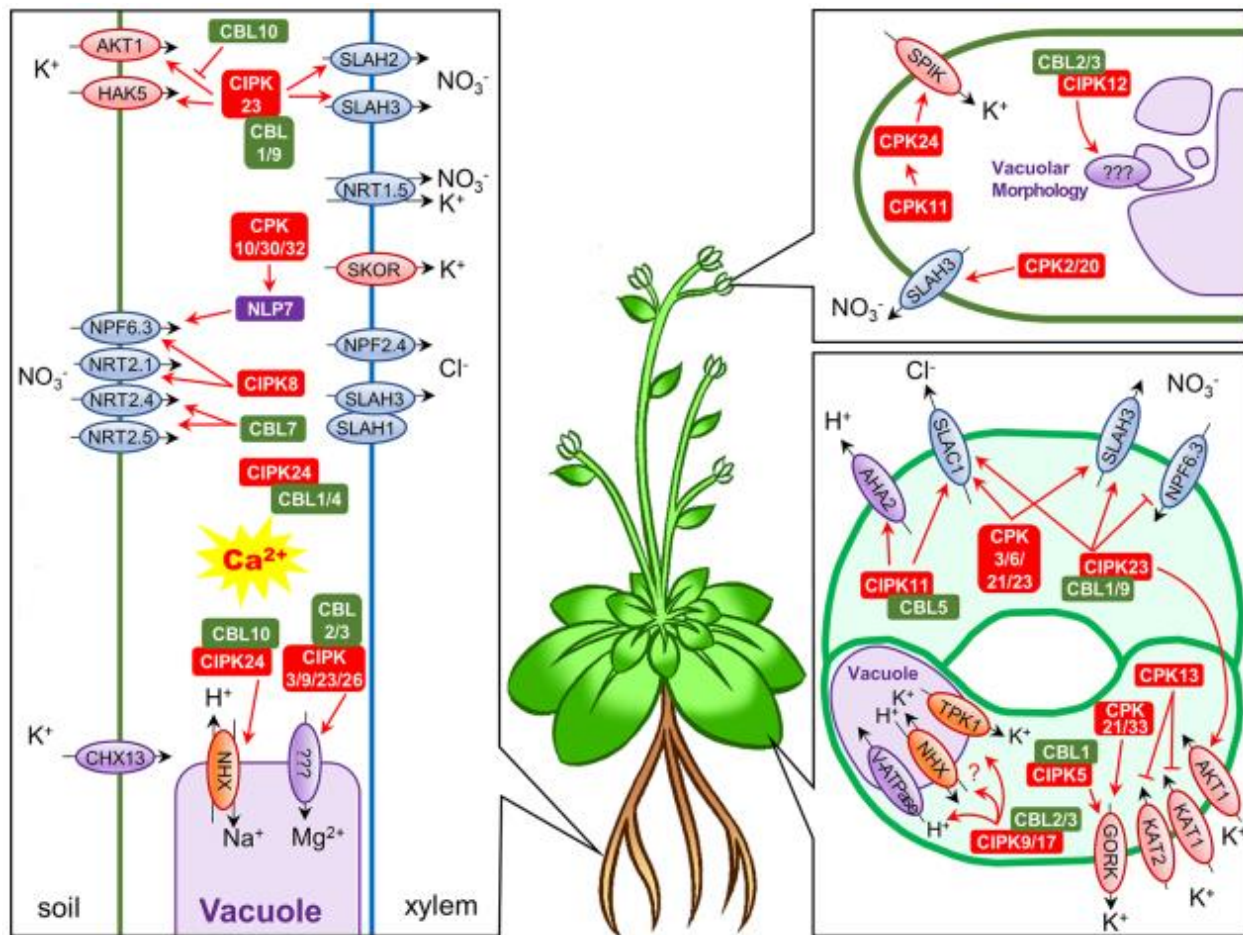


Figure 4: Calcium-regulated phosphorylation of K^+ and NO_3^- transport systems in *Arabidopsis thaliana*. Schematic representation of Ca^{2+} regulated K^+ and NO_3^- uptake in roots and translocation to shoots and flowers by diverse CBL/CIPK complexes. Adapted from Saito and Uozumi, 2020.

1.5. Crosstalk between K^+ and NO_3^- transport in *Arabidopsis thaliana*: The K^+/NO_3^- - H^+ antiporter NRT1.5

Regulation of K^+ transport has a close relationship with the NO_3^- transport at both transcriptional and posttranslational levels to coordinate the optimal growth and development of higher plants. The importance of co-regulate the K^+ and NO_3^- uptake and translocation in plants are required to maintain the balance of K^+ and NO_3^- within the plant (Engels and Marschner, 1993; Zhang et al., 2010; Ródenas et al., 2017).

NRT1.5, a member of the nitrate transporter1 family (NRT1) has been characterized as an exceptional example to observe the complex interconnection between nitrate and potassium transport in plants. NRT1.5 was described as a proton-coupled, low-affinity nitrate transporter involved in long-distance NO_3^- transport in *Arabidopsis thaliana* (Lin et al., 2008). NTR1.5 is expressed in root pericycle cells close to the xylem vessels and localizes to the plasma membrane, suggesting the involvement in xylem loading with nitrate. The expression of *NRT1.5* is dependent on nitrate and potassium availability. Under low nitrate nutrition, in *nrt1.5* mutants the root-to-shoot potassium transport is reduced, suggesting a regulatory loop at the level of xylem transport that maintains the balance between nitrate and potassium (Drechsler et al., 2015). A direct link of NRT1.5 to NO_3^- and K^+ homeostasis is supported by several observations. (1) Both NRT1.5 and the K^+ transporter SKOR contribute to K^+ translocation from root to shoot, with SKOR activity dominating under high NO_3^- and low K^+ supply, and NRT1.5 under low NO_3^- availability (Drechsler et al., 2015). (2) NRT1.5 was reported to perceive nitrate starvation-derived signals to prevent leaf senescence by facilitating foliar potassium accumulation (Meng et al., 2016). This might explain why the *NRT1.5* expression is highly upregulated during leaf senescence (Van Der Graaff et al., 2006). (3) Lateral root formation depends on *NRT1.5* under the deprivation of K^+ and low supply of NO_3^- (Zheng et al., 2016). (4) NRT1.5 functions as a proton-coupled H^+/K^+ antiporter loading K^+ to the xylem sap, whereas the proton gradient can promote NRT1.5-mediated K^+ release out the root parenchyma cells and facilitate K^+ loading into the xylem (Li et al., 2017a). (5) Although previous studies have shown that *NRT1.5* gene expression is influenced by changes in K^+/NO_3^- levels (Lin et al., 2008; Chen et al., 2012; Drechsler et al., 2015; Meng et al., 2016; Li et al., 2017a), the mechanistic basis of this gene expression regulation is not well characterized yet. The transcription factor MYB59 was the first and only one genetic component identified to positively regulate *NRT1.5*. MYB59 regulates K^+ and NO_3^- transport in response to low K^+/NO_3^- conditions by activating *NRT1.5* transcription (Du et al., 2019).

Other nutrients or toxic components have been reported to be linked to NRT1.5 besides nitrate and potassium. For example, NRT1.5 has been described as an important component in the regulation and modulation of phosphate deficiency responses in *Arabidopsis* (Cui et al., 2019) or together with proton pumps and ABA, NRT1.5 is involved in mechanisms to enhance the tolerance to cadmium in *Arabidopsis* (Wang et al., 2018). The toxicity by graphene oxide in plants reduced the expression of *NRT1.5* and other NRT1 family members, influencing the NO_3^- uptake rate, leading to adverse nitrate accumulation in stressed plants (Weng et al., 2020). Moreover, NRT1.5 was

identified as an indole-3-butyric acid (a precursor of the major auxin, IAA) transporter involved in root gravitropism (Watanabe et al., 2020).

1.6. Aim of the thesis

The diverse substrate specificities and the involvement of NRT1.5 in different ion networks could indicate physical and regulatory interaction between NRT1.5 and other nutrition-associated proteins. Preliminary data from this group identified some putative interaction partners of NRT1.5 by the split ubiquitin system in yeast (Drechsler, 2016) and the bimolecular fluorescent complementation assay (Zheng, 2018). Post-translational regulation of proteins is an essential mechanism controlling K^+ and NO_3^- homeostasis in plants, so the NRT1.5 interaction partners selected in this study are correlated with this regulation mechanism. The aim of my PhD thesis was the elucidation of molecular and physiological interactions of the AtNRT1.5 with novel proteins to comprehend the diverse functions of NRT1.5. The understanding of how they interact at a biological level and their role in the regulatory network of ion homeostasis in *Arabidopsis thaliana* was studied by different approaches. (1) Protein-protein interaction analysis by bimolecular complementation assays in *Nicotiana benthamiana* plants and the split ubiquitin system in *Saccharomyces cerevisiae*. (2) Genetic interaction studies using T-DNA knockout and knockdown mutants, complementation lines, and overexpression lines in *A. thaliana*. (3) Functional analysis and subcellular localization of plant proteins in *S. cerevisiae*. (4) Identification of protein binding sites by the introduction of mutations and the presence of protein-protein interaction was checked by the split ubiquitin system and bimolecular complementation assays. (5) Protein localization and promoter expression patterns using reporter genes like GFP or RFP (green or red fluorescent proteins) and GUS (β -glucuronidase) respectively in *A. thaliana*.

2. Material and methods

2.1. Materials

2.1.1. Enzymes and Kits

All restriction enzymes used in this study were purchased from company Thermo Fisher Scientific (Waltham, USA) or New England Biolabs (Frankfurt am Main, Germany). Without special indications, self-made Taq DNA polymerase was applied to all regular PCR reactions. Preparation of self-made Taq DNA polymerase was according to Desai and Pfaffle, 1995. The high fidelity DNA polymerases used for the high-proof amplification of DNA for cloning purpose were the Hybrid DNA polymerase (Roboklon) and Q5-DNA Polymerase (New England Biolabs).

The Molecular DNA marker to estimate DNA fragment sizes in agarose gels was the 2-log DNA ladder (0.1-10kb) from New England Biolabs.

All commercial kits used in this study were: NucleoSpin gel and PCR clean-up (MACHEREY NAGEL), Plasmid miniprep kit (Nippon Genetics), Power SYBR green PCR master mix (Thermo Fisher Scientific), Q5-site-directed mutagenesis kit (New England Biolabs) and NEBuilder HiFi DNA Assembly (New England Biolabs).

2.1.2. Oligonucleotides

All oligonucleotides were synthesized by Eurogentec Deutschland GmbH. Oligonucleotides for qRT-PCR are listed in Table 4, for genotyping PCR and RT-PCR are listed in Table 5 and for cloning are listed in Table 6.

Table 4: Oligonucleotides used for qRT-PCR. Without special indications, the sequences of the qRT-PCR oligonucleotides were generated by the Quantprime tool (Arvidsson et al., 2008). The amplicon lengths were between 60-200bp. F and R represent forward and reverse primers, respectively.

Gene name	Gene ID	Sequence (3' - 5')	Reference
<i>ACT2</i>	At3g18780	F: CTTCCTCAGCACATTCCAG R: AACATTGCAAAGAGTTTCAAGGT	Quantprime
<i>GAPC2 5'</i>	At1g13440	F: AAAGTTGTCGCTCAATGCAATC R: CGAAACCGTTGATTCCGATTC	(Parlitz et al., 2011)
<i>GAPC2 3'</i>	At1g13440	F: TTGGTGACAACAGGTCAAGCA	(Parlitz et al., 2011)

<i>NRT1.5</i>	At1g32450	R: AAACCTTGTCGCTCAATGCAATC F: TTGCTGGCATCGTCATTCTTCTG R: AGCACCAAGTTCACTCCAACTCC	(Drechsler et al., 2015)
<i>AHA2</i>	At4g30190	F: AGAAGAGCTGAGATCGCTAGGC R: TGTCCAAGCCCTTTAGCTTCACG	Quantprime
<i>CBL3</i>	At4g26570	F: TTGTTTGCAGACCGGGTATTTCG R: TGGGAGCATTTGGATGAAAGACAG	Quantprime
<i>PEP12</i>	At5g16830	F: TTGTCGATGACATCAGCTCTAACC R: TTGTCGATGACATCAGCTCTAACC	Quantprime
<i>SLAH1</i>	At1g62280	F: ATCTTCATGTCCCTGGTCTGTAGG R: AGAACCGACCGGATCTTTCACC	Quantprime
<i>SLAH3</i>	At5g24030	F: CCATGCCTGTGGACCGTTACTATG R: ACGATCTCTTCTTGAGGCCGTAGG	Quantprime
<i>VAMP722</i>	At2g33120	F: TCGTGGTACCGTTATCCTCGTTG R: GCACTGAGCAGCGATTGATGTG	Quantprime
<i>HAK5</i>	At4g13420	F: GGCAGGCTGCGTACCTAACTAAAC R: TGTTGGCCAGTATAACGGATCAGG	Quantprime
<i>AKT1</i>	At2g26650	F: TGCTTCGTCTTTGGCGTCTTCG R: AGTTGCGGTCTTTCTCTAGTCGG	Quantprime
<i>NHX1</i>	At5g27150	F: AAGAGCAGCGTTCGTCTTTCCG R: ACCAGACCACCAAATCACAACCTG	Quantprime
<i>TPK1</i>	At1g02880	F: ATGAAGATGGAGTTGTTGGAGCTG R: GTCGTGAGAGTTCCTGATTCATCG	Quantprime
<i>NRT1.1</i>	At1g12110	F: GCCACACACTGAACAATTCCGTTTC R: ATTCGAGGTAACCTCCCGCTTCC	Quantprime
<i>NRT1.2</i>	At1g69850	F: AAGGTTCTTCTTGCGGCTTCGG R: CTCGCAACCGCATTGCTTGAAC	Quantprime
<i>SKOR</i>	At3g02850	F: AGCTGGAGGTGACCCGAATAAG R: TCTAGAGGCTGCAAGATGCAAAGG	Quantprime
<i>UBQ10</i>	At4g05320	F: GGCCTTGATAATCCCTGATGAATAAG R: AAAGAGATAACAGGAACGGAAACATA	(Parlitz et al., 2011)
Oligo(dt) ₁₈	-	TTTTTTTTTTTTTTTTTTTT	-
<i>NRT1.8</i>	At4g21680	F: GGCTTCAGATTCTTGGATAG R: AACCCACAGAGTAGAGGATGG	(Li et al., 2010)

<i>NRT1.4</i>	At2g26690	F: ATCACTGCCGCTCTCATTCTTGGG R: TGTTGGCAGAGGTTGAACTTGGG	Quantprime
<i>CIPK23</i>	At1g30270	F: GCTCTACCTCAGCAAGTTCGAGAG R: CAAGACCACAAATCAGCCTTCGC	Quantprime
<i>AHA1</i>	At2g18960	F: GCCAGCTTGTTTGACAACAGGAC R: TTTGGCTGCAGACCGTGCAATG	Quantprime
<i>AHA3</i>	At5g57350	F: CCGTTACATACTAGCCGGAACAGC R: TTGCTTAGTGGTAAACGCAGTCC	Quantprime
<i>AHA4</i>	At3g47950	F: GGAGAGCTGAAATTGCTAGGTTGC R: ACCCAACTGAAATCAGCTTGCAC	Quantprime
<i>AHA5</i>	At2g24520	F: AAGCCAGGCTCTCATCTTCGTC R: ACTGCTATAAATGTCGCCACCAG	Quantprime
<i>AHA6</i>	At2g07560	F: GAAACGTGCAGAAGTTGCTAGGC R: TACCGACTCAACGTGGCCTTTG	Quantprime
<i>AHA7</i>	At3g60330	F: CAGCCAAGCGTTGATCTTCGTG R: CCGATATCACCGATGCAACCAG	Quantprime
<i>AHA8</i>	At3g42640	F: TGGCGACTGAATTCTCGTGGGATG R: TTCTTCCACAGGGATCCGCTCAAG	Quantprime
<i>AHA9</i>	At1g80660	F: TGTTGAACGTCCTGGCTTCTGG R: ACCGCAATCAAAGTAGCAATCAGC	Quantprime
<i>AHA10</i>	At1g17260	F: TGCCTTCATTCTTGCTCAACTTGC R: AGCAAAGCTGATGTTGGCATAAC	Quantprime
<i>AHA11</i>	At5g62670	F: CATTGGCGGTATCCCAATTGCC R: CCTCTTGGTTATTGCTCCCTGCTG	Quantprime

Table 5: Oligonucleotides used for genotyping PCR and RT-PCR to check the transcript in T-DNA insertion lines. Primers sequences for genotyping PCR to identify mutants were obtained from T-DNA primer design web (<http://signal.salk.edu/tdnaprimers.2.html>). LP and RP means left and reverse genomic primers. LB means left T-DNA border primer. F and R represent forward and reverse primers, respectively.

Primer name	Sequences (3' 5')
GAPC	F: GCAGCTCACTTGAAGGTTTG R: GACTTCGTTGGCGACAACAGG
LB_Gabi	CCATTTGGACGTGAATGTAGACAC
LBb1.3	ATTTTGCCGATTTTCGGAAC

LB1	GCCTTTTCAGAAATGGATAAATAGCCTTGCTTCC
LP_NRT1.5	CTCGAAGATTGCGTTTTTCAG
RP_NRT1.5	CCCGATGAGTGAGTATTGTGG
LP_AHA2	TGACAAAACCGGGACACTAAC
RP_AHA2	ATCACCACCTTTGCAATGAAC
LP_CBL3	GCCAACAAACAAAATAAATTTGG
RP_CBL3	GGAGCATAACATGCTTGAAACC
LP_PEP12	TGGCAAAAGATTTCCAATCAG
RP_PEP12	TGCTTAGACCAAGACAACGATG
LP_SLAH1	CGATATGAATTTCTTGCCTCG
RP_SLAH1	TCAGCAAATATGCACCATGAC
LP_SLAH3	AAAGCGGTAATGGTGATGATG
RP_SLAH3	GGTCGGTAGCCTTTGGTAGAG
LP_VAMP722	GATCTACAGTTTCGTGCTCG
RP_VAMP722	CTTCTCACCACGGTCAAGAA
LP_PHO1	GACGAGCTCTACCGTTGAAACGTTTTTTG
RT- NTR1.5	F: GGTCGCTGCAACGAAGAAATC R: CAAAGCGACGCTAAGGATGTC
RT- AHA2	F: TGGTTGGGATGCTTGCTGAT R: AGAGCAGGGGCATCATTGAC
RT-CBL3	F: TCGCAGTGCATAGACGGTTT R: GGTATCTTCCACCTGCGAGT
RT-PEP12	F: AGTTTCCAAGATCTCGAAGC R: CCAAGACAACGATGATGACA
RT-SLAH1	F: CCAGTGGTTCACAACGGAGA R: CCACCACGCGACATTGAATC
RT-SLAH3	F: GGCACCAAACCGGAATAACC R: CTCGTTGGTCGGTAGCCTTT
RT-VAMP722	F: AAGGGTTTGATTTTTCTTCTTCAA R: TCTCATCAACAGACCAAAGAAA

Table 6: Oligonucleotides used for conventional cloning, Gateway cloning, Gibson cloning and Q5 site mutagenesis. Restriction enzyme sites, Gateway and Gibson complementation attachment sites (highlighted and italic nucleotides) were integrated into the forward (F) and reverse (R) oligonucleotide sequences for amplification of coding DNA sequences (CDS).

Gene/Protein ID	Amplification	Sequence (3' 5')
Mutagenesis of <i>NRT1.5</i> and <i>AHA2</i>		
At4g30190 ¹	<i>AHA2</i> ^{D684V}	F:GATTGTCATGATGGTACCGACGTTAAGAATGGCAATGAT R: ATCATTGCCATTCTTAACGTCGGTACCATCATGACAATC
At4g30190	<i>AHA2</i> ^{AHYTV}	F: CAAGAAAGCTGGGTTCTAACTGGGAGTTTCAATGTCC R: GACATTGAAACTCCCAGTTAGAACCCAGCTTTCTTGT
At1g32450	<i>NRT1.5</i> ^{G209E}	F: GTGTTGAAAAGAGCGATTTCGAGGTTTAAAGCAAGGT R: GTGTTGAAAAGAGCGATTTCGAGGTTTAAAGCAAGGT
Yeast complementation constructs		
At4g30190	<i>AHA2</i> (BamHI/HindIII)	F: cgggatccATGTCGAGTCTCGAAGATATCAAG R: cccaagcttCTACACAGTGTAGTGACTGGGAG
At4g26570	<i>CBL3</i> (BamHI/PstI)	F: cgggatccATGTCGCAGTGCATAGACGGTTTC R: aactgcagTCAGGTATCTTCCACCTGCGAGTGG
At1g30270	<i>CIPK23</i> (BamHI/HindIII)	F: cgggatccATGGCTTCTCGAACAACGCCTTCACG R: cccaagcttTTATGTCGACTGTTTTGCAATTGTC
At5g16830	<i>PEP12</i> (PstI/HindIII)	F: gactagtATGAGTTTCCAAGATCTCGAAGCTG R: cccaagcttTTAGACCAAGACAACGATGATGAC
At1g62280	<i>SLAH1</i> (BamHI/PstI)	F: cgggatccATGGAAATTCCGAGGCAAGAAATT R: aactgcagCTAGTTTTGGTTAGTCGCATTGAG
At5g24030	<i>SLAH3</i> (SpeI/BamHI)	F: gactagtATGGAGGAGAAACCAAACCTATGTG R: cgggatccTTATGATGAATCACTCTCTTGAGT
At2g33120	<i>VAMP722</i> (BamHI/PstI)	F: cgggatccATGGCTTCTCGAACAACGCCTTCACG R: cccaagcttTTATGTCGACTGTTTTGCAATTGTC
PHO1p::<i>NRT1.5.e</i> GFP constructs		
p42212 ²	<i>eGFP</i> (PstI/PstI)	F: aaggattctaaagtctgcagATGGTGAGCAAGGGCGAG R: atacgaacgaaagctctgcagTACTTGTACAGCTCGTCCATG
Localization of <i>NRT1.5</i> and <i>AHA2</i>		
p42212 ²	<i>eGFP</i> (BamHI/HindIII)	F: cgggatccATGGTGAGCAAGGGCGAGGA R: cccaagcttTACTTGTACAGCTCGTCCA
At1g32450	<i>NRT1.5</i> (BamHI)	F: cgggatccATGTCTTGCCTAGAGATTA

2H5Q ³	mCherry (SpeI/HindIII)	F: <i>ccgactagt</i> GTGAGCAAGGGCGAGGAG R: <i>cccaagctt</i> TTACTTGTACAGCTCGTCCA
At4g30190	<i>AHA2</i> (BamHI/SpeI)	F: <i>cgggatcc</i> ATGTCGAGTCTCGAAGATATCA R: <i>ccgactagt</i> CACAGTGTAGTACTGGGAGT
Bimolecular complementation		
At1g30270	CIPK23 (attP2/attP3)	F:GGGGACAACCTTTGTATAATAAAGTTGGTATGGCTTCTCG AACAACG R:GGGGACCACTTTGTACAAGAAAGCTGGGTTTTATGTCTGA CTGTTTTGC

¹ ID gene number by TAIR10 (Arabidopsis.org). AtXgYYYYY structure means: At =organism. X= chromosome number 1,2,3,4,5. g= gene. Y=gene ID. ² ID gene number by Uniprot (<https://www.uniprot.org>). ³ ID protein number by PDB (protein data base).

2.1.3. Plasmids

All plasmids used in this work, acquired commercially or obtained from other studies are listed in Table 7.

Table 7: Plasmids acquired commercially or obtained by collaborations used in this work. Respective selection markers in bacteria (B), Plants (P) and Yeasts (Y) were abbreviated as following: Spec^R - spectinomycin resistance, Kan^R - kanamycin resistance, Amp^R - ampicillin resistance, Cam^R - chloramphenicol resistance, Leu^A - leucine auxotrophic marker, Trp^A - tryptophan auxotrophic marker, Ura^A - uracil auxotrophic marker, His^A - histidine auxotrophic marker and Ade^A - adenine auxotrophic marker.

Plasmid	Selective marker	Description	Reference
Yeast complementation			
p424	Amp ^R (B), Trp ^A (Y)	p42x are yeast expression vectors with <i>TEF</i> promoter	(Mumberg et al., 1995)
p425	Amp ^R (B), Ura ^A (Y)		
p426	Amp ^R (B), Leu ^A (Y)		
p425-SKOR	Amp ^R (B), Ura ^A (Y)	p425 vector with <i>SKOR</i>	(Drechsler et al., 2015)
p426-NRT1.5	Amp ^R (B), Leu ^A (Y)	p426 vector with <i>NRT1.5</i>	(Drechsler et al., 2015)
pDONR222	Kan ^R (B)	Gateway donor vector	Thermo Fisher Scientific
pDONR222-NRT1.5	Kan ^R (B)	Gateway donor vector with <i>NRT1.5</i>	(Drechsler, 2016)

pDONR222-AHA2 Split ubiquitin system	Kan ^R (B)	Gateway donor vector with <i>AHA2</i>	(Drechsler, 2016)
pBT3N-NRT1.5	Kan ^R (B), Leu ^A (Y)	Yeast expression vector with Cub- <i>NRT1.5</i> fusion	(Drechsler, 2016)
pBT3N-NRT1.8	Kan ^R (B), Leu ^A (Y)	Yeast expression vector with Cub- <i>NRT1.8</i> fusion	(Drechsler, 2016)
pBT3N-NRT1.10	Kan ^R (B), Leu ^A (Y)	Yeast expression vector with Cub- <i>NRT1.10</i> fusion	(Drechsler, 2016)
pNub-X-HA	Amp ^R (B), Trp ^A (Y)	Yeast gateway expression destination vector	ABRC stock #CD3-1739
pNub-AHA2	Amp ^R (B), Trp ^A (Y)	Yeast gateway expression destination vector with <i>AHA2</i>	(Drechsler, 2016)
BiFC2in1 assay			
pBiFC-2in1 NN	Spec ^R (B) Kan ^R (P)	pBiFC-2in1 destination vector with split <i>nYFP</i> and <i>cYFP</i>	(Grefen and Blatt, 2012)
pBiFC-2in1 NRT1.5/AHA2	Spec ^R (B) Kan ^R (B)	pBiFC-2in1 with split <i>nYFP AHA2</i> and <i>cYFP NRT1.5</i>	(Zheng, 2018)
pBiFC-2in1 NRT1.5/CBL3	Spec ^R (B) Kan ^R (B)	pBiFC-2in1 with split <i>nYFP CBL3</i> and <i>cYFP NRT1.5</i>	Yue Zheng (Freie Universität Berlin, DE)
pBiFC-2in1 NRT1.5/PEP12	Spec ^R (B) Kan ^R (B)	pBiFC-2in1 with split <i>nYFP PEP12</i> and <i>cYFP NRT1.5</i>	Yue Zheng (Freie Universität Berlin, DE)
pBiFC-2in1 NRT1.5/SLAH1	Spec ^R (B) Kan ^R (B)	pBiFC-2in1 with split <i>nYFP SLAH1</i> and <i>cYFP NRT1.5</i>	(Zheng, 2018)
pBiFC-2in1 NRT1.5/SLAH3	Spec ^R (B) Kan ^R (B)	pBiFC-2in1 with split <i>nYFP SLAH3</i> and <i>cYFP NRT1.5</i>	(Zheng, 2018)
pBiFC-2in1 NRT1.5/VAMP722	Spec ^R (B) Kan ^R (B)	pBiFC-2in1 with split <i>nYFP VAMP722</i> and <i>cYFP NRT1.5</i>	Yue Zheng (Freie Universität Berlin, DE)
pDONR221 p3-p2	Spec ^R (B) Kan ^R (B)	Gateway donor vector	Thermo Fisher Scientific
pDONR221 p3-p2 AHA2	Kan ^R (B)	Gateway donor vector with <i>AHA2</i>	(Zheng, 2018)
pDONR221 p1-p4 NRT1.5	Kan ^R (B)	Gateway donor vector with <i>NRT1.5</i>	(Drechsler, 2016)

Localization of NRT1.5 and AHA2	Kan ^R (B)	Binary vector with mCherry	My-Linh Du (Freie Universität Berlin, DE) (Herbst, 2019)
	pCAMBIA-mCherry	Donor vector with 35S promoter	
Complementation constructs	Cam ^R (B)	Binary T-DNA vector with 35Sp:: <i>NRT.5</i> and <i>eGFP</i>	(Drechsler et al., 2015)
	pGTkan3-35S:NRT1.5eGFP		
	pTkan ⁺ -PHO1:: <i>NRT1.5</i>	T-DNA vector with <i>NRT1.5</i>	(Drechsler et al., 2015)

2.1.4. Bacteria and yeast strains

Escherichia coli, *Agrobacterium tumefaciens* and *Saccharomyces cerevisiae* strains used in this work are listed and described in Table 8.

Table 8: Description of all bacteria and yeast strains used in this work.

Strain	Genotype	Description	Reference
<i>A. tumefaciens</i> GV3101::pMP90	Rifampicin and gentamycin resistant	Transformation of <i>N. benthamiana</i> or <i>A. thaliana</i>	(Koncz and Schell, 1986)
<i>E. coli</i> DH10β	<i>F</i> ⁻ <i>mcrA</i> Δ(<i>mrr-hsdRMS-mcrBC</i>) Φ80 <i>lacZ</i> Δ <i>M15</i> Δ <i>lacX74</i> <i>recA1</i> <i>endA1</i> <i>araD139</i> Δ(<i>ara,leu</i>)7697 <i>galU</i> <i>galK</i> <i>rpsL</i> <i>nupG</i> λ-	Homemade cells (Transformation efficiency ≈ 108 cfu/mg)	(Desai and Pfaffle, 1995)
NEB 5-α (DH5α)	<i>F</i> ⁻ φ80 <i>lacZ</i> Δ <i>M15</i> Δ(<i>lacZYA-argF</i>) <i>U169</i> <i>recA1</i> <i>endA1</i> <i>hsdR17</i> (<i>r_K⁻</i> , <i>m_K⁺</i>) <i>phoA</i> <i>supE44</i> λ ⁻ <i>thi-1</i> <i>gyrA96</i> <i>relA1</i>	Commercial high-efficiency strain	New England Biolabs
<i>S. cerevisiae</i>			

BY4741	<i>MATa, his3Δ1, leu2Δ, met15Δ, ura3Δ</i>	Wild type strain	(Brachmann et al., 1998)
BYT12	BY4741 <i>trk1Δ::loxP trk2Δ::loxP</i>	Lack the main K ⁺ uptake systems (<i>trk1, trk2</i>)	(Petrezselyova et al., 2010)
BYT45	BY4741 <i>nha1Δ::loxP ena1-5Δ::kanMX</i>	Lack the main K ⁺ efflux systems (<i>nha1, ena1</i>)	(Zahrádka and Sychrová, 2012)
THY.AP4	<i>MATa ura3 leu2 his3 trp1 ade2 lexA::lacZ lexA::HIS3 lexA::ADE2</i>	Mating based split-ubiquitin assays	(Obrdiik et al., 2004)

2.1.5. Plant material

In this work, *Arabidopsis thaliana* wild type plants are the ecotype Columbia-0 (Col-0) since all mutants have the Col-0 genetic background. The T-DNA insertion lines and the overexpression lines used are listed in Table 9. All single T-DNA insertion lines were obtained from the Arabidopsis Biological Resource Center, overexpression lines were obtained from Drechsler, 2016; Zheng, 2018 and double mutants were generated through crossing of two homozygous single T-DNA insertion mutants.

Table 9: *Arabidopsis thaliana* lines used in this work.

Abbreviations: Kanamycin (Kan), Sulfadiazine (Sulfa), and BASTA herbicide (phosphinothricin).

Lines	Target gene	Description	Tolerance
GABI_347B03	<i>NRT1.5</i> (At1g32450)	<i>nrt1.5</i> T-DNA knockout (Drechsler, 2016)	Sulfa
GABI_219D04	<i>AHA2</i> (At4g30190)	<i>aha2</i> T-DNA knockout (Zheng, 2018)	Sulfa
GABI_956D04	<i>CBL3</i> (At4g26570)	<i>cbl3</i> T-DNA mutant	Sulfa
SAIL_580_C04	<i>PEP12</i> (At5g16830)	<i>pep12</i> T-DNA mutant	BASTA
SALK_039811c	<i>SLAH1</i> (At1g62280)	<i>slah1</i> T-DNA mutant	Kan
GABI_317G03	<i>SLAH3</i> (At5g24030)	<i>slah3</i> T-DNA mutant	Sulfa
SALK_103189C	<i>VAMP722</i> (At2g33120)	<i>vamp722</i> T-DNA mutant	Kan
GABI_756D01	<i>NRT1.8</i> (At4g21680)	<i>nrt1.8</i> T-DNA mutant (Zheng, 2018)	Sulfa
SALK_072700	<i>NRT1.10</i> (At5g62680)	<i>nrt1.10</i> T-DNA mutant	
<i>NRT1.5p::uidA</i>	<i>NRT1.5</i> (At1g32450)	<i>NRT1.5p::GUS</i> (Zheng et al., 2016)	Kan

<i>35S::eGFPSLAH1</i>	<i>SLAH1</i> (At1g62280)	<i>SLAH1</i> with <i>eGFP</i> under 35S promoter (Yue Zheng, AG Kunze)	BASTA
<i>35S::eGFPSLAH3</i>	<i>SLAH3</i> (At5g24030)	<i>SLAH3</i> with <i>eGFP</i> under 35S promoter (Yue Zheng, AG Kunze)	BASTA

2.1.6. Database and Software

All databases and software used in this work are listed in Table 10.

Table 10: Databases and software used in this work.

Name	Application	Reference
ABRC	Order Arabidopsis T-DNA insertion lines	http://abrc.osu.edu/
Aramemnon	Plant membrane protein database	(Schwacke et al., 2003)
CCTOP	Constrained consensus TOPology predictor	http://cctop.enzim.ttk.mta.hu/
eFP Browser	Visualization of gene expression data	http://bar.utoronto.ca/
Excel	Calculations and creation of plots	Microsoft corporation
Inkscape	Creation of figures and tables	https://inkscape.org/
Leica LAS AF	Confocal microscopy imaging	Leica Microsystems
LRRfinder	Identification of LRR motifs	http://lrrfinder.com/lrrfinder.php
NCBI	PubMed and BLASTs	https://ncbi.nlm.nih.gov/
PROMALS3D	Alignments for multiple protein sequences	http://prodata.swmed.edu
Quantprime	Design of qPCR primers	https://quantprime.mpimp-golm.mpg.de/
RADAR	Detection and alignment of repeats in protein sequences	https://ebi.ac.uk/Tools/pfa/radar/
SnapGene	Visualization of DNA sequences	GSL Biotech LLC, Chicago, US
SUBA4	Subcellular localization of proteins	https://suba.live/
TAIR10	<i>Arabidopsis thaliana</i> data base	https://arabidopsis.org/
Weblogo	Creation of sequence logos	https://weblogo.berkeley.edu/logo.cgi

2.1.7. Sequencing

DNA sequencing from plasmid DNA or PCR products was done by LGC Genomics GmbH Biotechnologie using the flexi run service. Approximately 100ng of DNA with respective primer added (20 μ M) in a total volume of 12 μ l was sent for sequencing.

2.1.8. Medium and selection

2.1.8.1. Medium for cultivating bacteria

Standard growth of *E. coli* or *A. tumefaciens* was in Lysogeny broth (LB) medium (70g/l). For solid medium, 1.2% agar was added before autoclaving. To select the recombinant cultures, the media were supplemented with the corresponding antibiotic stock solutions (**Table 11**) after autoclaving. *E. coli* was generally grown at 37°C and *A. tumefaciens* at 28°C.

Table 11: Antibiotics and other components added in LB medium for *E. coli* and *A. tumefaciens* growth.

Component in LB medium	Concentration
Antibiotics	
Ampicillin	100mg/ml
Chloramphenicol	34mg/ml
Gentamycin	25mg/ml
Kanamycin	50mg/ml
Rifampicin	50mg/ml
Spectinomycin	75mg/ml
Other components	
Acetosyringone	150 μ M
IPTG	0.1M
Silvet L-77	0.025% v/v
X-Gal	40 μ g/ml

2.1.8.2. Medium for cultivating *Saccharomyces cerevisiae*

The general growth of *S. cerevisiae* was carried out with yeast extract, peptone, dextrose and adenine (YPAD) liquid or solid medium (50g/l of YPAD broth and 70g/l of YPAD agar respectively) (Formedium) at 30°C. For the selection of recombinant yeast cells, the synthetic defined minimal media YNB (Yeast Nitrogen Base) was used supplemented with glucose, (NH₄)₂SO₄, and the indicated auxotrophic amino acids (**Table 12**). Additionally, an YNB media variation without potassium content (Austrian modification form Formedium #CYN7502) was used to evaluate yeast growth in the split ubiquitin system assay. To support the growth of BYT12 and BYT45 mutants, 0.1M or 1M KCl were added to YPAD or YNB medium. In the split-ubiquitin assay, to inhibit the autoactivation, 20mM 3-amino-1,2,4-triazole (3-AT, competitive inhibitor of the *HIS3* gene product) was additionally added to the YNB medium. The pH of media was adjusted with NaOH to around 5.5 and 5.8. To make solid medium, 2% agar was added before autoclaving.

Table 12: Minimal yeast medium composition.

Yeast medium	Composition
YNB minimal medium	6.9 g/l YNB ¹ , 20% w/v glucose and 0.05% w/v (NH ₄) ₂ SO ₄
YNB -Ura	YNB minimal medium with 0.77g/l CSM drop out (-Ura) ²
YNB -Leu	YNB minimal medium with 0.69g/l CSM drop out (-Leu) ²
YNB -Trp	YNB minimal medium with 0.64g/l CSM drop out (-Leu, -Trp) ² and 100mg/l L-leucine ³
YNB -Ura -Leu	YNB minimal medium with 0.67g/l CSM drop out (-Ura -Leu) ²
YNB -Leu -Trp	YNB minimal medium with 0.64g/l CSM drop out (-Leu, -Trp) ²
YNB -Ura -Leu -Trp	YNB minimal medium with 0.57g/l CSM drop out (-Ade -His -Leu -Trp -Ura -Met) ² , 20mg/l adeninsulfat ³ , 20mg/l L-histidine ³ , and 20 mg/l L-methionin.
YNB -Leu -Trp -His -Ade	YNB minimal medium with 0.59g/l CSM drop out (-Ade -His -Leu -Trp -Met) ² , and 20 mg/l L-methionin ³

¹ YNB, yeast nitrogen base medium without amino acids and without (NH₄)₂SO₄ (Formedium). ²

Complete supplement mixture (CSM) drop out (Formedium). ³ Amino acids filtered sterile (Formedium).

2.1.8.3. Medium for cultivating *Arabidopsis thaliana*

For *in vitro* assays, *A. thaliana* seeds were surface sterilized and stratified in darkness for 2 days at 4°C. The surface sterilization was performed with 70% v/v EtOH for 2 min, followed by 10% v/v NaClO and 1% w/v SDS for 3min, and then followed by 3 times 3 minute washing in sterile deionized water. Pre-germination was carried out in commercial 1/2MS (Murashige-Skoog medium) plates (pH= 5.5) containing 1% w/v sucrose and 0.3% w/v gelrite in a growth chamber under long-day conditions (16h/8h light/dark, 22°C, light intensity of 120 μ mol m⁻² s⁻¹, relative humidity of 40%) for 5 days. Modified 1/2 MS plates were used to manipulate the concentrations of K⁺ and NO₃⁻, 0.6% w/v agarose, 1.5mM CaCl₂, 1mM MgSO₄, 0.5mM NaH₂PO₄, 0.05mM H₃BO₃, 0.05mM MnSO₄, 0.05mM FeNa-EDTA, 15 μ M ZnSO₄, 2.5 μ M KI, 0.5 μ M Na₂MoO₄, 0.05 μ M CuSO₄, 0.05 μ M CoCl₂, 0.5% MS vitamins, 0.5g/l MES, 1% w/v sucrose and pH 5.5 adjusted with NaOH. K⁺ and NO₃⁻ were added to the indicated concentrations with KCl and Ca(NO₃)₂, respectively. For soil assays plants were pre germinated in a 1:1 mixture of commercial type P soil and unfertilized type 0 soil in long day growth conditions. After 5 days, the seedlings were transferred to either the same soil as control or unfertilized type 0 soil (mixture 4:1 with sand) and supplemented with nutrient solutions as indicated in each case. Nutrient solutions are given in Table S1, and composition of commercial type P or 0 soils are described in Drechsler et al., 2015.

2.2. Methods

2.2.1. Transformation into bacteria, yeast and plants

2.2.1.1. Chemical transformation of *Escherichia coli*

50 μ l of chemical competent *E. coli* cells (stored at -80°C) were thawed on ice, followed by mixing with about 1-100ng of plasmid DNA. After 30min incubation on ice, cells were heat shocked at 42°C for 45s in water bath and immediately chilled on ice for 2min. 950 μ l of LB medium was added, then cell were incubated at 37°C for 1h by shaking at 220rpm. 200 μ l cell culture was plated in LB plates with corresponding antibiotics (**Table 11**), and the plates were inversely incubated at 37°C overnight.

2.2.1.2. Transformation of *Agrobacterium tumefaciens* by electroporation

50µl of electro competent *A. tumefaciens* cells (stored at -80°C) were thawed on ice, followed by mixing with 1ng plasmid DNA and incubated on ice for 10min. The mixture was then transferred to an electroporation cuvette followed by electroporation at 2.2 kV for 5ms. After that, the cells were immediately transferred with 950µl LB medium and then cultured at 28°C for 3h at 220 rpm. 20µl culture was plated on LB plates within required antibiotics (**Table 11**) and inversely incubated at 28°C for 2 days.

2.2.1.3. Chemical transformation of *Saccharomyces cerevisiae*

The *S. cerevisiae* transformation protocol is adapted from Ito et al., 1984. One single colony was inoculated in 10ml YPAD medium and was cultured overnight by shaking at 30°C, 220 rpm. After OD_{600nm} measurement, a second cell culture was generated in 50ml fresh YPAD medium to OD_{600nm}=0.2, followed by culturing to final OD_{600nm} to 0.8 by shaking at 30°C, 220 rpm.

Cell cultures were centrifuged at 3000g for 5min at room temperature. Cell pellets were resuspended in 25ml sterile deionized H₂O. The centrifugation was repeated at 3000g for 5min at room temperature. Supernatants were removed, and pellets were resuspended in 400µl of 0.1M LiAc. For transformation, 240µl 50% PEG4000, 36µl 1M LiAc, 50µl ssDNA (1µg/µl) and 1000ng of plasmid were added into 50µl competent cells, followed by vortex. Transformed competent cells were incubated at 30°C for 30 min and then 20min at 42°C. Cells were centrifuged 30s at 3300g. Pellet with the transformed cells was resuspended in 600µl sterile H₂O. 200µl cells were plated in YNB agar selective medium (**Table 12**) and followed by an inversely incubation at 30°C for 2 to 4 days.

2.2.1.4. *Agrobacterium tumefaciens*-mediated transformation of *Arabidopsis thaliana*

A. thaliana plants were transformed by the floral-dip method (Clough and Bent, 1998). 200ml recombinant *A. tumefaciens* 24h culture in low salt LB medium (10g/l tryptone, 2.5g/l NaCl and

5g/l yeast extract) with 150 μ M Acetosyringon was centrifuged at 5000rpm for 15min at room temperature. The pellet was resuspended in freshly prepared infiltration medium (MS with 150 μ M Acetosyringon, 0.025% Silwet L-77 v/v, and 5% sucrose w/v, pH 5.8) to OD_{600nm}= 0.8. 30-days old *Arabidopsis thaliana* plants with healthy flowers were dipped in medium with *A. tumefaciens* for about 90s. Infiltrated plants were placed in darkness and high humidity for 24-36h and then were put back to light condition in long day chambers and grew further for seed harvesting.

2.2.1.5. *Agrobacterium tumefaciens*-mediated transformation of *Nicotiana benthamiana*

For the transient expression of plant proteins in *N. benthamiana*, glycerol stocks of GV3101::pMP90 *Agrobacterium* transformed with the respective plasmid constructs were streaked in the LB plates with appropriate antibiotics and incubate at 28°C for 2 days. Then, single colonies of *Agrobacterium* from plates were inoculated in 5ml liquid LB medium with appropriate antibiotics and grown in a shaker at 28°C, 220rpm overnight. 2ml overnight culture was harvested by centrifugation at 4000g for 15min at room temperature. Pellet was washed two times with infiltration buffer (10mM MES, pH 5.6, 10mM MgCl₂ and 150 μ M Acetosyringone). Cells were all adjusted to OD_{600nm}=0.5. Subsequently, cultures were incubated for 2h at room temperature, and then cells were infiltrated into *N. benthamiana* leaves (8-week old plants) with a syringe.

2.2.2. Molecular biological methods

2.2.2.1. Classical cloning of constructs for yeast complementation

The full-length CDS of *NRT1.5*, *AHA2*, *CBL3*, *CIPK23*, *PEP12*, *SLAH1*, *SLAH3* and *VAMP722* were amplified with corresponding restriction enzyme attachment sites, the oligonucleotides listed in Table 6. cDNA from *Arabidopsis* root was used as PCR templates. The amplified gene products were then successively ligated into the yeast expression vectors p424TEF, p425TEF and p426TEF via the restriction sites mentioned in Table 6.

The NRT1.5^{G209E} mutant was generate using the Q5-site-directed mutagenesis kit (New England BioLabs). A guanine in position 626 of NRT1.5 full length DNA was replaced for an adenine, this

point mutation changed the codon GGA codifying to a glycine (G) in the codon GAA codifying to a glutamic acid (E). The mutation then is called NRT1.5^{G209E}. The primers used are listed in Table 6. The new vectors generated were p426-NRT1.5^{G209E}, p425-AHA2, p424-CBL3, p425-CIPK23, p425-PEP12, p424-SLAH1, p425-SLAH3 and p424-VAMP722.

2.2.2.2. Gibson cloning of constructs for plant complementation

The eGFP coding sequence lacking the initial ATG codon was amplified from the pGTkan3-35S:NRT1.5eGFP vector with overhands to be cloned by Gibson assembly into pTkan⁺-PHO1NRT1.5 vector. The stop codon TAA of *NRT1.5* was removed by PCR.

pTkan⁺-PHO1NRT1.5 vector was opened by restriction enzyme digestions with BamHI and PstI and ligated with eGFP fragment with the NEBuilder HiFi DNA assembly kit (New England Biolabs). pTkan⁺-PHO1NRT1.5^{G209E}eGFP vector was obtained from the previous Q5 site mutagenesis of pTkan⁺-PHO1NRT1.5eGFP vector. The primers used are listed in Table 6.

2.2.2.3. Gibson cloning of constructs for protein localization

The eGFP and mCherry coding sequence lacking the initial ATG codon was amplified from the pGTkan3-35S:NRT1.5eGFP and pCAMBIA-mCherry vectors respectively with overhangs to be cloned by Gibson assembly into p426 and p425 vectors respectively. The oligonucleotides used are listed in Table 6. The vectors p426, p426-NRT1.5, p426-NRT1.5^{G209E}, p425, and p425-AHA2 were digested and opened with BamHI and HindIII restriction enzymes. The ligation of vector and inserts were carried out by NEBuilder HiFi DNA assembly kit (New England Biolabs). The new vectors generated were p425-mCherry, p425-AHA2mCherry, p425-AHA2^{D684V}mCherry, p426-eGFP, p426-NRT1.5eGFP and p426-NRT1.5eGFP^{G209E}.

2.2.2.4. Gateway cloning of constructs for split-ubiquitin assay

The entry gateway vectors pDONR222-NRT1.5 and pDONR222-AHA2 were mutagenized with the Q5-site-directed mutagenesis kit (New England Biolabs) with the oligonucleotides listed in Table 6 to create the mutants: pDONR222-NRT1.5^{G209E}, pDONR222-AHA2^{D684V}, and

pDONR222-AHA2^{AHYTV}. N-terminal Nub-AHA2 mutants fusion were then generated by a LR reaction between pDONR222-AHA2^{D684V} or pDONR222-AHA2^{AHYTV} and the gateway-compatible yeast expression vector pNub-X-HA. C-terminal pBT3N-NRT1.5^{G209E} fusion were then generated by a LR reaction between the pDONR222-NRT1.5^{G209E} vector and the gateway-compatible yeast expression vector pBT3N-X.

2.2.2.5. Gateway cloning of constructs for the pBiFC-2in1 assay

The gateway entry vectors pDONR221p1-p4-NRT1.5 and pDONR221p2-p3-AHA2 were mutagenized with the Q5-site-directed mutagenesis kit (New England Biolabs) with the oligonucleotides listed in Table 6 to create the mutants: pDONR221p1-p4-NRT1.5^{G209E}, pDONR221p2-p3-AHA2^{D684V}, and pDONR221p2-p3-AHA2^{AHYTV}. Then pDONR221 p1-p4 NRT1.5 and pDONR221 p3-p2-AHA2 containing the different mutations were cloned into destination vector pBiFC-2in1-NN by LR reaction.

Full length of CIPK23 was amplified and cloned with the attachment sites attB2/attB3 into the Gateway vector pDONR221p2-p3 via BP reaction. The oligonucleotides used are listed in Table 6. Then the vector pDONR221p2-p3-CIPK23 with pDONR221p1-p2-NRT1.5 were cloned into destination vector pBiFC2in1 NN by LR reaction.

2.2.3. Genomic DNA isolation

Total genomic DNA from *Arabidopsis thaliana* plants was extracted from frozen plant material using 2% Cetrimonium bromide (CTAB) method (Chen and Ronald, 1999).

Frozen *Arabidopsis thaliana* tissue in liquid N₂ was ground, mixed and homogenized together with 2 metal balls by a mixer mill (Retsch MM 400). 600µl of 2% CTAB buffer (100mM Tris-Cl pH 8, 1.4M NaCl, 20mM EDTA and 2%CTAB w/v) was added to the ground material and mixed by vortex, followed by an incubation at 65°C for 20min. The tubes were inverted every 5min and were centrifuged at room temperature for 10min at 13000g. The supernatant was transferred together with one volume of chloroform:isoamyl alcohol (24:1) and mixed well by inverting, followed by centrifuging at 13500g for 5 min. The upper phase was then transferred and mixed together with one volume of isopropanol to precipitate the DNA, followed by incubating at 4°C for 10min.

Precipitated DNA was obtained by centrifuging at 13000g for 10min. Pellet was washed with 70% EtOH, followed by centrifuging at 13000g for 3min at room temperature. Pellet was air dried, resuspended in 200µl of H₂O with 20 µg/ml RNAasa and incubated at 50°C for 30min.

2.2.4. *Arabidopsis thaliana* RNA isolation

Total RNA from *Arabidopsis thaliana* seedlings, roots or shoots were extracted from frozen plant material using the citric acid extraction method (Oñate-Sánchez and Vicente-Carbajosa, 2008).

Frozen plant tissue in liquid N₂ was ground, mixed and homogenized together with 2 metal balls by a mixer mill (Retsch MM 400) for 40s. 600µl of cell lysis buffer (2% SDS, 68mM sodium citrate, 132mM citric acid and 1mM EDTA) was added and incubated for 2min at room temperature. 200µl of precipitation buffer (4M NaCl, 16mM sodium citrate and 32mM citric acid) was added on ice and well mixed by shaking, and then incubated for 10min. Samples were centrifuged for 10min 14000g at 4°C and the supernatant was mixed together with one volume of isopropanol for 30min on ice to precipitate the RNA. The pellet was obtained by centrifugation for 10min 14000g at 4°C and then washed with 70% EtOH. After air drying, the pellet was dissolved in 25µl RNAase free H₂O. Concentrations and purity of RNAs were analyzed by using Nanodrop ND-1000 spectrophotometer (Thermo Fisher Scientific).

2.2.5. cDNA synthesis

1U of DNase I (Thermo Fisher Scientific) digested for 1h at 37°C total genomic DNA from all different RNA samples. Then, for the cDNA synthesis, RNA samples were incubated with 100µmol of oligo(dt)₁₈ for 5min at 65°C, then 200U of RevertAid reverse transcriptase (Thermo Fisher Scientific) was used for a total 20µl cDNA synthesis reaction followed by 60min at 42 °C incubation and then 10min at 70°C. To examine whether cDNA has genomic DNA contamination, primers span the intron of glyceraldehyde-3-phosphate dehydrogenase C subunit 1 (*GAPCI*) were used to carry on a standard PCR (Oligonucleotide sequences in Table 4).

2.2.6. Quantitative real time PCR

The CFX connect real-time PCR detection system (Bio-Rad Laboratories) was used for qRT-PCR measurements. Each 5µl reaction mix contained 2.5µl SYBR green PCR master mix (Thermo Fisher Scientific), 0.5µl cDNA and 2µl forward and reverse primers mix (0.5µM each). The qRT-PCR procedure program is as follows: 95°C for 10 min, 95°C for 15 s, and 60°C for 60s (last 2 steps for 40 cycles). For the melting curve analysis the temperature increased from 65°C to 95°C within 30min. All qRT-PCR assays were performed with 3 biological replicates and 3 technical replicates. The cDNA ends integrity was checked by the expression of the housekeeping gene *GAPC2* (At1g13440, glyceraldehyde-3-phosphate dehydrogenase 2) at 3' and 5' ends as (Parlitz et al., 2011) reported. The expression values of the individual genes were normalized to the CT value of the reference gene *ACT2* (At3g18780.2) or *UBQ10* (At4g05320). All qRT-PCR oligonucleotides used are listed in Table 4.

2.2.7. Elemental analyses

The plant material was dried for 48h at 75°C, weighed into polytetrafluorethylene digestion tubes, and digested in HNO₃ under pressure using a microwave digester (Ultraclave 4, MLS GmbH). The concentrations of macro and microelements were determined by Inductively coupled plasma atomic emission spectroscopy (ICP-OES) using an iCAP 6500 Dual OES Spectrometer (Thermo Fischer Scientific) by a collaboration partnership with the group of Prof. Dr. Nicolaus von Wirén at the Leibniz institute of Plant Genetics and Crop Plant in Gatersleben, Germany.

2.2.8. Nitrate measurement

Nitrate was determined calorimetrically according to the protocol of Cataldo et al., 1975. 50mg of frozen and homogenized plant material (roots or shoots) was mixed with 1mL of deionized water and centrifuged for 5min at 4°C and 12000g, then 40mL of supernatant was mixed with 160mL of 1% w/v salicylic acid in concentrated sulfuric acid. For background measurement, 40mL of supernatant were mixed with 160mL of deionized water. After a 20min incubation on ice, 1.8mL

of cooled 4M NaOH was added and mixed carefully. When the samples reached room temperature, the Abs_{410nm} was determined with a microplate reader (BioTek), and the values were compared to a nitrate standard curve (0 - 8mM KNO_3).

2.2.9. Histochemical detection of GUS

Transgenic seedlings expressing GUS were incubated with GUS staining solution (0.1% X-Gluc, 0.1% Triton X-100, 50mM sodium phosphate buffer, pH 7.2) and was infiltrated under vacuum for 1min. After 16h incubation at 37°C, the staining solution was replaced by fixing solution (3:1 v/v of 100% ethanol, glacial acetic acid). The fixing solution was removed after 16h and decolorizing solution (100% ethanol) was added. The plant material was preserved in 70% ethanol and observed in a binocular.

2.2.10. Extracellular acidification assay

The extracellular acidification was assayed as described Haruta et al., 2010 with modifications. Five day-old seedlings were incubated in 200 μ l of modified 1/4 MS media (pH 5.5, unbuffered without MES) with 30 μ g/ml fluorescein isothiocyanate/dextran (M_r 10,000, Sigma-Aldrich) fluorescent dye for 16h in a long day plant room (16h/8h light/dark, 22°C, light intensity of 120 μ mol $m^{-2} s^{-1}$, relative humidity of 40%). Fluorescent emission of the dye was detected at 535nm and excitation at 485nm, using a microplate reader (BioTek). Media pH was obtained from a calibrated standard curve by measuring the fluorescence of commercial MS media (buffered) with a pH range from 4 to 7.4.

2.2.11. Split root assay

The split-root experiments were performed as described Zhang et al., 2014 with modification. In brief, the primary root of 3 days-old *Arabidopsis thaliana* seedlings grown in MS medium were removed to induce the formation of lateral roots. After growth for 7 days more, the seedlings were transferred to two-compartment plates. One lateral root was placed in MS medium in one compartment, and the other lateral root was placed in modified MS medium (0mM K^+ 1mM NO_3^-

) in the other compartment. The photographs were taken after 7 days, and the root growth was analyzed.

2.2.12. Confocal microscopy

Confocal laser scanning microscope (CLSM) was performed in a Leica TCS SP5 confocal microscope with 20x and 63x water immersion objectives (Leica Microsystems).

Bimolecular fluorescent complementation assays were performed at three days post infiltration in *N. benthamiana* leaves. Simultaneous excitation of YFP ($\lambda_{\text{excitation}}= 488\text{nm}$, $\lambda_{\text{emission}}= 568\text{-}587\text{nm}$) with the argon laser, mRFP ($\lambda_{\text{ex}}= 561\text{nm}$, $\lambda_{\text{em}}= 608\text{-}642\text{nm}$) and autofluorescence of chlorophyll ($\lambda_{\text{ex}}= 561\text{nm}$, $\lambda_{\text{em}}= 642\text{-}702\text{nm}$) with diode-pumped solid state (DPSS) laser were performed.

Overnight yeast cell cultures at 30°C expressing fluorescent tags as eGFP and mCherry were observed by CLSM. Cell cultures were centrifuged for 10min 10.000g. Pellets were washed 2 times in 1X TBS buffer (50mM Tris-Cl, pH 7.6 and 150mM NaCl). Simultaneous excitation of eGFP and mCherry was performance by argon ($\lambda_{\text{ex}}=488\text{nm}$ and $\lambda_{\text{em}}=493\text{-}555\text{nm}$) and DPSS ($\lambda_{\text{ex}}=561\text{nm}$ and $\lambda_{\text{em}}= 608\text{-}640\text{nm}$) lasers respectively.

Finally, the fluorescence signal of eGFP in roots and leaves of *Arabidopsis* transgenic lines was performed by CLSM. Simultaneous excitation of eGFP ($\lambda_{\text{ex}}=488\text{nm}$ and $\lambda_{\text{em}}= 493\text{nm}\text{-}555\text{nm}$) and autofluorescence of chlorophyll ($\lambda_{\text{ex}}= 561\text{nm}$, $\lambda_{\text{em}}= 642\text{-}702\text{nm}$) was performed using the argon laser and the DPSS laser, respectively.

Post-acquisition image processing was performed using the Leica LAS-AF software.

3. Results

3.1. Protein sequence analysis of the NRT1.5 transporter in *Arabidopsis thaliana*

3.1.1. NRT1.5 protein alignment unveils low conservation of motifs involved in NO₃⁻/H⁺ transport within NTR1 transporter family

The *Arabidopsis thaliana* NRT1.5 gene encodes a 614 amino acid protein, and little is known about protein features or motifs involved in the attributed functions of NRT1.5 in plant nutrition. In addition, like all members of the NRT1 family, NRT1.5 was predicted to contain 12 putative transmembrane domains (TM) and a long hydrophilic loop between TM6 and TM7 (Lin et al., 2008) but no protein structure has been yet described and characterized. Using the I-TASSER (Iterative Threading ASSEmbly Refinement) approach to protein structure and function prediction, the alignment of NRT1.5 protein sequence against all proteins in the PDB library found as a first match the nitrate transporter NRT1.1, which means it was the closest protein structural similarity found by the predictor program used (**Figure 5B**). The crystal structure of the *A. thaliana* NRT1.1 was resolved and unveiled some molecular determinants of the NO₃⁻ and H⁺ selectivity of the NRT1 transport members (Parker and Newstead, 2014; Sun et al., 2014). To identify features in NRT1.5 involved in nitrate and proton coupling, the unique or conserved known features involved in these functions in NRT1.1 were highlighted and extrapolated in the alignment with the NRT1 family members. The amino acid sequence alignment disclosed different motifs, domains or specific amino acids that are highly conserved among plant NRT1.5 orthologues but poorly conserved in other *Arabidopsis* NRT1 family members (**Figure 5A**). For example, (1) the residue Thr¹⁰¹ located at the beginning of TM3 in NRT1.5 is conserved among plant NRT1 family members (except for NRT1.2 and NRT1.3). Thr¹⁰¹ represents one of the hallmarks of the dual-affinity nitrate transport function of NTR1.1 (Parker and Newstead, 2014; Sun et al., 2014). (2) The nitrate substrate-binding pocket of NRT1.1 is mostly hydrophobic, except for one histidine residue, His³⁵⁶ in TM7, which is critical in nitrate recognition (Sun and Zheng, 2015). Notably, His³⁵⁶ is not conserved in NRT1.5 or other NRT1/PTR family members, suggesting that the differences in the substrate-binding sites in between NRT1/PTR members may have different recognition mechanisms and could explain why they have diverse substrate recognition as diverse as nitrate, peptides, and plant hormones. (3) The central loop containing Arg²⁶⁴-Arg²⁶⁶-Lys²⁶⁷ involved in nitrate affinity of NRT1.1 (Wen and Kaiser, 2018) is missing in the NRT1.5, where non-charged amino acids are found in position 266

potential motifs and residues involved in nitrate and proton transport was done by BLASTp (NCBI) using AtNRT1.5 as a query. From 100 eudicots orthologues, the individual logos were generated using Weblogo (<http://weblogo.berkeley.edu/logo.cgi>). The height of each amino acid symbol in Weblogo indicates amino acid residue conservation at a given position. Amino acids are colored according to their chemical properties: polar amino acids (G,S,T,Y,C,Q,N) are green, basic (K,R,H) blue, acidic (D,E) red and hydrophobic (A,V,L,I,P,W,F,M) amino acids are black. Black arrows show the position of each residue or motif involved in proton coupling or nitrate transport. **B.** Overlay of the homology models of nitrate transporter NRT1.1 and NRT1.5. The predicted NRT1.5 structure is shown in orange, while the NRT1.1 structural analog is displayed using violet. Protein structure assembly simulation was done by I-TASSER online tool to align the NRT1.5 protein sequence against all structures in the PDB library.

3.2. Phenotypical analysis of the *nrt1.5* knockout mutant

3.2.1. Ion homeostasis-associated genes are differentially regulated in *nrt1.5* at low nutrition supply

The lack of *NRT1.5* in roots of *Arabidopsis thaliana* generates an accumulation of K^+ in roots and a reduction in shoots under the limitation of K^+ and NO_3^- (Drechsler et al., 2015; Zheng, 2018). Moreover, the K^+ transport activity of NRT1.5 was detected by heterologous expression in *Xenopus* oocytes in acidic conditions (Li et al., 2017a). These results demonstrated that the translocation of K^+ from root-to-shoot is directly regulated by NRT1.5 in the acidic cellular pH of the xylem. Yet, the NO_3^- transport function of NRT1.5 or the dependency of nitrate in K^+ transport under acidic conditions is not discussed in detail.

Here, under low fertilization conditions (0mM K^+ and 1mM NO_3^-), the nitrate content in *nrt1.5* mutant roots and shoots was higher than that in wild-type shoots (**Figure 6**). However, increasing to 2mM of K^+ was enough to eliminate this difference. This shows that NO_3^- accumulation in roots and shoots is impaired in *nrt1.5* mutant in a K^+ -dependent manner and that NRT1.5 cannot be attributed to a direct root-to-shoot nitrate transport function.

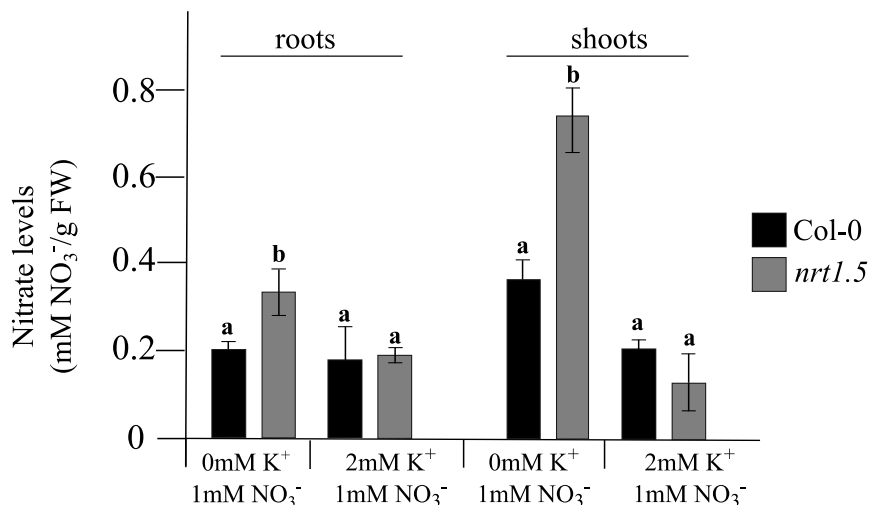


Figure 6: NO₃⁻ quantification in root and shoots of Col-0 and *nrt1.5* seedlings under different fertilization conditions. Plants were pre-germinated in MS media and after five days transferred to 0mM K⁺ /1mM NO₃⁻ or 2mM K⁺ /1mM NO₃⁻ mediums. Nitrate levels are represented as mM of nitrate per g of fresh weigh (FW). Different letters indicate statistically significant differences (Student's *t*-test) between *nrt1.5* and Col-0 in the different treatments with $P < 0.05$, (means \pm SD, n=12).

Taking advantage that transcriptional regulation of ion transporters and channels can change ions contents in different organs under nutrient deficiencies, the gene expression of K⁺ and NO₃⁻ transporters and channels in *nrt1.5* mutant was analyzed.

The expression of several K⁺ and NO₃⁻ transporters and channels was significantly altered in Col-0 and *nrt1.5* mutant at low fertilization conditions (0mM K⁺ and 1mM NO₃⁻) (**Figure 7**). Regarding K⁺ uptake, the high-affinity K⁺ transporter *HAK5* was \approx 40-fold down-regulated in *nrt1.5* roots, supporting earlier findings at low-N supply conditions (Drechsler et al., 2015). In addition, expression of the selective inward-rectifying potassium channel *AKT1* and the K⁺ transporter *KUP7* was approximately 2.5-fold up-regulated without significant differences between Col-0 and *nrt1.5*. The vacuolar K⁺/H⁺ antiporter *NHX1* and the K⁺-selective tonoplast ion channel *TPK1* were \approx 2-fold down-regulated in Col-0 but they were not altered in *nrt1.5* mutant roots. Moreover, K⁺ root-to-shoot translocation systems such as the selective outward-rectifying potassium channel *SKOR* was 2-fold up-regulated in *nrt1.5* roots, whereas in Col-0 it was \approx 2-fold down-regulated.

Concerning NO₃⁻ uptake and root-to-shoot translocation, the dual affinity transporter *NRT1.1*, the low-affinity transporter *NRT1.2*, and the NO₃⁻ transporter *NRT1.8* were not regulated. In contrast, *NRT1.8* is 32-fold up-regulated in *nrt1.5* roots under low-N conditions (Drechsler et al., 2015), suggesting that the low fertilization condition using here is impacting the *NRT1.8* transcription.

Finally, the low-affinity proton-dependent nitrate transporter *NRT1.4* involved in nitrate xylem translocation had an 8-fold down-regulation in Col-0 and *nrt1.5* roots.

Considering the elemental composition in *nrt1.5* roots/shoot and the root transcript patterns, NRT1.5 is modulating the indirect accumulation of NO_3^- in plant organs and is influencing the expression of transporters and channels that might contribute to the plant nutrient status.

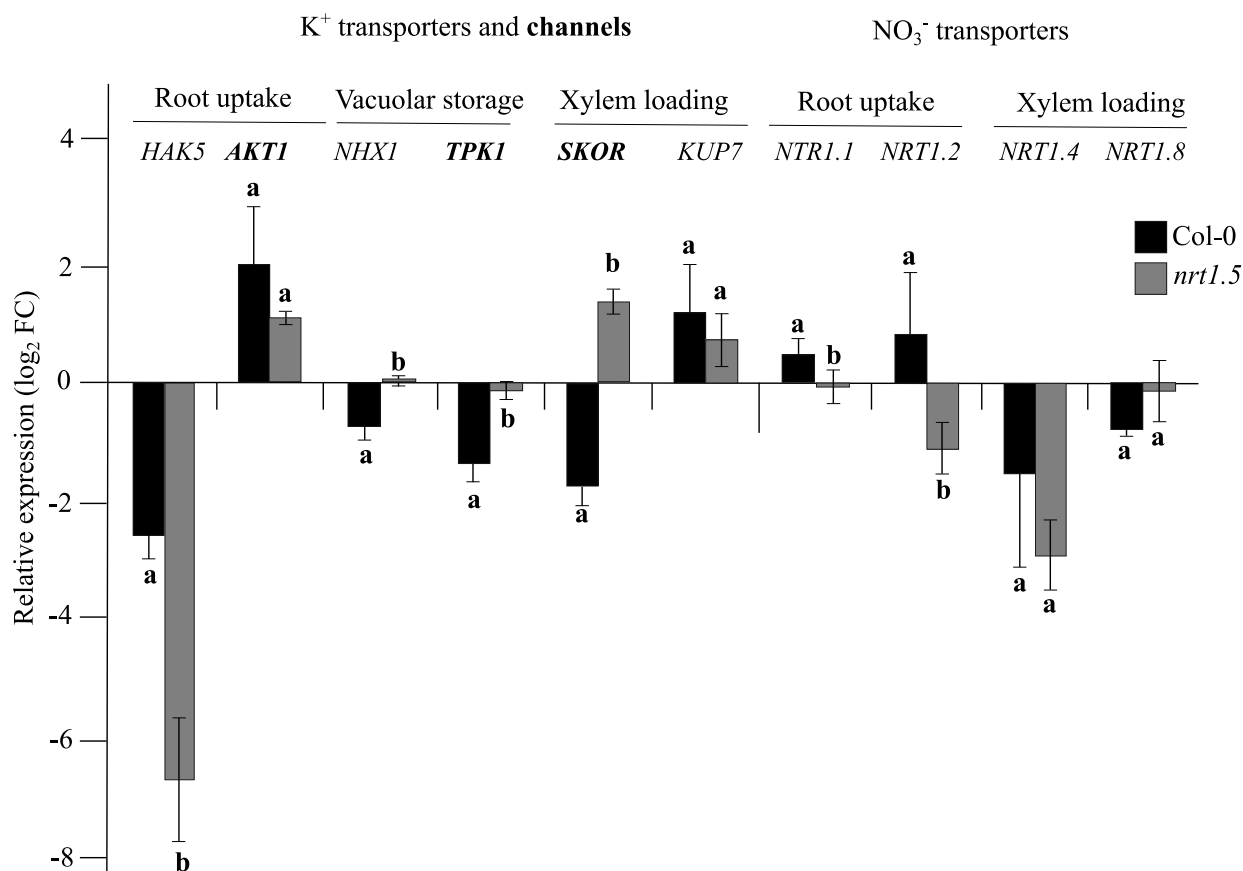


Figure 7: Expression changes of ion transporters and channels at low fertilized supply. Gene expression of different K⁺ and NO₃⁻ transporters and channels (bold cases) by qPCR in Col-0 and *nrt1.5* roots under low fertilization supply (0mM K⁺/1mM NO₃⁻). The relative gene expression (log₂FC) was normalized with *UBQ10* as a housekeeping gene and relative to Col-0 under growth conditions in MS medium. Different letters indicate statistically significant differences (Student's *t*-test) between *nrt1.5* and Col-0 in the different treatments with $P < 0.05$, (means \pm SD, n=3).

3.2.2. *NRT1.5* promoter activity in roots depends on K^+ uptake

To identify if the *NRT1.5* promoter is inducible by different potassium and nitrate availabilities in the medium, its activity and tissue specificity in *Arabidopsis* roots at low fertilization supply was determined (**Figure 8**). The transgenic line *NRT1.5p::uidA* (Zheng et al., 2016) containing the GUS reporter gene *uidA* (β -glucuronidase) under the control of the *NRT1.5* promoter was used. Seedlings grown in MS medium showed *NRT1.5* promoter activity in the primary vascular cylinder, formation of lateral roots and root cap, while the root cortex and root hairs were not stained. GUS staining is more intense at lateral root primordia mainly at the central basal domain. After being pre-germinated in MS medium for five days and later transferred to a low fertilized medium (0mM K^+ /1mM NO_3^- pH=5.5), the intensity of GUS staining (*NRT1.5* promoter activity) was stronger in comparison with MS medium and the signal was also detected in the root cortex. Interestingly, *NRT1.5* promoter activity was strongly reduced in roots after the treatment with 2mM CsCl, a K^+ uptake blocker that acts as a K^+ competitive inhibitor (**Figure 8**).

This shows that the *NRT1.5* promoter is constitutively active in MS medium, but its activity increases under low fertilization conditions (0mM K^+ /1mM NO_3^-). However, when the K^+ uptake is completely blocked (by CsCl) the *NRT1.5* expression is reduced, indicating the existence of a mechanism that tightly regulates K^+ uptake and translocation to the xylem. *NRT1.5* expression may depend on the K^+ uptake and could be modulated by the K^+ status in roots.

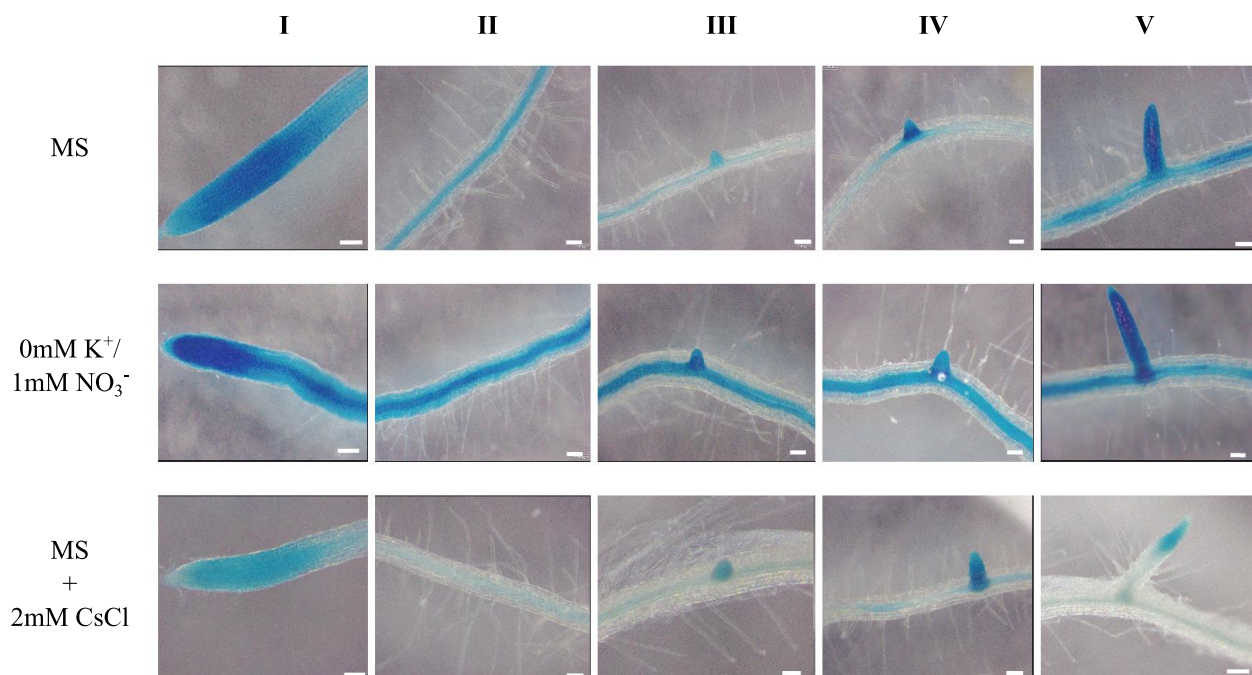


Figure 8: *NRT1.5* promoter activity in roots of *NRT1.5p::uidA* seedlings. Seedlings were grown for five days in MS medium and then transferred to MS medium (pH=5.5), 0mM K⁺/1mM NO₃⁻ (pH=5.5), or MS medium supplemented with 2mM CsCl (pH=5.5) for five more days before the histochemical detection of GUS activity. The *NRT1.5p::uidA* line is described in (Zheng et al., 2016). Each picture represents, I root tip, II lateral root pre-initiation events, III lateral root initiation, IV lateral root emergence, and V lateral root formation. The figure represents similar observations on two independent experiments. The white bars represent 100µm.

3.2.3. *NRT1.5* is not required for the perception of external K⁺ contents

Plants can sense the external nutrient conditions and regulate root growth accordingly. The sensing and perception mechanisms that control plant responses to nutrient deprivation are not well characterized, but few K⁺ and NO₃⁻ transporters and channels have been identified as novel components for nutrient perception and sensing, like the nitrate transporter *NRT1.1* and the potassium channel *AKT1* (Ho et al., 2009; Li et al., 2017b). The external K⁺ and NO₃⁻ levels directly determine the root (primary and lateral) and shoot growth and development of plants lacking *NRT1.5* at specific nutrient contents (Drechsler et al., 2015; Meng et al., 2016; Zheng et al., 2016; Li et al., 2017a). However, if *NRT1.5* is involved in the perception of external nutrient contents was not investigated. Here, along with the drop of external K⁺ concentrations and stable concentration of NO₃⁻ at 1mM, gradual senescence phenotypes were observed in both wild-types (*Col-0*) and the *nrt1.5* mutant. However, the *nrt1.5* mutant developed senescence symptoms up to 1mM K⁺ in contrast to *Col-0* that was up to 0.1mM K⁺ (**Figure 9A**). In addition, *nrt1.5* mutants had a reduced lateral root density in comparison to *Col-0*, and the mutant was not able to produce new lateral roots when the medium contains less than 0.1mM of K⁺. *Col-0* plants also had a reduced lateral root density but even at 0mM of K⁺ they still were able to produce new lateral roots (**Figure 9B**). These data indicate that both *Col-0* and *nrt1.5* can sense the local K⁺ concentrations and grow accordingly, suggesting *NRT1.5* is not involved in K⁺ perception. However, the K⁺ concentration ranges or thresholds where wild-type plants responded were different to the *nrt1.5*.

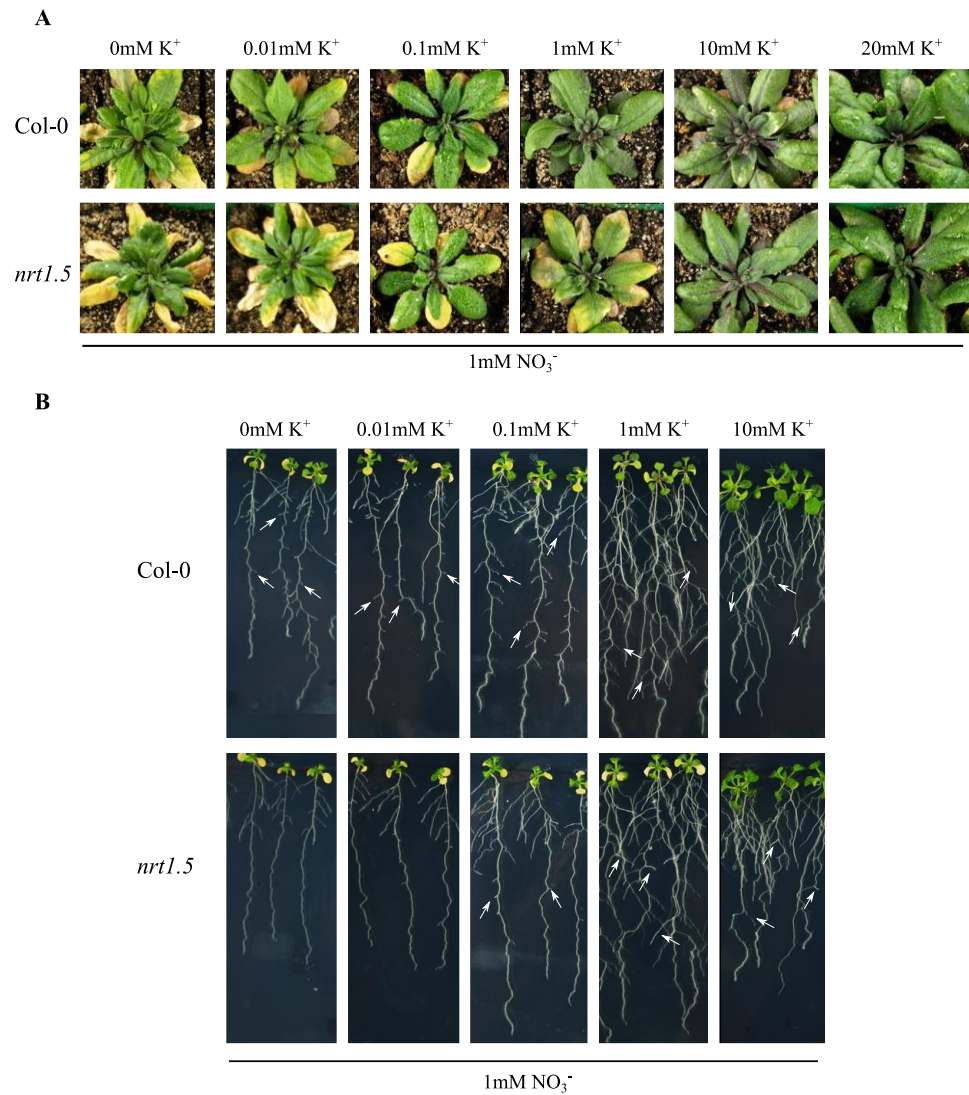


Figure 9: Shoot and root phenotypes of Col-0 and *nrt1.5* mutant under different external K⁺ concentrations and stable NO₃⁻ supply. **A.** Col-0 and *nrt1.5* seedlings were transferred after seven days of pre-germination in fertilized soil to non-fertilization soil. Two times a week, plants were watered with fertilizer solutions containing K⁺ and NO₃⁻ concentrations as indicated. Details of solutions are given in Table S1. **B.** Col-0 and *nrt1.5* seedlings were pre-germinated in MS medium for seven days and transferred to medium containing different K⁺ and NO₃⁻ conditions as indicated for another ten days. White arrows represent the formation of new lateral roots.

3.2.4. NRT1.5 modulates the root architecture in dependency of extracellular potassium, nitrate, and pH

NRT1.5 has been described as a nitrate and potassium transporter involved in NO_3^- and K^+ xylem loading by H^+ coupling, and both functions are described at basic (pH=7.4) or acidic (pH=5.5) pH conditions respectively (Lin et al., 2008; Li et al., 2017a). As mentioned before, root architecture is affected in the *nrt1.5* mutant under K^+ and NO_3^- deficiency conditions (Zheng et al., 2016). Therefore, it was tempting to investigate whether the *nrt1.5* mutant also exhibits an altered root architecture in response to different nitrate and potassium supply in combination with acidic or basic conditions.

To test whether K^+ or NO_3^- contents and pH in the medium influence the root growth, Col-0 and *nrt1.5* seedlings were grown under different nutrient supplies and pH conditions. At 0mM K^+ and acidic conditions (stable 1mM NO_3^-), the *nrt1.5* mutant showed a reduction of lateral root density in comparison to Col-0, similar to the observations of Zheng et al., 2016 at pH=5.8. In contrast, when plants were grown at basic pH a recovery of lateral root density to wild-type level was observed (**Figure 10**). Surprisingly, at 0mM NO_3^- and acidic conditions (stable 1mM K^+) the lateral root density of *nrt1.5* was not different from Col-0, whereas at basic pH the lateral root density of *nrt1.5* seedlings was reduced (**Figure 10**). No root phenotypes were observed when plants were grown at 1mM of K^+ and NO_3^- either in acidic or basic conditions, evidencing that the changes in root growth are linked to pH conditions and low nutrient availability.

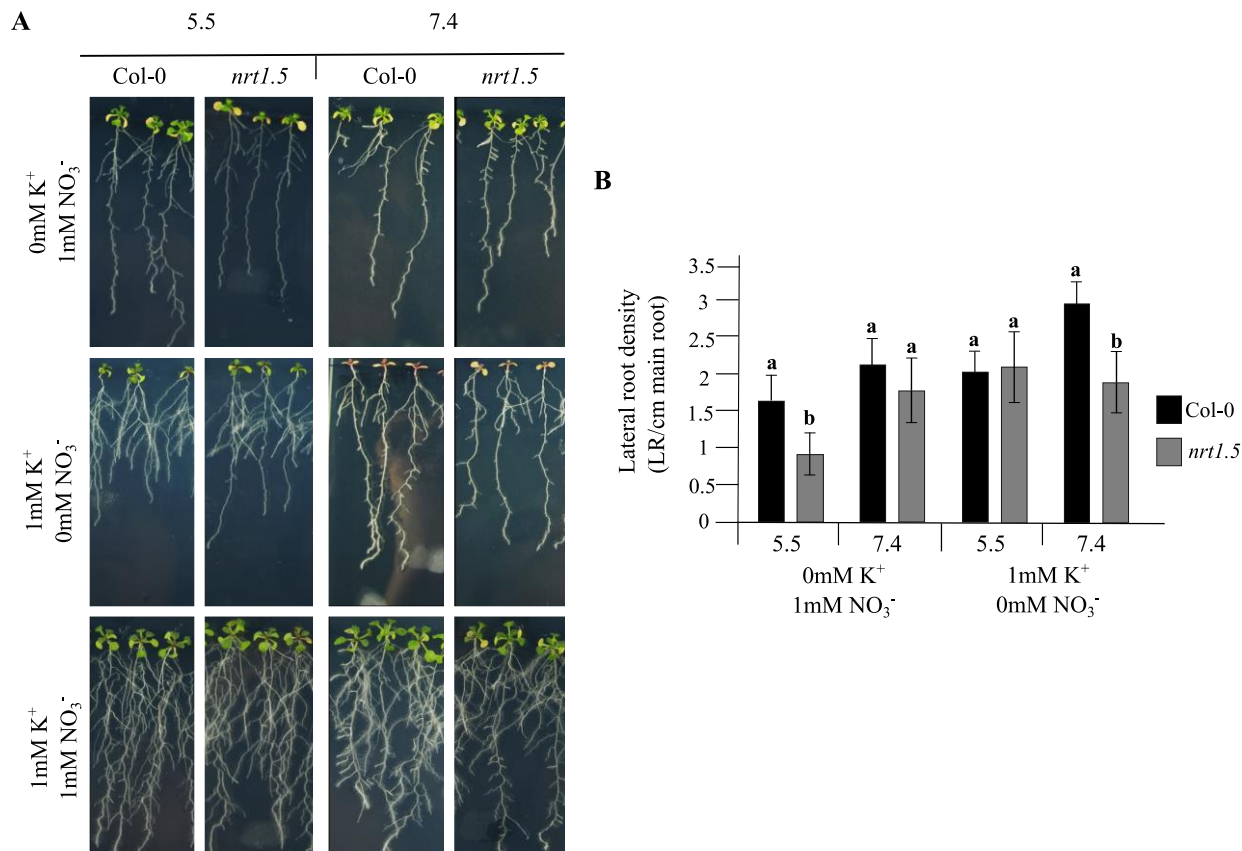


Figure 10: Root growth of Col-0 and *nrt1.5* under different potassium and nitrate contents in acidic or basic conditions in the medium. **A.** Seedlings were pre-germinated five days in MS medium (pH=5.5) and later transferred to 0mM K⁺/1mM NO₃⁻, 1mM K⁺/0mM NO₃⁻, or 1mM K⁺/1mM NO₃⁻ either at pH=5.5 or 7.4 for ten days further. **B.** Lateral root density quantification of Col-0 and *nrt1.5* seedlings grown at 0mM K⁺/1mM NO₃⁻ and 1mM K⁺/0mM NO₃⁻ either at acidic or basic conditions. Different letters indicate statistically significant differences (Student's *t*-test) between *nrt1.5* and Col-0 in the different treatments with *P*<0.05, (means ± SD, n ≥20).

3.2.5. The NRT1.5^{G209E} expression does not complement phenotypically the *nrt1.5* mutant

The phenotype and ion content analysis of a *nrt1.5* complementation line (PHO1p:NRT1.5) demonstrated that *NRT1.5* expression in root cells is needed to meet the K⁺ demand of the leaf (Drechsler et al., 2015). Here, a complementation line with a mutant version of *NRT1.5* (*NRT1.5*^{G209E}) attached to a fluorescent tag was created and analyzed to evaluate the impact of the mutation on *NRT1.5* function and localization in living plant cells. The amino acid substitution

from Gly²⁰⁹ to a Glu (G209E) was proposed to lose the ability of NRT1.5 to transport K⁺ (Li et al., 2017a).

nrt1.5 mutant plants were transformed with a vector containing the promoter of the *PHO1* gene (At3g23430) with expression primarily directed to the root vasculature (Hamburger et al., 2002), and the *NRT1.5* coding region without stop codon fused to eGFP fluorescent tag at the C-terminus. Four independently transformed *PHO1p::NRT1.5eGFP* and *PHO1p::NRT1.5^{G209E}eGFP* lines in *nrt1.5* background that are homozygous for a single insertion of the transgene were used for further studies.

Previously, it has been shown that the *nrt1.5* mutant displays impaired root architecture, and developed an early senescence phenotype when plants grew in media lacking potassium (**Figure 9**). Additionally, *nrt1.5* seedlings developed a Hygromycin B (HygB) sensitivity due to a reduction in the plasma membrane potential (Drechsler et al., 2015). Homozygous *PHO1p::NRT1.5eGFP* and *PHO1p::NRT1.5eGFP^{G209E}* T3 plants were evaluated phenotypically under lack of K⁺ and addition of HygB. The root growth assay indicated that *PHO1p::NRT1.5eGFP* plants can rescue the reduction in root density (**Figure 11A and B**) and the early senescence phenotype of *nrt1.5* (**Figure 11C**) under K⁺ deprivation, supporting previous studies of this complementation line without the fluorescent tag (Drechsler et al., 2015). These observations demonstrate that the attachment of the fluorescent tag does not interfere with the NRT1.5 function. The introduction of the mutation G209E into NRT1.5 in the transgenic line *PHO1p::NRT1.5^{G209E}eGFP* showed the *nrt1.5* root and shoot phenotypes, demonstrating that the mutation G209E prevents complementation of the *nrt1.5* mutant. Moreover, HygB is used as an indicator of the plasma membrane potential status, where wild type roots are sensitive to the toxic drug. When the plasma membrane potential is altered the toxic drug is not able to enter into the cells and the plants develop an enhanced HygB tolerance, like *nrt1.5* mutants due to the alteration in ion transport (Drechsler et al., 2015). Here, two independent *PHO1p::NRT1.5eGFP* lines were sensitive to 5µg/ml HygB (reduction of root growth and yellow cotyledons), whereas the *PHO1p::NRT1.5^{G209E}eGFP* lines were more resistant, indicating plasma membrane potential was restored after the introduction of NRT1.5 in *nrt1.5* mutant background. Contrarily, the NRT1.5^{G209E} mutant is not able to complement the *nrt1.5* mutant, most likely because of a direct influence in the ion transport function of NRT1.5, such as a defective protein activity, incorrect protein folding, or influence in the interaction with other components at the plasma membrane.

3. Results

Finally, live-cell imaging was carried in roots of *PHO1p::NRT1.5eGFP* and *PHO1p::NRT1.5^{G209E}eGFP* transgenic lines by epifluorescence microscopy. The detection of GFP signal in both lines verified that NRT1.5 wild-type and the mutated version NRT1.5^{G209E} are expressed in both transgenic lines and they seem to localize to the plasma membrane, however, the exact cellular localization cannot be determined on these pictures (**Figure 11D**).

These results demonstrate that the *NRT1.5* expression in the plasma membrane of roots is indeed required and essential for the lateral root development and nutrient transport to shoots under K⁺ and NO₃⁻ limiting conditions. Moreover, glycine 209 is critically required for the NRT1.5 activity in the control of ion homeostasis in living plants.

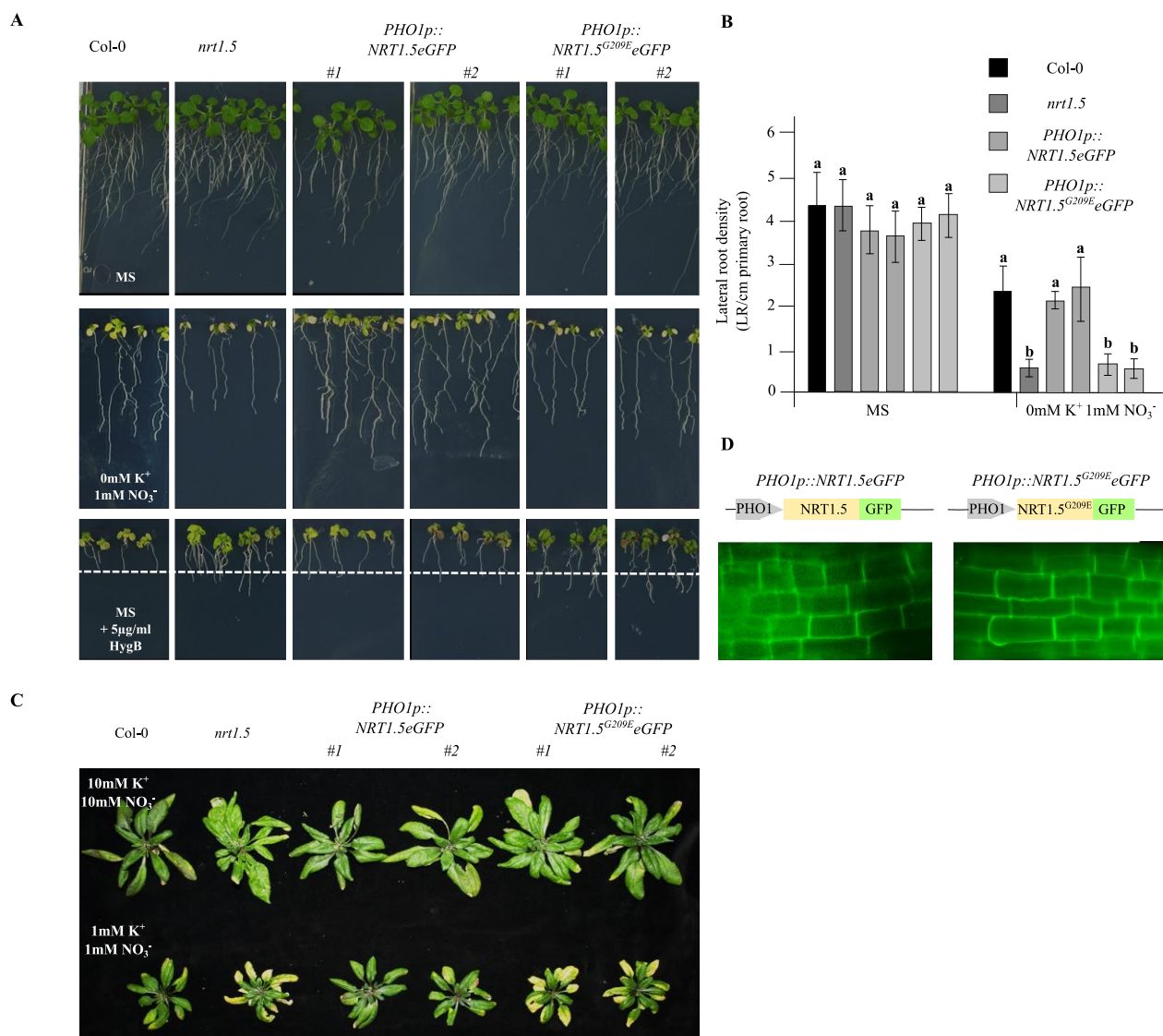


Figure 11: Phenotypes of the complementation lines *PHO1p::NRT1.5eGFP* and *PHO1p::NRT1.5^{G209E}eGFP*. **A.** Root phenotypes. Col-0, *nrt1.5*, two independent *PHO1p::NRT1.5eGFP* (#1

and #2), and two independent *PHO1p::NRT1.5^{G209E}eGFP* (#1 and #2) were pre-germinated in MS medium for five days and transferred to plates containing MS, 0mM K⁺/1mM NO₃⁻, or MS + 5μg/ml HygB for ten days more. Dotted white line represents maximum root growth of Col-0 in MS + 5μg/ml HygB. **B.** Lateral root density quantification of plants in MS or 0mM K⁺/1mM NO₃⁻ conditions in part A. Different letters indicate statistically significant differences (Tukey's test) between mutants and Col-0 in the different treatments with $P < 0.05$, (means \pm SD, $n \geq 20$). **C.** Shoot phenotypes. Plants were pre-germinated in fertilized soil for seven days, and transferred to unfertilized type soil and supplemented with MS-based fertilization solution containing 1mM/1mM or 10mM/10mM of K⁺/NO₃⁻ (Table S1) for forty days further. **D.** Epifluorescence microscopy. Detection of GFP signal from 10 days-old *PHO1p::NRT1.5eGFP* and *PHO1p::NRT1.5^{G209E}eGFP* seedlings grew in MS medium (pH=5.5).

3.3. Identification of novel regulatory components involved in nutrient translocation in plants

From unpublished data of our group, several putative interaction partners of NRT1.5 were identified by the *S. cerevisiae* split ubiquitin system and a few of them were verified by bimolecular fluorescence complementation (BiFC) in *N. benthamiana* assays (Drechsler, 2016; Zheng, 2018) (**Table 13**). Among these are the plasma membrane H⁺ ATPase AHA2 (At4g30190), the calcium sensor protein CBL3 (At4g26570), the CBL-interacting protein kinase CIPK23 (At1g30270), two putative anion efflux channels that have been reported to be essential for anion homeostasis SLAH1 (At1g62280) and SLAH3 (At5g24030), the SNARE vesicle transport protein PEP12 (At5g16830), and the vesicle-associated membrane protein VAMP722 (At2g33120).

Table 13: Summary of all identified potential interaction partners of the potassium/nitrate transporter NRT1.5 up to date. Most of the physical interactions between NRT1.5 and the interaction partners were identified by the split ubiquitin system in *Saccharomyces cerevisiae*²⁻¹⁰, bimolecular complementation assay in *Nicotiana benthamiana*^{2,7,8,9} and ChIP-qPCR assay in *Arabidopsis thaliana*¹. Abbreviations: PM, plasma membrane. VM, vacuolar membrane. Most of the NRT1.5 protein interactions have not been published yet.

Interaction partner	Protein function	Expressed in *	References about identification of interaction
¹ MYB59	MYB-type transcription factor	Nucleus	(Du et al., 2019)
² AHA2	H ⁺ ATPase proton pump	PM	(Drechsler, 2016; Zheng, 2018)
³ CBL3	Ca ²⁺ sensor	PM and VM	(Drechsler, 2016)

⁴ CIPK23	CBL-interacting protein kinase 23	PM, cytosol	(Zheng, 2018)
⁵ PEP12	SNARE, syntaxin of plants 21	VM, Golgi, PM	(Drechsler, 2016)
⁶ VAMP722	Vesicle associate membrane protein 722	PM	(Drechsler, 2016)
⁷ SLAH1	Silent S-type anion channel	PM	} (Drechsler, 2016; Zheng, 2018)
⁸ SLAH3	Silent S-type anion channel	PM	
⁹ NRT1.10	Glucosinolate-specific transporter	PM	
¹⁰ DMP2	DUF679 membrane protein	PM , vacuole	(Kasaras, 2012)

^{*}Prediction of protein subcellular localization from SUBA4 database (www.suba.live).

3.2.1. NRT1.5 interacts with AHA2, CBL3, CIPK23, PEP12, SLAH1, SLAH3, and VAMP722 in the bimolecular fluorescence complementation (BiFC) assay in *N. benthamiana*

Since not all potential NRT1.5 interaction candidates were evaluated by BiFC assays by (Zheng, 2018), here it was checked if the protein-protein interactions that (Drechsler, 2016) observed in heterologous yeast cells also occur in living plant cells. NRT1.5 was fused to cYFP and the potential NRT1.5 interaction partners AHA2, CBL3, CIPK23, PEP12, SLAH1, SLAH3, and VAMP722 were fused to nYFP in the pBiFC-2in1 system by Gateway cloning (Grefen and Blatt, 2012) (**Figure 12A**). As a negative control, the pBiFC-2in1 construct with unfused nYFP and NRT1.5 fused to cYFP was used. The pBiFC-2in1 constructs were transformed into *A. tumefaciens* for transient expression in *N. benthamiana*. Two days post-infiltration (dpi), fluorescence signals from the epidermis basal cell layer of transfected *N. benthamiana* were analyzed by confocal fluorescence microscopy. The RFP signal is a positive control for the successful transformation and expression of the pBiFC-2in1 constructs in *N. benthamiana* leaves. The negative control did not show a signal, whereas all interaction partner candidates of NRT1.5 were able to reconstitute the fluorescent YFP signal, at the plasma membrane (**Figure 12B**). This data confirms the interaction between NRT1.5 and all interaction partners at the plant plasma membrane.

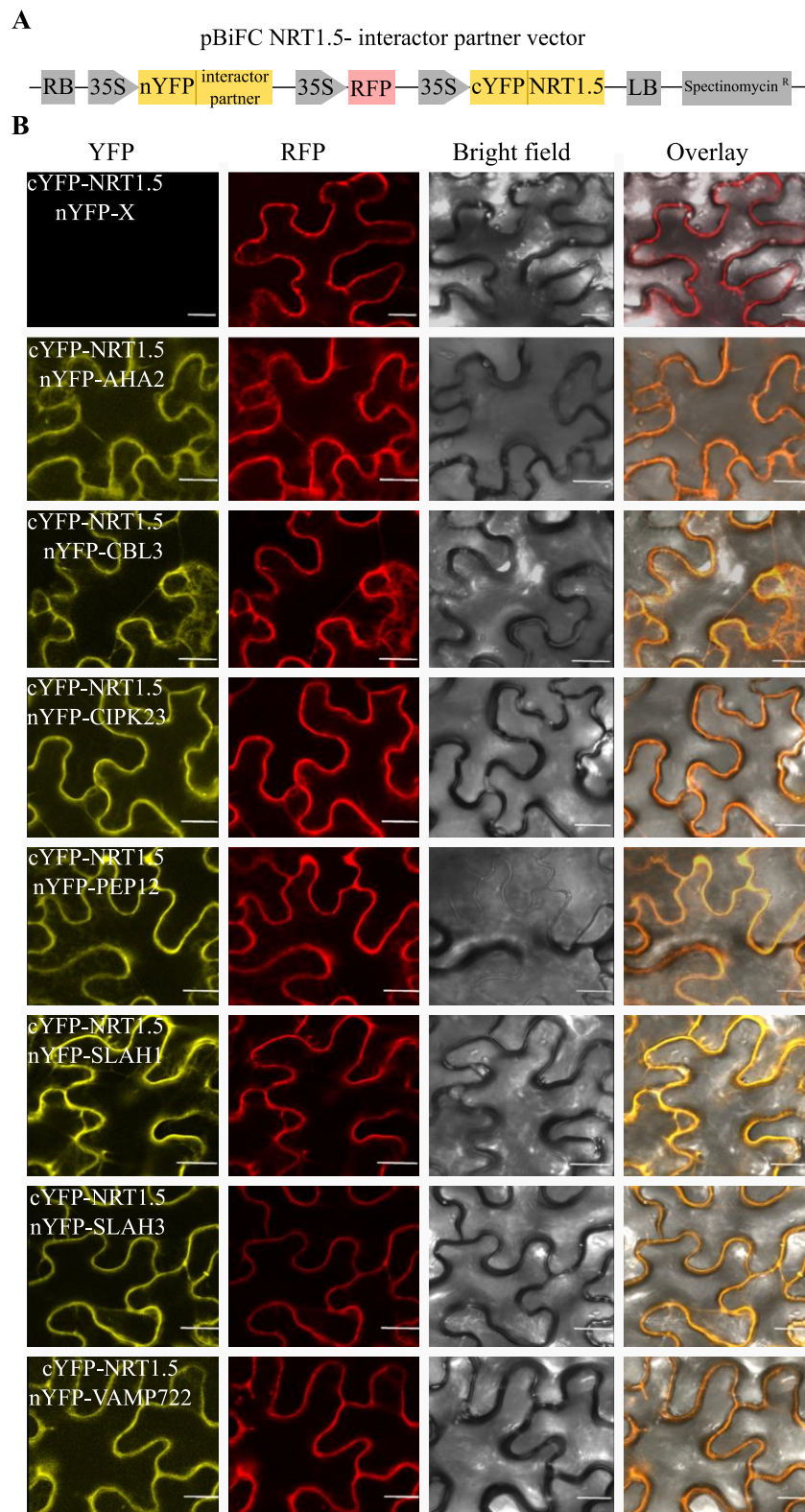


Figure 12: NRT1.5 interaction with potential interaction candidates by BiFC assay in *Nicotiana benthamiana* leaves. **A.** Schematic representation of the T-DNA from the pBiFC-2in1 vector containing NRT1.5 and the potential interaction partners. Abbreviations: RB/LB: right/left border of T-DNA. 35S: 35S

promoter of cauliflower mosaic virus (CaMV). RFP: red fluorescent protein marker. nYFP and cYFP are two yellow fluorescent protein moieties (nYFP: 1-155 amino acids and cYFP: 156–239 amino acids). **B.** Confocal microscopy images of epidermis cells expressing cYFP-NRT1.5 and non-fused nYFP, nYFP-AHA2, nYFP-CBL3, nYFP-CIPK23, nYFP-PEP12, nYFP-SLAH1, nYFP-SLAH3, or nYFP-VAMP722 at three days after infiltration (dpi). The channels observed are YFP fluorescence showing the existence of interaction (yellow), RFP fluorescence as a positive control for the success transformation (red), bright field (grey) and the overlay of the three channels. The white scale bar represents 20µm.

3.3.2. Gene expression of *AHA2*, *CBL3*, *PEP12*, *SLAH1*, *SLAH3*, and *VAMP722* is affected by low nutrition supply in the *nrt1.5* mutant

As a first approximation to comprehend the biological importance between the interaction of NRT1.5 with *AHA2*, *CBL3*, *CIPK23*, *PEP12*, *SLAH1*, *SLAH3*, and *VAMP722* (so-called NRT1.5 interaction partners) confirmed in Figure 11, the molecular involvement of them was investigated in relation to nutrient availability and the lack of *NRT1.5*. To achieve that, the *AHA2*, *CBL3*, *CIPK23*, *PEP12*, *SLAH1*, *SLAH3*, and *VAMP722* expression levels were measured in Col-0 and *nrt1.5* plants at low potassium and nitrate supply (0mM K⁺/1mM NO₃⁻) by qRT-PCR. In wild-type (Col-0) roots, all interaction partners of NRT1.5 were slightly induced (about 2- fold up) as well as in the *nrt1.5* mutant where the expression of all interaction partners was even stronger than wild type (between 2 and 11-fold up). The S-type anion channels *SLAH1* and *SLAH3* were the most highly induced genes in the *nrt1.5* roots with 11 and 6-fold up-regulation respectively, supporting earlier findings under N-deprivation (Drechsler et al., 2015). The H⁺-ATPase, *AHA2*, involved in pH homeostasis and the SNARE, *VAMP722*, involved in protein trafficking to plasma membrane were also significantly up-regulated (≈4-fold up). Moreover, the calcium sensor, *CBL3*, and another component of the SNARE network, *PEP12*, were 2-fold up-regulated in *nrt1.5* roots. The expression of the *CIPK23* kinase was ≈2-fold up-regulated but did not show statistical differences between Col-0 and the *nrt1.5* mutant (**Figure 13**). This indicates that the molecular regulation of the NRT1.5 interaction partners is affected by K⁺ and NO₃⁻ availability and is linked to the lack of NRT1.5.

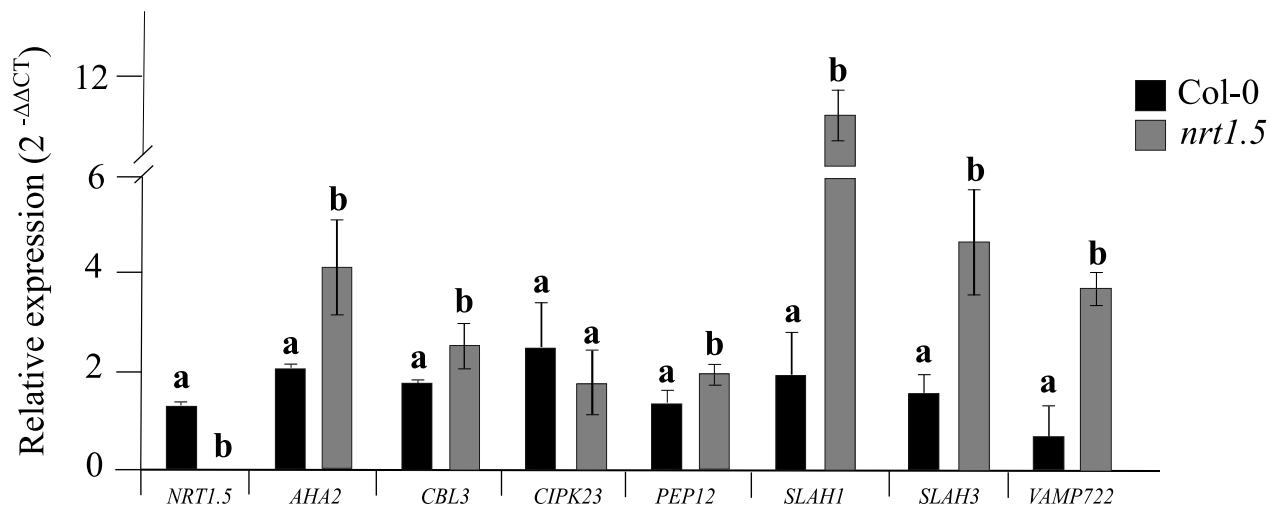
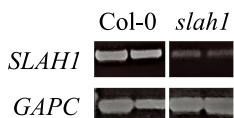
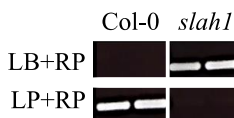
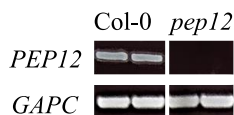
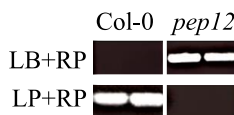
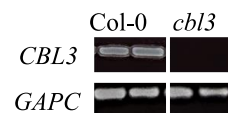
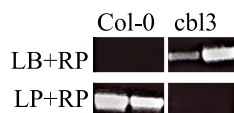
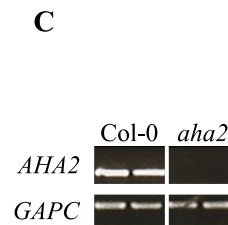
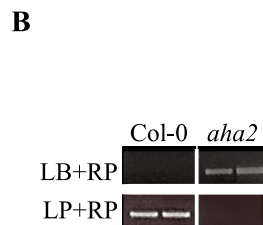
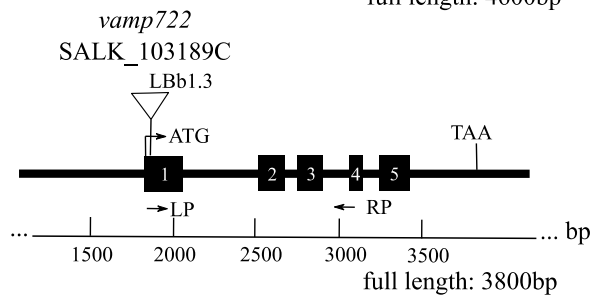
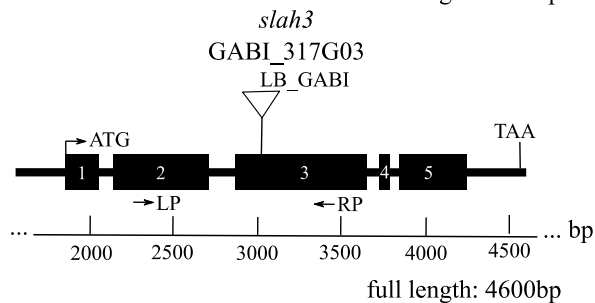
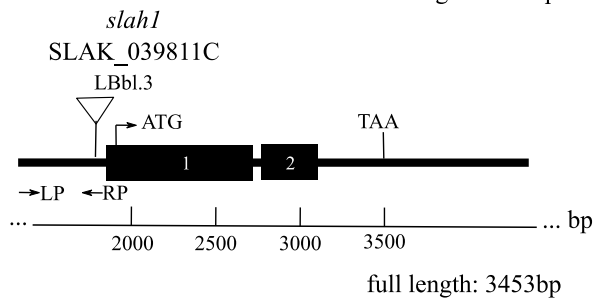
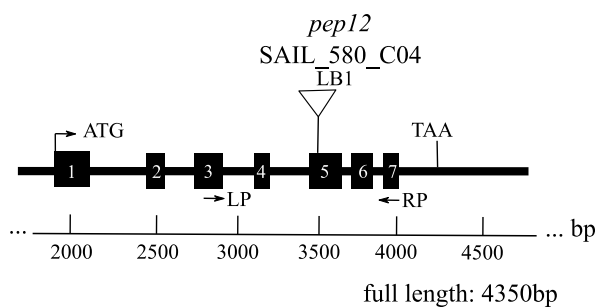
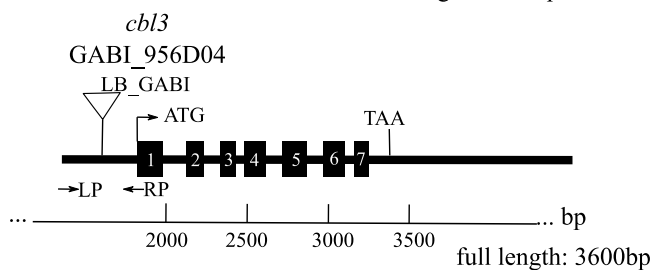
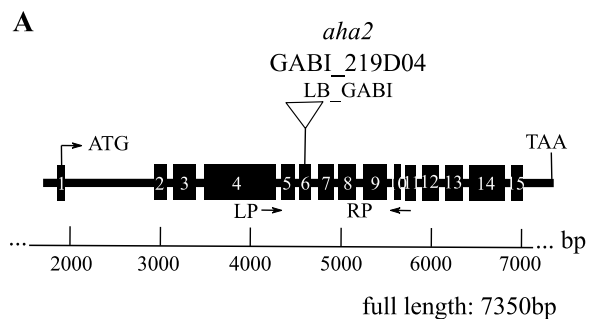


Figure 13: Gene expression of NRT1.5 interaction partners in Col-0 and *nrt1.5* roots by qPCR. Col-0 and *nrt1.5* were pre-germinated in MS medium for five days and later transferred to either MS or 0mM K⁺/1mM NO₃⁻ mediums. Relative expression ($2^{-\Delta\Delta CT}$) was calculated by the expression of each gene under 0mM K⁺/1mM NO₃⁻ compared with MS medium. *UBQ10* was used as a housekeeping gene. Different letters indicate statistically significant differences (Student's *t*-test) between *nrt1.5* and Col-0 with $P < 0.05$, (means \pm SD, n=3).

3.3.3. Identification of homozygous lines and transcript levels of *aha2*, *cbl3*, *pep12*, *slah1*, *slah3*, and *vamp722* mutants

To investigate the physiological significance of the interactions between NRT1.5 and its interacting partners, T-DNA insertion mutants from the candidates (**Figure 14A**) were ordered as segregating lines in the T3 generation from the Arabidopsis Biological Resource Center (ABRC). Homozygotes of each mutant were identified by PCR on genomic DNA (**Figure 14B**), and semi-quantitative RT-PCR was carried out to verify the absence of full-length gene transcripts in the homozygous mutants. Except for *slah1*, which showed residual transcription, all mutants turned out to be knockout lines (**Figure 14C**).



Zheng, 2018

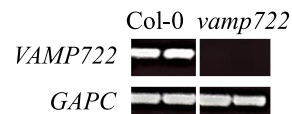
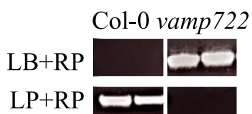


Figure 14: Schematic representations of *AHA2*, *CBL3*, *PEP12*, *SLAH1*, *SLAH3*, and *VAMP722* gene structures, identification of homozygous lines, and detection of transcript levels in T-DNA *Arabidopsis thaliana* mutants. **A.** Gene structures and T-DNA insertion sites of every mutant line. T-DNA insertions are identified with a triangle, black bars represent exons, initial codon ATG, and stop codon TAA are shown as a reference. The localization of LP and RP primers for genotyping PCRs are represented as black arrows. The full length of genomic DNA is shown with a scale at the bottom of each gene representation. **B.** Identification of homozygous T-DNA mutants. Two paired PCR reactions, LB+RP and LP+RP, are shown using genomic DNA as a template. No PCR products are expected in the LB+RP reaction for Col-0 and PCR products are expected for homozygotes and heterozygotes mutant lines. PCR products are expected in LP+RP reaction in Col-0 and heterozygote mutant lines and no PCR products are expected for homozygote mutant lines. **C.** RT-PCR analysis of cDNAs from all mutants was performed with exon-specific primers for *AHA2*, *CBL3*, *PEP12*, *SLAH1*, *SLAH3*, and *VAMP22*. GAPC was used as a housekeeping gene (band fragment for cDNA \approx 543bp) and all cDNAs were synthesized from 2 μ g of RNA. gDNA from Col-0 was used as wild type control. Primers used for genomic PCRs and RT-PCRs are listed in Table 4.

3.3.4. Shoot phenotypes of *aha2*, *cbl3*, *pep12*, *slah1*, *slah3*, and *vamp722* mutants are not phenocopies of *nrt1.5* at low nutrition supply

To investigate if the *AHA2*, *CBL3*, *PEP12*, *SLAH1*, *SLAH3*, and *VAMP722* are correlated with the maintenance of potassium and nitrate homeostasis, single mutants of each interaction partner were grown in different NO_3^- and K^+ regimens and the phenotypes were analyzed. After 30 days of growth in high fertilized soil (10mM K^+ /10mM NO_3^-), none of the mutants showed lesion-symptoms. In low fertilized soil (1mM K^+ /1mM NO_3^-) only *nrt1.5* developed visible early senescence (**Figure 15A**), supporting earlier observations (Drechsler et al., 2015; Meng et al., 2016). The quantification of the senescence phenotypes was carried out by measuring the percentage of lesion formation in leaves. Upon growth under 1mM K^+ and 1mM NO_3^- the *nrt1.5* mutant developed 53% of lesions, whereas the *aha2*, *cbl3*, *pep12*, *slah1*, *slah3*, and *vamp722* single mutants developed like wild type plants, 20%-30% of lesions (**Figure 15B**). This shows at first glance that *AHA2*, *CBL3*, *PEP12*, *SLAH1*, *SLAH3*, and *VAMP722* are not linked with the K^+ root-to-shoot translocation.

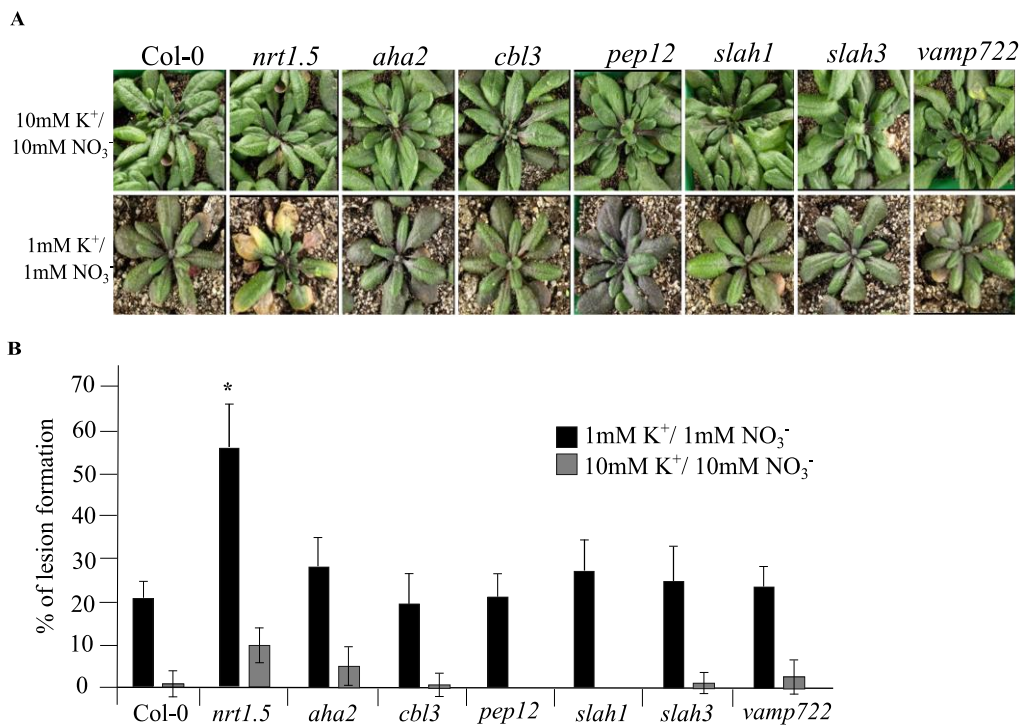


Figure 15: Shoot phenotypes of *nrt1.5*, *aha2*, *cbl3*, *pep12*, *slah1*, *slah3*, and *vamp722* mutants under different fertilization conditions. **A.** Wild type (Col-0) and mutant plants were pre-germinated in fertilized soil for seven days and then transferred to unfertilized soil and watered with given solutions (1mM K⁺/1mM NO₃⁻ or 10mM K⁺/10mM NO₃⁻) for thirty days further. **B.** Percentage of lesions formation in leaves in the fertilization conditions in A. The asterisk (*) indicates statistically significant differences (Student's *t*-test) between mutants and Col-0 in each treatment with $P < 0.01$, (means \pm SD, n=12).

Subsequently, *aha2*, *cbl3*, *pep12*, *slah1*, *slah3*, and *vamp722* homozygous single knockout mutants were crossed with *nrt1.5* respectively to generate the double mutants. The analysis of all lines is described in the following chapters of this thesis.

3.4. Elucidation of the physiological significance of the interaction between NRT1.5 and the proton pump, AHA2

3.4.1. AHA2 contributes in K⁺ root-to-shoot translocation under low nutrition supply

To investigate if NRT1.5 and AHA2 physical interaction has involvement in K⁺ root-to-shoot translocation in Arabidopsis, the double mutant *nrt1.5/aha2* was phenotypically analyzed. Col-0, *nrt1.5*, *aha2*, and *nrt1.5/aha2* plants were grown under different NO₃⁻/K⁺ regimens as described in

Drechsler et al., 2015. In all plant lines including Col-0, early shoot chlorosis accompanied by yellow leaf tips and pale green inner rosette leaves occurred only on low fertilized soil (1mM K^+ /1mM NO_3^-) (**Figure 16A**), and all plants showed a reduction in the fresh weight at these conditions in comparison with high fertilized soil (10mM K^+ /10mM NO_3^-) (**Figure 16C**), suggesting that the leaf chlorosis phenotype of plants and the reduction of weight were due to the low K^+ and NO_3^- contents in the soil. *nrt1.5* and *nrt1.5/aha2* mutants are the most affected with 63% and 75% of the leaf surface having lesions respectively, whereas Col-0 and *aha2* showed around 30% lesions (**Figure 16B**).

The lack of *AHA2* does not cause an obvious shoot phenotype under the different treatments, however, the lack of both *AHA2* and *NRT1.5* showed a slight increase (not statistically significant) in the % of lesions in leaves, demonstrating a possible functional interaction of *NRT1.5* and *AHA2* under low fertilized soil conditions.

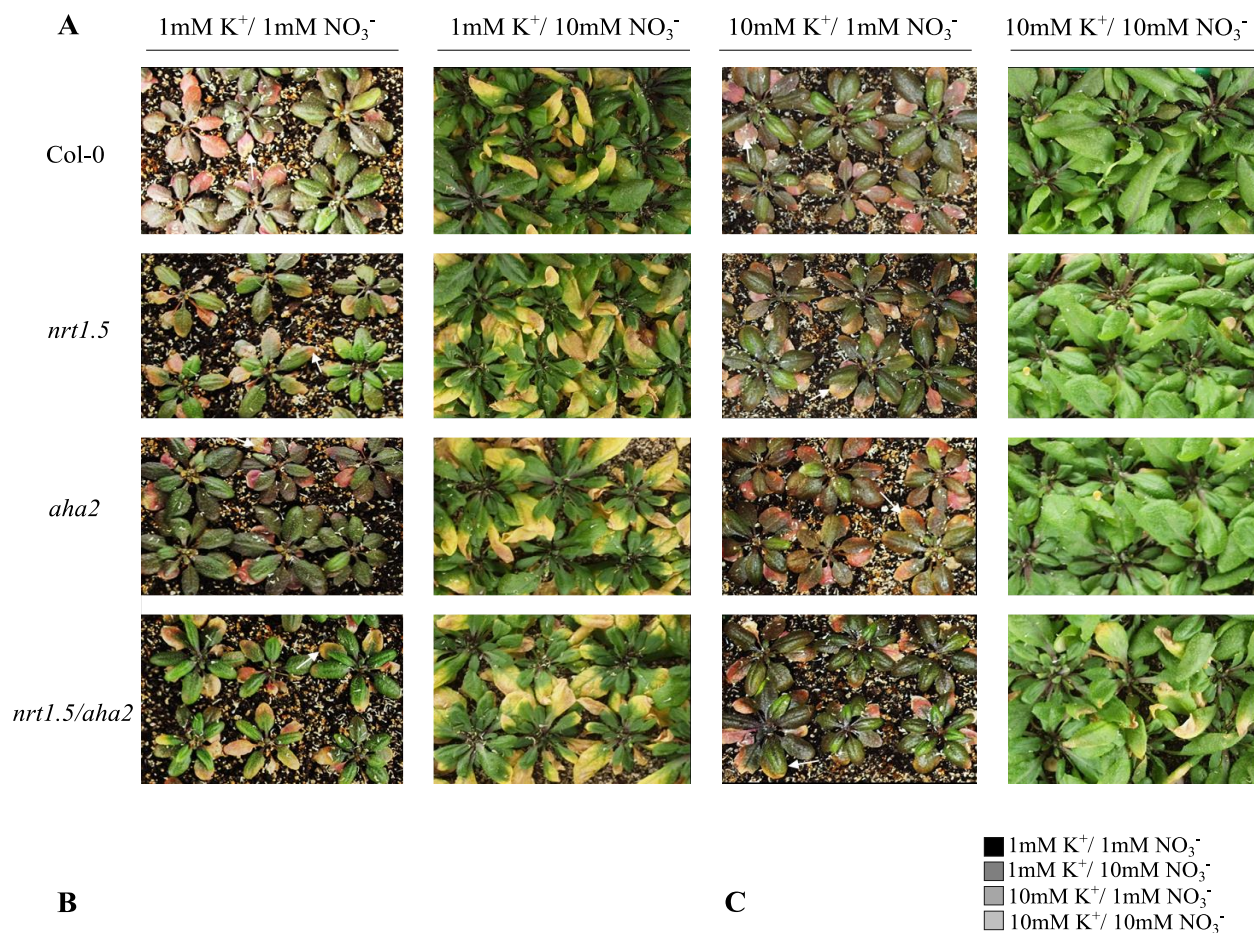


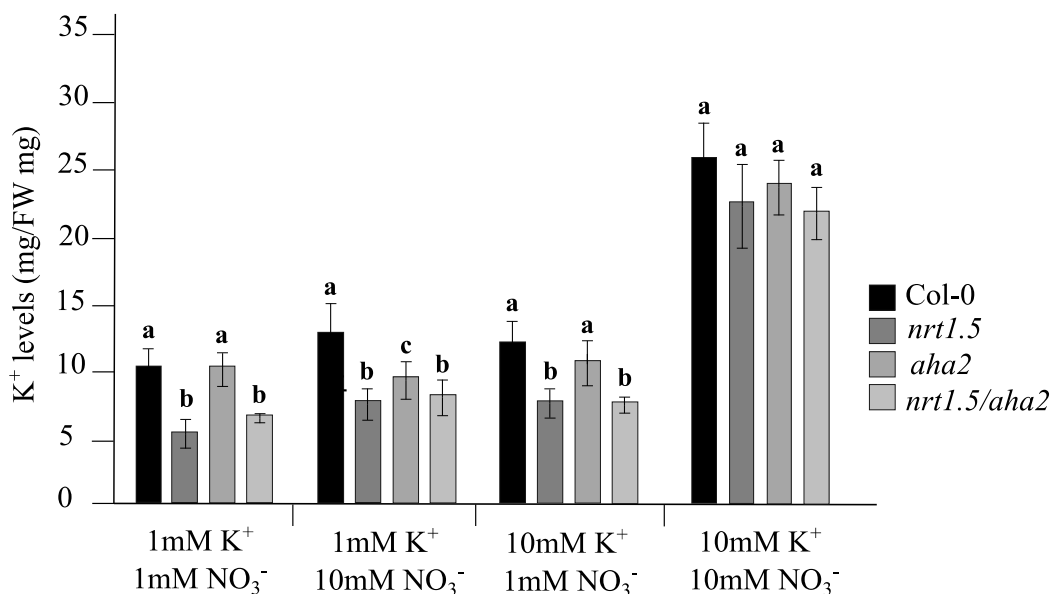
Figure 16: Shoot phenotypes of Col-0, *nrt1.5*, *aha2*, and *nrt1.5/aha2* under different K⁺/NO₃⁻ supplies. **A.** Col-0, *nrt1.5*, *aha2*, and *nrt1.5/aha2* plants were pre-germinated in fertilized soil for seven days and later transferred to unfertilized soil type and watered with different nitrate and potassium concentration regimens (see solution composition on Supplementary Table 1) for thirty days further. White arrows show leaf lesions. **B.** % of leaf lesions from treatments in A. **C.** Rosette fresh weight (FW) of Col-0, *aha2*, *nrt1.5*, and *nrt1.5/aha2* plants from treatments in A. Different letters indicate statistically significant differences (Tukey's test) between mutants and Col-0 with $P < 0.05$, (means \pm SD, n=8).

To uncover cross-talk between macronutrient and micronutrient homeostasis in plants, the macronutrients Calcium (Ca), Magnesium (Mg), Phosphorus (P), Potassium (K), and Sulphur (S), and the micronutrients Boron (B), Manganese (Mn), Zinc (Zn), and Aluminum (Al) were measured in Col-0, *nrt1.5*, *aha2*, and *nrt1.5/aha2* plants by inductively coupled plasma optical emission spectrometry (ICP-OES) under different potassium and nitrate concentrations in the medium. It is speculated that the deficiency or excess of K^+ or NO_3^- could cause imbalances between the uptake and translocation to shoots of other macronutrients or micronutrients.

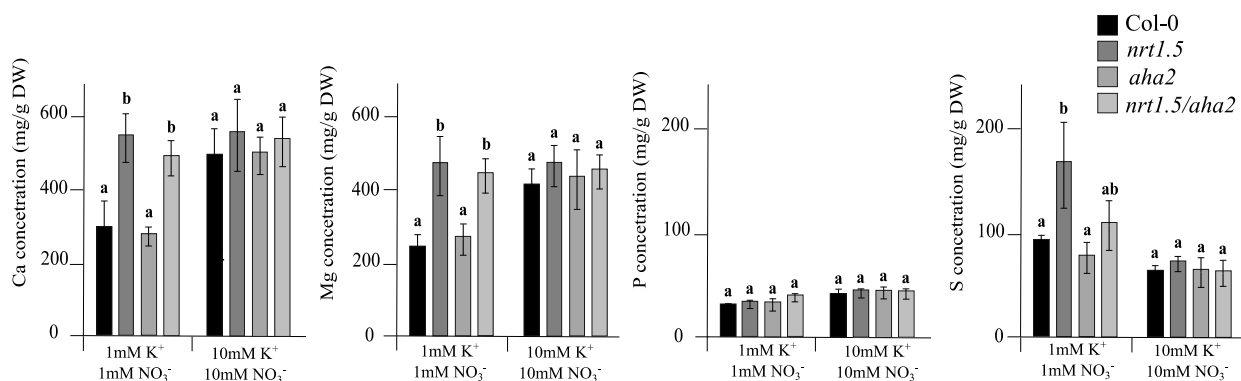
Most of the macronutrient contents were increased in *nrt1.5* and *nrt1.5/aha2* leaves (**Figure 17B**) except for K^+ where the levels decreased under low fertilization conditions (1mM K^+ /1mM NO_3^-) (**Figure 17A**). The deficiency of K^+ in shoots of *nrt1.5* and *nrt1.5/aha2* mutants detected here, explains the early senescence phenotype (**Figure 15A**) in the same conditions since deficiency of K^+ in shoots triggers early senescence phenotypes (Armengaud et al., 2004; Li et al., 2012; Meng et al., 2016). The *aha2* mutant showed the same K^+ levels compared with Col-0 in all conditions except under low K^+ and high NO_3^- supply (1mM K^+ /10mM NO_3^-) where the K^+ reduction in *aha2* mutant was statistically significant in comparison with wild-type (**Figure 17A**).

K^+ deficiency is often accompanied by increased tissue concentrations of other cationic elements, which are partially compensating for the charge imbalances in the plant (Drechsler et al., 2015). Indeed, a remarkable increase mainly in the two macronutrients Ca (1.8- to 1.6-fold) and Mg (1.8- to 1.7-fold) was observed in leaves of *nrt1.5* and *nrt1.5/aha2* plants, respectively under low fertilization conditions. The *aha2* mutant showed no changes in comparison with Col-0 (**Figure 17B**). Under high fertilization conditions no changes in macronutrient or micronutrient contents were detected (**Figure 17B and C**).

A



B



C

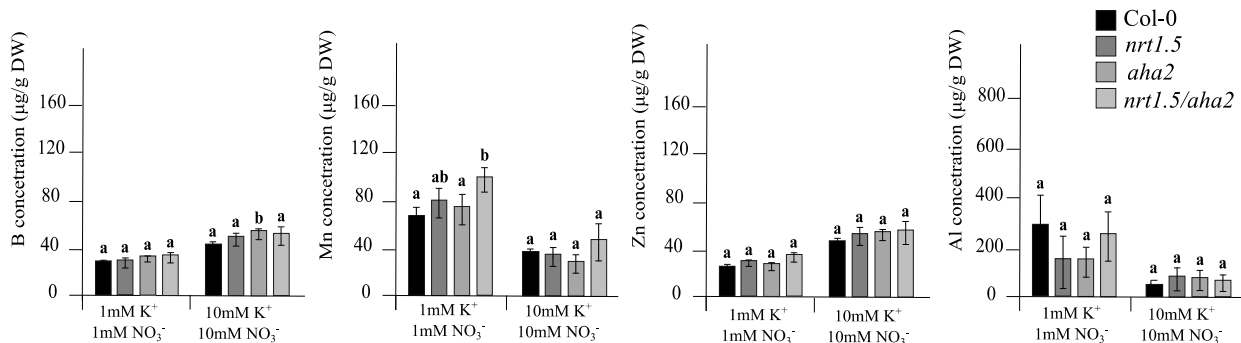


Figure 17: Elemental analysis of Col-0, *nrt1.5*, *aha2*, and *nrt1.5/aha2* leaves in different K⁺ and NO₃⁻ regimens by ICP-OES. **A.** K⁺ levels (mg/FW mg) in Col-0, *nrt1.5*, *aha2*, and *nrt1.5/aha2* shoots. Plants were pre-germinated in fertilized soil for seven days and later transferred to unfertilized type soil and watered with different K⁺ and NO₃⁻ regimens for thirty days further. **B.** Macronutrients and **C.** Micronutrients measurement in shoots of Col-0, *nrt1.5*, *aha2*, and *nrt1.5/aha2* from A. Here only 1mM

$K^+/1mM NO_3^-$ and $10mM K^+/10mM NO_3^-$ regimens are represented. Different letters indicate statistically significant differences (Tukey's test) between mutants and Col-0 with $P < 0.05$, (means \pm SD, $n=8$).

These results indicate that AHA2 affects the K^+ root-to-shoot translocation only at low potassium (1mM) and high (10mM) of nitrate conditions, however, the reduction of K^+ levels was low and no visible phenotype was observed in shoots of *aha2* mutant. A possible explanation could be the redundancy of the AHA family. From the 11 family members of H^+ ATPases in *A. thaliana* (Table 3), AHA2 plays a major role in the root epidermal cells but AHA1, AHA4, AHA7, and AHA11 expression were found in roots as well (Gaxiola et al., 2007).

3.4.2. NRT1.5 and AHA2 are involved in the modulation of root architecture under low nutrition supply

NRT1.5 and *AHA2* are mainly expressed in the root pericycle cells (Fuglsang et al., 2007; Lin et al., 2008). To test if AHA2 is involved in the modulation of the root architecture together with NRT1.5, a root growth test was carried out in *aha2* and *nrt1.5/aha2* mutants under different nutritional supplies. First, Col-0, *nrt1.5*, *aha2*, and *nrt1.5/aha2* were grown in MS medium for five days and then transferred into low ($0mM K^+/1mM NO_3^-$) or high ($10mM K^+/10mM NO_3^-$) nutrition supply. Reduction of root density in *nrt1.5* mutants under $0mM K^+/1mM NO_3^-$ medium was observed, supporting earlier findings (Zheng et al., 2016). Interestingly, *aha2* and *nrt1.5/aha2* double mutant showed also a significant reduction in lateral root density in comparison to wild type. Another observation is that the reduction in the root density in the mutants is directly related to no formation of new lateral roots after the transfer to low nutrition supply conditions (Figure 18A and B). Moreover, the root hair architecture of plants was qualitatively checked and clear differences in root hair formation were observed at $0mM K^+/1mM NO_3^-$ supply in comparison with roots at high nutrition conditions. A reduction of root hairs in all mutants in comparison with Col-0 was observed, at low nutrition supply where the double mutant *nrt1.5/aha2* was the most affected (Figure 18C). This indicates that AHA2 expression in roots is important for the root architecture under $0mM K^+/1mM NO_3^-$.

Finally, another phenotype in the seedlings was observed. Shoots of all mutants, *nrt1.5*, *aha2*, and *nrt1.5/aha2* developed a chlorosis phenotype in the cotyledons at low nutrition supply after a week of growth (Figure 18D). This data in an early developmental phase of the plant growth demonstrate

3. Results

a potential link of NRT1.5 and AHA2 with root architecture development and K^+ root-to-shoot translocation in a K^+/NO_3^- dependent manner.

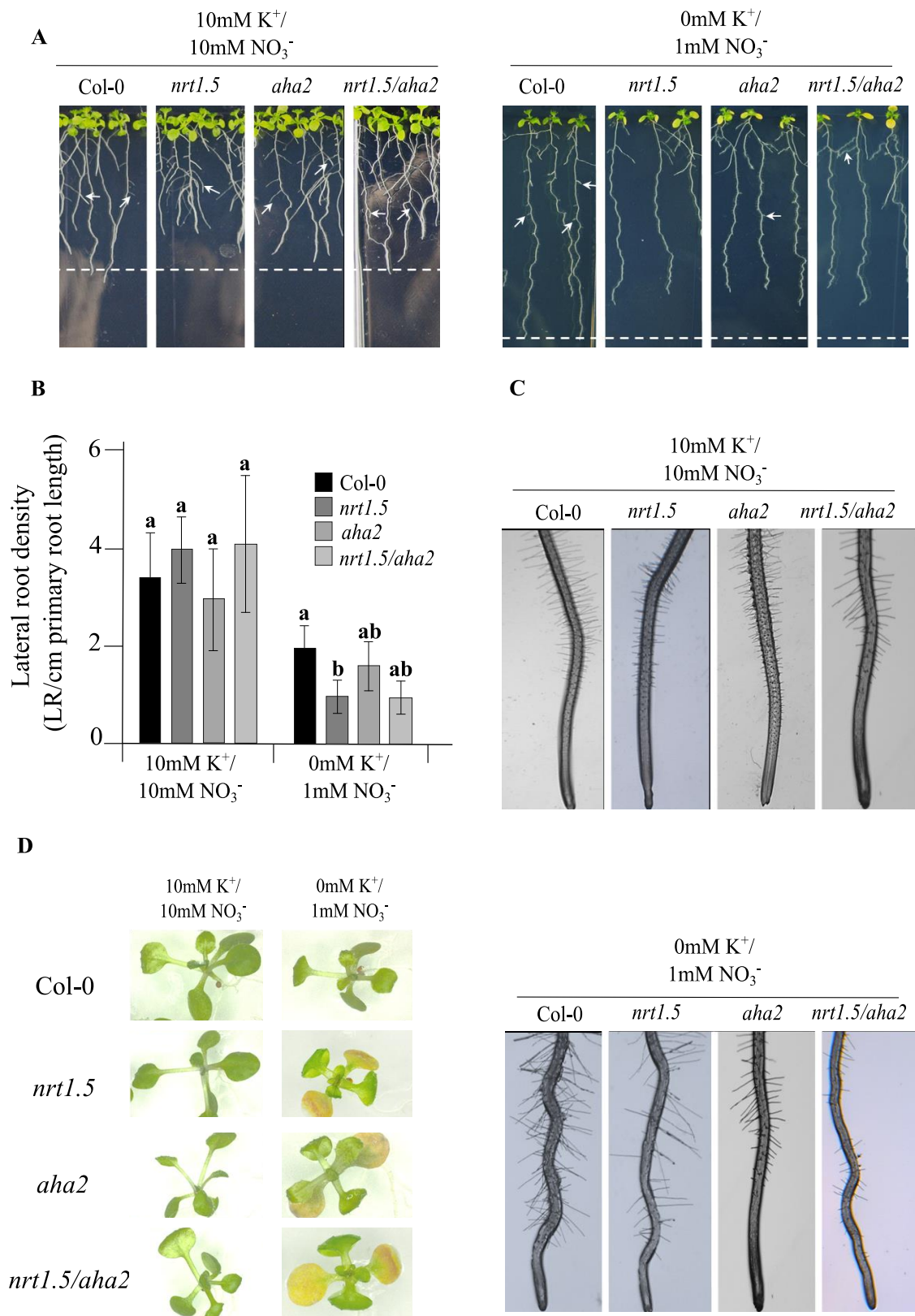


Figure 18: Phenotypes of Col-0, *nrt1.5*, *aha2*, and *nrt1.5/aha2* seedlings at low (0mM K⁺/1mM NO₃⁻) or high (10mM K⁺/10mM NO₃⁻) nutritional supply. **A.** Root phenotypes. Seedlings were pre-germinated in MS medium for five days and then transferred to 0mM K⁺/1mM NO₃⁻ or 10mM K⁺/10mM NO₃⁻ media for fourteen days further. White arrows show lateral root formation. Dashed lines represent the maximum primary root growth of Col-0 in each condition. **B.** Quantification of the density of lateral roots from A. The number of lateral roots formed/main length of the primary root was plotted as lateral root density. Different letters indicate statistically significant differences (Tukey's test) between mutants and Col-0 with $P < 0.05$, (means \pm SD, n=12). **C.** Root hair phenotypes of seedlings in A. **D.** Shoot phenotypes of seedlings in A after a week of growth in the conditions indicated.

3.4.3. NRT1.5 and AHA2 are not functional as a K⁺ sensors

To assess if NRT1.5 and AHA2 interaction has a role in K⁺ sensing in *Arabidopsis thaliana*, root growth assays were conducted in *nrt1.5*, *aha2*, and *nrt1.5/aha2* mutants. The growth of the root system in response to the external concentration of nutrients is a joint operation of sensor or receptor proteins. The primary root growth of wild-type plants is often affected by low nutrition supply, while mutants affected in sensor proteins could maintain unaffected the primary root growth (Li et al., 2017b). If NRT1.5 and AHA2 are involved in K⁺ sensing, the root growth might differ in the knockout mutant *nrt1.5* and *aha2* in comparison to Col-0. When wild-type and mutant seedlings were transferred from MS to 0mM K⁺/1mM NO₃⁻ media, the primary root growth was enhanced in all plants (**Figure 19A**). Usually, when plant roots spot a low K⁺ region they stop the growth, whereas N deficiency stimulates the growth of a more exploratory root system with longer lateral roots (Gruber et al., 2013). The nutritional conditions used here are a combination of K⁺ deprivation and low NO₃⁻ supply, suggesting that the enhanced root growth (**Figure 19A**) is attributed to this combination.

Moreover, to determine if NRT1.5 and AHA2 have a role in sensing the local K⁺ and NO₃⁻ levels, a split-root assay was performed. Two different primary roots from the same seedling were placed either in MS or 0mM K⁺/1mM NO₃⁻. The primary root growth of wild-type, *nrt1.5*, *aha2*, and *nrt1.5/aha2* plants was enhanced in 0mM K⁺/1mM NO₃⁻ in contrast with MS medium after a week of treatment, indicating that the roots were able to sense the lack of nutrients (**Figure 19B**). This shows that NRT1.5 and AHA2 are not correlated with K⁺ and NO₃⁻ sensing since their lack (in *nrt1.5*, *aha2*, and *nrt1.5/aha2* mutants) did not show phenotypes in the split root assay.

Finally, cesium chloride (CsCl) was used as a K^+ transport blocker to impede the K^+ root uptake. If NRT1.5 and AHA2 proteins are involved in K^+ perception, the loss of function mutants *nrt1.5* and *aha2* should not be affected by CsCl treatment. The addition of $15\mu\text{M}$ CsCl in MS medium did not affect the root growth of all tested plants. Even 2mM CsCl did not impair root growth (data not shown). However, under 0mM K^+ and 1mM NO_3^- supply, the application of $15\mu\text{M}$ CsCl inhibited the primary root and lateral root growth of all plants. Under these conditions, more than $15\mu\text{M}$ CsCl is lethal for plants (data not shown). The double mutant *nrt1.5/aha2* showed a visible reduction in lateral root and root length growth in comparison with wild-type and single mutants (**Figure 19C**).

These data indicate that neither NTR1.5 nor AHA2 are required for perception of external K^+ or NO_3^- since seedlings are still able to sense and respond to deficiency of K^+ and NO_3^- , modulating the root growth accordingly. Nevertheless, the root phenotype of double mutant *nrt1.5/aha2* when K^+ uptake is blocked by CsCl suggests that both NRT1.5 and AHA2 may influence the root development in dependency of the K^+ status in roots.

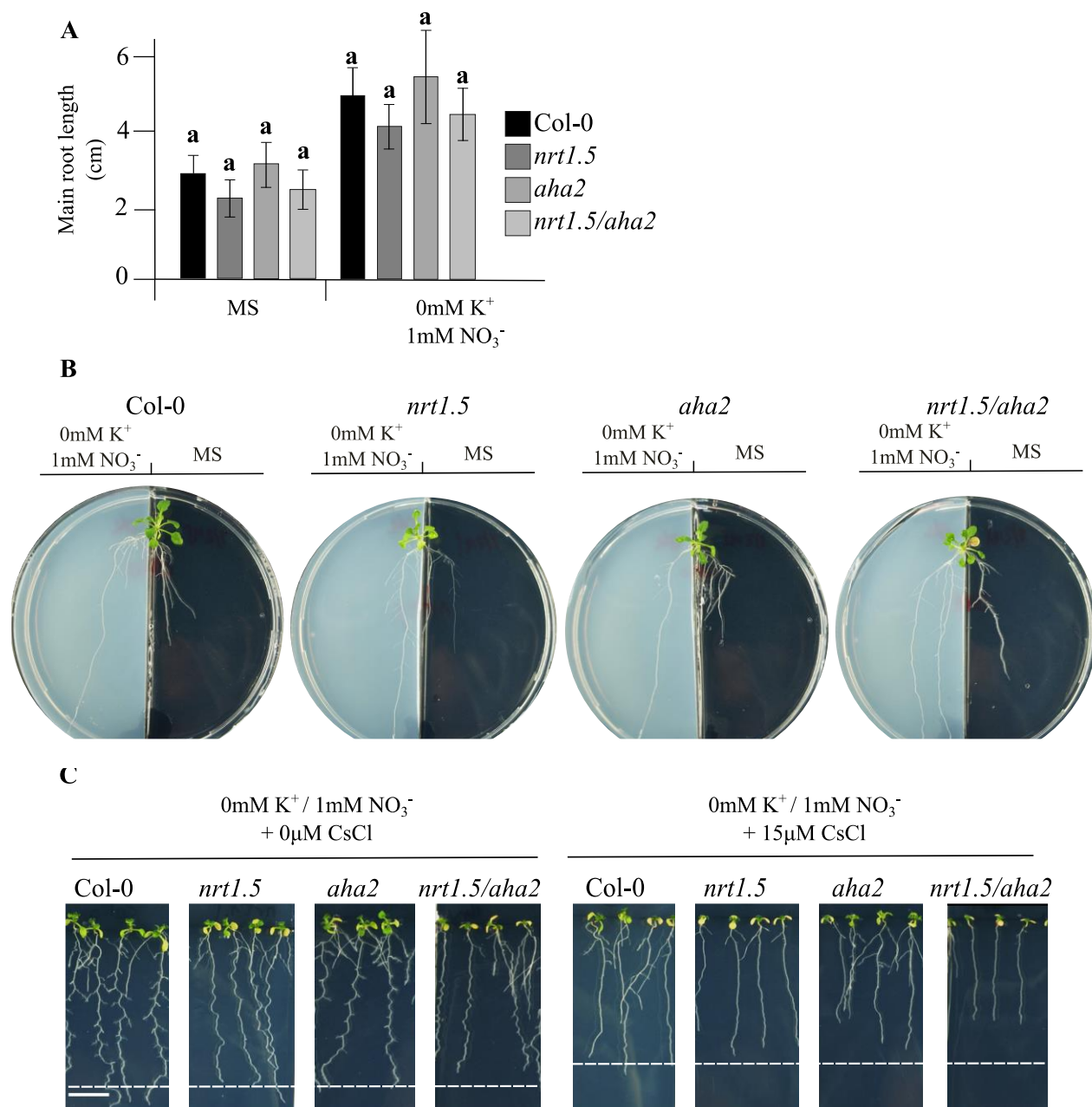


Figure 19: Nutrient perception of the primary roots of Col-0, *nrt1.5*, *aha2*, and *nrt1.5/aha2* plants. **A.** Primary root length. Five days-old seedlings were transferred from pre-germination in MS medium to 0mM K⁺/1mM NO₃⁻ or MS plates for seven days further. The main root length was measured and plotted. Different letters indicate statistically significant differences (Tukey's test) between mutants and Col-0 with $P < 0.05$, (means \pm SD, $n=12$). **B.** Split root assay. Ten days-old seedlings with the induction of two primary roots (see material and methods section 2.2.11) were transferred from MS medium to a split plate with 0mM K⁺/1mM NO₃⁻ in one side (left) and MS medium on the other (right). The two primary roots were placed on each side. After growing for seven more days, the photographs were taken. **C.** Root phenotypes after treatment with a K⁺ uptake blocker. Seedlings were pre-germinated in MS medium for five days and then

transferred to MS or 0mM K⁺/1mM NO₃⁻ medium with or without 15μM of the K⁺ transport blocker CsCl for seven days further. The white bar represents 1cm, and dashed white lines represent the maximum root growth of Col-0 in each CsCl treatment.

3.4.4. NRT1.5 and AHA2 are ion transporters involved in plasma membrane depolarization in *Arabidopsis thaliana* and *Saccharomyces cerevisiae*

Ion homeostasis in plant cells depends on the coordinated action of multiple ion transporters and channels at the plasma membrane of plant cells. Together, proton and ion pumps, nutrient cotransporters, and channels determine ionic cellular distribution, which is critical for the maintenance of membrane potential, pH control, and the transport of nutrients (Sze and Chanroj, 2018). Higher plant cells have a steep electrical gradient ($\Delta\psi$) of about -150 to -250 mV (negative inside) and a pH gradient (ΔpH) of 1.5 to 2 (acidic outside) across the plasma membrane. Since NRT1.5 and AHA2 are both involved in ion transport, the hypothesis about an interplay between them to maintain the ΔpH and $\Delta\psi$ homeostasis across the plasma membrane was addressed. The next chapters describe how the lack or overexpression of *NRT1.5* and *AHA2*, in *Arabidopsis* and yeast cells respectively, influences the plasma membrane potential and the extracellular pH.

The uptake of the toxic cationic drug HygB is dependent on the membrane potential in yeast and plants. Cells sensitivity to HygB is often linked to changes in the plasma membrane potential, which can be provoked by alterations in K⁺ homeostasis in *S. cerevisiae* (Barreto et al., 2011) or alterations in H⁺ homeostasis in *Arabidopsis thaliana* (Haruta and Sussman, 2012).

Here, a HygB sensitivity test in Col-0, *nrt1.5*, *aha2*, and *nrt1.5/aha2* seedlings was carried out to examine the plasma membrane potential. The growth of Col-0 seedlings is extremely sensitive to 5μg/mL HygB, whereas *nrt1.5*, *aha2*, and *nrt1.5/aha2* mutants are resistant (**Figure 20**). These observations strongly imply that the lack of *NRT1.5* and *AHA2* indeed influences the plasma membrane potential.

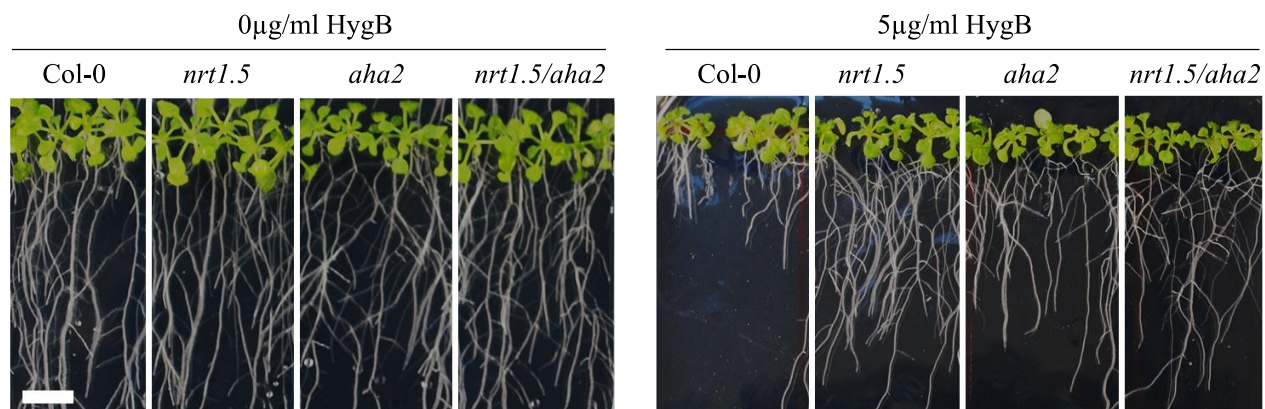


Figure 20: Hygromycin B sensitivity of Col-0, *nrt1.5*, *aha2*, and *nrt1.5/aha2* seedlings. Seedlings were pre-germinated in MS medium for seven days before transfer to MS medium supplemented with or without 5 μ g/ml HygB for another fifteen days. The white bar represents 1cm.

The overexpression of *NRT1.5* in yeast cells causes hyperpolarization of the yeast plasma membrane in the K⁺ uptake deficient mutant BYT12, indicating that *NRT1.5* is active in yeast cells and influences the plasma membrane potential (Drechsler et al., 2015).

To investigate whether *NRT1.5* and *AHA2* influence the plasma membrane potential in this yeast expression system, both genes were co-expressed in wild-type BY4741 and mutant BYT12 cells. Subsequently, the yeast growth was monitored in plates containing a HygB gradient and high K⁺ content (0.1M) to support the BYT12 mutant growth (**Figure 21**). The overexpression of the *NRT1.5*^{G209E} mutant was included in the assay to see the impact of the mutation in the yeast system. The expression of *NRT1.5*, *NRT1.5*^{G209E}, and *AHA2* did not influence the growth of BY4741 and BYT12 cells in the absence of HygB and 0.1M KCl (**Figure 21A**). Under a HygB gradient up to 5 μ g/ml the expression of *NRT1.5* in BYT12 cells induced hypersensitivity to high HygB concentrations, as previously reported by Drechsler et al., 2015, and the mutant *NRT1.5*^{G209E} showed a modest growth recovery to the BYT12 phenotype, indicating the mutation might be avoiding the K⁺ translocation in the yeast system (**Figure 21B**).

Moreover, expression of *AHA2* in BYT12 cells resulted in a strong HygB sensitivity compared to BYT12 cells with the empty vectors and even with *NRT1.5* expression, proving that the plasma membrane potential is strongly influenced by the expression of *AHA2*. To test for an interaction of *NRT1.5* and *AHA2*, both were co-expressed in BYT12 cells. Yeast growth of the double transformant was indistinguishable from the single transformant with *AHA2*, indicating no direct influence of *NRT1.5* in *AHA2* (**Figure 21B**).

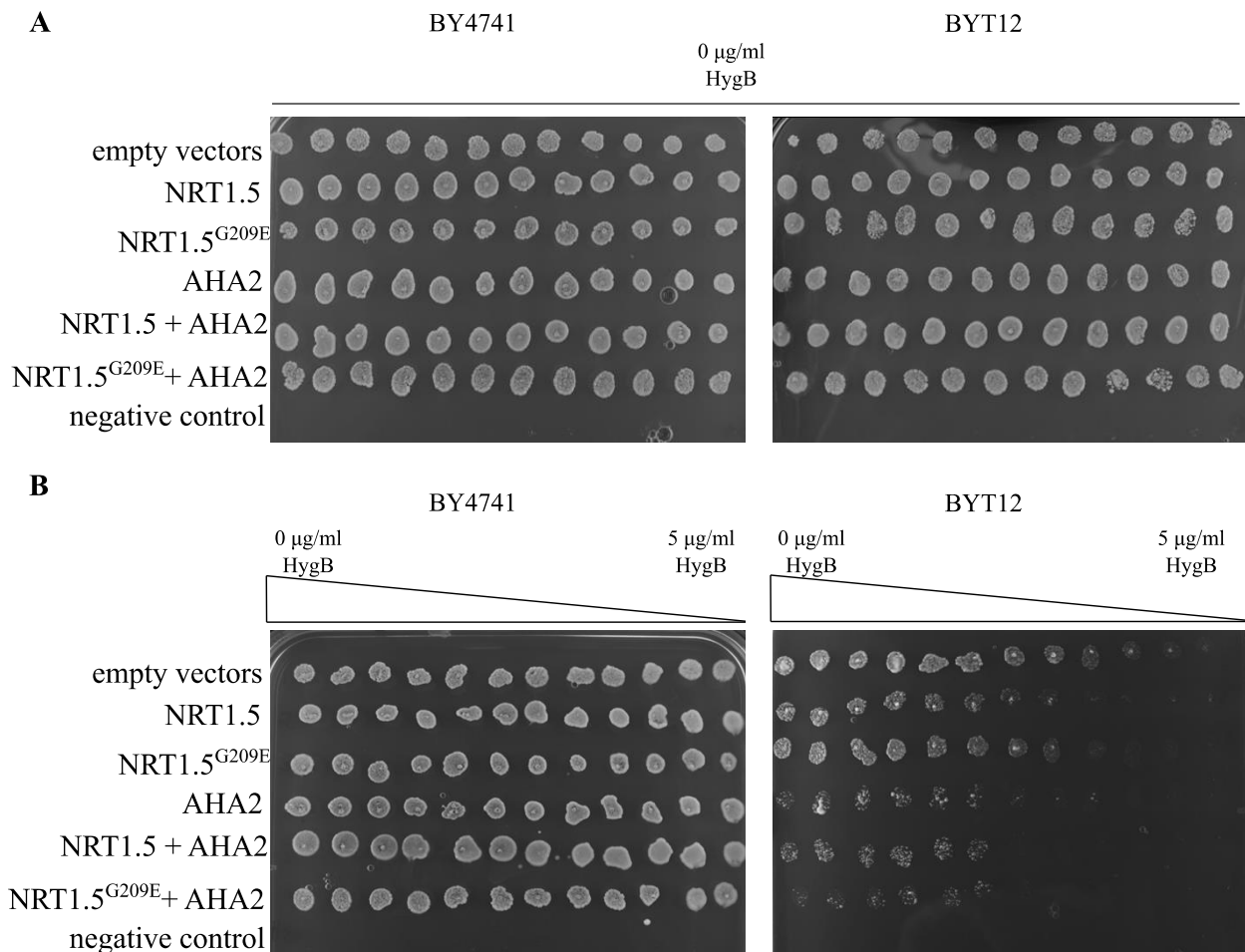


Figure 21. Hygromycin B sensitivity test in different yeast cells overexpressing NRT1.5, NRT1.5^{G209E}, and AHA2. BY4741 wild-type, and BYT12 mutant strains were transformed with the expression constructs indicated on the left (under *TEF* promoter expression). Twelve drops of each transformed yeast cell suspension ($OD_{600nm} = 1$) were distributed in YNB pH= 5.5 (-Leu -Ura) plates containing 0.1M KCl and 0µg/ml HygB (**A**) or a HygB gradient from 0 to 5µg/ml (**B**). Plates were incubated at 30°C for two days. The negative control was water. Representative pictures of six independent experiments are shown.

3.4.5. NRT1.5 and AHA2 mediate changes in extracellular pH at low nutrition supply in *Arabidopsis thaliana*

NRT1.5 promotes K^+ release out of the root cells into the xylem vessels at external acidic pH conditions as in the xylem sap (Li et al., 2017a), and AHA2 is the major plasma membrane proton pump in root cells (Haruta et al., 2010) (**Figure 22A**). Since cellular pH homeostasis is maintained by the concerted activity of different players (see introduction 1.4.2), pH measurement was

conducted in Col-0, *nrt1.5*, *aha2*, and *nrt1.5/aha2* seedlings to investigate if NRT1.5 and AHA2 cooperatively control the cellular pH.

The fluorescent dye, fluorescein isothiocyanate-dextran (FITC-dextran) was used to measure the extracellular pH in roots of *A. thaliana* seedlings. The dye specificity for the extracellular space is due to the inability of FITC-dextran to penetrate the plasma membrane (Hoffmann and Kosegarten, 1995). FITC-dextran has been widely used to visualize pH changes at the root surface in *Arabidopsis* (Haruta et al., 2010; Haruta et al., 2018), and the sensitivity of the dye is comparable with a pH-sensitive microelectrode (Pitann et al., 2009). Here, the extracellular pH of wild-type, *nrt1.5*, *aha2*, and *nrt1.5/aha2* roots was determined under two nutritional conditions: under high (10mM K⁺/10mM NO₃⁻) or low (0mM K⁺/1mM NO₃⁻) nutrition supplies.

At high-nutrition supply, the extracellular pH of Col-0 and the *nrt1.5* mutant roots were similar with pH≈5.35 but *aha2* and *nrt1.5/aha2* mutants showed a slight but significant increase to pH≈5.5 (Figure 22B). This data indicates that the lack of *AHA2* influences the external pH values.

Wild-type roots showed a reduction in extracellular pH to pH≈4.9 at 0mM K⁺/1mM NO₃⁻, supporting that low nutrition supply induces acidification of the extracellular space (Behl and Raschke, 1987), whereas the *nrt1.5*, *aha2*, and *nrt1.5/aha2* mutants were unable to reduce the pH like Col-0. The *nrt1.5/aha2* double mutant was the most affected (Figure 22B). These data show that both NRT1.5 and AHA2 contribute to the pH maintenance under K⁺ deprivation and low NO₃⁻ supply.

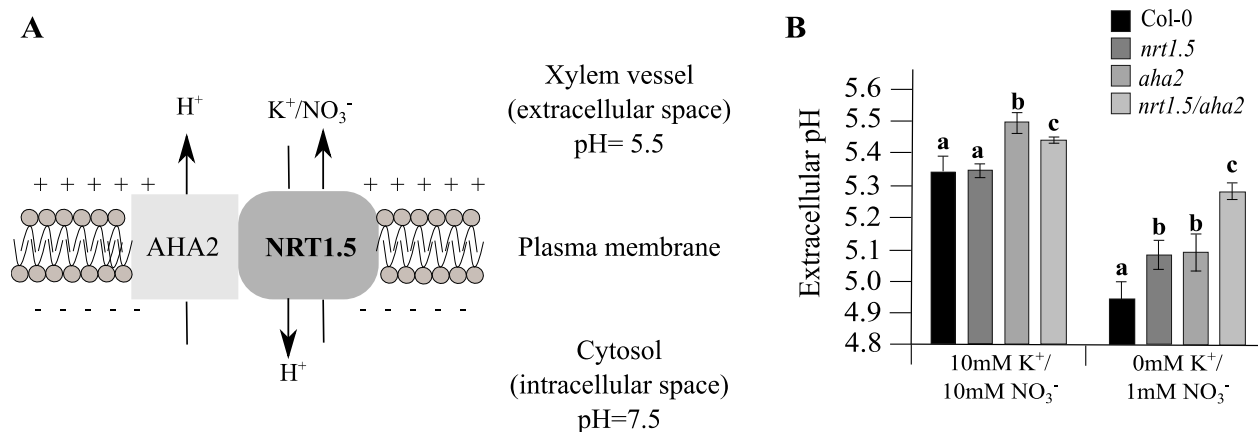


Figure 22: Extracellular pH measurement in Col-0, *nrt1.5*, *aha2* and *nrt1.5/aha2*. **A.** Representation of NRT1.5 and AHA2 interaction in the plasma membrane of pericycle cells in plant roots. Under physiological conditions, the intracellular pH is slightly alkaline (pH≈ 7.4-7.5) and the extracellular pH in xylem vessels is slightly acidic (pH≈ 5.5). The plasma membrane is charged negatively in the intracellular space (-) and less negatively in the extracellular space (+). **B.** Extracellular pH measurements in Col-0, *nrt1.5*, *aha2*, and

nrt1.5/aha2 roots under high (10mM K⁺/10mM NO₃⁻) and low (1mM K⁺/0mM NO₃⁻) nutrition supply. Seedlings were pre-germinated in MS medium for five days and then transferred to a modified MS medium with 10mM K⁺/10mM NO₃⁻ or 0mM K⁺/1mM NO₃⁻ for another five days. The ten days-old seedlings were incubated with 1/4MS liquid medium supplemented with 30μg/ml of FITC-dextran overnight at room temperature. Media pH was obtained by the fluorescence of a standard curve with a pH range from 4 to 7.4. Different letters indicate statistically significant differences (Tukey's test) between mutants and Col-0 with $P < 0.05$, (means \pm SD, n=10).

3.4.6. *NRT1.5* and *AHA2* expression in *Saccharomyces cerevisiae* is not directly correlated with K⁺ export function under acidic conditions

Expression of *NRT1.5* in a yeast mutant strain lacking the endogenous K⁺ export systems *ENA1* and *NHA1* (so-called BYT45) did not complement the defective growth of the mutant at pH=6 and high K⁺ conditions (Drechsler et al., 2015), indicating that *NRT1.5* itself is not able to export K⁺. Since *NRT1.5* was described as a K⁺ transporter at pH=5.5 (Li et al., 2017a), the failure in complementation by *NRT1.5* could be explained if *NRT1.5* was not fully functional in yeast cells because the growth conditions regarding pH were not optimal, or also if *NRT1.5* requires activation by auxiliary proteins to be functional in the yeast system. To investigate if changes in extracellular pH can influence the K⁺ export activity of *NRT1.5*, the co-expression in the absence or presence of *AHA2* was carried out in the yeast mutant BYT45 at acidic or basic conditions. Yeast growth was assayed in a high-K⁺ medium (1M KCl) to force cells to export the high levels of K⁺. The main export K⁺ channel in roots, *SKOR* served as positive control and was able to induce the growth of the defective BYT45 yeast background, indicating that *SKOR* has a K⁺ export function and detoxified the BYT45 cells. The *NRT1.5* and *AHA2* expression were not able to restore the growth retardation of BYT45 cells in a medium containing 1M KCl either at acidic or basic conditions. Finally, to test for an interaction of *NRT1.5* and *AHA2*, both proteins were co-expressed in BYT45 cells. Yeast growth of the double transformant was indistinguishable from the single transformants, indicating no direct influence of *AHA2* in the K⁺ export function of *NRT1.5* under these conditions in yeast (**Figure 23**).

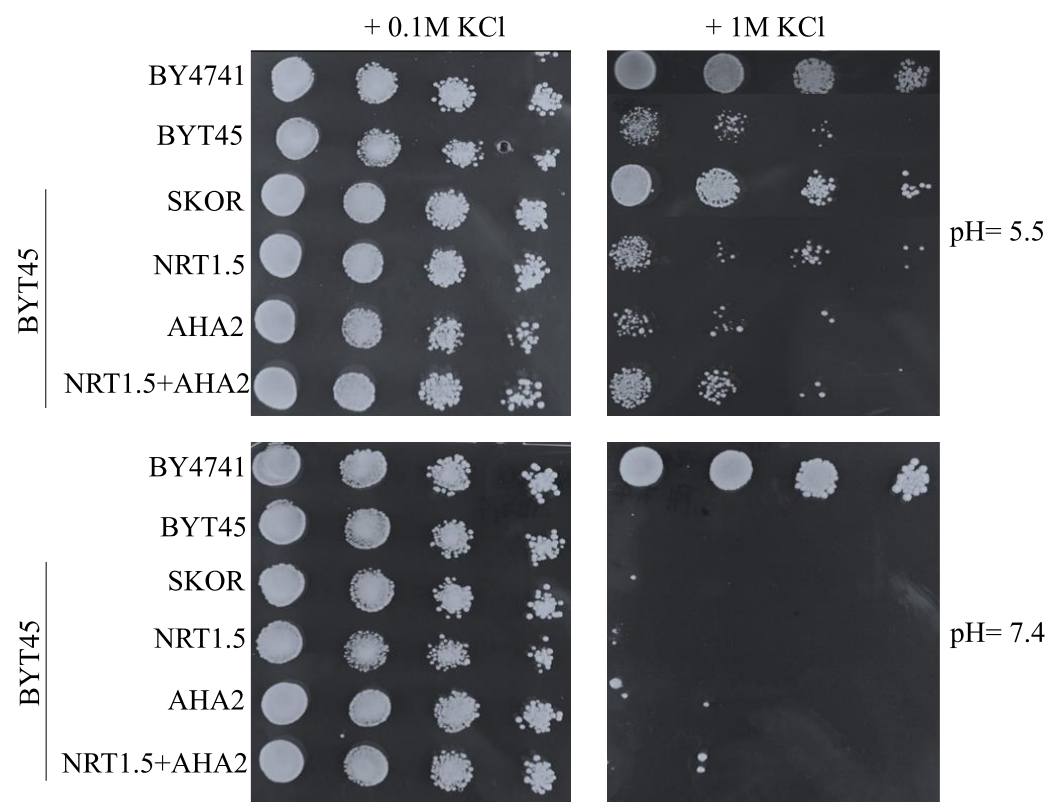


Figure 23: Functional analysis of *NRT1.5* and *AHA2* in yeast. Potassium export ability was analyzed in the defective *S. cerevisiae* K^+ export mutant BYT45 (*ena1* and *nha1*). Cells were transformed with the expression constructs indicated on the left under the expression of the *TEF* promoter. Cell suspensions from $OD_{600nm} = 10^{-2}$ to 10^{-5} were dropped in YNB (-Ura -Leu) agar plates supplemented with 0.1 or 1M KCl at acidic (pH=5.5) or basic (pH=7.4) conditions. Plates were grown for two days at 30°C. BY4741 wild-type strain transformed with empty vectors was used as a control.

In *S. cerevisiae*, the K^+/H^+ antiporter encoded by *NHA1* and the Na^+/K^+ -ATPase encoded by *ENA1* are responsible for the cytosolic detoxification of cations, maintenance of stable intracellular K^+ concentrations, and control of pH levels (Ariño et al., 2010). To investigate if the expression of *NRT1.5* and *AHA2* in *S. cerevisiae* is functional in the H^+ transport, the extracellular pH was measured when BYT45 cells (lacking *NHA1* and *ENA1*) express *NRT1.5* and *AHA2*.

Supplementation with 0.1M or 1M KCl in yeast medium did not cause growth differences between the BYT45 cells expressing *NRT1.5* and *AHA2* (**Figure 23**). However, the extracellular pH measurements showed that the expression of *NRT1.5* and *AHA2* in the wild type BY4741 and BYT45 mutant are affecting the extracellular pH. This data demonstrates that *NRT1.5* and *AHA2* are expressed and the proteins are active in yeast (**Figure 24**). Overall, BYT45 mutant background either at 0.1 or 1M KCl had an increase of pH in comparison to the wild-type BY4741, suggesting

that the extracellular space of BYT45 cells is less acid than the wild type, most likely as a result of the defective K^+ and H^+ transport activity. Interestingly, the single and double expression of *NRT1.5* and *AHA2* in BYT45 cells affected the pH to more acid levels either at 0.1 or 1M KCl, a tendency to restore wild-type values.

This data shows that *NRT1.5* and *AHA2* are expressed, functional, and capable to control the cellular pH in the heterologous expression system.

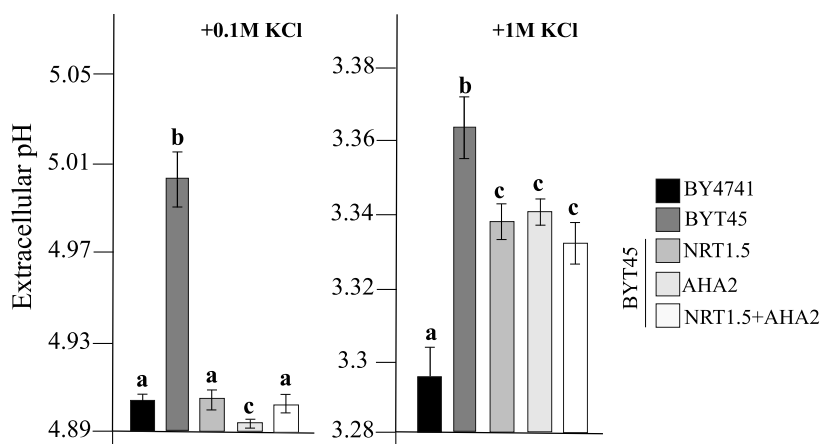


Figure 24: Extracellular pH measurements of *NRT1.5* and *AHA2* expression in yeast. Cultures of BYT45 mutant cells (*enal* and *nha1*) expressing *NRT1.5* and *AHA2* in liquid YNB (-Leu -Ura) medium supplemented with 0.1M or 1M KCl (pH=5.5) were incubated at 30°C, 220rpm overnight. Overnight cultures were adjusted to $OD_{600nm}=1$ and supernatants were incubated with 30 μ g/ml FITC-dextran. pH was obtained from the fluorescence of a standard curve of YNB medium with a pH range from 3 to 6. Different letters indicate statistically significant differences (Tukey's test) between mutants and Col-0 with $P < 0.05$, (means \pm SD, n=10).

3.4.7. *NRT1.5* and *AHA2* protein-protein interaction depends on the K^+ and H^+ transport activity respectively

NRT1.5 and *AHA2* protein-protein interaction was identified by the split-ubiquitin system in *S. cerevisiae* (Drechsler, 2016) and confirmed by BiFC in *N. benthamiana* (Figure 12 and Zheng, 2018). These studies did not offer further details of the protein-protein interaction binding sites. To investigate the potential amino acid residues or motifs involved in the protein-protein interaction, different mutant versions of *NRT1.5* and *AHA2* were created. The protein structure representations and the position of each mutation are represented in Figure 25A.

Leucine-rich repeats (LRR) serve as platforms that mediate specific protein-protein interactions (Kobe and Kajava, 2001). Based on that, the analysis of the NRT1.5 protein sequence by web-based tools was carried out to identify repeated sequences (<https://www.ebi.ac.uk/Tools/pfa/radar/>) and specifically LRR repeats (LRRfinder). Three highly conserved protein repeats (I, II, and III) were identified and each of them contained a potential LRR motif. Moreover, the glycine 209 located in TM5 of NRT1.5 that was critically required to complement NRT1.5 (**Figure 11**) is overlapping an LRR motif in the repeat III (**Figure 25B**). Since the protein repeat III is also highly conserved in NRT1.5 orthologues of other plant species (**Figure 25B**), the mutation G209E is a good candidate to check protein-protein interaction. Subsequently, the mutant NRT1.5^{G209E} was used to determine the effect of blocking K⁺ export activity and altering an LRR motif in the interaction with AHA2.

AHA2 has a charged residue, the Asp⁶⁸⁴ in TM6, identified as an essential proton acceptor during proton translocation. Substitution at Asp⁶⁸⁴ in the D684V mutation resulted in a mutant with a complete deficiency in proton pumping (Buch-Pedersen and Palmgren, 2003). Additionally, the cytosolic C-terminal end of AHA2 has a short binding site (His⁹⁴⁵Tyr⁹⁴⁶Thr⁹⁴⁷Val⁹⁴⁸ or HYTV) for 14-3-3 proteins to modulate the activity of the proton pump by phosphorylation (Jahn et al., 1997; Fuglsang et al., 1999). To elucidate the effect of altering the proton pump activity of AHA2 with the NRT1.5 interaction, the AHA2^{D684V} substitution and AHA2^{ΔHYTV} deletion mutants were used. Further, the analysis of their physical interaction was investigated by the yeast mating-based split-ubiquitin system (mbSUS). The mbSUS assay takes advantage of protein fusions with the N- and C-terminal halves (Nub and Cub respectively) of ubiquitin. Reassembly of ubiquitin leads to transactivator cleavage from the Cub fusion, its transit to the nucleus, reporter gene activation, and yeast growth in selective media (**Figure 25C**) (Grefen et al., 2007). The full-length CDS of AHA2 (Drechsler, 2016), AHA2^{D684V}, or AHA2^{ΔHYTV} were fused with the N-terminal ubiquitin moiety Nub. The full-length CDS of NRT1.5 (Drechsler, 2016) or NRT1.5^{G209E} were fused with the C-terminal ubiquitin moiety Cub. Subsequently, these constructs were transformed in the auxotrophic yeast strain THY.AP4 (**Figure 25C**). Co-expression of NRT1.5-Cub with Nub-AHA2 or Nub-AHA2^{ΔHYTV} led to yeast growth, which indicates NRT1.5 could directly interact with AHA2 and the mutant version AHA2^{ΔHYTV}. In contrast, co-expression of NRT1.5^{G209E}-Cub with Nub-AHA2 and NRT1.5-Cub with Nub-AHA2^{D684V} did not lead to yeast growth, indicating mutations G209E and D684V are directly interfering in the protein-protein interaction (**Figure 25D**). A yeast nitrogen base growth media lacking K⁺ was used to evaluate the protein-protein interactions dependency

with potassium content in the media. Yeast growth is critically affected by the lack of potassium, suggesting either an unfavorable effect since the growth control (-Leu -Trp) is also affected or a potential K^+ -dependency in the protein-protein interaction between NRT1.5 and AHA2.

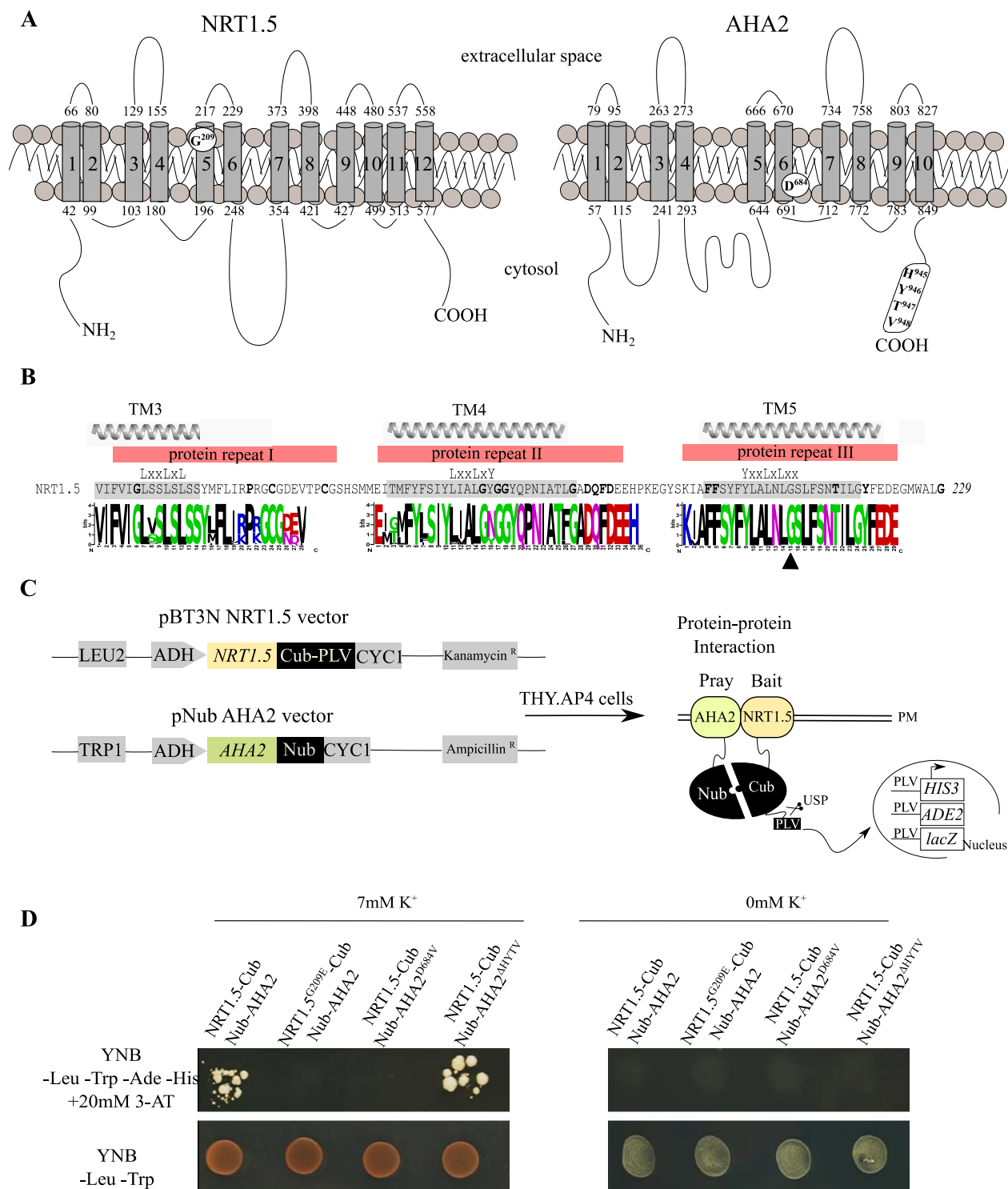


Figure 25: The interaction between NRT1.5 and AHA2 was investigated in different mutants in the yeast split ubiquitin system. **A.** Schematic representation of the protein structure of NRT1.5 and AHA2, and the

position of the different mutations used in this work. The amino acids mutated and their locations are represented. The protein structure prediction was done by CCTOP (Constrained Consensus TOPology) server. **B.** Split ubiquitin assay representation. The ubiquitin-protein is split into two halves, the N-terminal domain (Nub, from N-ubiquitin), and the C-terminal domain (Cub, from C-ubiquitin). These halves are each fused to the CDS of AtAHA2 and AtNRT1.5 in the vectors pNub-AHA2 and pBT3N-NRT1.5 respectively. The Cub peptide is also bound to an artificial reporter transcription factor PLV. After being co-expressed into THY.AP4 yeast cells, if Cub and Nub halves are brought together into proximity, they associate to form the full-length ubiquitin and the reporter transcription factor is released by ubiquitin-specific proteases (UBP). The free transcription factor then enters the nucleus and activates the transcription of reporter genes (*HIS3*, *ADE2*, and *lacZ*). Abbreviations: ADH: alcohol dehydrogenase I promoter from *S. cerevisiae*. LEU2 (L-leucine) and TRP1 (L-tryptophan): autotrophic markers. CYC1: CYC1 terminator from *S. cerevisiae*. PM: plasma membrane. **C.** Protein repeats in the NRT1.5 sequence. The secondary structure of NRT1.5 is shown above and transmembrane domains are highlight in grey. The 3 sequence repeats (I-III) found in NRT1.5 protein (by RADAR and LRRfinder) are indicated in light red, and the location of mutation G209E is marked with a black arrow in TM5. Below the NRT1.5 protein sequence, the protein repeats I, II, and III were aligned against NRT1.5 orthologues from 100 different plant species using BLASTp (NCBI) and subsequently represented using WEBLOGO (<http://weblogo.berkeley.edu/logo.cgi>). **D.** The protein-protein interaction between NRT1.5 and AHA2 wild types and mutants. THY.AP4 cells were transformed with NRT1.5 wild type or mutant fused to Cub and AHA2 wild type or mutants fused to Nub. For the selection of transformants, twelve μ l of yeast cell cultures ($OD_{600nm}=1$) were dropped in YNB (-Leu -Trp) medium as a growth control and the detection of protein-protein interactions was carried out in YNB -Leu -Trp -His -Ade. The YNB medium contains from the manufacturer either 7mM or 0mM of K^+ . The addition of 20mM of 3-amino-1,2,4-triazole (3-AT) was used to reduce the non-specific yeast growth not based on protein-protein interactions. Plates were incubated at 30°C for three days and then photographed.

To evaluate whether the protein-protein interactions observed in yeast cells also occur in plant cells, a BiFC assay was carried out (Grefen and Blatt, 2012). NRT1.5 or NRT1.5^{G209E} mutant were fused to cYFP, and AHA2, AHA2^{D684V}, or AHA2 ^{Δ HYTV} mutants were fused to nYFP in the pBiFC-2in1 system by Gateway cloning. As a negative control, the pBiFC-2in1 construct with unfused nYFP and NRT1.5-fused cYFP was used. The generated pBiFC-2in1 constructs were transformed into *A. tumefaciens* for transient expression in *N. benthamiana*. Two days post-infiltration the fluorescence signals from underside epidermis cells of transfected *N. benthamiana* leaves were recorded by confocal fluorescence microscopy. The negative control did not conduct YFP signal, and the RFP signal showed the successful transformation and expression of the pBiFC-2in1 constructs (**Figure**

26, RFP channel). The co-expression of cYFP-NRT1.5 with nYFP-AHA2 or nYFP-AHA2^{AHYTV} led to YFP fluorescence signal. However, the expression of cYFP-NRT1.5^{G209E} with nYFP-AHA2 did not lead to YFP signal, as well as cYFP-NRT1.5 with nYFP-AHA2^{D684V} (Figure 26, YFP channel), supporting the observation in the split ubiquitin system (Figure 25) that G209E and D684V mutations are affecting NRT1.5 and AHA2 interaction.

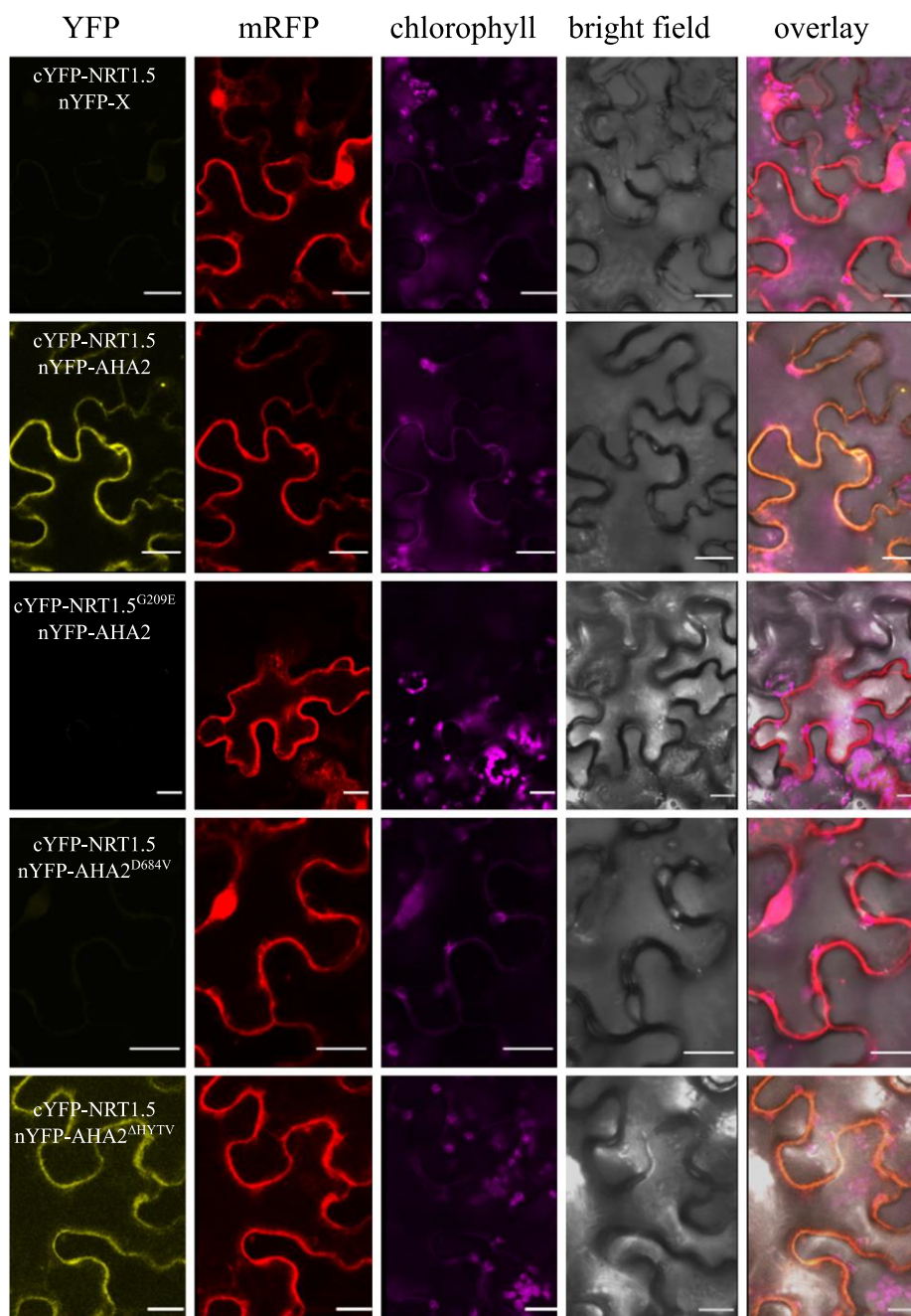


Figure 26: Verification of the protein-protein interaction of NRT1.5 and AHA2 and their mutant versions by BiFC-2in1 assay in epidermis of *N.benthamiana*. Confocal microscope images of epidermis cells expressing non-fused nYFP and cYFP-NRT1.5 (cYFP-NRT1.5 nYFP-X), nYFP-AHA2 and cYFP-NRT1.5, nYFP-AHA2 and cYFP-NRT1.5^{G209E}, nYFP-AHA2^{D684V} and cYFP-NRT1.5, and nYFP-AHA2^{ΔHYTV} and cYFP-NRT1.5, after two days post-infection. Different channels are represented: RFP fluorescence signals in red, YFP fluorescence signals in yellow, the autofluorescence of chlorophyll (artificially represented in violet), the bright field, and the overlay of the four channels. The scale bar represents 20μm.

3.4.8. NRT1.5, NRT1.5^{G209E}, AHA2, and AHA2^{D684V} proteins localize in cellular membranes of *Saccharomyces cerevisiae* and *Nicotiana benthamiana*

Previously, some specific amino acids from NRT1.5 and AHA2 were identified as crucial for the protein-protein interaction (**Figures 25 and 26**). To test, if the NRT1.5^{G209E} and AHA2^{D684V} mutations are interfering with the protein localization, subcellular localization assays were carried out here using different fluorescent tags in *S. cerevisiae* and *N. benthamiana*.

To determine the subcellular localization in *S. cerevisiae* cells, C-terminal fusions of NRT1.5 or NRT1.5^{G209E} with the green fluorescent protein eGFP and AHA2 or AHA2^{D684V} with the red fluorescent protein mCherry were created (**Figure 27A**) and imaged by confocal microscopy.

Since the yeast THY.AP4 strain was used for the split ubiquitin system, where the NRT1.5 and AHA2 interaction binding sites were detected, the same strain was used also for the localization assay. Free eGFP and mCherry were localized in the cytosol of yeast cells. Surprisingly, NRT1.5eGFP and NRT1.5eGFP^{G209E} displayed intense fluorescence signals in cytosolic compartments. The same observation applied to AHA2-mCherry and AHA2^{D684V}mCherry constructs (**Figure 27B**). Additionally, the background of BYT45 cells was checked since the K⁺ export activity is altered there. The localization of NRT1.5 and AHA2 wild-types and mutants with the fluorescent tags was still in the cytosol compartments (**Figure 27C**) even when they grew under high KCl concentrations (1M KCl) (data is not shown). Since fluorescent organelle markers were not used here, it is not possible to identify in which cytosolic compartments the signal is displayed. These data demonstrate that NRT1.5 and AHA2 proteins are expressed in yeast cells, but they localize not at the plasma membrane as in *Arabidopsis thaliana*. Nevertheless, the wild-type and mutant versions of NRT1.5 and AHA2 seem to be located in the same subcellular compartments in yeast cells, thus allowing their interaction (**Figure 25**).

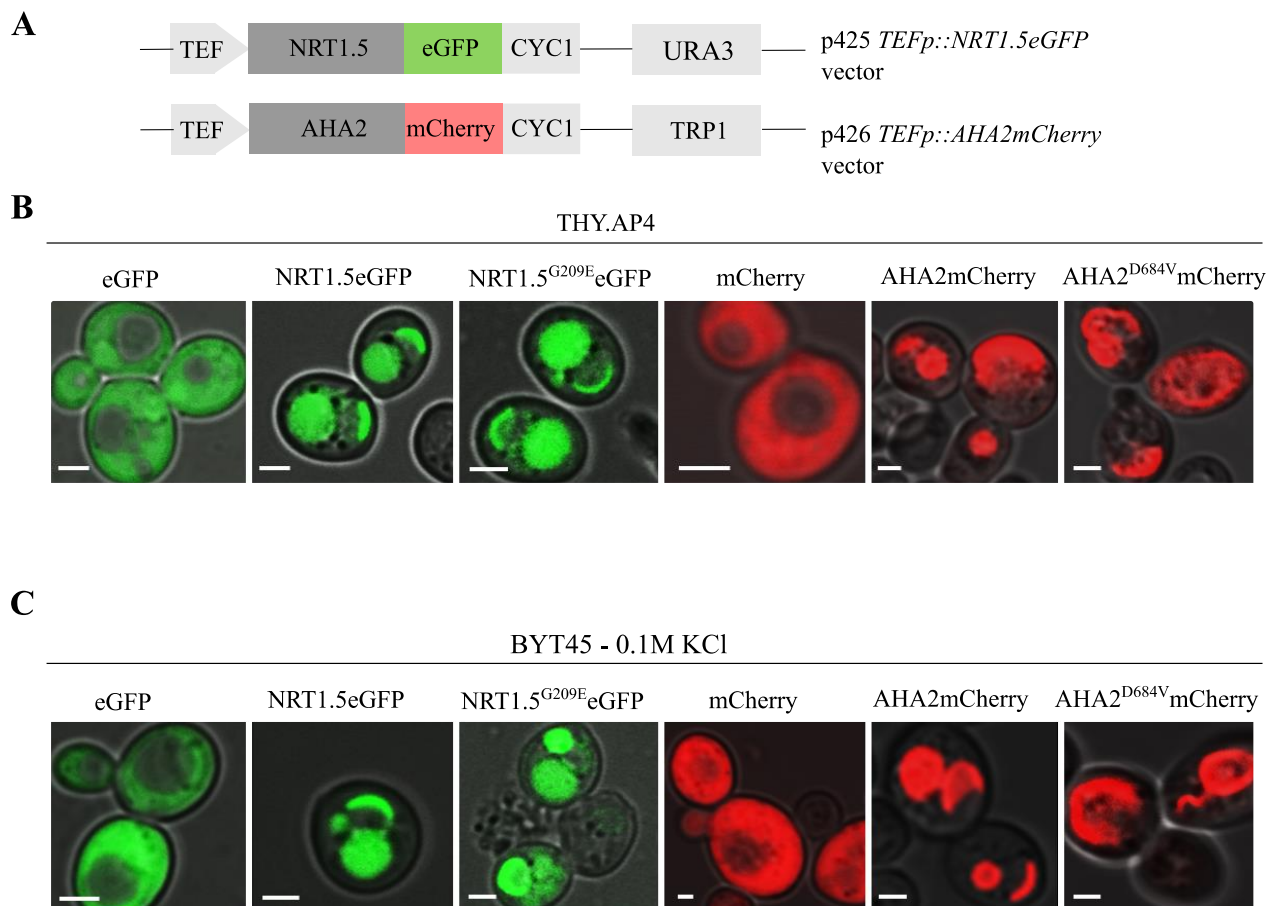


Figure 27: Cellular localization of NRT1.5 and AHA2 in *S. cerevisiae* cells by confocal microscopy. **A.** Schematic representation of the genetic cassette of the p42x vectors (Mumberg et al., 1995), containing NRT1.5 and AHA2 wild-types and their respective mutants fused to eGFP or mCherry respectively at the C-terminus. Abbreviations: TEF: promoter. CYC1: terminator. wo TAA: without stop codon TAA. wo ATG: without initial codon ATG. URA3 and TRP1: auxotrophic markers. **B.** THY.AP4 strain or **C.** BYT45 strain expressing eGFP, NRT1.5eGFP, NRT1.5^{G209E}eGFP, mCherry, AHA2mCherry, or AHA2^{D684V}mCherry driven by TEF promoter. Yeast cultures were grown in YNB medium (-Leu -Ura, pH=5.5) at 30°C overnight. Cell pellets were obtained and after being PBS washed, the confocal microscopy was carried out. The white bars represent 2μm.

Alternatively, co-expression of NRT1.5 and AHA2 (wild-type and mutants) in yeast was carried out to investigate if the co-expression of NRT1.5 and AHA2 can interfere in the protein targeting to the yeast plasma membrane. Wildtype and mutant proteins co-localized in yeast cells as is indicated by the overlap of green and red fluorescence signals (**Figure 28**) but the subcellular localization still seems to not be at the plasma membrane.

Further studies in planta are required to prove that NRT1.5, NRT1.5^{G209E}, AHA2, and AHA2^{D684V} are located in the plasma membrane. *S. cerevisiae* is not suitable for *in vivo* localization studies of the NRT1.5 and AHA2 transporters.

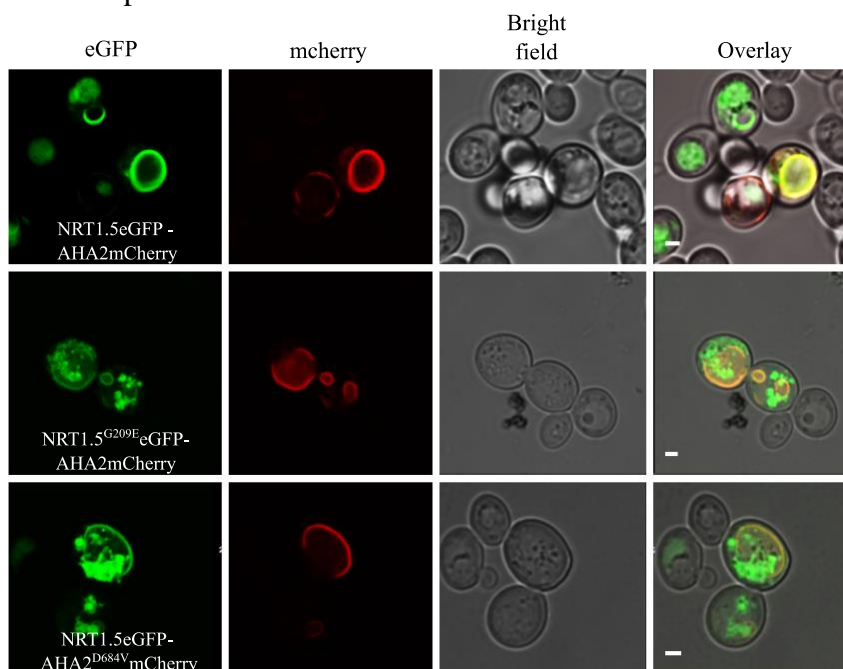


Figure 28: NRT1.5 and AHA2 co-localization in *S. cerevisiae* cells. THY.AP4 yeast cells co-expressed NRT1.5eGFP-AHA2mCherry, or NRT1.5^{G209E}eGFP-AHA2mCherry, or NRT1.5eGFP-AHA2^{D684V}mCherry constructs. Yeast cultures were grown in liquid YNB medium (-Leu -Ura pH=5.5) at 30°C, overnight. From the overnight cultures, the pellets were obtained, PBS washed, and observed by confocal microscopy. Different channels represented are eGFP, mCherry, bright field, and the overlay of the three channels. The white bars represent 2µm.

To determine the subcellular localization of NRT1.5, NRT1.5^{G209E}, AHA2, and AHA^{D648V} in plant cells, the open reading frames were amplified and subsequently cloned upstream of the *eGFP* or *mCherry* reporter genes and downstream of the *35S* promoter (**Figure 29A**). The resulting constructs were then transiently expressed in *N. benthamiana* leaves and fluorescence signals were observed two days after infiltration. Fluorescent signals are recorded from transfected leaves with free GFP, free mCherry, NRT1.5eGFP, NRT1.5^{G209E}eGFP, AHA2mCherry, and AHA^{D648V}mCherry. However, the exact subcellular localization cannot be assumed from these observations (**Figure 29B**). Plasmolysis was induced by treatment of transfected *N. benthamiana* epidermis cells with 5% NaCl. The characteristic Hechtian strands (Oparka, 1994) typical of plasma membrane retracting from the cell wall in mesophyll cells were observed in epidermis

3. Results

expressing NRT1.5 and AHA2, either wild type or mutants versions, evidencing the plasma membrane localization. In contrast, plasmolysing cells expressing free eGFP or mCherry did not display Hechtian strands, supporting the cytosol localization of these free tags (**Figure 29B**).

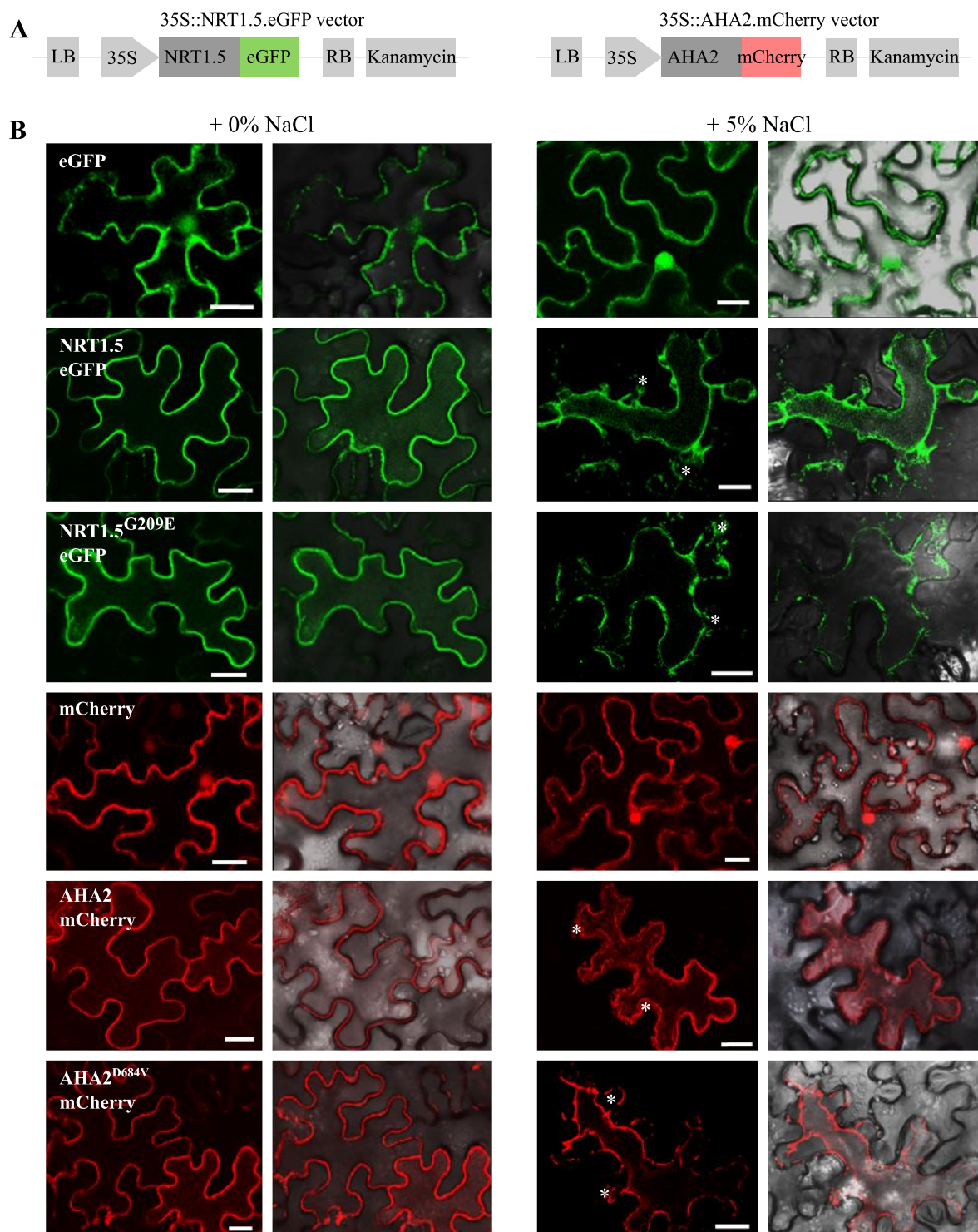


Figure 29: Cellular localization of NRT1.5 and AHA2 in *N. benthamiana* epidermis cells. **A.** Schematic representation of pCAM-HA vector (Herbst, 2019) containing NRT1.5 or AHA2 wild-type and their respective mutants fused to eGFP or mCherry respectively at the C-terminus. Abbreviations: 35S: 35S promoter from cauliflower mosaic virus. RB/LB: right/left border of T-DNA **B.** *N. benthamiana* epidermis cells overexpressing eGFP, NRT1.5eGFP, NRT1.5^{G209E}eGFP, mCherry, AHA2mCherry, and AHA2^{D684V}mCherry two days after infiltration. Cellular plasmolysis was induced by incubation in NaCl 5% during visualization in the microscope. Asterisks indicate areas between plasmolyzed cells and where Hechtian strands are noticeable. Two channels are represented: eGFP (green) or mCherry (red) in left panels, and the overlay with the bright field in right panels. The scale bar represents 20µm.

3.4.9. Plasma membrane H⁺-ATPase family members are transcriptionally regulated by low nutrition supply

To investigate whether plasma membrane H⁺-ATPase (PM H⁺-ATPase) gene family members are regulated by different K⁺ and NO₃⁻ supplies, and if functional redundancy between family members exists, the expression of all PM H⁺-ATPase genes (*AHA1-AHA11*) was examined in *Arabidopsis thaliana* seedlings lacking *NRT1.5* and *AHA2* under 0mM K⁺/1mM NO₃⁻ supply using real-time qPCR. The transcript levels of the eleven PM H⁺-ATPase genes revealed significant expression changes of *AHA4* and *AHA6* isoforms with ≈7-fold up-regulation in Col-0 plants at 0mM K⁺/1mM NO₃⁻ in comparison to MS medium. In contrast, the *nrt1.5* mutant showed ≈3.5-fold upregulation of *AHA1* and *AHA2*, whereas *AHA4* expression was 17-fold upregulated. The *aha2* mutant displayed an up-regulation of *AHA6* and *AHA9* with 18 and 8 fold-up respectively. Interestingly, the lack of both proteins, NRT1.5 and AHA2, had a strong influence on the expression of all *AHAs* where none of the 11 genes were regulated (**Figure 30**). PM H⁺-ATPase root transcript patterns indicate an influence of NRT1.5 and AHA2 dependent on K⁺ and NO₃⁻ levels.

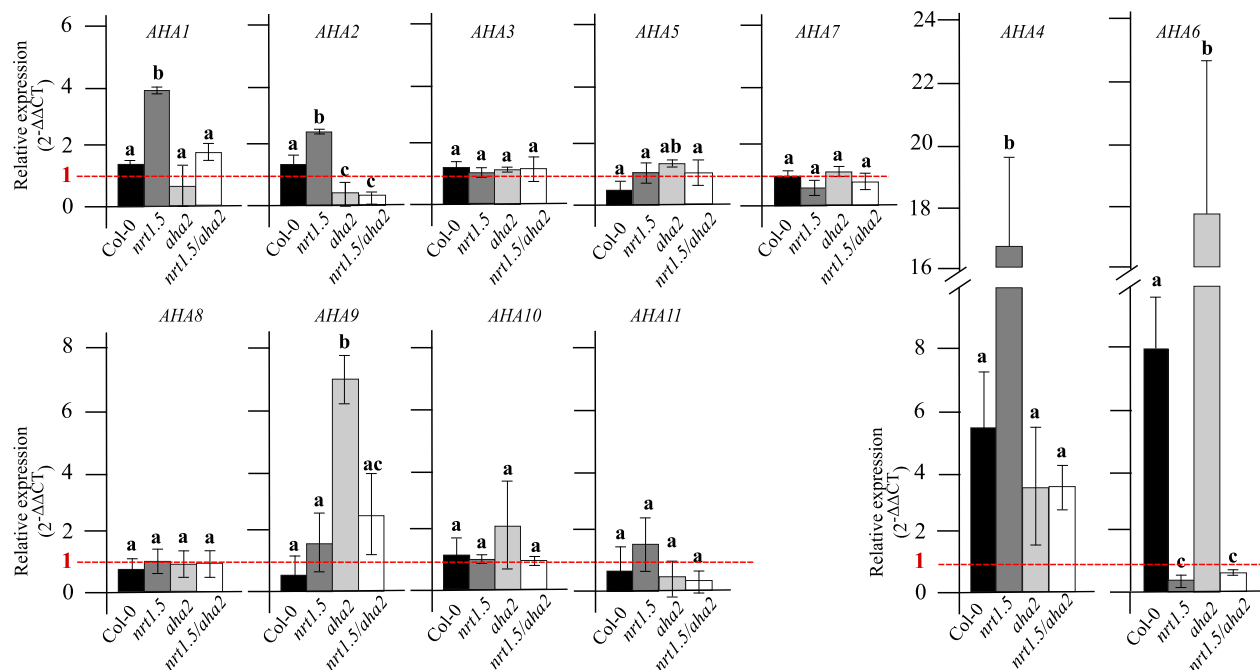


Figure 30: Expression of the 11 H⁺-ATPase family members (*AHA1*–*AHA11*) in Col-0, *nrt1.5*, *aha2*, and *nrt1.5/aha2* seedlings under 0mM K⁺/1mM NO₃⁻ supply. Seedlings grew in MS medium for five days and were then transferred to MS or 0mM K⁺/1mM NO₃⁻ media for fourteen days more. The values plotted are the relative fold change expression (2^{-ΔΔCT}) generated by the normalization to the housekeeping gene *UBQ10*, and then to the expression of 0mM K⁺/1mM NO₃⁻ of each genotype compared with MS medium. The dotted red lines represent 2^{-ΔΔCT}=1. Different letters indicate statistically significant differences (Tukey’s test) between mutants and Col-0 with *P*<0.05, (means ± SD, n=3).

3.4.10. AHA2 interaction with other NRT1 family members

The nitrate transporter NRT1.8 is expressed in parenchyma cells and plays a role in removing NO₃⁻ from xylem sap to parenchyma cells (Li et al., 2010), an opposite function of NRT1.5 activity (**Figure 1**). Even though both transporters are located in the same tissue, unpublished data from our group showed NRT1.5 and NRT1.8 were not physically interacting (Drechsler, 2016). Another NRT1 member, NRT1.10, has been described to transport a wide range of glucosinolates (Jørgensen et al., 2017) and interestingly has been identified to interact physically with NRT.1.5 by split ubiquitin (Drechsler, 2016) and by bimolecular complementation (Zheng, 2018) assays. A split ubiquitin assay was carried out here to observe if AHA2 can interact with other NRT1 family members to better understand the interaction of the proton pump with this family of nitrate transporters. The full-length CDS of NRT1.8 and NRT1.10 was fused with the C-terminal ubiquitin

moiety Cub. Subsequently, together with the constructs NRT1.5-Cub and AHA2-Nub (Drechsler, 2016) in which AHA2 was fused to the N-terminal ubiquitin moiety Nub, the constructs were transformed in the auxotrophic yeast strain THY.AP4 (-Leu, -Trp, -His, -Ade, -Ura). Co-expressions of NRT1.5-Cub with AHA2-Nub and NRT1.10-Cub with AHA2-Nub led to yeast growth, which indicates that NRT1.5 and NRT1.10 interact with AHA2. Unfused Nub was co-expressed with NRT1.5-Cub to serve as negative control. The co-expression of NRT1.8-Cub with AHA2-Nub shows the negative control growth background, which indicates NRT1.8 does not interact with AHA2 (**Figure 31A**).

To understand if a connection exists between NRT1.5 with NRT1.8 and NRT1.10 in the maintenance of K^+ and NO_3^- homeostasis, a phenotypical analysis was carried out. The analysis of the knockout mutants, *nrt1.8* and *nrt1.10*, did not show shoot phenotypes under low K^+ supply (**Figure 31B**). However, *nrt1.8* and *nrt1.10* showed a reduction of the lateral root density at low K^+ and NO_3^- supply conditions, mimicking the *nrt1.5* phenotype (**Figure 31C**).

The Glycine 209 in the TM5 of NRT1.5 was detected as an important residue for the interaction with AHA2 (**Figure 25C, 26**). The Gly²⁰⁹ is not found fully conserved when the amino acid sequence of NRT1.5 was aligned with NRT1.8 and NRT1.10. However, at position 209 a non-polar residue is located in the three nitrate transporters (**Figure 31D**), indicating that a non-polar residue in position 209 is not enough for the existence of the interaction of AHA2 with NRT1 family members. All these data propose that NRT1.5, NRT1.8, and NRT1.10 are correlated with the modulation of the root architecture under low K^+/NO_3^- supply.

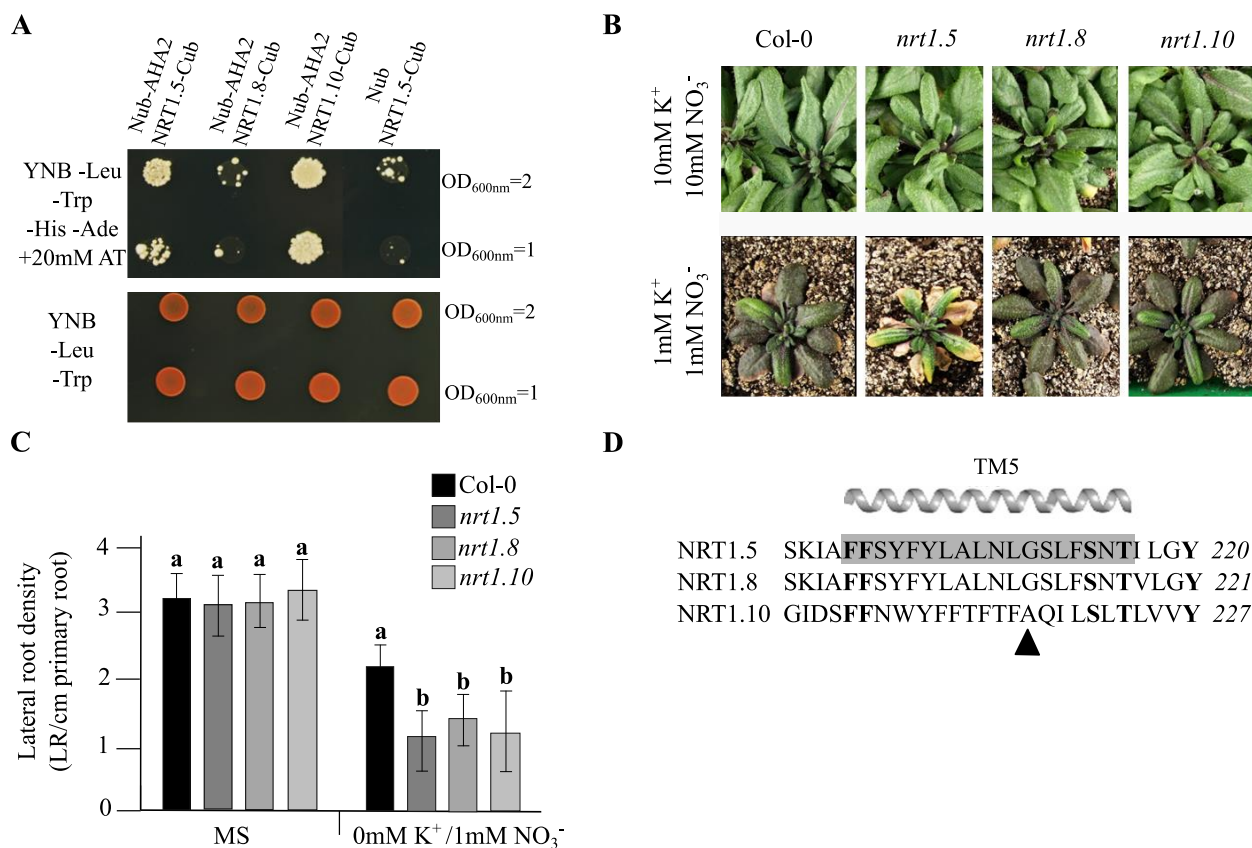


Figure 31: AHA2 interaction with other NRT1 family members. **A.** Split ubiquitin assay in *S. cerevisiae* to detect the interaction between AHA2 with NRT1.5, NRT1.8, or NRT1.10. AHA2 was fused to Nub and the NRT15, NRT1.8, and NRT1.10 were fused to Cub. Unfused Nub co-expressed with NRT1.5-Cub is the negative control. After transformation in THY.AP4 cells, selection of the transformants yeast cells was done in YNB (-Leu -Trp) media. The detection of protein-protein interactions was carried out in the YNB-Leu-Trp-His-Ade medium. The addition of 20mM of 3-AT was used to reduce the nonspecific yeast growth not based on protein-protein interactions. Plates were incubated at 30°C for four days. **B.** Shoot phenotypes of Col-0, *nrt1.5*, *nrt1.8*, and *nrt1.10* plants grown on unfertilized soil and watered with 10mM K⁺/10mM NO₃⁻ or 1mM of K⁺/1mM NO₃⁻ for forty days more. **C.** Lateral root density of Col-0, *nrt1.5*, *nrt1.8*, and *nrt1.10*. Seedlings were pre-germinated in MS for five days and then transferred to either MS medium or a modified MS with 0mM K⁺/1mM NO₃⁻ for fourteen days further. Different letters indicate statistically significant differences (Tukey's test) between mutants and Col-0 with $P < 0.05$, (means \pm SD, $n > 20$). **D.** Segment of the protein sequence alignment between NRT1.5, NRT1.8, and NRT1.10. The model-based sequence alignment was done using the Promals3d server. Conserved amino acid residues are shown in bold, and NRT1.5 transmembrane domain 5 is highlight in grey. The position of G209 residue is indicated with a black arrow. The secondary structure of NRT1.5 is shown above the alignment.

3.5. Elucidation of the physiological significance of the interaction between NRT1.5 and the anion channels SLAH1 and SLAH3

Chloride and nitrate are the major counterions for K^+ uptake and they play crucial roles in plant nutrition (Hedrich and Geiger, 2017). *SLAH1* and *SLAH3* genes were strongly up-regulated in *nrt1.5* mutant roots under 0mM K^+ and 1mM NO_3^- conditions (**Figure 13**), and their up-regulation might indicate that both proteins could be linked to the NRT1.5 function. In addition, NRT1.5 is physically interacting with SLAH1 and SLAH3 in the split ubiquitin and bimolecular complementation assays (Drechsler, 2016; Zheng, 2018; **Figure 11**), and the SLAH1 and SLAH3 proteins are expressed like NRT1.5 in the root xylem-pole pericycle (Cubero-Font et al., 2016), suggesting a potential biological interaction. Here in this section, the phenotypical analysis of *slah1* and *slah3* loss of function mutants, the double mutants with *nrt1.5*, and overexpression of SLAH1 and SLAH3 were carried out.

3.5.1. *slah1/nrt1.5* and *slah3/nrt1.5* mutants do not show phenotypes at low nutrition supply

To investigate the relationship between the Cl^-/NO_3^- channels SLAH1 and SLAH3 with NRT1.5 in the root-to-shoot translocation of nutrients, single (*slah1*, *slah3*) and double mutants (*slah1/nrt1.5* and *slah3/nrt1.5*) were phenotyped under different K^+ and NO_3^- regimens. Both single mutants did not show morphological shoot differences compared to Col-0 (**Figure 15**), but *nrt1.5/slaha1* and *nrt1.5/slaha3* double mutants developed the *nrt1.5* phenotype under low fertilization conditions (1mM $K^+/1mM NO_3^-$). (**Figure 32A**). The analysis of the lateral root density at low fertilization conditions also did not show phenotypes in the *slah1* and *slah3* single mutants in comparison with Col-0. The *nrt1.5/slaha1* and *nrt1.5/slaha3* mutants showed a reduction of lateral root density, similar to *nrt1.5* where new lateral roots are not formed after seedlings are transferred from MS media to low fertilization conditions (**Figure 32B**). From these data, it is shown that the K^+/NO_3^- translocation from root-to-shoot and modulation of root architecture is not affected by SLAH1 and SLAH3 and both anion transporters do not seem to link to NRT1.5.

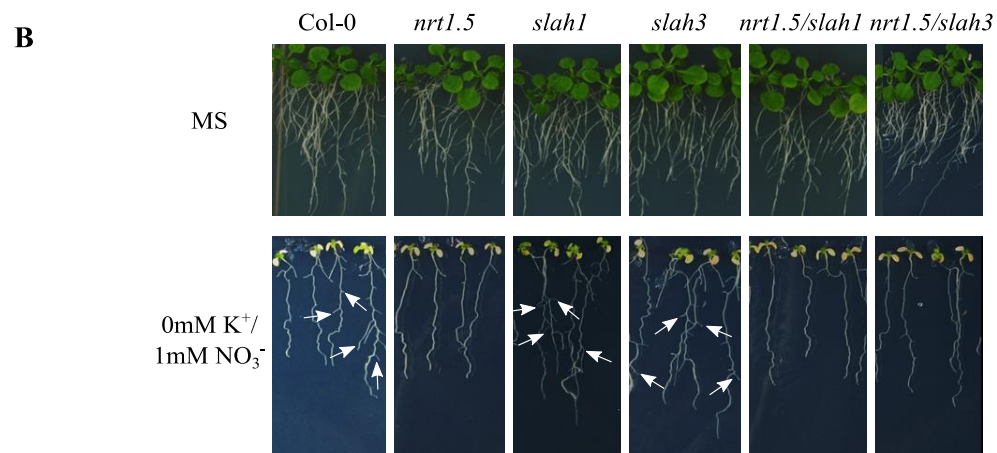
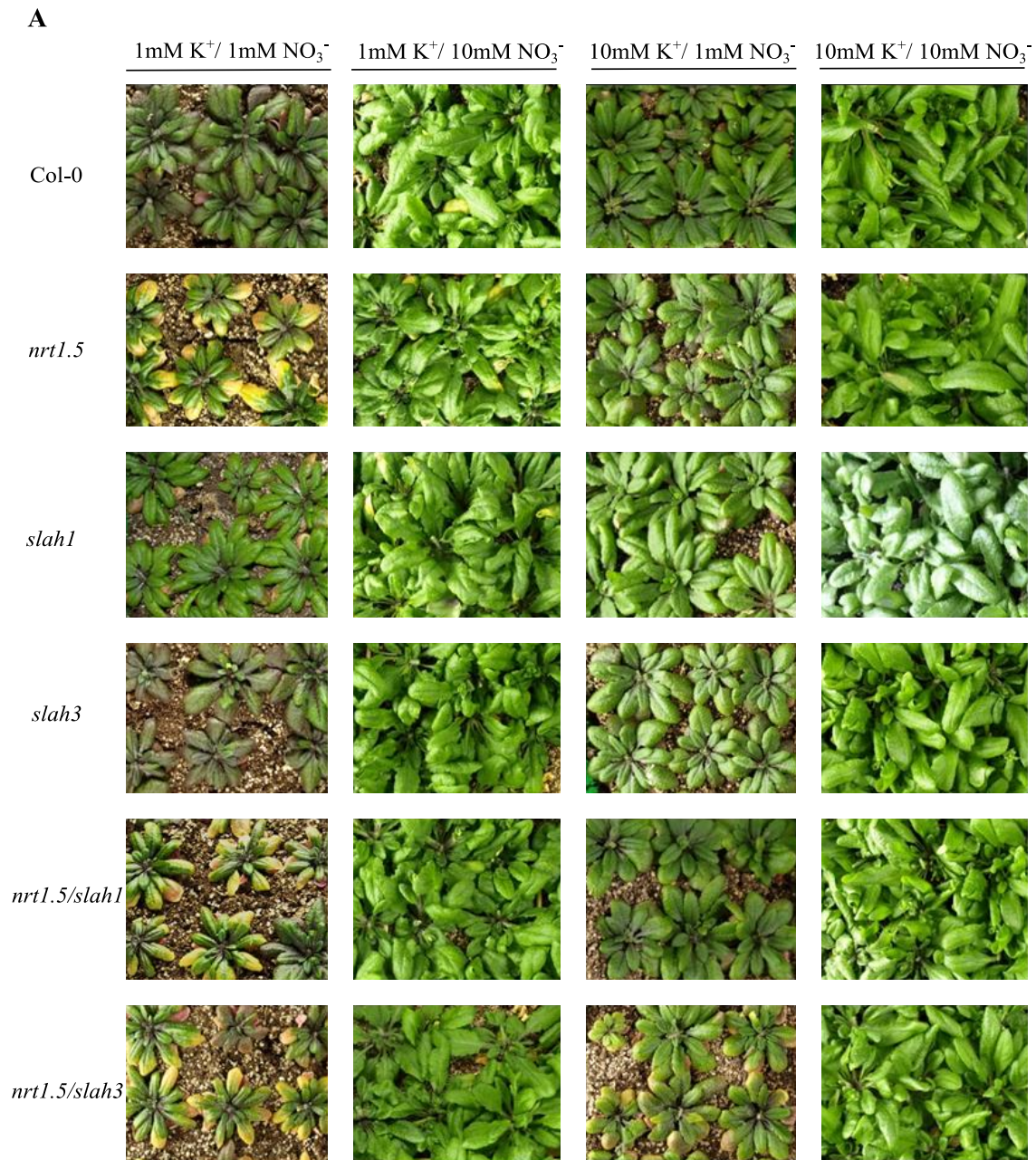


Figure 32: Phenotypes of Col-0, *nrt1.5*, *slah1*, *slah3*, *slah1/nrt1.5*, and *slah3/nrt1.5* mutants under different K^+ and NO_3^- regimens. **A.** Shoot phenotype of plants. Plants were pre-germinated in fertilized soil for seven days and later transferred to unfertilized soil and watered with modified nutrient solutions, containing different NO_3^- and K^+ regimens indicated in the figure. The plants grew for forty days further and were watered two times a week. **B.** Root phenotypes. Seedlings were pre-germinated in MS medium for five days and later transferred to MS medium or 0mM K^+ /1mM NO_3^- for seven days further. White arrows indicate lateral roots formation.

3.5.2. Overexpression of SLAH1 and SLAH3 in Arabidopsis do not show shoot phenotypes at low nutrition supply

The activity of Slow-type anion channels, like SLAC and SLAHs, have been described to affect negatively the activity of K^+ transport systems (Zhang et al., 2016). To investigate if SLAH1 and SLAH3 are negative regulators of NRT1.5, the phenotyping of 35S::SLAH1eGFP and 35S::SLAH3eGFP overexpression lines was carried out. The stable overexpression of 35S::SLAH1eGFP and 35S::SLAH3eGFP lines were successful in *Arabidopsis thaliana* transgenic plants since 20 and 8-fold up expression of *SLAH1* and *SLAH3* was detected by qPCR respectively (**Figure 33A**). Since the 35S::SLAH1eGFP and 35S::SLAH3eGFP lines contain SLAH1 and SLAH3 attached to a fluorescent tag (GFP), the detection of GFP signal in *A. thaliana* epidermis and roots by confocal microscopy revealed the success of the protein expression (**Figure 33B**).

The plant phenotypes under different K^+/NO_3^- supplies showed that 35S::SLAH1eGFP and 35S::SLAH3eGFP lines did not phenocopy the *nrt1.5* mutant, rejecting the hypothesis of a negative regulation between SLAH1 and SLAH3 with NRT1.5 (**Figure 33C**).

In addition, anion transport usually affects K^+ transport systems at transcriptional level (see 1.4.4). To check if the expression of *SLAH1* or *SLAH3* can influence the transcriptional expression of *NRT1.5*, the gene expression of *NRT1.5* was checked in the background of 35S::SLAH1eGFP and 35S::SLAH3eGFP lines. The transcript levels of *NRT1.5* were not regulated in the background of the overexpression lines (**Figure 33D**).

These data indicate that SLAH1 and SLAH3 might not be correlated with the negative regulation of NRT1.5 by a physical or molecular interaction.

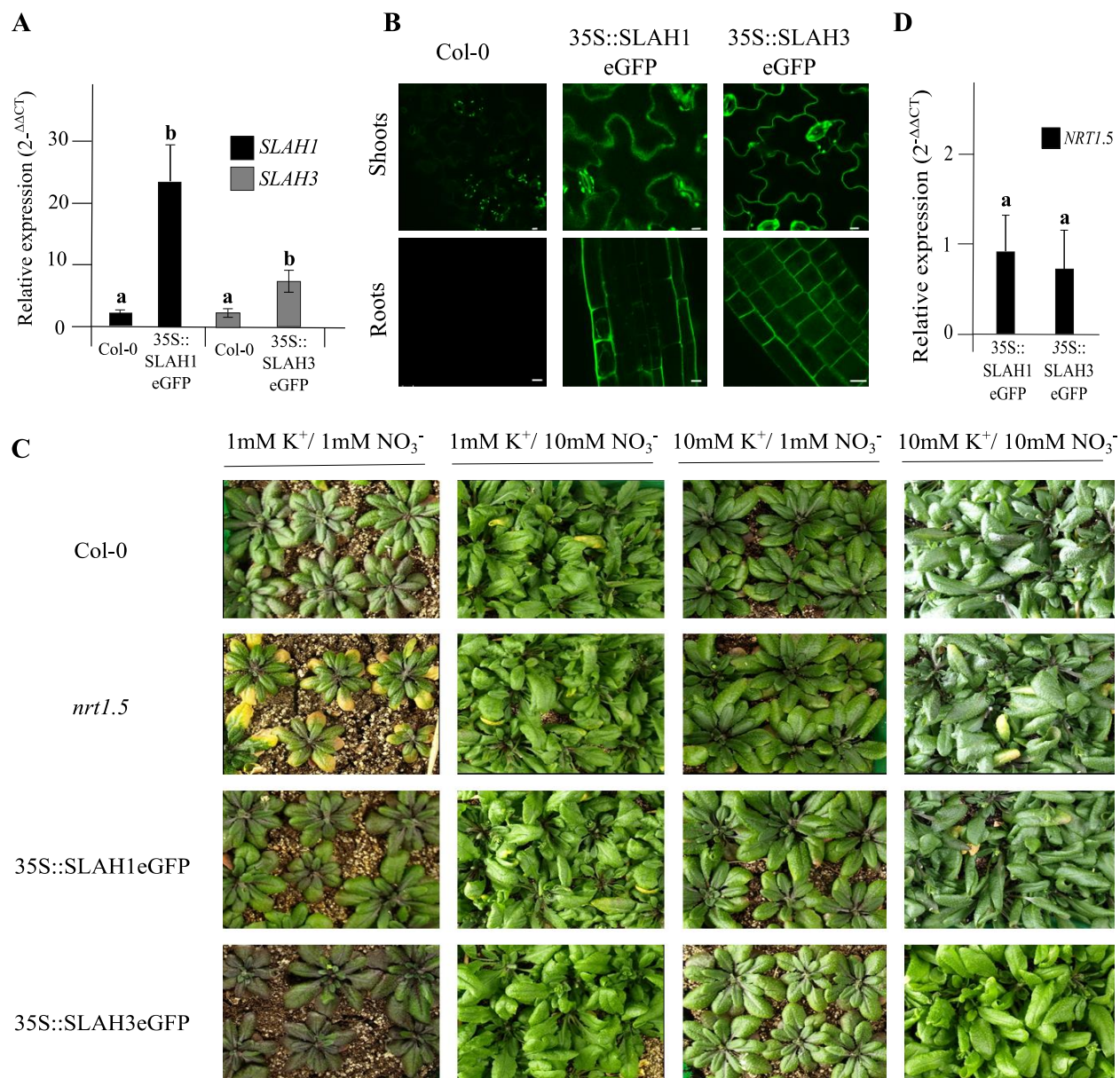


Figure 33: Phenotypes of 35S::SLAH1eGFP and 35S::SLAH3eGFP lines under different K⁺ and NO₃⁻ regimens. **A.** Expression of *SLAH1* and *SLAH3* by qPCR. Seedlings (T3 generation) were grown in MS plates for fifteen days and later harvested for RNA extractions. The relative transcript level (2^{-ΔΔCT}) was measured by qPCR. The housekeeping gene *UBQ10* was used for normalization. Data represent three biological replicates. **B.** Col-0, 35S::SLAH1eGFP, and 35S::SLAH3eGFP plants grew in MS medium for ten days. GFP signal was registered in roots and shoots by confocal microscopy. The white bars represent 10μm. **C.** Shoot phenotypes. Plants were pre-germinated in fertilized soil for seven days, and transferred to unfertilized soil, and watered with different K⁺ and NO₃⁻ regimens as indicated for thirty days more. **D.** Expression of *NRT1.5* in 35S::SLAH1eGFP and 35S::SLAH3eGFP overexpression seedlings. Seedling grew in MS medium for ten days, later RNA was extracted. The housekeeping gene *UBQ10* was used for normalization and the relative expression (2^{-ΔΔCT}) was calculated as relative to *NRT1.5* expression in Col-0.

(mean \pm SD; n = 3). Different letters indicate statistically significant differences (Tukey's test) between mutants and Col-0 with $P < 0.05$

3.5.3. SLAH1, SLAH3 and NRT1.5 contribute to the maintenance of the plasma membrane potential

To analyze the effect of lacking or overexpressing SLAH1 and SLAH3 with NRT1.5, a HygB sensibility assay as described in chapter 3.4.4 was carried out. *slah1*, *slah3*, *nrt1.5/slah1*, *nrt1.5/slah3*, 35S::SLAH1eGFP and 35S::SLAH3eGFP mutants grew in MS medium supplemented with 5 μ g/ml HygB. Mutants displayed a resistant phenotype by enhancing root growth and the presence of green cotyledons, mimicking the *nrt1.5* phenotype (**Figure 34A and B**). However, a synergistic or additive effect between NRT1.5 with SLAH1 or SLAH3 was not observed. These observations demonstrate that the plasma membrane potential is altered in the different knockout mutants, even in the knockdown line *slah1*, and also in the overexpression lines 35S::SLAH1eGFP and 35S::SLAH3eGFP. This proves that lack or overexpression of SLAH1 and SLAH3 influence the plasma membrane potential due to the ion transport function across the plasma membrane.

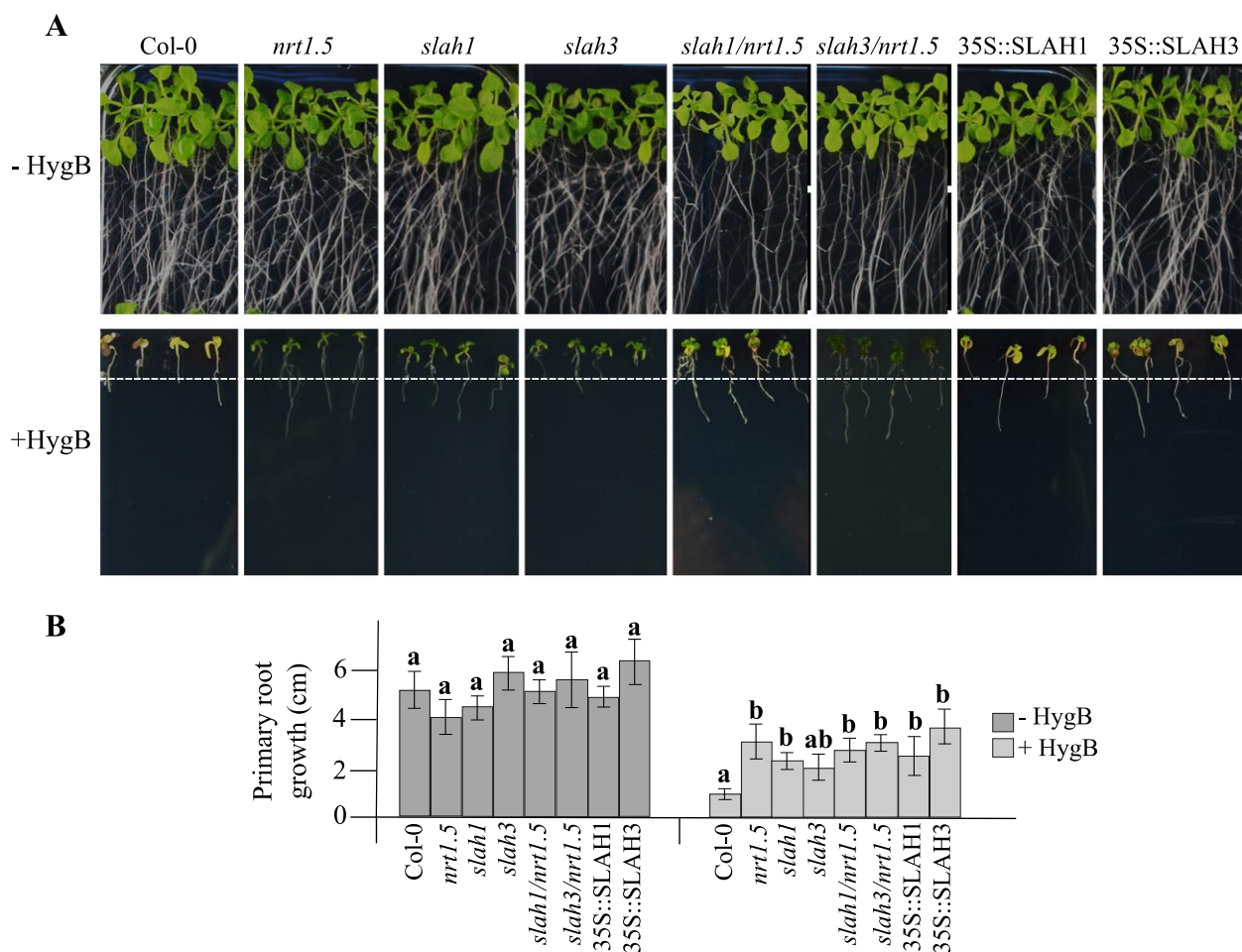


Figure 34: Hygromycin B sensitivity. **A.** Col-0, *nrt1.5*, *slah1*, *slah3*, *nrt1.5/slah1*, *nrt1.5/slah3*, 35S::SLAH1eGFP, and 35S::SLAH3eGFP seedlings were pre-germinated in MS medium for four days and then transferred to MS supplemented with or without 5 μ g/ml HygB for ten days more. The white dotted line represents the maximum root growth of Col-0 in MS medium with 5 μ g/ml HygB. **B.** Primary root growth of plants in A. (mean \pm SD; n = 10). Different letters indicate statistically significant differences (Tukey's test) between mutants and Col-0 with $P < 0.05$. The white dotted line represents the maximum root growth of Col-0 in MS medium with 5 μ g/ml HygB.

3.6. Elucidation of the physiological significance of the interaction between NRT1.5 with CBL3, PEP12, and VAMP722

Phosphorylation of K⁺ channels and NO₃⁻ transporters appears to be an important way to regulate their function and the CBL and CIPK proteins are well-studied components in this pathway (Xu et al., 2006; Ho et al., 2009; Ragel et al., 2015). In addition to phosphorylation-mediated regulation, K⁺ channels can also be regulated by plasma membrane trafficking by SNARE proteins in plant

cells (Grefen et al., 2010; Eisenach et al., 2012). If NRT1.5 can be regulated by CBL3, PEP12, and VAMP722 as a response to K^+ and NO_3^- deficiency is investigated here by the phenotype analysis of the double mutants of *nrt1.5* with *cbl3*, *vamp722*, and *pep12*.

3.6.1. The lack of *CBL3*, *VAMP722* and *PEP12* genes do not show a link with NRT1.5 under low nutrition supply in *Arabidopsis thaliana*

To investigate the possible physiological significance of the interaction between NRT1.5 with CBL3, PEP12, and VAMP722 in *A. thaliana*, the single T-DNA insertion mutants *cbl3* (GABI_956D04), *pep12* (SAIL_580_C04) and, *vamp722* (SALK_103189C) were crossed with *nrt1.5*. The homozygote double mutants with *nrt1.5* from F3 generation were phenotypically analyzed. Col-0, *nrt1.5*, *cbl3*, *pep12*, *vamp722*, *cbl3/nrt1.5*, *pep12/nrt1.5*, and *vamp722/nrt1.5* plants grew on non-fertilized soil and were weekly watered with two different K^+ and NO_3^- regimens (1mM K^+ /1mM NO_3^- and 10mM K^+ /10mM NO_3^-). Compared to *nrt1.5*, Col-0, *cbl3*, *pep12*, and *vamp722* did not show visible morphological changes under both fertilization regimens. Double mutants *nrt1.5/cbl3*, *nrt1.5/pep12* and *nrt1.5/vamp722* showed the leaf chlorosis phenotype of *nrt1.5* under 1mM of K^+ / NO_3^- supply (**Figure 35A**). Analysis of the root growth in *cbl3*, *pep12*, and *vamp722* mutants under low K^+ supply did not show phenotypes in comparison with Col-0 (**Figure 35B**). This data shows that the lack of *CBL3*, *PEP12*, and *VAMP722* is not influencing the root architecture or the root-to-shoot translocation of nutrients and they may not collaborate with NRT1.5.

As a last attempt to approach a link between CBL3, PEP12, and VAMP722 with ion homeostasis, the phenotypes of single and double mutants exposed to HygB were analyzed to observe if the plasma membrane potential is affected in the mutants. The *vamp722* single mutant showed an evident resistance against HygB treatment, developing green cotyledons and enhanced root growth compared to Col-0, indicating that the lack of *VAMP722* is affecting the plasma membrane potential. In contrast, *cbl3* and *pep12* mutants showed more sensitivity to HygB than *vamp722* since seedlings developed yellow cotyledons but the root growth of seedlings mimic *nrt1.5*, demonstrating that the lack of both proteins is also sufficient to change the plasma membrane. Double mutants are showing the same phenotype as the *nrt1.5* single mutant, indicating a non-additive effect occurring in between proteins (**Figure 35C**).

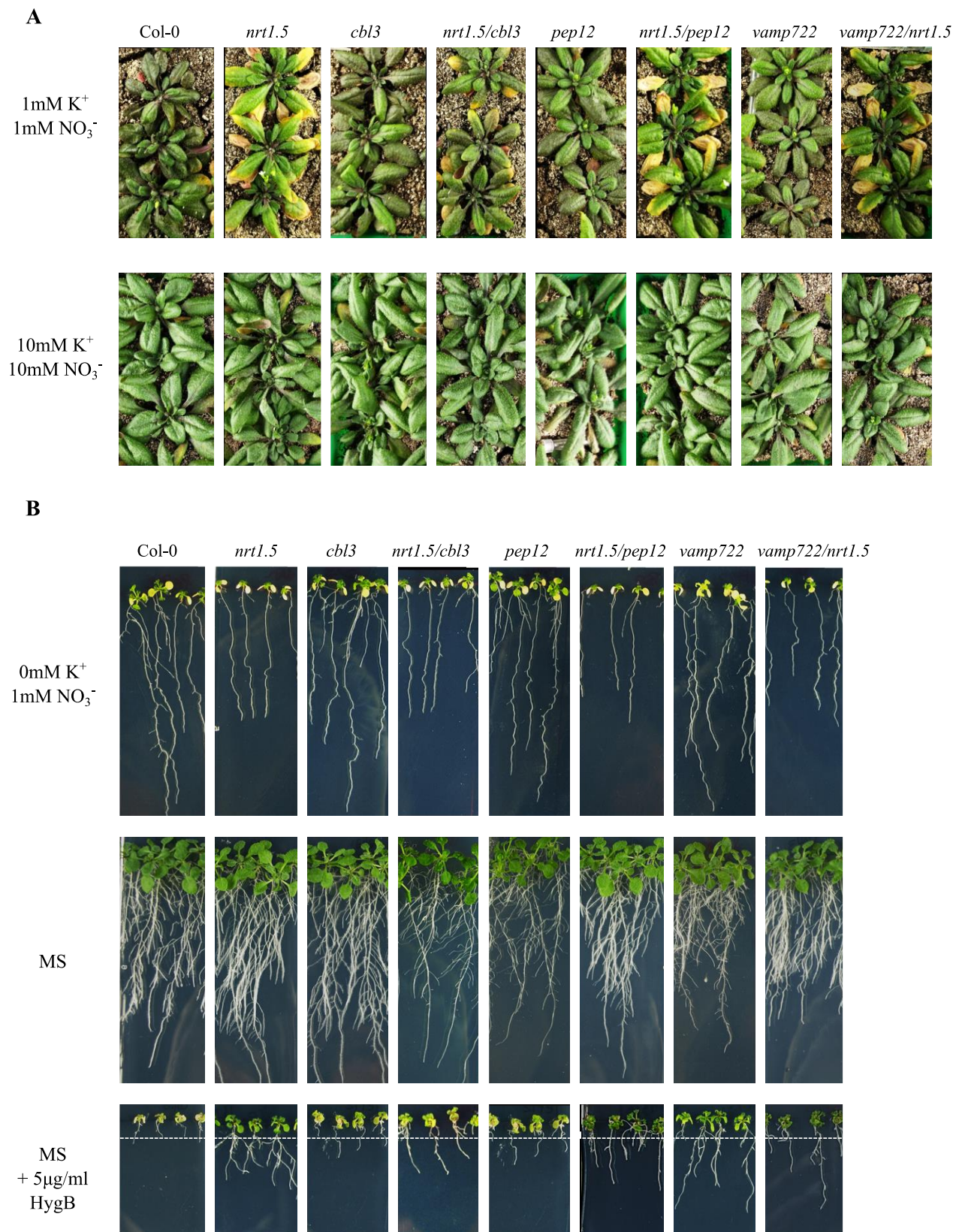


Figure 35: Root and shoot phenotypes of Col-0, *nrt1.5*, *cbl3*, *pep12*, *vamp722*, *nrt1.5/cbl3*, *nrt1.5/pep12*, and *nrt1.5/vamp722* plants growing under different K⁺ and NO₃⁻ regimens. **A.** Seedlings were pre-

germinated in fertilized soil for seven days and transferred to unfertilized soil and supplemented with different solutions as indicated (1mM K⁺/1mM NO₃⁻ or 10mM K⁺/10mM NO₃⁻) for thirty days more. **B.** Root phenotypes. Seedlings were pre-germinated for five days in MS medium and transferred to MS, 0mM K⁺/1mM NO₃⁻ or MS supplemented with 5μg/mL HygB for fourteen days further. The white dotted line represents the maximum root growth of Col-0 in MS medium with 5μg/ml HygB.

3.6.2. Co-expression of CBL3 and CIPK23 or PEP12 and VAMP722 does not influence the K⁺ export activity and localization of NRT1.5 in yeast

Plant ion transporters and channels have been reported to require multiple genes to reconstitute the complete function in yeast systems. One example of the use of yeast as a tool to reconstitute a functional plant ion transport system is the SOS (salt overly sensitive) signaling pathway. SOS3 is a calcium sensor (from CBL family), and recruits the SOS2 protein kinase to the plasma membrane upon activation by calcium. SOS2, once activated by SOS3, is able to phosphorylate SOS1 (Na⁺/H⁺ antiporter) and increase its Na⁺ transport activity. SOS1 confers a weak phenotype of Na⁺ tolerance when expressed in yeast mutants lacking the endogenous Na⁺ extrusion systems. Overexpression of SOS2 and SOS3 in the yeast mutant strain overexpressing SOS1 dramatically rescues the Na⁺ sensitivity phenotype, while overexpression of SOS2 or SOS3 in yeast in the absence of SOS1 does not confer any phenotype (Quintero et al., 2002).

Here it was studied if co-expression of proteins involved in calcium-regulated phosphorylation (CIPK23 and CBL3) or involved in vesicle traffic to the plasma membrane (PEP12 and VAMP722) that are interaction partners of NRT1.5 can reconstitute K⁺ export activity and subcellular localization of NRT1.5 in yeast. As shown before, the expression of NRT1.5 alone in BYT45 cells lacking the endogenous K⁺ export systems ENA1 and NHA1 did not restore K⁺ export at high K⁺ (1M KCl) and acidic pH, and the co-expression of the proton pump AHA2 did not influence the K⁺ export activity of NRT1.5 (**Figure 23**). These results can be explained if NRT1.5 was not fully functional in yeast and required activation by ancillary proteins, such as CBL3 and CIPK23 or PEP12 and VAMP722. Cells expressing any of these proteins alone or together with NRT1.5 did not show growth differences at 0.1M KCl. This is also the case at 1M KCl, but cell growth was dramatically reduced (**Figure 36A**). These results indicate that the protein kinase CIPK23, the Ca²⁺ sensor CBL3, PEP12, and VAMP722 were not sufficient for the activation of K⁺ export in yeast by NRT1.5.

3. Results

Surprisingly, the subcellular localization of NRT1.5 in yeast cells was in cytosol compartments and not in the plasma membrane as it was expected from plant cells (**Figure 27B, 28**). A cellular localization assay was carried out to investigate if co-expression of NRT1.5 with CBL3 and CIPK23 or PEP12 and VAMP722 can change the subcellular localization of NRT1.5. Using the THY.AP4 yeast strain, NRT1.5eGFP was co-expressed with the combination of CBL3 and CIPK23 or PEP12 and VAMP722. NRT1.5 localization was still in the cytosol compartments with or without the expression of the interaction partners of NRT1.5 (**Figure 36B**). These observations advise that the heterologous expression of CBL3 and CIPK23 and PEP12 and VAMP722 are not influencing the cellular localization of NRT1.5 in yeast cells, by their respective calcium-regulated phosphorylation and vesicle trafficking functions.

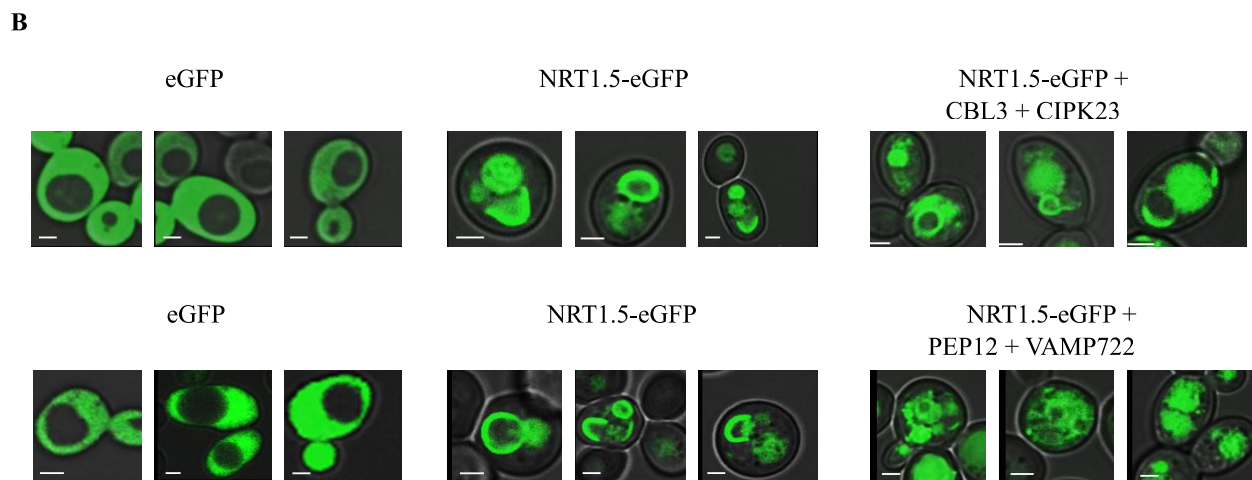
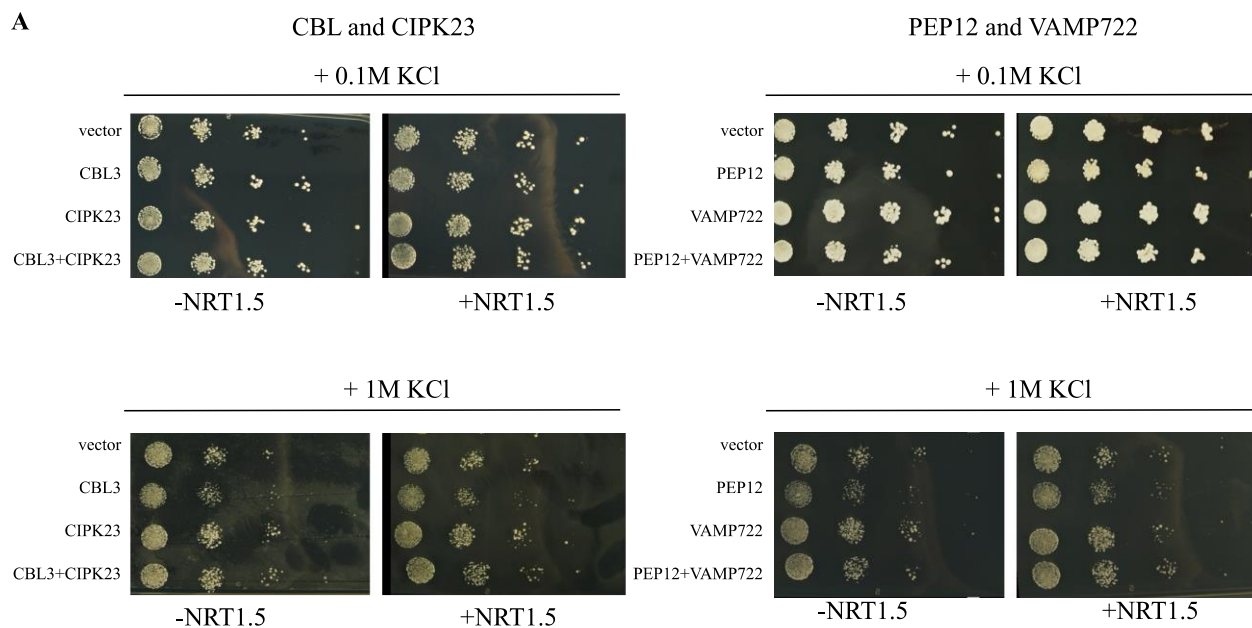


Figure 36: Influence of CBL3 and CIPK23 or PEP12 and VAMP722 co-expressions in the K⁺ export activity and subcellular localization of NRT1.5 in yeast cells. **A.** K⁺ export activity of NRT1.5 co-expressing CBL3/CIPK23 and PEP12/VAMP722. Yeast strain BYT45 lacking the main K⁺ export transporters was transformed with the empty vector or the indicated combination of cDNAs on the left. Cell suspension concentrations from OD_{600nm}= 10⁻¹ to 10⁻⁵ were dropped in YNB (-Ura -Leu -Trp) agar plates supplemented with 0.1 or 1M KCl. Plates were grown for two days at 30°C. **B.** NRT1.5eGFP and CBL3 and CIPK23 or PEP12 and VAMP722 co-expression in THY.AP4 *S. cerevisiae* cells by confocal microscopy. Yeast cultures were grown from a single colony in YNB liquid medium (-Leu -Ura -Trp pH=5.5) at 30°C overnight. The overnight pellets were PBS washed and observed in confocal microscopy. Three representative microscopies are shown of each construct. Microscopies were generated by excitation of GFP, and overlapping the images with the bright field channel. The white bars represent 2µm.

4. Discussion

4.1. AtNRT1.5 protein sequence analysis unveils different characteristic features of the NRT1 family proteins

The low-affinity NO_3^- transporters NRT1/PTR are a ubiquitous family that exists in all kingdoms of life (Steiner et al., 1995). In contrast to the low number of family members in some organisms, such as in *Saccharomyces cerevisiae* (one), *Drosophila* (three), *Caenorhabditis elegans* (four), and humans (six), the NRT1/PTR family is prevalent in higher plants, where Arabidopsis and rice contain 53 and 80 NRT1/PTR members, respectively (Tsay et al., 2007), which implies that these proteins have diverse and complex functions in higher plants. Here, six different known sequence motifs from the NRT1.1 transporter that have been shown by structural and functional studies to be essential for proton-coupled nitrate transport are used to inquire about the NRT1.5 protein features. From the AtNRT1.5 protein alignment against all NRT1 family members, sequence motifs and residues involved in proton coupling, nitrate transport, and recognition are not all present in NRT1.5 in comparison to other NRT1 members (**Figure 5A**). The first two features are implicated in proton and nitrate binding and transport: a conserved motif named ExxER/K, located in the first transmembrane helix (TM1) and a His residue in TM7 that has been observed in some bacterial, algal, and plants transporters (Longo et al., 2018). NRT1.5 has not the ExxER motif in TM1 (instead it has a QxxAT) or a His residue in TM7, indicating NRT1.5 must have an unknown and alternative mechanism for H^+ coupling. Removal of charged residues in the ExxER motif abolished both H^+ binding and NO_3^- transport activity of NRT1.1 (Sun et al., 2014). Moreover, the stoichiometry of H^+/NO_3^- transport through NRT1.1 is at least $2\text{H}^+:1\text{NO}_3^-$, and it was proposed that the ExxER motif in TM1 binds one H^+ , leaving His³⁵⁶ in TM7 to bind another H^+ and NO_3^- (Parker and Newstead, 2014). It is well known that histidine residues are important H^+ binding amino acids involved in the regulation or activity of pH-dependent transporters in bacteria, yeast, mammals, and plants because they can ionize within the physiological pH range (Wiebe et al., 2001; Ortiz-Ramirez et al., 2011). In a high-affinity NO_3^- transporter in rice, OsNRT2.3b, the His¹⁶⁷ was located in the cytoplasmic side and has been confirmed to play a critical role in sensing cytosolic pH (Fan et al., 2016). The H167R mutation does not fully eliminate the basic activity of OsNRT2.3b as an H^+ -coupled NO_3^- transporter but results in the loss of cytosolic pH sensing (Fan

et al., 2016). In addition, in a maize homolog of AtNRT1.1, the His³⁶² was described as essential for nitrate transport (Wen et al., 2017), supporting that this feature is crucial for both proton-coupling mechanisms and the presence of a nitrate binding site in different higher plants. NRT1.5 protein sequence contains only seven His residues but only one is located in a transmembrane domain, the His⁴³³ at TM9. This residue should be considered in future investigations as potential and novel H⁺ binding site in NRT1.5.

NRT1.8, another NRT1 family member in Arabidopsis, participates in the unloading of nitrate from the xylem and is the most similar NRT1 family member to NRT1.5 (\approx 80% identity at the protein sequence level). NRT1.8 is the only NRT1 family member having the same QxxAT motif as NRT1.5 instead of the proton coupling ExxER conserved motif in TM1. Additional functional and phylogenetic studies are needed to clarify how NRT1.5 and NRT1.8 can transport protons, and how the QxxAT motif evolved.

The third feature of plant NPFs is the cytosolic loop linking the two six-helical bundles between TM6 and TM7. This structure of approximately 80 amino acid center loop contains three conserved positively charged residues, Arg²⁶⁴-Arg²⁶⁶-Lys²⁶⁷ in NRT1.1 (Parker and Newstead, 2014) whereas NRT1.5 has evolved non-charged amino acids at positions 266 and 267 which are poorly conserved in plant orthologues. These residues have been shown to play a role in stabilizing the protein. Indeed, Ho and Frommer, 2014 confirmed the importance of these structural elements where nitrate transport activity is inhibited in an Arg^{264A}-Arg^{266A}-Lys^{267A} mutant, and it was suggested that the stable amphipathic alpha-helix in the N-terminal region (including Arg²⁶⁴-Arg²⁶⁶-Lys²⁶⁷) of the center loop could be a potential protein-docking site (Sun et al., 2014). How NRT1.5 stabilizes the protein from the intracellular side is still unknown, and it will need further investigation of which residues are involved in the protein stabilization.

The fourth and fifth features are involved in the formation of an inter-helical salt bridge between residues on TM4 and TM10 that influences the outward-open conformation of NRT1/POT transporters (Newstead, 2017). The salt bridge can potentially form between Lys¹⁶⁴ on TM4 and Glu⁴⁷⁶ on TM10 in NRT1.1 (Parker and Newstead, 2014). The analysis of the residues that can form the salt-bridge between TM4 and TM10 in NRT1.5 reveals that at position 164 a non-charged amino acid is present, and the negatively charged amino acid on TM10 is present in NRT1.5 and in all NRT1 family members. The no conservation of both residues related to the formation of the salt bridge demonstrated that the outward-open conformation of NRT1.5 should have an alternative mechanism. Finally, the residue Thr¹⁰¹ has been one of the features highly conserved in the NRT1

family. Under low NO_3^- conditions, NRT1.1 is toggling from a low to a high-affinity nitrate transport system by phosphorylation at the threonine residue 101 (O'Brien et al., 2016). Initially, NRT1.5 was described with a dual NO_3^- transport function (Lin et al., 2008), so to have a better understanding of the nitrate affinity state of NRT1.5, mutations at this crucial residue can be informative.

In summary, from the amino acid sequence alignment analysis of NRT1 family members, different motif and residues related to NO_3^- and H^+ transport or structural conformation of the transporters are weakly conserved in NTR1.5. These may explain the diverse substrate specificity of the NRT1.5 and suggest the need for further biochemical and structural studies of individual NRT1 for a better understanding of the transport mechanism in this family of transporters. However, the regions corresponding to the features are weakly conserved in the NRT1 family and are highly conserved in NRT1.5 plant orthologues, suggesting an important and complex role of these motifs and residues in the NRT1.5 protein function.

4.2. NRT1.5 is a significant component correlated with the molecular regulation of potassium and nitrate transport in Arabidopsis roots

4.2.1. Transcriptional analysis of *nrt1.5* at low nutrition supply suggests changes in the ion contents in shoots

Transcriptional analyses of selected ion transporters and channels in the *nrt1.5* mutant at K^+ and NO_3^- deficiency conditions support that the loss of the NRT1.5 function has a significant impact on potassium and nitrate homeostasis in roots and shoots.

The expression data from *nrt1.5* mutant roots grown at 0mM K^+ and 1mM NO_3^- conditions shows similarities with Drechsler et al., 2016 expression data from N-deficient plants. For example, HAK5, a transporter involved in high-affinity K^+ uptake is down-regulated in Col-0 and *nrt1.5* roots at K^+ and NO_3^- starvation (**Figure 7**). It is known that K^+ deprivation enhanced the transcription of *HAK5* as a strategy to induce the K^+ uptake under the starvation condition (Rubio et al., 2014). The increase of root K^+ contents in *nrt1.5* mutant in comparison with Col-0 (Li et al., 2017a; Zheng, 2018) is supporting this transcriptional response. Alternatively, changes in the concentration of one nutrient trigger a signaling cascade that modifies not only the amount,

localization, expression, and/or activity of this nutrient-specific transport system but also transport systems related to other nutrients (Ragel et al., 2019). For example, NO_3^- , PO_4^{3-} , and SO_4^{2-} deficiencies reduced root K^+ uptake in tomato and Arabidopsis plants (Ródenas et al., 2017). It is conceivable that the combination of K^+ and NO_3^- deficiencies affect negatively the K^+ uptake by the modulation of the high-affinity transporter *HAK5*.

The vacuolar K^+/H^+ antiporter *NHX1* and the K^+ channel *TPK1* are involved in the sequestration of K^+ from the cytosol to vacuoles. Cytosolic K^+ concentration is thought to decline only when the vacuolar K^+ reserve has been depleted below the thermodynamical equilibrium with the cytosolic pool (Walker et al., 1996). The overexpression of the *AtNHX1* induced K^+ -deficiency symptoms despite transgenic plants having greater vacuolar K^+ contents. The intense sequestration of K^+ in *NHX1*-overexpressing plants reduced cytosolic K^+ activity and elicited disorders related to K^+ deprivation (Leidi et al., 2010). Here, the reduction in cytosolic K^+ caused by K^+ -starvation triggers downregulation of *NHX1* and *TPK1* in wild-type plants, most likely to avoid K^+ storage into vacuoles, whereas in the *nrt1.5* mutant the expression of both genes is not altered, probably because the accumulation of K^+ in roots by *nrt1.5* mutation is compensating the external low K^+ supply.

Regarding nitrate homeostasis, the lack of *NRT1.5* generates an accumulation of NO_3^- in roots and shoots at K^+ and NO_3^- deficiency conditions (**Figure 6**). The expression of NO_3^- uptake transport systems (*NRT1.1* and *NRT1.2*) and the xylem translocation systems (*NRT1.4* and *NRT1.8*) are not regulated by K^+ and NO_3^- deficiency and it cannot explain the accumulation of NO_3^- in roots and shoots (**Figure 7**). Two members of the slow anion channel-associated homolog *SLAH1* and *SLAH3* involve in nitrate efflux from pericycle cells into the root xylem vessels are highly up-regulated (**Figure 13**), similar as under N-deprivation (Drechsler et al., 2015). Their up-regulation in *nrt1.5* roots may support the accumulation of nitrate in shoots, indicating *SLAH1* and *SLAH3* might positively correlate with the lack of *NRT1.5* in pericycle cells. However, the high nitrate contents in roots cannot be explained by these transcriptional data.

Nutrients contents in the media and transcriptional control of K^+ and NO_3^- transport systems support that *NRT1.5* influences, directly and indirectly, the root-to-shoot translocation of K^+ and NO_3^- in plants. However, the combination of both potassium and nitrate starvation reveal that the linkage between NO_3^- and K^+ transport by *NRT1.5* is more intimate than the mere balancing of charges as previously thought.

4.2.2. *NRT1.5* promoter is regulated by nutrient availability and uptake

The promoter-GUS analyses carried out in this work showed that the activity of the *NRT1.5* promoter in roots is dependent on the cellular K^+ status (**Figure 8**). In contrast to the studies published so far, which always focused on the *NRT1.5* promoter activity in roots under K^+ and NO_3^- sufficient conditions (Lin et al., 2008; Drechsler, 2016; Zheng et al., 2016; Watanabe et al., 2020), results from this thesis indicate additional *NRT1.5* function in response at K^+ and NO_3^- limitation presumably as a mechanism to enhance the xylem loading.

Promoter activity and tissue specificity of multiple nitrate and potassium transporters and channels are altered by different ion supplies as a strategy to improve the transport mechanisms. For example, the promoter activity and tissue specificity of the high-affinity nitrate uptake systems, *NRT2.1* and *NRT2.4*, were affected in N-deprived plants (Kiba et al., 2012). In addition, the promoter activity of the K^+ uptake transporters *AtHAK5* (Gierth et al., 2005) and the K^+/H^+ transporter *AtCHX13* (Zhao et al., 2008) was induced by a low supply of K^+ . Surprisingly, the *NRT1.5* promoter activity is strongly reduced in the root vasculature upon blocking K^+ uptake by CsCl (**Figure 8**). Recently, tight coordination between K^+ uptake and translocation in plants was demonstrated, where K^+ translocation may act in K^+ uptake via a feedback mechanism to adapt K^+ uptake rates to the K^+ translocation ones (Nieves-Cordones et al., 2019). For instance, lack of the main K^+ translocation transporter, *SKOR*, has a negative impact on Rb^+ uptake (an analog for K^+) and K^+ uptake transporter *HAK5* expression in plants with K^+ deprivation (Nieves-Cordones et al., 2019). The authors speculate that K^+ uptake and translocation are linked in such a way that if one slows down, the other follows suit.

Thus, it is tempting to speculate that xylem loading via *NRT1.5* might be regulated by K^+ uptake. Changes in the promoter activity of *NRT1.5* did not provide conclusive evidence for a feedback mechanism between K^+ uptake and translocation, further research in this line is required.

4.3. *NRT1.5* has an important role in root architecture and plant development

4.3.1. *NRT1.5* is not involved in root K^+ perception

Nutrient distribution is heterogeneous in soil, and plant roots have to detect the nutrient content and exploit the nutrient-rich zones to acquire more nutrition for plant growth and development, which

requires nutrient sensors in plant roots. These sensors must perceive the external nutrient concentrations in a wide range and have the ability to regulate root growth according to the nutrient concentration. Plants perceive external K^+ concentrations and modulate their root architecture to grow towards the K^+ -rich zones. In general, deficiency of K^+ produced a root system that became shorter and the primary root length decreased, which is an important morphological response to K^+ deficiency (Gruber et al., 2013). On another hand, nitrate deficiency stimulated the growth of a more exploratory lateral root system but an unaffected primary root growth (Sun et al., 2017). In the present study, a root growth experiment indicated that wild-type *Arabidopsis* roots can sense the different local K^+ concentrations when nitrate levels are stably low at 1mM (**Figure 9**).

The molecular mechanism for the perception of external nutrient signals to modulate root growth is still not well described. A few examples exist in the literature about proteins acting as nutrient sensors. The K^+ channel, AKT1, is involved in the perception of changing K^+ conditions in the external environment. Other than in wild type plants, the root growth of the *akt1* mutant was almost unaffected by external K^+ , proving an implication of AKT1 in *Arabidopsis* response to low K^+ (Li et al., 2017b). Also NRT1.1 acts in external NO_3^- sensing, and is located upstream of the transcription factor ANR1 in the NO_3^- signaling pathway that triggers increased lateral root elongation (Remans et al., 2006).

Since some of the NRT1.5 properties were consistent with a role in K^+ sensing, I hypothesized that NRT1.5 could also be involved in the perception of nutrient availability. First, mutants of NRT1.5 were shown to display a root development phenotype under very specific conditions of K^+ , NO_3^- , and PO_4^- (Drechsler, 2016; Zheng, 2018) that could not be related to NRT1.5 transport activity. Second, nutrient sensors in root cells must perceive the external nutrient concentrations in a wide range and have the ability to regulate root growth according to the nutrient concentration (Li et al., 2017b). NRT1.5 mediates K^+ transport over an ample range of K^+ concentrations, from 0.01mM to 1mM (Li et al., 2017a; Zheng, 2018), which might facilitate the perception of various K^+ concentrations in the external environment. Third, the transcription rate of *NRT1.5* is unaffected by external K^+ supply (Zheng, 2018). Thus, the abundance of NRT1.5 is relatively stable, which may ensure a steady response under different K^+ conditions. However, root and shoot growth of wild-type and the *nrt1.5* mutant showed gradually affected phenotypes by external K^+ gradient, demonstrating mutant plants are still able to perceive the external K^+ . This indicates that NRT1.5 is not involved in K^+ sensing (**Figure 9 and 19**).

4.3.2. NRT1.5 modulates the root architecture in dependency of external nitrate, potassium and pH

This study showed that NRT1.5 not only governs root growth by external nitrate and potassium contents in the medium, also the external pH status has a strong impact on the root architecture. The *nrt1.5* mutant shows a reduction in lateral root formation under acidic pH and K⁺ deprivation, supporting previous observations (Zheng et al., 2016), and also under basic pH and NO₃⁻ deprivation (**Figure 10**). How the root architecture is modulated in dependency of NRT1.5, nutrient availability in the media, and pH is a complex physiological observation that may combine other components.

Several studies showed interconnections between pH, nutrient availability, and root growth in higher plants. For example, aluminum and low pH (pH≤4.5) influence the root elongation (Koyama et al., 1995), phosphorus and pH (acidic and basic) alter the root morphology (Robles-Aguilar et al., 2019). In addition, hormone contents have been described recently as another component influencing root growth together with pH and nutrient availability (Meier et al., 2020). Auxin diffusion is described as a mechanism to coordinate the plasticity of the root system architecture under fluctuating nutrient availabilities, and if NRT1.5 is directly or indirectly involved in auxin transport was already discussed in the literature (Zheng et al., 2016). As an indirect involvement of hormones, it has been described that ammonium transporters acidify the root apoplast, which increases the pH-dependent import of protonated auxin into cortical and epidermal cells, promoting the emergence of lateral roots. In nitrogen-deficient plants, auxin also accumulates in the root vasculature, but a more alkaline apoplast leads to retention of auxin in these tissues and prevents lateral root formation (Meier et al., 2020). Nitrate and potassium transport also acidify the root apoplast by H⁺-coupled ion transport to maintain the electrochemical balance and contribute to intracellular pH homeostasis (see introduction 1.4.2). Based on the observation that the lateral root is influenced by NRT1.5 at low K⁺ in combination with acidic conditions or low NO₃⁻ combined with basic pH (**Figure 10**), it is therefore tempting to speculate that NRT1.5 activity can modulate the root architecture by pH changes that influence the hormone homeostasis.

Alternatively, NRT1.5 has been described recently as a potential transporter of Indole-3-butyric acid (IBA), a precursor of the major endogenous auxin indole-3-acetic acid (IAA) (Watanabe et al., 2020). In line with this, NRT1.5 activity can influence the lateral root growth by the direct control of the hormone status. Interestingly, the nitrate transporter NRT1.1 has a dual NO₃⁻ and auxin

transport activity and it controls auxin accumulation in lateral root tips in response to low NO_3^- supply ($<0.2\text{mM}$) through the modification of auxin transport (Krouk et al., 2010). NRT1.5 might control the lateral root in the same way. To better understand the implication of NRT1.5 in root growth with auxin, nutrients availability, and pH, the analysis of *DR5::GUS/nrt1.5* transgenic line is suggested. *DR5::GUS* is a synthetic auxin-responsive promoter fused to the GUS reporter gene (Ulmasov et al., 1997). This transgenic reporter in the background of *nrt1.5* will provide novel insights about how auxin distribution in roots depends on the NRT1.5 function.

4.4. Identification of interaction partners of NRT1.5 uncovers mechanisms of posttranslational regulation

The multifaceted influence of NRT1.5 in nutrient homeostasis can be based on the regulatory interaction with other possible nutrient-associated proteins. This study verified and confirmed the protein-protein interactions of NRT1.5 with seven proteins by BiFC assay (**Figure 12**). Those proteins are involved with pH regulation in roots (H^+ -ATPase AHA2), protein targeting by secretory pathway (the SNARE proteins PEP12 and VAMP722), specific Ca^{2+} signature and phosphorylation events (Ca^{2+} sensor CBL3 and the kinase CIPK23), and anion transport (S-type anion channels SLAH1 and SLAH3). Most of these mechanisms are involved in post-translational regulation of proteins, which would allow to rapidly adapt the transporter activity to changes in nutrient availability. A recent publication shows that NRT1.5 expression is not epigenetically regulated by DNA methylation, a mechanism controlling other NRT family members as NRT1.1 and NRT2.1. The authors suggest that other regulatory mechanisms, for instance, transcription factor binding or post-translational modifications, might be involved in the regulation of NRT1.5 (Hua et al., 2020). MYB59 was directly bound to the *NRT1.5* promoter and positively regulated its expression (Du et al., 2019), but no post-translational mechanisms were identified up to date.

AHA2, CBL3, SLAH1, SLAH3, and VAMP722 could interact with NRT1.5 as they are expressed in the same tissues, pericycle root cells and root vasculature, in the plasma membrane (Fuglsang et al., 2007; Liu et al., 2013; Zheng et al., 2015; Cubero-Font et al., 2016). In the literature, none of the interaction partners were linked directly with NRT1.5. Nevertheless, some family members of them were well described in interaction with other K^+ and NO_3^- transport systems in *Arabidopsis thaliana* or other higher plants. **Figure 37** shows a hypothetical model of potential functions of the interaction partners of NRT1.5 (named from A to D) in the plasma membrane of pericycle cells.

(A) Many nutrient transport proteins in plant cells are energized by electrochemical H^+ gradients across the plasma membrane due to the action of H^+ -ATPase (Palmgren, 2001). NRT1.5 activity might need the interaction with AHA2 to maintain the electrochemical gradient homeostasis. (B) CBL-CIPK modules are well known to regulate the activity of HAK5 (Ragel et al., 2015), AKT1 (Sánchez-Barrena et al., 2020), AKT2 (Held et al., 2011), GORK1 (Förster et al., 2019), and NRT1.1 (Ho et al., 2009) transport systems. Phosphorylation of NRT1.5 by CBL3 and CIPK23 might be an activation mechanism. (C) The vesicle-trafficking SNARE pathway through VAMP and PEP proteins controls the ion transport and activity of KC1 and KAT1 (Waghmare et al., 2019). Based on that, the NRT1.5 targeting to the plasma membrane via the SNARE pathway is postulated. (D) Negative regulation of NRT1.5 by SLAH1 and SLAH3 is hypothesized since these S-type anion channels are essential negative regulators of K^+ transporters like KAT1 (Zhang et al., 2016).

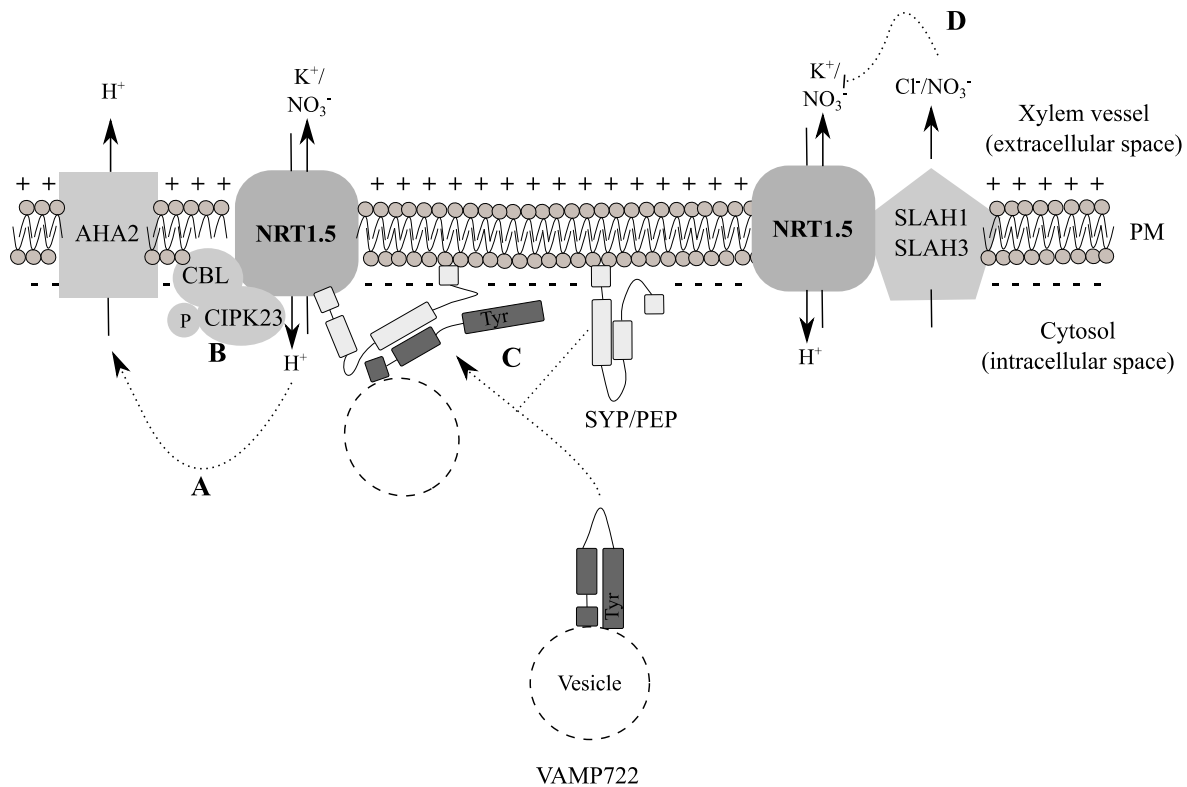


Figure 37: Hypothetical model represents how NRT1.5 may interact in the plasma membrane of root cells with AHA2, CBL3, CIPK23, PEP12, SLAH1, SLAH3, and VAMP722. NRT1.5 interaction with **A**, the proton pump AHA2, **B**, the complex between the calcineurin B-like 3 (CBL) and a CBL-Interacting protein kinase (CIPK23), **C**, the cooperation of the SNARE proteins SYP/PEP and VAMP722, and **D**, the regulation by the anion channels SLAH1 and SLAH3. Abbreviations: Try, tyrosine residue in VAMP722. P, phosphorylation site of CIPK23. Dotted arrows and lines represent the hypothetical interaction between

NRT1.5 with the different proteins. PM, plasma membrane. + and –, positive and negative net charges in the extra or intracellular space.

4.5. NRT1.5 and AHA2 are correlated with the maintenance of the plasma membrane potential and cellular pH

Protein-protein interaction between NRT1.5, and the plasma membrane H⁺-ATPase, AHA2 was confirmed in plants by the BiFC assay (**Figure 13**). The plant plasma membrane H⁺-ATPases or so-called AHAs (AUTOINHIBITED H⁺-ATPases) are found as a multigene family, where AHA2 is the central isoform in roots, expressed mainly in the epidermis, root cortex cells, xylem, and root hairs (Fuglsang et al., 2007; Hoffmann et al., 2019). AHAs facilitate an acidic cell wall environment by extrusion of protons to the apoplast, which is essential for cell wall expansion and cell growth. They generate a proton electrochemical gradient which provides the driving force for the uptake and efflux of ions and metabolites across the plasma membrane (Sze et al., 1999). The *aha2* mutant shows an up-regulation of the K⁺ transporters HAK5 and CHX17 indicating a close link between proton transport and K⁺ fluxes at the plasma membrane, especially at low K⁺ supply (Haruta and Sussman, 2012). Potassium is not the only nutrient linked to this AHA isoform, it was shown that the *AHA2* expression levels are affected by different nitrate supplies (Młodzińska et al., 2015) and at a protein level, AHA2 was identified as a protein involved in the regulation of nitrogen starvation responses (Gilbert et al., 2021).

Here, besides the physical interaction, the physiological importance of NRT1.5 and AHA2 interaction was described. The lack of *NRT1.5* and *AHA2* in plants triggered a slight but significant accumulation of K⁺ in leaves only under low K⁺ supply (**Figure 17A**), indicating an involvement of both proteins in K⁺ xylem loading. No phenotypes are observed in adult plants, but in roots and shoots at an early developmental stage of seedlings. The lateral root, root hair, and shoots of *aha2* mutants are affected (**Figure 18**), and the expression levels of *AHA2* are *NRT1.5* are regulated by K⁺ and NO₃⁻ deficiencies (**Figure 13**). Collectively, these analyses reveal a novel and coordinated function of the protein-protein interaction between NRT1.5 and AHA2 in the maintenance of potassium homeostasis in roots and shoots of Arabidopsis that impact the plant development.

Additionally, eliminating or overexpressing *NRT1.5* and *AHA2* in Arabidopsis and yeast respectively, had a strong effect on the plasma membrane potential (**Figure 20 and 21**) and extracellular pH (**Figure 22 and 24**), where the last one was directly related to K⁺ and NO₃⁻ status

in the media. Interestingly, plants lacking AHA2 altered the extracellular pH in MS media, which is consistent with previous studies (Haruta et al., 2010). When wild-type plants face K^+ deprivation, the extracellular space becomes acidic (Walker et al., 1998), whereas *aha2*, *nrt1.5* and *nrt1.5/aha2* mutants are unable to acidify the extracellular space (**Figure 22**), suggesting that NRT1.5 and AHA2 cooperatively modify the extracellular pH at K^+ and NO_3^- deficiencies since the double mutant *nrt1.5/aha2* shows a different phenotype from the single *nrt1.5* and *aha2* knockouts.

The pH homeostasis in different cellular compartments and plasma membrane potential was mentioned in the introduction of this thesis as the result of the collaboration between H^+ pumps and H^+ -coupled K^+ / NO_3^- transporters and channels at the plasma membrane.

For example, an immediate physiological response of root cells to NH_4^+ and NO_3^- exposure is a transient change of plasma membrane potential, which is caused by NH_4^+ and NO_3^- influx carrying H^+ into the cell and compensated by activation of the plasma membrane H^+ -ATPase to repolarize and maintain the plasma membrane potential (Wang et al., 1994; Liu and Von Wirén, 2017).

Regarding potassium transport, in the bread red mold *Neurospora crassa*, depolarization is caused by K^+ inward movement in co-transport with H^+ , where the entry of $1K^+$ with $1H^+$ would electrically balance the extrusion of $2H^+$ per ATP hydrolyzed by plasma membrane H^+ ATPase (Rodriguez-Navarro et al., 1986). And in Arabidopsis, the K^+ channel GORK mediates K^+ efflux from root cells, which alongside H^+ efflux by AHA2, repolarizes membrane potential, and restores the ion homeostasis (van Kleeff et al., 2018). In line with these examples, a model is hypothesized where the NRT1.5 transporter activity may require the PM H^+ -ATPase, AHA2 in roots. NRT1.5 exports nutrients to the xylem, leading to the interaction with the proton pump AHA2 to activate the proton extrusion, which acidifies the apoplast space to keep the proton homeostasis required for NRT1.5 activity.

4.6. NRT1.5 requires the conserved Gly²⁰⁹ in TM5 to interact with AHA2 at the plasma membrane

Mutations in NRT1.5 and AHA2 directly influenced their physical interaction (**Figure 25, 26**). Specifically, the mutations affecting the K^+ activity of NRT1.5 (substitution G209E) or the H^+ pump activity of AHA2 (substitution E684V) impacted the protein-protein interaction in yeast and plants. Initially, to the identification of new key components involved in K^+ absorption or

translocation in plants, a low-K⁺-sensitive mutant (so-called *lks*) was characterized (Li et al., 2017a). The *lks2* mutant was identified as a single-nucleotide mutation in *NRT1.5*, which resulted in a substitution of Gly²⁰⁹ to Glu (G209E). Here, the introduction of NRT1.5^{G209E} is not able to complement the *nrt1.5* phenotype either in roots or shoots of Arabidopsis (**Figure 11**), and the overexpression of the NRT1.5^{G209E} in yeast does not phenocopy the plasma membrane potential status of cells expressing NRT1.5 (**Figure 21**). In addition, the Gly²⁰⁹ is not a unique required residue via NRT1 family members interact with AHA2, since protein-protein interaction occurs between AHA2 and NRT1.10 (Ala in position 209) but not NRT1.8 (Gly in position 209) (**Figure 31**).

The presence of a non-polar (Gly, Ala, or Val) residue at position 209 is conserved in all NRT1 family members and among other NRT1.5 plant orthologues (**Figure 25C**), suggesting an important role of this residue in the protein function. Non-polar amino acids seem to have high plasticity of replacement among them (most frequently the protein function is not affected), whereas the exchange to a charged one is a radical replacement that can lead to changes in protein structure or function (Castro-Chavez, 2010). Indeed, here the substitution from a non-polar (Gly) amino acid to an acidic charged residue (Glu) results in a loss of function mutation (**Figure 11**). Here, it is proposed that the transmembrane Gly²⁰⁹ residue plays a vital role in maintaining NRT1.5 function under K⁺ and NO₃⁻ deficiency. However, the mechanism of how Gly is maintaining the protein function at the plasma membrane remains unknown.

Moreover, the Gly²⁰⁹ is located inside of a potential motif from the family of the Leucine-Rich Repeats (LRR). There are multiple sub-families of LRR domain types, each with consensus amino acid motifs slightly differing from the minimal canonic L₁xxL₂xL₃ motif (Martin et al., 2020). NRT1.5 protein sequence showed three protein repeats (named here as I, II, III) with potential LRR motifs at the transmembrane domain 3, 4, and 5 (**Figure 25C**). The motif I included the canonic L₁xxL₂xL₃ motif at TM3, and repeat II contains a variation from the LRR canonic motif when L₃ is replaced by another hydrophobic amino acid (L₁xxL₂xY₃) at TM4. Supporting this the Kobe and Kajava classification of LRR motifs described that one leucine often replaces for another hydrophobic residue (Kobe and Kajava, 2001). Interestingly, the Gly²⁰⁹ at TM5 is flanking the repeat motif III that contains an extension of the motif LRR (Y₁xxL₂xL₃xx). It is been shown that mutations at conserved locations in LRR repeat often disturb protein-protein interactions and functions in plants (Martin et al., 2020). In this context, the substitution G209E may affect the

NRT1.5 function by distortion of protein-protein interaction with other important components that support the K⁺ export function.

4.7. NRT1.5 and AHA2 protein localization is independent of G209E and E684V mutations respectively

Cellular localization of NRT1.5 and AHA2 have been reported and predicted at the plasma membrane in *Xenopus* oocytes, or seedlings and protoplasts, respectively (Li et al., 2017a; Haruta et al., 2018). The introduction of G209E and E684V mutations in NRT1.5 and AHA2 do not change the cellular localization of both proteins in yeast or plant cells (**Figure 11, 27, 29**), meaning that the mutations are not influencing the protein trafficking to the cellular membrane. To understand how the protein-protein interaction is affected by the lack of function of NRT1.5 and AHA2, the concept of protein mobility in cellular membranes is introduced here.

Several studies have shown that the polar localization of mineral nutrient transporters in plant cells (cell asymmetry) is involved in efficient uptake and translocation of the nutrients. For example, the iron transporter IRT1 is localized at the outer polar domain of the plasma membrane of root epidermal cells (Barberon et al., 2014). In contrast, the borate exporter BOR1 localizes to the inner domain of root endodermis cells (Takano et al., 2010). Moreover, the potato (*Solanum tuberosum*) high-affinity phosphate transporter PT2 localizes to the apical (shoot-oriented) surface of the epidermal plasma membrane (Gordon-Weeks et al., 2003), and the nitrate transporter NRT2.4 was identified to the outer plasma membrane domain in epidermal cells for efficient capture and uptake of NO₃⁻ from the soil into roots (Kiba et al., 2012).

Nutrient availability is an important environmental signal that influences the protein distribution in the plasma membrane. For example, when boron levels increase, BOR4 protein becomes enriched at the outer domain of the membrane in the root elongation zone to dampen boron-associated toxicity. Importantly, this localization directs boron export in the soil-ward direction, opposite to the direction utilized for nutrient uptake (Miwa et al. 2007). How the protein mobility or polarities are established, maintained, and dynamically modulated, or if protein-protein interactions are affected by this mechanism are still largely unclear for most of the proteins (Raggi et al., 2020; Yang et al., 2020). NRT1.5 and AHA2 protein functions in loading the xylem vessels from the pericycle cells might emerge as good candidates to present membrane asymmetries because of the specific spatial direction of their transport. In the approach taken here, NRT1.5 and NRT1.5^{G209E}

in root cells appeared not to be asymmetrically localized (**Figure 11**). In addition protein localization of AHA2 and AHA2^{D684V} in planta was not observed here since only overexpression with 35S promoter in tobacco or TEF promoter in yeast was done (**Figure 27, 28, and 29**). The expression of AHA2 and AHA2^{D684V} fused to a fluorescent tag under control of the *PHO1* or *AHA2* promoters will be useful to observe if AHA2 shows protein asymmetry along the root plasma membrane and if the mutation D684V influences the protein localization.

Together with the 4.6 and 4.5 sections, a hypothetical model about how NRT1.5 and AHA2 interact together at the root plasma membrane is shown (**Figure 38**). Temporary, the ion transport activity of NRT1.5 generates a ΔpH between the cytosol and the extracellular space by a still unknown mechanism since motifs related to H^+ transport are not present in NRT1.5. This is supported by the pH and plasma membrane potential observations in NRT1.5 loss or gain of function mutants (**Figure 20, 21, and 22**) and with the already discussed mechanisms of other nitrate and potassium transporters that generate a ΔpH . Subsequently, AHA2 might restore the pH, pumping out protons to the extracellular space. NRT1.5 mutated at Gly²⁰⁹ is still able to localize to the PM (**Figure 11 and 29**) but the interaction with AHA2 does not occur most likely because the mutation in a highly conserved LRR motif affects the protein-protein interaction with AHA2. Alternatively, the NRT1.5^{G209E} and AHA2^{D684V} mutations might affect a proper asymmetric accumulation within the plasma membrane. This could explain why the protein-protein interaction between NRT1.5 and AHA2 takes not place even when proteins are located at the plasma membrane (**Figure 38**).

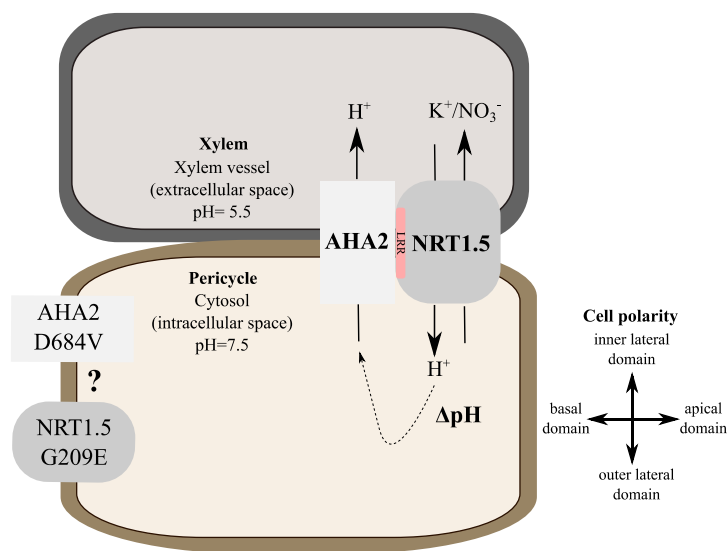


Figure 38: Hypothetical model about the interaction of NRT1.5 with AHA2 at the root plasma membrane. Both proteins potentially work together to keep the K⁺, NO₃⁻ and pH homeostasis in plant roots. The question mark represents the loss of function NRT1.5^{G209E} and AHA2^{D684V} mutants with an altered localization at the plasma membrane.

4.8. Different H⁺-ATPase family proton pumps are correlated with K⁺ and NO₃⁻ homeostasis

The *Arabidopsis thaliana* genome encodes 11 plasma membrane H⁺-ATPase (AHAs) proteins of around 950 amino acids (**Table 3**), although AHA1 and AHA2 are the most predominantly expressed in the plants (Baxter et al., 2003; Haruta et al., 2010).

AHA1 is a housekeeping protein found all over the plant but it is described as the major isoform in guard cells (Ueno et al., 2005; Haruta et al., 2010). AHA2 plays a critical role in establishing the proton gradient at the root surface (Fuglsang et al., 2007), AHA4 controls proton homeostasis in the root endodermis (Vitart et al., 2001), AHA6 and AHA9 are detected specifically to guard cell protoplasts (Ueno et al., 2005) and are required for pollen development (Hoffmann et al., 2020).

Interestingly, the gene expression of AHA family members is regulated under K⁺ and NO₃⁻ deficiencies and is correlated with *NRT1.5* and *AHA2* (**Figure 30**). Some plasma membrane H⁺-ATPases respond also to other abiotic stresses. For instance, roles for *AHA1* in red light stress (Ando and Kinoshita, 2018), *AHA2* in iron transport (Santi and Schmidt, 2009), and together with *AHA7* in phosphorus stress (Yuan et al., 2017), and *AHA4* in salt stress (Gévaudant et al., 2007), have been reported.

In this work, H⁺-ATPase isoforms *AHA4* in roots and *AHA6* in guard cells are up-regulated in wild-type plants under K⁺ and NO₃⁻ deficiency. Surprisingly, in *nrt1.5* mutant, an increased expression of *AHA1*, *AHA2*, and *AHA4* was detected (**Figure 30**). The expression patterns and protein abundances of AHA1 and AHA2 together generate up to 80% of the overall H⁺-ATPase activity in plants (Haruta and Sussman, 2012). The expression of AHA1 and AHA2 are correlated with *NRT1.5*, perhaps directly or indirectly due to the lack of macro and micronutrients in shoots (**Figure 17**), or the alteration in the expression of K⁺ and NO₃⁻ transporters and channels (**Figure 7**), or the root extracellular pH changes (**Figure 22**), or changes in plasma membrane potential (**Figure 21**). In addition, AHA4 is strongly expressed in the root endodermis (Vitart et al., 2001). The root endodermis serves as a border between the outer cortex and the inner vascular system and is involved in the regulation of the nutrient uptake from the soil (Barberon et al., 2016), so it is conceivable that the alteration in K⁺ and NO₃⁻ root homeostasis triggers the activation of the proton pump AHA4 in root endodermis.

Additionally, the lack of the proton pump AHA2 in roots induced expression of the pollen tube isoforms *AHA6* and *AHA9* (**Figure 30**). Since AHA2 is the main proton pump involved in root

acidification, *AHA6* and *AHA9* expression may compensate for the lack of *AHA2* in roots. However, further investigation of these novel molecular interactions should be addressed in the direction of the spatial expression of those isoforms since it occurs in different plant organs.

Remarkably in the double mutant *nrt1.5/aha2*, no H⁺-ATPase members are regulated (**Figure 30**), evidencing a strong influence and molecular interaction between *NRT1.5* and *AHA2* in the genetic regulation of proton pumps in plants.

4.9. K⁺ export activity of NRT1.5 is not detected in *Saccharomyces cerevisiae*

There have been many successful examples of functional characterization of plant K⁺ transporters and channels using the heterologous expression system in *S. cerevisiae*. Using yeast mutants lacking the main K⁺ export (*ENA1* and *NHA1*) or import (*TRK1* and *TRK2*) transporters, it was found that *KAT1* (Anderson et al., 1992), *AKT1* (Sentenac et al., 1992), *HAK5* (Rubio et al., 2000), *KUP1* (Fu and Luan, 1998), *KT3/KUP4* (Rigas et al., 2001), *HKT1* (Schachtman and Schroeder, 1994), and *CHX13* (Zhao et al., 2008) most of them from *Arabidopsis thaliana* can complement the function in the yeast mutants. However, functional analyses by the heterologous expression of plant genes in yeast have several limitations. For instance, not all plant membrane proteins are correctly folded, processed, assembled, or localized in yeast due to the absence of specific machinery. Also, they may lose activity due to the different composition of the membrane lipids, or not all plant genes are properly expressed in yeast due to codon-usage bias (Locascio et al., 2019).

The implementation of the yeast system to characterize *NRT1.5* as a K⁺ export/import transporter has been employed without success at pH=6 (Drechsler et al., 2015). Here, the strategy of co-expressing *NRT1.5* with regulatory proteins to complement the yeast growth was used. For example, the potassium channel *AKT1* and potassium transporter *HAK5* were able to complement yeast mutants only when they were co-expressed together with *SYP121* and *CIPK23/CBL1*, respectively (Honsbein et al., 2009; Ragel et al., 2015). Alternatively, different yeast growth conditions, like nutrients availability or pH conditions, could affect the ion reconstitution in yeast. Unfortunately, adjusting the pH to 5.5 to simulate the xylem vessel conditions or the reconstitution of the K⁺ transport system by co-expression with the H⁺-ATPase controlling the extracellular pH, or with *CBL3* and *CIPK23* involved in phosphorylation mechanisms or, with *VAMP722* and

PEP12 related to the vesicle trafficking to the plasma membrane was not enough to reconstitute the K^+ export activity of NRT1.5 in yeast (**Figure 23 and 36A**).

The failure to recover the K^+ transport activity of NRT1.5 might be caused by incomplete or no translation, incorrect folding, sorting, or even degradation of the NRT1.5 in the yeast cell system. However, NRT1.5 successfully is expressed in yeast cells but the protein localization was not at the plasma membrane (**Figure 27**). This shows that NRT1.5 is not (fully) functional as a K^+ transporter in yeast due to the wrong intracellular localization, which could not be restored by the introduction of NRT1.5 interaction partners involved in post-translational mechanisms (**Figure 27B, 28, and 36B**).

AHA2 expression in yeast also has led to an incorrect cellular localization but functional activity was detectable in the heterologous expression system in *S. cerevisiae*. For example, extracellular pH (**Figure 24**) and plasma membrane potential (**Figure 21**) were altered when AHA2 is expressed in yeast. Few studies about the functional evaluation of plant proteins in the heterologous expression system in yeast showed an incorrect cellular localization by retention in different subcellular compartments together with residual functional activity. More than 25 years ago, H^+ -ATPases from *A. thaliana* were shown to be retained in internal membranes and only weakly complemented the growth defect of the *pma1* mutant (lacking main yeast proton pump systems). Truncated versions in the C-terminus were able to partially localize to the plasma membrane and fully complemented the growth defect (Palmgren and Christensen, 1993).

4.10. Interaction between NRT1.5 with the anion channels SLAH1 and SLAH3

In *Arabidopsis thaliana*, SLAH3 is an anion channel involved in chloride and nitrate transport in guard cells, while SLAH1 together with SLAH3 are engaged in root nitrate and chloride acquisition, and anion translocation to the shoots (Hedrich and Geiger, 2017). SLAH1 and SLAH3 proteins independently are interacting with NRT1.5 at the plasma membrane of plant cells (**Figure 12** and Zheng, 2018). Also, transcriptional levels of *SLAH1* and *SLAH3* are highly induced by low K^+ and NO_3^- supply conditions in the *nrt1.5* mutant (**Figure 13**). Other types of abiotic stresses, such as salinity, water deficit, low pH, and low N, were linked to transcriptional regulation of those anion channels (Drechsler et al., 2015; Cubero-Font et al., 2016; Zhang et al., 2016; Qiu et al., 2017), demonstrating a wide function under different types of stresses. The physiological interaction between NRT1.5 with SLAH1 and SLAH3 can be explained either as a positive

regulation due to the shared function of NO_3^- transport or as negative regulation of K^+ loading into the xylem since anion channel activity has been linked to reducing the activity of K^+ transport (Laanemets et al., 2013; Zhang et al., 2016). However, the lack or overexpression of SLAH1 and SLAH3 in Arabidopsis plants did not cause morphological or development changes compared to wild type plants under different NO_3^- and K^+ regimes, and did not reveal a link to NRT1.5 activity (**Figure 15, 32, 33**). These data show that the individual contribution of SLAH1 and SLAH3 is not directly correlated with NRT1.5 in the maintenance of nutrient homeostasis. Alternatively, the creation of the triple mutant of *slah1/slah3/nrt1.5* can provide additional information of a possible contribution of SLAH1-SLAH3 module in K^+ and NO_3^- homeostasis.

Besides the contribution of S-type of anion channels in plant nutrition, other roles largely attributed to these anion channels are the regulation of the cellular ion charge balance to control physiological processes. For example, expanding cells need to accumulate osmolytes to keep up cell turgor and for this reason, they require anion channels. Active anion channels would cause ion leakage and thus create a futile cycle with ion uptake systems. However, various stimuli activate anion channels and lead to a rapid reduction in osmolytes that leads to loss of turgor (Roelfsema et al., 2012). Here, the anion channels SLAH1 and SLAH3 are components controlling the plasma membrane potential in root cells (**Figure 34**). If the changes in plasma membrane potential by SLAH1 and SLAH3 can affect the NRT1.5 activity directly or indirectly is not possible to answer with this data, so further investigation is needed.

4.11. Potential posttranslational regulation of NRT1.5 by CBL3 and CIPK23

Cytosolic moieties of K^+ and NO_3^- transporters and channels share a common regulatory mechanism in which a protein complex between a Calcineurin B-like (CBL) and a CBL-Interacting Protein Kinase (CIPK) decodes a specific calcium signature to phosphorylate and activate ion transport. In Arabidopsis, diverse ion transport systems are regulated by CBL-CIPK complexes, including channels or transporters that mediate transport of potassium (KAT1, KAT2, GORK, AKT1, AKT2, HAK5, SPIK), sodium (SOS1), ammonium (AMT1.1, AMT1.2), nitrate and chloride (SLAC1, SLAH2, SLAH3, NRT1.1, NRT2.4, NRT2.5), and protons (AHA2, V-ATPase) (Reviewed by Saito and Uozumi, 2020). From the 10 members of CBLs and 26 members of CIPKs

present in the *Arabidopsis thaliana* genome, here it is confirmed by the BiFC assay that CBL3 and CIPK23 are physically interacting with NRT1.5 in planta (**Figure 12**).

Remarkably, the *cipk23* and *nrt1.5* mutants were isolated as low-K⁺-sensitive (*lks*) mutants and they showed similar phenotypes under low K⁺ conditions, regarding ion contents and leaf chlorosis phenotypes (Xu et al., 2006; Li et al., 2017a). These data together indicate that NRT1.5 and CIPK23 regulate K⁺ transport and the speculation of a joint role between them is pointed out here. Nevertheless, *CIPK23* expression is not affected under low K⁺ and NO₃⁻ supply either in wildtype or *nrt1.5* plants (**Figure 13**), suggesting the interaction between NRT1.5 and CIPK23 is not affecting their molecular regulation. CIPK23 kinase has been identified in the regulation of NO₃⁻ transport by the physical interaction with NRT1.1. The dual high and low-affinity function of NRT1.1 is exchangeable by the phosphorylation of NRT1.1 at Thr¹⁰¹ by CIPK23 (Rashid et al., 2020). NRT1.5 contains the Thr¹⁰¹ residue (**Figure 5**), so it is presumed that this key residue will need further investigation to unveil the NRT1.5 and CIPK23 interaction.

Additionally, Calcineurin B-like 3 (CBL3) is also implicated in nutrient homeostasis. The CBL3-CIPK9 module is involved in regulating K⁺ transporter and channel functions under K⁺ limitation (Liu et al., 2013); CBL3 might contribute to the activation of K⁺/H⁺ exchangers such as NHX1/2 (Song et al., 2018) and NHX5/6 (Zhang et al., 2020); the two-pore K⁺ (TPK) channels may be activated by CBL2 and CBL3 (Tang et al., 2020); and several CBLs affect protein phosphorylation of the high-affinity NO₃⁻ transporter, NRT2.1 (Cui Chu et al., 2020).

In this thesis, the *cb13* single mutant (**Figure 14**) does not show an obvious phenotype linked to low K⁺ and NO₃⁻ supply, as well as no alteration in the plasma membrane potential (**Figure 15 and 36**). It is been shown that CBL3 and CBL2 share 92% identity in amino acid sequence and their genes may originate from a duplication event (Kolukisaoglu et al., 2004). CBL2 and CBL3 genes are broadly expressed in plant tissues but display overlapping expression patterns in *Arabidopsis* roots (Tang et al., 2012). Genetic analysis has shown that the two genes overlap in their function as *cb12* or *cb13* single mutants closely resemble wild-type, but the double mutant displays evident abnormalities in development and ionic sensitivity (Tang et al., 2012), reduction on K⁺ contents (Eckert et al., 2014), and recently *cb12/cb13* double mutant phenotype was described hypersensitive to low-K⁺ conditions (Tang et al., 2020). The absence of *cb13* phenotypes in this thesis could be explained by the redundancy of the CBL family since the functional redundancy among calcium-dependent kinases, and the number of targets that they phosphorylate is a difficult cellular scene. However, the *CBL3* expression is regulated under low K⁺ and NO₃⁻ supply in the *nrt1.5* mutant

(**Figure 13**). A similar *CBL3* up-regulation was reported in Arabidopsis roots by other abiotic stresses such as salt, drought, and cold (Kilian et al., 2007), suggesting a molecular regulation of *CBL3* by different abiotic stresses.

Finally, CIPK23 and other CIPK kinases physically interacts with CBL2 and CBL3 and they have been described in Mg^{2+} homeostasis (Tang et al., 2015) and K^+ starvation (Tang et al., 2020) in Arabidopsis. In this context, the triple interaction between NRT1.5, CBL3, and CIPK23 could be investigated as a potential module involved in the regulation of K^+ and NO_3^- homeostasis (**Figure 37**).

4.12. Interaction between NRT1.5 and the vesicle trafficking proteins PEP12 and VAMP722

One group of regulators of membrane trafficking is the SNARE family (soluble N-ethylmaleimide sensitive factor attachment protein receptors), they mediate membrane fusion between transport vesicles and target organelles (Lipka et al., 2007). R-SNAREs usually are localized to the vesicle membrane and often are referred to as vesicle-associated membrane proteins (VAMPs). In Arabidopsis, the R-SNAREs assemble in complex with plasma membrane Q-SNAREs (Qa so-called syntaxins, Qb and Qc) to mediated-vesicle trafficking of proteins (Karnik et al., 2013; Karnik et al., 2015). Here, a novel syntaxin member (PEP12/SYP21) and an R-SNARE component (VAMP722) are confirmed to interact with NRT1.5 in plants (**Figure 12**). Both proteins were previously detected in a split ubiquitin screening to interact with NRT1.5 (Drechsler, 2016).

Some SNAREs are known to interact with ion channels and affect their regulation, and the family member of Qa-SNARE proteins is the best-known example. SYP121 interacts with the K^+ channels KC1 and KAT1, altering channel gating to promote K^+ uptake (Honsbein et al., 2009; Lefoulon et al., 2018), and promoting secretory vesicle traffic to the plasma membrane (Karnik et al., 2017).

Yet, the Arabidopsis Qa-SNARE protein PEP12/SYP21 is poorly characterized concerning N and K^+ homeostasis. PEP12/SYP21 was originally identified in a genetic screen for mutants with altered vacuolar morphology or by a defective delivery of vacuolar proteins to *S. cerevisiae* vacuoles (Becherer et al., 1996). Transient overexpression of PEP12/SYP21 in tobacco plants targeted it to the vacuolar sorting pathway (Foresti et al., 2006). Nevertheless, the *syp21/syp22* double mutant phenotypes revealed a redundant and interchangeable function of SYP21 and SYP22 proteins (Uemura et al., 2010), suggesting complex unknown functions for SYP21/PEP12 protein.

Recently, SYP22 (sharing 79% of protein similarity with SYP21/PEP12) has been described as an important component in the control of the hormone receptor BRI1 plasma membrane targeting to modulate brassinosteroids signaling (Zhu et al., 2019). In this work, even though an up-regulation of *PEP12* is detected under K^+ and NO_3^- low supply in *nrt1.5* mutant (**Figure 13**), the *pep12* single mutant and the double mutant with *nrt1.5* do not show phenotypes (**Figure 15 and 35**), evidencing no cooperation between NRT1.5 and PEP12 in K^+/NO_3^- translocation. Moreover, the plasma membrane potential is not altered in the *pep12* mutant, indicating that the lack of the Qa-syntaxin does not affect the cellular ion transport (**Figure 35**). The redundancy and interchangeability of SYP21 and SYP22 can explain these observations, so further investigation of SYP22 could give more insights into how Qa-syntaxins may regulate nutrient transport systems such as NRT1.5.

Contrastingly, the subfamily members of R-SNARE (VAMP7) localized in secretory vesicles and the vesicles are addressed and tethered to the plasma membrane (Uemura et al., 2004). VAMP722 and VAMP721 depletion by constitutive gene silencing or homozygous double mutations result in severe growth defect or lethality, respectively (Kwon et al., 2008; Zhang et al., 2011). VAMP721 and VAMP722 showed $\approx 95\%$ of protein identity and 88% in coding sequences identity (data is not shown), this observation corroborates the redundancy of the phenotypes. Surprisingly, no phenotypes in *vamp722* single mutant are observed under K^+ and NO_3^- deficiency (**Figure 15 and 36**), however, the plasma membrane potential of mutant plants is affected (**Figure 35**), demonstrating that VAMP722 is correlated with ion homeostasis. Also, *VAMP722/VAMP721* were transcriptionally up-regulated by diverse stresses (Kwon et al., 2008; Yun et al., 2013) and in this thesis, a transcriptional response of *VAMP722* is observed under K^+ and NO_3^- limitation in the *nrt1.5* mutant (**Figure 13**), demonstrating R-SNARE proteins are transcriptionally regulated by K^+ and NO_3^- availability.

Typically, vesicle fusion with the plasma membrane requires four different SNAREs (Qa, Qb, Qc, and R) that form the quaternary tight SNARE complex (**Figure 3**). In plants, the first identified SNARE complex comprises the SYP121 (Qa-SNARE) attached to the plasma membrane, SNAP33 (containing both Qb and Qc-SNARE), and the secretory vesicle residing VAMP721/722 (Collins et al., 2003; Kwon et al., 2008). Some years later, a SYP121/VAMP722/VAMP721 complex has been identified to be regulating the K^+ activity of KAT1 and KC1 channels (Zhang et al., 2015). Evidence of more SNARE complexes is unknown, but the possibility that PEP12 and VAMP722 are working together to regulate NRT1.5 is conceivable. In this context, the triple mutant between

NRT1.5, PEP12, and VAMP722 could be useful to investigate the potential protein-protein interaction between VAMP722 and PEP12 together with NRT1.5.

4.12. Conclusions and perspectives

The NRT1.5 transporter fulfills a wide variety of tasks in root cells. Results presented in this thesis reveal experimental evidence that its function is dependent on the media availability of nitrate, potassium, and pH status. However, even though the *nrt1.5* mutant shows a root growth dependency with NO_3^- , K^+ contents and pH in the media, it is still unknown whether NRT1.5 is controlling directly or indirectly the plasticity of the root architecture. To decipher this in future experiments, the auxin status in roots might be studied (discussed in section 4.3.2).

The NRT1.5 interaction with proteins involved in post-translational mechanisms such as ion homeostasis (SLAH1, SLAH3, and AHA2), calcium-regulated phosphorylation (CBL3 and CIPK23), and vesicle trafficking to the plasma membrane (PEP12 and VAMP722) offers first indications of the elucidation of a potential regulatory network in plant nutrition. The detailed exploration of these molecular interactions represents a promising approach to further exploring the multiple functions of NRT1.5. However, the physiological significance in which the NRT1.5 transporter interacts with all partners has not yet been clarified within the scope of this doctoral thesis. Electrophysiological measurements in *Xenopus* oocytes could clarify whether the simultaneous expression of NRT1.5 and one or more interaction partners change the transport properties. To shed light on the influence of multiple interaction partners on the ion balance, phenotypic and physiological analysis of *slah1* and *slah3*, *pep12* and *vamp722*, and *cbl3* and *cipk23* double and triple mutants with *nrt1.5* could be carried out.

Finally, the potential cross-talk between the different post-translational mechanisms may give indications about the potential regulation of NRT1.5. Cellular regulation of proteins is a complex mechanism that cannot be studied by single protein-protein interactions.

A comprehensive study of the NRT1.5 interactions could make an important contribution to the further decoding of the complex nutrient-dependent signal and transport network in *Arabidopsis*.

5. References

- Almagro A, Shan HL, Yi FT** (2008) Characterization of the Arabidopsis nitrate transporter NRT1.6 reveals a role of nitrate in early embryo development. *Plant Cell* **20**: 3289–3299
- Almeida P, Katschnig D, de Boer AH** (2013) HKT transporters-state of the art. *Int J Mol Sci* **14**: 20359–20385
- Amrutha RN, Sekhar PN, Varshney RK, Kishor PBK** (2007) Genome-wide analysis and identification of genes related to potassium transporter families in rice (*Oryza sativa* L.). *Plant Sci* **172**: 708–721
- Anderson JA, Huprikar SS, Kochian L V., Lucas WJ, Gaber RF** (1992) Functional expression of a probable Arabidopsis thaliana potassium channel in *Saccharomyces cerevisiae*. *Proc Natl Acad Sci U S A* **89**: 3736–3740
- Ando E, Kinoshita T** (2018) Red light-induced phosphorylation of plasma membrane H⁺-ATPase in stomatal guard cells. *Plant Physiol* **178**: 838–849
- De Angeli A, Monachello D, Ephritikhine G, Frachisse JM, Thomine S, Gambale F, Barbier-Brygoo H** (2006) The nitrate/proton antiporter AtCLCa mediates nitrate accumulation in plant vacuoles. *Nature* **442**: 939–942
- Ariño J, Ramos J, Sychrova H** (2010) Alkali Metal Cation Transport and Homeostasis in Yeasts. *Microbiol Mol Biol Rev* **74**: 95–120
- Armengaud P, Breitling R, Amtmann A** (2004) The potassium-dependent transcriptome of Arabidopsis reveals a prominent role of jasmonic acid in nutrient signaling. *Plant Physiol* **136**: 2556–2576
- Armengaud P, Sulpice R, Miller AJ, Stitt M, Amtmann A, Gibon Y** (2009) Multilevel analysis of primary metabolism provides new insights into the role of potassium nutrition for glycolysis and nitrogen assimilation in Arabidopsis roots. *Plant Physiol* **150**: 772–785
- Arvidsson S, Kwasniewski M, Riaño-Pachón DM, Mueller-Roeber B** (2008) QuantPrime - A flexible tool for reliable high-throughput primer design for quantitative PCR. *BMC Bioinformatics* **9**: 1–15
- Barberon M, Dubeaux G, Kolb C, Isono E, Zelazny E, Vert G** (2014) Polarization of iron-regulated transporter 1 (IRT1) to the plant-soil interface plays crucial role in metal homeostasis. *Proc Natl Acad Sci U S A* **111**: 8293–8298
- Barberon M, Vermeer JEM, De Bellis D, Wang P, Naseer S, Andersen TG, Humbel BM, Nawrath C, Takano J, Salt DE, et al** (2016) Adaptation of root function by nutrient-

- induced plasticity of endodermal differentiation. *Cell* **164**: 447–459
- Barragán V, Leidi EO, Andrés Z, Rubio L, de Luca A, Fernández JA, Cubero B, Pardo JM** (2012) Ion exchangers NHX1 and NHX2 mediate active potassium uptake into vacuoles to regulate cell turgor and stomatal function in *Arabidopsis*. *Plant Cell* **24**: 1127–1142
- Barreto L, Canadell D, Petrežsélyová S, Navarrete C, Marešová L, Peréz-Valle J, Herrera R, Olier I, Giraldo J, Sychrová H, et al** (2011) A genomewide screen for tolerance to cationic drugs reveals genes important for potassium homeostasis in *Saccharomyces cerevisiae*. *Eukaryot Cell* **10**: 1241–1250
- Bassham DC, Brandizzi F, Otegui MS, Sanderfoot AA** (2008) The secretory system of *Arabidopsis*. *Arabidopsis Book* **65**: 1–29
- Bassil E, Zhang S, Gong H, Tajima H, Blumwald E** (2019) Cation specificity of vacuolar NHX-type cation/H⁺ Antiporters. *Plant Physiol* **179**: 616–629
- Batistič O, Kudla J** (2009) Plant calcineurin B-like proteins and their interacting protein kinases. *Biochim Biophys Acta - Mol Cell Res* **1793**: 985–992
- Baumert M, Maycox PR, Navone F, De Camilli P, Jahn R** (1989) Synaptobrevin: An integral membrane protein of 18000 daltons present in small synaptic vesicles of rat brain. *EMBO J* **8**: 379–384
- Baxter I, Tchieu J, Sussman MR, Boutry M, Palmgren MG, Gribskov M, Harper JF, Axelsen KB** (2003) Genomic comparison of P-type ATPase ion pumps in *Arabidopsis* and rice. *Plant Physiol* **132**: 618–628
- Becherer KA, Rieder SE, Emr SD, Jones EW** (1996) Novel syntaxin homologue, Pep12p, required for the sorting of luminal hydrolases to the lysosome-like vacuole in yeast. *Mol Biol Cell* **7**: 579–594
- Behl R, Raschke K** (1987) Close coupling between extrusion of H⁺ and uptake of K⁺ by barley roots. *Planta* **172**: 531–538
- Benito B, Haro R, Amtmann A, Cuin TA, Dreyer I** (2014) The twins K⁺ and Na⁺ in plants. *J Plant Physiol* **171**: 723–731
- Bennett MK, Calakos N, Scheller RH** (1992) Syntaxin: A synaptic protein implicated in docking of synaptic vesicles at presynaptic active zones. *Science* (80-) **257**: 255–259
- Bock JB, Matern HT, Peden AA, Scheller RH** (2001) A genomic perspective on membrane compartment organization. *Nature* **409**: 839–841
- Brachmann CB, Davies A, Cost GJ, Caputo E, Li J, Hieter P, Boeke JD** (1998) Designer

- deletion strains derived from *Saccharomyces cerevisiae* S288C: A useful set of strains and plasmids for PCR-mediated gene disruption and other applications. *Yeast* **14**: 115–132
- Britto DT, Kronzucker HJ** (2005) Nitrogen acquisition, PEP carboxylase, and cellular pH homeostasis: New views on old paradigms. *Plant, Cell Environ* **28**: 1396–1409
- Buch-Pedersen MJ, Palmgren MG** (2003) Conserved Asp684 in transmembrane segment M6 of the plant plasma membrane P-type proton pump AHA2 is a molecular determinant of proton translocation. *J Biol Chem* **278**: 17845–17851
- Cao Y, Jin X, Huang H, Derebe MG, Levin EJ, Kabaleeswaran V, Pan Y, Punta M, Love J, Weng J, et al** (2011) Crystal structure of a potassium ion transporter, TrkH. *Nature* **471**: 336–341
- Castro-Chavez F** (2010) The rules of variation: Amino acid exchange according to the rotating circular genetic code. *J Theor Biol* **264**: 711–721
- Cataldo DA, Haroon MH, Schrader LE, Youngs VL** (1975) Rapid colorimetric determination of nitrate in plant tissue by nitration of salicylic acid. *Commun Soil Sci Plant Anal* **6**: 71–80
- Cellier F, Conéjéro G, Ricaud L, Doan TL, Lepetit M, Gosti F, Casse F** (2004) Characterization of AtCHX17, a member of the cation/H⁺ exchangers, CHX family, from *Arabidopsis thaliana* suggests a role in K⁺ homeostasis. *Plant J* **39**: 834–846
- Cerezo M, Tillard P, Filleur S, Muños S, Daniel-Vedele F, Gojon A** (2001) Major alterations of the regulation of root NO₃⁻ uptake are associated with the mutation of Nrt2.1 and Nrt2.2 genes in *Arabidopsis*. *Plant Physiol* **127**: 262–271
- Chanroj S, Wang G, Venema K, Zhang MW, Delwiche CF, Sze H** (2012) Conserved and diversified gene families of monovalent cation/H⁺ antiporters from algae to flowering plants. *Front Plant Sci* **3**: 1–18
- Chen CZ, Lv XF, Li JY, Yi HY, Gong JM** (2012) *Arabidopsis* NRT1.5 is another essential component in the regulation of nitrate reallocation and stress tolerance. *Plant Physiol* **159**: 1582–1590
- Chen DH, Ronald PC** (1999) A rapid DNA miniprep method suitable for AFLP and other PCR applications. *Plant Mol Biol Report* **17**: 53–57
- Chen Y, Hu L, Punta M, Bruni R, Hillerich B, Kloss B, Rost B, Love J, Siegelbaum S, Hendrickson W** (2010) Homolog Structure of the SLAC1 Anion Channel for Closing Stomata in Leaves. *Nature* **467**: 1074–1080
- Chiba Y, Shimizu T, Miyakawa S, Kanno Y, Koshiha T, Kamiya Y, Seo M** (2015)

- Identification of *Arabidopsis thaliana* NRT1/PTR FAMILY (NPF) proteins capable of transporting plant hormones. *J Plant Res* **128**: 679–686
- Chopin F, Orsel M, Dorbe MF, Chardon F, Truong HN, Miller AJ, Krapp A, Daniel-Vedele F** (2007) The *Arabidopsis* ATNRT2.7 nitrate transporter controls nitrate content in seeds. *Plant Cell* **19**: 1590–1602
- Clough SJ, Bent AF** (1998) Floral dip: A simplified method for *Agrobacterium*-mediated transformation of *Arabidopsis thaliana*. *Plant J* **16**: 735–743
- Collins NC, Thordal-Christensen H, Lipka V, Bau S, Kombrink E, Qiu JL, Hüchelhoven R, Steins M, Freialdenhoven A, Somerville SC, et al** (2003) SNARE-protein-mediated disease resistance at the plant cell wall. *Nature* **425**: 973–977
- Corratgé-Faillie C, Ronzier E, Sanchez F, Prado K, Kim JH, Lanciano S, Leonhardt N, Lacombe B, Xiong TC** (2017) The *Arabidopsis* guard cell outward potassium channel GORK is regulated by CPK33. *FEBS Lett* **591**: 1982–1992
- Coskun D, Britto DT, Kronzucker HJ** (2017) The nitrogen–potassium intersection: membranes, metabolism, and mechanism. *Plant Cell Environ* **40**: 2029–2041
- Cubero-Font P, Maierhofer T, Jaslan J, Rosales MA, Espartero J, Díaz-Rueda P, Müller HM, Hürter AL, AL-Rasheid KAS, Marten I, et al** (2016) Silent S-type anion channel subunit SLAH1 gates SLAH3 open for chloride root-to-shoot translocation. *Curr Biol* **26**: 2213–2220
- Cui Chu L, Offenborn JN, Steinhorst L, Wu XN, Xi L, Li Z, Jacquot A, Lejey L, Kudla J, Schulze WX** (2020) Plasma membrane CBL Ca²⁺ sensor proteins function in regulating primary root growth and nitrate uptake by affecting global phosphorylation patterns and microdomain protein distribution. *New Phytol* 0–2
- Cui YN, Li XT, Yuan JZ, Wang FZ, Wang SM, Ma Q** (2019) Nitrate transporter NPF7.3/NRT1.5 plays an essential role in regulating phosphate deficiency responses in *Arabidopsis*. *Biochem Biophys Res Commun* **508**: 314–319
- Czempinski K, Zimmermann S, Ehrhardt T, Müller-Röber B** (1997) New structure and function in plant K⁺ channels: KCO1, an outward rectifier with a steep Ca²⁺ dependency. *EMBO J* **16**: 2565–2575
- Czerny DD, Padmanaban S, Anishkin A, Venema K, Riaz Z, Sze H** (2016) Protein architecture and core residues in unwound α -helices provide insights to the transport function of plant AtCHX17. *Biochim Biophys Acta - Biomembr* **1858**: 1983–1998

- Daram P, Urbach S, Gaymard F, Sentenac H, Chérel I** (1997) Tetramerization of the AKT1 plant potassium channel involves its C-terminal cytoplasmic domain. *EMBO J* **16**: 3455–3463
- Davenport RJ, Muñoz-Mayor A, Jha D, Essah PA, Rus A, Tester M** (2007) The Na⁺ transporter AtHKT1;1 controls retrieval of Na⁺ from the xylem in Arabidopsis. *Plant, Cell Environ* **30**: 497–507
- Demidchik V, Straltsova D, Medvedev SS, Pozhvanov GA, Sokolik A, Yurin V** (2014) Stress-induced electrolyte leakage: The role of K⁺-permeable channels and involvement in programmed cell death and metabolic adjustment. *J Exp Bot* **65**: 1259–1270
- Desai U., Pfaffle P.** (1995) Single-step purification of a thermostable DNA polymerase expressed in *Escherichia coli*. *Biotechniques* **19**: 780–782
- Doyle DA, Cabral JM, Pfuetzner RA, Kuo A, Gulbis JM, Cohen SL, Chait BT, MacKinnon R** (1998) The structure of the potassium channel: Molecular basis of K⁺ conduction and selectivity. *Science* (80-) **280**: 69–77
- Drechsler N** (2016) Der Nitrattransporter AtNRT1.5/AtNPF7.3- Ein Schlüsselprotein in der Regulierung des pflanzlichen Kaliumhaushaltes. Freie Universität Berlin
- Drechsler N, Zheng Y, Bohner A, Nobmann B, von Wiren N, Kunze R, Rausch C** (2015) Nitrate-dependent control of shoot K homeostasis by the nitrate transporter1/peptide transporter family member NPF7.3/NRT1.5 and the stelar K⁺ outward rectifier skor in arabidopsis. *Plant Physiol* **169**: 2832–2847
- Dreyer I, Gomez-Porrás JL, Riaño-Pachón DM, Hedrich R, Geiger D** (2012) Molecular evolution of slow and quick anion channels (SLACs and QUACs/ALMTs). *Front Plant Sci* **3**: 1–12
- Dreyer I, Uozumi N** (2011) Potassium channels in plant cells. *FEBS J* **278**: 4293–4303
- Du XQ, Wang FL, Li H, Jing S, Yu M, Li J, Wu WH, Kudla J, Wang Y** (2019) The transcription factor MYB59 regulates K⁺/NO₃⁻ translocation in the arabidopsis response to low K⁺ stress. *Plant Cell* **31**: 699–714
- Eckert C, Offenborn JN, Heinz T, Armarego-Marriott T, Schültke S, Zhang C, Hillmer S, Heilmann M, Schumacher K, Bock R, et al** (2014) The vacuolar calcium sensors CBL2 and CBL3 affect seed size and embryonic development in *Arabidopsis thaliana*. *Plant J* **78**: 146–156
- Eisenach C, Chen ZH, Grefen C, Blatt MR** (2012) The trafficking protein SYP121 of

- Arabidopsis connects programmed stomatal closure and K⁺ channel activity with vegetative growth. *Plant J* **69**: 241–251
- Engels C, Marschner H** (1993) Influence of the form of nitrogen supply on root uptake and translocation of cations in the xylem exudate of maize (*Zea mays* L). *J Exp Bot* **44**: 1695–1701
- Espen L, Nocito FF, Cocucci M** (2004) Effect of NO₃⁻ transport and reduction on intracellular pH: An in vivo NMR study in maize roots. *J Exp Bot* **55**: 2053–2061
- Fan SC, Lin CS, Hsu PK, Lin SH, Tsay YF** (2009) The Arabidopsis nitrate transporter NRT1.7, expressed in phloem, is responsible for source-to-sink remobilization of nitrate. *Plant Cell* **21**: 2750–2761
- Fan X, Naz M, Fan X, Xuan W, Miller AJ, Xu G** (2017) Plant nitrate transporters: From gene function to application. *J Exp Bot* **68**: 2463–2475
- Fan X, Tang Z, Tan Y, Zhang Y, Luo B, Yang M, Lian X, Shen Q, Miller AJ, Xu G** (2016) Overexpression of a pH-sensitive nitrate transporter in rice increases crop yields. *Proc Natl Acad Sci U S A* **113**: 7118–7123
- Fasshauer D, Sutton RB, Brunger AT, Jahn R** (1998) Conserved structural features of the synaptic fusion complex: SNARE proteins reclassified as Q- and R-SNAREs. *Neurobiol Commun* by Peter B Moore **95**: 15781–15786
- Von Der Fecht-Bartenbach J, Bogner M, Dynowski M, Ludewig U** (2010) CLC-b-mediated NO₃⁻/H⁺ exchange across the tonoplast of Arabidopsis vacuoles. *Plant Cell Physiol* **51**: 960–968
- Fecht-Bartenbach J Von Der, Bogner M, Krebs M, Stierhof YD, Schumacher K, Ludewig U** (2007) Function of the anion transporter AtCLC-d in the trans-Golgi network. *Plant J* **50**: 466–474
- Felle HH** (2001) pH: Signal and messenger in plant cells. *Plant Biol* **3**: 577–591
- Feng H, Fan X, Miller AJ, Xu G** (2020) Plant nitrogen uptake and assimilation: regulation of cellular pH homeostasis. *J Exp Bot* **5**: 1–13
- Feng H, Yan M, Fan X, Li B, Shen Q, Miller AJ, Xu G** (2011) Spatial expression and regulation of rice high-affinity nitrate transporters by nitrogen and carbon status. *J Exp Bot* **62**: 2319–2332
- Forde BG** (2000) Nitrate transporters in plants: Structure, function and regulation. *Biochim Biophys Acta - Biomembr* **1465**: 219–235

- Foresti O, DaSilva LLP, Denecke J** (2006) Overexpression of the Arabidopsis syntaxin PEP12/SYP21 inhibits transport from the prevacuolar compartment to the lytic vacuole in vivo. *Plant Cell* **18**: 2275–2293
- Förster S, Schmidt LK, Kopic E, Anschütz U, Huang S, Schlücking K, Köster P, Waadt R, Larrieu A, Batistič O, et al** (2019) Wounding-induced stomatal closure requires jasmonate-mediated activation of GORK K⁺ channels by a Ca²⁺ sensor-kinase CBL1-CIPK5 complex. *Dev Cell* **48**: 87–99
- Fu HH, Luan S** (1998) AtKUP1: A dual-affinity K⁺ transporter from arabidopsis. *Plant Cell* **10**: 63–73
- Fuglsang AT, Guo Y, Cuin TA, Qiu Q, Song C, Kristiansen KA, Bych K, Schulz A, Shabala S, Schumaker KS, et al** (2007) Arabidopsis protein kinase PKS5 inhibits the plasma membrane H⁺-ATPase by preventing interaction with 14-3-3 protein. *Plant Cell* **19**: 1617–1634
- Fuglsang AT, Kristensen A, Cuin TA, Schulze WX, Persson J, Thuesen KH, Ytting CK, Oehlenschläger CB, Mahmood K, Sondergaard TE, et al** (2014) Receptor kinase-mediated control of primary active proton pumping at the plasma membrane. *Plant J* **80**: 951–964
- Fuglsang AT, Visconti S, Drumm K, Jahn T, Stensballe A, Mattei B, Jensen ON, Aducci P, Palmgren MG** (1999) Binding of 14-3-3 protein to the plasma membrane H⁺-ATPase AHA2 involves the three C-terminal residues Tyr946-Thr-Val and requires phosphorylation of Thr947. *J Biol Chem* **51**: 36774–36780
- Gambale F, Uozumi N** (2006) Properties of Shaker-type potassium channels in higher plants. *J Membr Biol* **210**: 1–19
- Garciadeblás B, Senn ME, Bañuelos MA, Rodríguez-Navarro A** (2003) Sodium transport and HKT transporters: The rice model. *Plant J* **34**: 788–801
- Gaxiola RA, Palmgren MG, Schumacher K** (2007) Plant proton pumps. *FEBS Lett* **581**: 2204–2214
- Gaymard F, Pilot G, Lacombe B, Bouchez D, Bruneau D, Boucherez J, Michaux-Ferrière N, Thibaud JB, Sentenac H** (1998) Identification and disruption of a plant shaker-like outward channel involved in K⁺ release into the xylem sap. *Cell* **94**: 647–655
- Gazzarrini S, Lejay L, Gojon A, Ninnemann O, Frommer WB, Von Wirén N** (1999) Three functional transporters for constitutive, diurnally regulated, and starvation-induced uptake of

- ammonium into Arabidopsis roots. *Plant Cell* **11**: 937–947
- Geelen D, Lurin C, Bouchez D, Frachisse JM, Lelièvre F, Courtial B, Barbier-Brygoo H, Maurel C** (2000) Disruption of putative anion channel gene AtCLC-a in Arabidopsis suggests a role in the regulation of nitrate content. *Plant J* **21**: 259–267
- Geiger D, Becker D, Vosloh D, Gambale F, Palme K, Rehers M, Anshuetz U, Dreyer I, Kudla J, Hedrich R** (2009) Heteromeric AtKC1·AKT1 channels in Arabidopsis roots facilitate growth under K⁺-limiting conditions. *J Biol Chem* **284**: 21288–21295
- Geiger D, Maierhofer T, Al-Rasheid KAS, Scherzer S, Mumm P, Liese A, Ache P, Wellmann C, Marten I, Grill E, et al** (2011) Stomatal closure by fast abscisic acid signaling is mediated by the guard cell anion channel SLAH3 and the receptor RCAR1. *Sci Signal* **4**: 1–13
- Gerendás J, Schurr U** (1999) Physicochemical aspects of ion relations and pH regulation in plants - A quantitative approach. *J Exp Bot* **50**: 1101–1114
- Gévaudant F, Duby G, Von Stedingk E, Zhao R, Morsomme P, Boutry M** (2007) Expression of a constitutively activated plasma membrane H⁺-ATPase alters plant development and increases salt tolerance. *Plant Physiol* **144**: 1763–1776
- Gierth M, Mäser P** (2007) Potassium transporters in plants - Involvement in K⁺ acquisition, redistribution and homeostasis. *FEBS Lett* **581**: 2348–2356
- Gierth M, Mäser P, Schroeder JI** (2005) The potassium transporter AtHAK5 functions in K⁺ deprivation-induced high-affinity K⁺ uptake and AKT1 K⁺ channel contribution to K⁺ uptake kinetics in Arabidopsis roots. *Plant Physiol* **137**: 1105–1114
- Gilbert M, Li Z, Wu XN, Rohr L, Gombos S, Harter K, Schulze WX** (2021) Comparison of path-based centrality measures in protein-protein interaction networks revealed proteins with phenotypic relevance during adaptation to changing nitrogen environments. *J Proteomics* **235**: 1–12
- Gobert A, Isayenkov S, Voelker C, Czempinski K, Maathuis FJM** (2007) The two-pore channel TPK1 gene encodes the vacuolar K⁺ conductance and plays a role in K⁺ homeostasis. *Proc Natl Acad Sci U S A* **104**: 10726–10731
- Gordon-Weeks R, Tong Y, Davies TGE, Leggewie G** (2003) Restricted spatial expression of a high-affinity phosphate transporter in potato roots. *J Cell Sci* **116**: 3135–3144
- Van Der Graaff E, Schwacke R, Schneider A, Desimone M, Flügge UI, Kunze R** (2006) Transcription analysis of arabidopsis membrane transporters and hormone pathways during

- developmental and induced leaf senescence. *Plant Physiol* **141**: 776–792
- Grabov A** (2007) Plant KT/KUP/HAK potassium transporters: Single family - Multiple functions. *Ann Bot* **99**: 1035–1041
- Grefen C, Blatt MR** (2012) A 2in1 cloning system enables ratiometric bimolecular fluorescence complementation (rBiFC). *Biotechniques* **53**: 311–314
- Grefen C, Blatt MR, Chen Z, Honsbein A, Donald N, Hills A** (2010) A novel motif essential for SNARE interaction with the K⁺ channel KC1 and channel gating in Arabidopsis. *Plant Cell* **22**: 3076–3092
- Grefen C, Lalonde S, Obrdlik P** (2007) Split-Ubiquitin system for identifying protein-protein interactions in membrane and full-length proteins. *Curr. Protoc. Neurosci.* pp 1–41
- Greiner T, Ramos J, Alvarez MC, Gurnon JR, Kang M, Van Etten JL, Moroni A, Thiel G** (2011) Functional HAK/KUP/KT-like potassium transporter encoded by chlorella viruses. *Plant J* **68**: 977–986
- Gruber BD, Giehl RFH, Friedel S, von Wirén N** (2013) Plasticity of the Arabidopsis root system under nutrient deficiencies. *Plant Physiol* **163**: 161–179
- Guan P** (2017) Dancing with hormones: A current perspective of nitrate signaling and regulation in Arabidopsis. *Front Plant Sci* **8**: 1–20
- Hamburger D, Rezzonico E, MacDonald-Comber Petétot J, Somerville C, Poirier Y** (2002) Identification and characterization of the Arabidopsis PHO1 gene involved in phosphate loading to the xylem. *Plant Cell* **14**: 889–902
- Han M, Wu W, Wu WH, Wang Y** (2016) Potassium transporter KUP7 is involved in K⁺ acquisition and translocation in Arabidopsis root under K⁺-limited conditions. *Mol Plant* **9**: 437–446
- Haruta M, Burch HL, Nelson RB, Barrett-Wilt G, Kline KG, Mohsin SB, Young JC, Otegui MS, Sussman MR** (2010) Molecular characterization of mutant Arabidopsis plants with reduced plasma membrane proton pump activity. *J Biol Chem* **285**: 17918–17929
- Haruta M, Sussman MR** (2012) The effect of a genetically reduced plasma membrane protonmotive force on vegetative growth of Arabidopsis. *Plant Physiol* **158**: 1158–1171
- Haruta M, Tan LX, Bushey DB, Swanson SJ, Sussman MR** (2018) Environmental and genetic factors regulating localization of the plant plasma membrane H⁺-ATPase. *Plant Physiol* **176**: 364–377
- Hedrich R, Geiger D** (2017) Biology of SLAC1-type anion channels - from nutrient uptake to

- stomatal closure. *New Phytol* 1–16
- Held K, Pascaud F, Eckert C, Gajdanowicz P, Hashimoto K, Corratgé-Faillie C, Offenborn JN, Lacombe B, Dreyer I, Thibaud JB, et al** (2011) Calcium-dependent modulation and plasma membrane targeting of the AKT2 potassium channel by the CBL4/CIPK6 calcium sensor/protein kinase complex. *Cell Res* **21**: 1116–1130
- Herbst J** (2019) Der Einfluss von Tetratricopeptidrepeat Proteinen auf die Chlorophyllbiosynthese und Chloroplastenbiogenese. Humboldt-Universität
- Herdean A, Nziengui H, Zsiros O, Solymosi K, Garab G, Lundin B, Spetea C** (2016) The Arabidopsis thylakoid chloride channel AtCLCe functions in chloride homeostasis and regulation of photosynthetic electron transport. *Front Plant Sci* **7**: 1–15
- Ho CH, Frommer WB** (2014) Fluorescent sensors for activity and regulation of the nitrate transceptor CHL1/NRT1.1 and oligopeptide transporters. *Elife* **2014**: 1–21
- Ho CH, Lin SH, Hu HC, Tsay YF** (2009) CHL1 functions as a nitrate sensor in plants. *Cell* **138**: 1184–1194
- Hoffmann B, Kosegarten H** (1995) FITC-dextran for measuring apoplast pH and apoplastic pH gradients between various cell types in sunflower leaves. *Physiol Plant* **95**: 327–335
- Hoffmann RD, Olsen LI, Ezike C V., Pedersen JT, Manstretta R, López-Marqués RL, Palmgren M** (2019) Roles of plasma membrane proton ATPases AHA2 and AHA7 in normal growth of roots and root hairs in Arabidopsis thaliana. *Physiol Plant* **166**: 848–861
- Hoffmann RD, Portes MT, Olsen LI, Damineli DSC, Hayashi M, Nunes CO, Pedersen JT, Lima PT, Campos C, Feijó JA, et al** (2020) Plasma membrane H⁺-ATPases sustain pollen tube growth and fertilization. *Nat Commun* **11**: 1–15
- Hong JP, Takeshi Y, Kondou Y, Schachtman DP, Matsui M, Shin R** (2013) Identification and characterization of transcription factors regulating Arabidopsis HAK5. *Plant Cell Physiol* **54**: 1478–1490
- Honsbein A, Sokolovski S, Grefen C, Campanoni P, Pratelli R, Paneque M, Chen Z, Johansson I, Blatt MR** (2009) A tripartite SNARE K⁺ channel complex mediates in channel-dependent K⁺ nutrition in Arabidopsis. *Plant Cell* **21**: 2859–2877
- ten Hoopen F, Cuin TA, Pedas P, Hegelund JN, Shabala S, Schjoerring JK, Jahn TP** (2010) Competition between uptake of ammonium and potassium in barley and Arabidopsis roots: Molecular mechanisms and physiological consequences. *J Exp Bot* **61**: 2303–2315
- Hsu PK, Tsay YF** (2013) Two phloem nitrate transporters, NRT1.11 and NRT1.12, are

- important for redistributing xylem-borne nitrate to enhance plant growth. *Plant Physiol* **163**: 844–856
- Hu HC, Wang YY, Tsay YF** (2009) AtCIPK8, a CBL-interacting protein kinase, regulates the low-affinity phase of the primary nitrate response. *Plant J* **57**: 264–278
- Hua YP, Zhou T, Huang JY, Yue CP, Song HX, Guan CY, Zhang ZH** (2020) Genome-wide differential dna methylation and mirna expression profiling reveals epigenetic regulatory mechanisms underlying nitrogen- limitation-triggered adaptation and use efficiency enhancement in allotetraploid rapeseed. *Int J Mol Sci* **21**: 1–28
- Huang L, Kuang L, Wu L, Shen Q, Han Y, Jiang L, Wu D, Zhang G** (2020) The HKT transporter HvHKT1;5 negatively regulates salt tolerance. *Plant Physiol* **182**: 584–596
- Huang NC, Liu KH, Lo HJ, Tsay YF** (1999) Cloning and functional characterization of an Arabidopsis nitrate transporter gene that encodes a constitutive component of low-affinity uptake. *Plant Cell* **11**: 1381–1392
- Ishikawa S, Ito Y, Sato Y, Fukaya Y, Takahashi M, Morikawa H, Ohtake N, Ohyama T, Sueyoshi K** (2009) Two-component high-affinity nitrate transport system in barley: Membrane localization, protein expression in roots and a direct protein-protein interaction. *Plant Biotechnol* **26**: 197–205
- Ito H, Murata K, Kimura A** (1984) Transformation of intact yeast cells treated with alkali cations or thiol compounds. *Agric Biol Chem* **48**: 341–347
- Jahn T, Fuglsang AT, Olsson A, Bruntrup IM, Collinge DB, Volkmann D, Sommarin M, Palmgren MG, Larsson C** (1997) The 14-3-3 protein interacts directly with the C-terminal region of the plant plasma membrane H⁺-ATPase. *Plant Cell* **9**: 1805–1814
- Jegla T, Busey G, Assmann SM** (2018) Evolution and structural characteristics of plant voltage-gated K⁺ channels. *Plant Cell* **30**: 2898–2909
- Jørgensen ME, Xu D, Crocoll C, Motawia MS, Ernst HA, Ramı D, Olsen CE, Mirza O, Nour-eldin HH, Halkier BA** (2017) Origin and evolution of transporter substrate specificity within the NPF family. *Elife* 1–31
- Jossier M, Kroniewicz L, Dalmas F, Le Thiec D, Ephritikhine G, Thomine S, Barbier-Brygoo H, Vavasseur A, Filleur S, Leonhardt N** (2010) The Arabidopsis vacuolar anion transporter, AtCLC_c, is involved in the regulation of stomatal movements and contributes to salt tolerance. *Plant J* **64**: 563–576
- Karnik R, Grefen C, Bayne R, Honsbein A, Köhler T, Kioumourtzoglou D, Williams M,**

- Bryant NJ, Blatt MR** (2013) Arabidopsis Sec1/Munc18 protein SEC11 is a competitive and dynamic modulator of SNARE binding and SYP121-dependent vesicle traffic. *Plant Cell* **25**: 1368–1382
- Karnik R, Waghmare S, Zhang B, Larson E, Lefoulon C, Gonzalez W, Blatt MR** (2017) Commandeering channel voltage sensors for secretion, cell turgor, and volume control. *Trends Plant Sci* **22**: 81–95
- Karnik R, Zhang B, Waghmare S, Aderhold C, Grefen C, Blatt MR** (2015) Binding of SEC11 indicates its role in SNARE recycling after vesicle fusion and identifies two pathways for vesicular traffic to the plasma membrane. *Plant Cell* **27**: 675–694
- Kasaras A** (2012) Characterization of the senescence-associated membrane protein DMP1 and the DMP family in Arabidopsis thaliana. Freie Universitat Berlin
- Kiba T, Feria-Bourrellier AB, Lafouge F, Lezhneva L, Boutet-Mercey S, Orsel M, Bréhaut V, Miller A, Daniel-Vedele F, Sakakibara H, et al** (2012) The Arabidopsis nitrate transporter NRT2.4 plays a double role in roots and shoots of nitrogen-starved plants. *Plant Cell* **24**: 245–258
- Kilian J, Whitehead D, Horak J, Wanke D, Weigl S, Batistic O, D'Angelo C, Bornberg-Bauer E, Kudla J, Harter K** (2007) The AtGenExpress global stress expression data set: Protocols, evaluation and model data analysis of UV-B light, drought and cold stress responses. *Plant J* **50**: 347–363
- Kinoshita T, Hayashi Y** (2011) New insights into the regulation of stomatal opening by blue light and plasma membrane H⁺-ATPase. *Int. Rev. Cell Mol. Biol.* pp 89–115
- van Kleeff PJM, Gao J, Mol S, Zwart N, Zhang H, Li KW, de Boer AH** (2018) The Arabidopsis GORK K⁺-channel is phosphorylated by calcium-dependent protein kinase 21 (CPK21), which in turn is activated by 14-3-3 proteins. *Plant Physiol Biochem* **125**: 219–231
- Kobe B, Kajava A V.** (2001) The leucine-rich repeat as a protein recognition motif. *Curr Opin Struct Biol* **11**: 725–732
- Kolukisaoglu Ü, Weigl S, Blazevic D, Batistic O, Kudla J** (2004) Calcium sensors and their interacting protein kinases: Genomics of the Arabidopsis and rice CBL-CIPK signaling networks. *Plant Physiol* **134**: 43–58
- Koncz C, Schell J** (1986) The promoter of TL-DNA gene 5 controls the tissue-specific expression of chimaeric genes carried by a novel type of Agrobacterium binary vector.

- MGG Mol Gen Genet **204**: 383–396
- Koyama H, Toda T, Yokota S, Dawair Z, Hara T** (1995) Effects of aluminum and pH on root growth and cell viability in *Arabidopsis thaliana* strain landsberg in hydroponic culture. *Plant Cell Physiol* **36**: 201–205
- Krouk G, Lacombe B, Bielach A, Perrine-Walker F, Malinska K, Mounier E, Hoyerova K, Tillard P, Leon S, Ljung K, et al** (2010) Nitrate-regulated auxin transport by NRT1.1 defines a mechanism for nutrient sensing in plants. *Dev Cell* **18**: 927–937
- Kwon C, Neu C, Pajonk S, Yun HS, Lipka U, Humphry M, Bau S, Straus M, Kwaaitaal M, Rampelt H, et al** (2008) Co-option of a default secretory pathway for plant immune responses. *Nature* **451**: 835–840
- Laanemets K, Wang Y, Lindgren O, Wu J, Soomets U, Kangasjärvi J, Schroeder JI, Kollist H** (2013) Mutations in SLAC1 anion channel slow stomatal opening and severely reduce K⁺ uptake channel activity via enhanced cytosolic [Ca²⁺] and increased Ca²⁺ sensitivity of K⁺ uptake channels. *New Phytol* **197**: 88–98
- Lacombe B, Pilot G, Michard E, Gaymard F, Sentenac H, Thibaud JB** (2000) A shaker-like K⁺ channel with weak rectification is expressed in both source and sink phloem tissues of *Arabidopsis*. *Plant Cell* **12**: 837–851
- Latz A, Becker D, Hekman M, Müller T, Beyhl D, Marten I, Eing C, Fischer A, Dunkel M, Bertl A, et al** (2007) TPK1, a Ca²⁺-regulated *Arabidopsis* vacuole two-pore K⁺ channel is activated by 14-3-3 proteins. *Plant J* **52**: 449–459
- Lefoulon C, Waghmare S, Karnik R, Blatt MR** (2018) Gating control and K⁺ uptake by the KAT1 K⁺ channel leveraged through membrane anchoring of the trafficking protein SYP121. *Plant Cell Environ* **41**: 2668–2677
- Leidi EO, Barragán V, Rubio L, El-Hamdaoui A, Ruiz MT, Cubero B, Fernández JA, Bressan RA, Hasegawa PM, Quintero FJ, et al** (2010) The AtNHX1 exchanger mediates potassium compartmentation in vacuoles of transgenic tomato. *Plant J* **61**: 495–506
- Léran S, Edel KH, Pervent M, Hashimoto K, Corratge-Faillie C, Offenborn JN, Tillard P, Gojon A, Kudla J, Lacombe B** (2015) Nitrate sensing and uptake in *Arabidopsis* are enhanced by ABI2, a phosphatase inactivated by the stress hormone abscisic acid. *Sci Signal* **8**: 1–7
- Li B, Byrt C, Qiu J, Baumann U, Hrmova M, Evrard A, Johnson AAT, Birnbaum KD, Mayo GM, Jha D, et al** (2016) Identification of a stelar-localized transport protein that

- facilitates root-to-shoot transfer of chloride in arabidopsis. *Plant Physiol* **170**: 1014–1029
- Li B, Wang Y, Zhang Z, Wang B, Eneji AE, Duan L, Li Z, Tian X** (2012) Cotton shoot plays a major role in mediating senescence induced by potassium deficiency. *J Plant Physiol* **169**: 327–335
- Li H, Yu M, Du XQ, Wang ZF, Wu WH, Quintero FJ, Jin XH, Li HD, Wang Y** (2017a) NRT1.5/NPF7.3 functions as a proton-coupled H⁺/K⁺ antiporter for K⁺ loading into the xylem in arabidopsis. *Plant Cell* **29**: 2016–2026
- Li J, Wu W-H, Wang Y** (2017b) Potassium channel AKT1 is involved in the auxin-mediated root growth inhibition in Arabidopsis response to low K⁺ stress. *J Integr Plant Biol* **59**: 895–909
- Li JY, Fu YL, Pike SM, Bao J, Tian W, Zhang Y, Chen CZ, Zhang Y, Li HM, Huang J, et al** (2010) The Arabidopsis nitrate transporter NRT1.8 functions in nitrate removal from the xylem sap and mediates cadmium tolerance. *Plant Cell* **22**: 1633–1646
- Lin SH, Kuo HF, Canivenc G, Lin CS, Lepetit M, Hsu PK, Tillard P, Lin HG, Wang YY, Tsai CB, et al** (2008) Mutation of the Arabidopsis NRT1.5 nitrate transporter causes defective root-to-shoot nitrate transport. *Plant Cell* **20**: 2514–2528
- Lipka V, Kwon C, Panstruga R** (2007) SNARE-ware: The role of SNARE-domain proteins in plant biology. *Annu Rev Cell Dev Biol* **23**: 147–174
- Liu H, Tang R, Zhang Y, Wang C, Lv Q, Gao X, Li WB, Zhang H** (2010) AtNHX3 is a vacuolar K⁺/H⁺ antiporter required for low-potassium tolerance in Arabidopsis thaliana. *Plant, Cell Environ* **33**: 1989–1999
- Liu K, Tsay Y** (2003) Switching between the two action modes of the dual-affinity nitrate transporter CHL1 by phosphorylation. *EMBO J* **22**: 1005–1013
- Liu LL, Ren HM, Chen LQ, Wang Y, Wu WH** (2013) A protein kinase, Calcineurin B-Like Protein-interacting Protein Kinase9, interacts with calcium sensor Calcineurin B-Like Protein3 and regulates potassium homeostasis under low-potassium stress in Arabidopsis. *Plant Physiol* **161**: 266–277
- Liu Y, Von Wirén N** (2017) Ammonium as a signal for physiological and morphological responses in plants. *J Exp Bot* **68**: 2581–2592
- Locascio A, Andrés-Colás N, Mulet JM, Yenush L** (2019) *Saccharomyces cerevisiae* as a tool to investigate plant potassium and sodium transporters. *Int J Mol Sci*. doi: 10.3390/ijms20092133

- Longo A, Miles NW, Dickstein R** (2018) Genome mining of plant NPFs reveals varying conservation of signature motifs associated with the mechanism of transport. *Front Plant Sci* **871**: 1–17
- Ma Q, Tang RJ, Zheng XJ, Wang SM, Luan S** (2015) The calcium sensor CBL7 modulates plant responses to low nitrate in Arabidopsis. *Biochem Biophys Res Commun* **468**: 59–65
- Ma TL, Wu WH, Wang Y** (2012) Transcriptome analysis of rice root responses to potassium deficiency. *BMC Plant Biol* **12**: 1–13
- Maathuis FJM, Filatov V, Herzyk P, Krijger GC, Axelsen KB, Chen S, Green BJ, Li Y, Madagan KL, Sánchez-Fernández R, et al** (2003) Transcriptome analysis of root transporters reveals participation of multiple gene families in the response to cation stress. *Plant J* **35**: 675–692
- Maierhofer T, Diekmann M, Offenborn JN, Lind C, Bauer H, Hashimoto K, Al-Rasheid KAS, Luan S, Kudla J, Geiger D, et al** (2014) Site- and kinase-specific phosphorylation-mediated activation of SLAC1, a guard cell anion channel stimulated by abscisic acid. *Sci Signal* **7**: 1–12
- Marmagne A, Vinauger-Douard M, Monachello D, De Longevialle AF, Charon C, Allot M, Rappaport F, Wollman FA, Barbier-Brygoo H, Ephritikhine G** (2007) Two members of the Arabidopsis CLC (chloride channel) family, AtCLCe and AtCLCf, are associated with thylakoid and Golgi membranes, respectively. *J Exp Bot* **58**: 3385–3393
- Martin EC, Sukarta OCA, Spiridon L, Grigore LG, Constantinescu V, Tacutu R, Govere A, Petrescu AJ** (2020) LRRpredictor -A new LRR motif detection method for irregular motifs of plant NLR proteins using an ensemble of classifiers. *Genes (Basel)* **11**: 1–26
- Martinoia E, Meyer S, De Angeli A, Nagy R** (2012) Vacuolar transporters in their physiological context. *Annu Rev Plant Biol* **63**: 183–213
- Mäser P, Thomine S, Schroeder JI, Ward JM, Hirschi K, Sze H, Talke IN, Amtmann A, Maathuis FJM, Sanders D, et al** (2001) Phylogenetic relationships within cation transporter families of Arabidopsis. *Plant Physiol* **126**: 1646–1667
- Meharg AA, Blatt MR** (1995) NO₃⁻ transport across the plasma membrane of Arabidopsis thaliana root hairs: Kinetic control by pH and membrane voltage. *J Membr Biol* **145**: 49–66
- Meier M, Liu Y, Lay-Pruitt KS, Takahashi H, von Wirén N** (2020) Auxin-mediated root branching is determined by the form of available nitrogen. *Nat Plants* **6**: 1136–1145
- Meng S, Peng JS, He YN, Zhang G Bin, Yi HY, Fu YL, Gong JM** (2016) Arabidopsis NRT1.5

- mediates the suppression of nitrate starvation-induced leaf senescence by modulating foliar potassium level. *Mol Plant* **9**: 461–470
- Menz J, Li Z, Schulze WX, Ludewig U** (2016) Early nitrogen-deprivation responses in Arabidopsis roots reveal distinct differences on transcriptome and (phospho-) proteome levels between nitrate and ammonium nutrition. *Plant J* **88**: 717–734
- Młodzińska E, Klobus G, Christensen MD, Fuglsang AT** (2015) The plasma membrane H⁺-ATPase *AHA2* contributes to the root architecture in response to different nitrogen supply. *Physiol Plant* **154**: 270–282
- Monachello D, Allot M, Oliva S, Krapp A, Daniel-Vedele F, Barbier-Brygoo H, Ephritikhine G** (2009) Two anion transporters *AtClCa* and *AtClCe* fulfil interconnecting but not redundant roles in nitrate assimilation pathways. *New Phytol* **183**: 88–94
- Mumberg D, Müller R, Funk M** (1995) Yeast vectors for the controlled expression of heterologous proteins in different genetic backgrounds. *Gene* **156**: 119–122
- Murashige T, Skoog F** (1962) A revised medium for rapid growth and bio assays with tobacco tissue cultures. *Physiol Plant* **15**: 473–497
- Negi J, Matsuda O, Nagasawa T, Oba Y, Takahashi H, Kawai-Yamada M, Uchimiya H, Hashimoto M, Iba K** (2008) CO₂ regulator *SLAC1* and its homologues are essential for anion homeostasis in plant cells. *Nature* **452**: 483–486
- Newstead S** (2017) Recent advances in understanding proton coupled peptide transport via the POT family. *Curr Opin Struct Biol* **45**: 17–24
- Nguyen CT, Agorio A, Jossier M, Depré S, Thomine S, Filleur S** (2016) Characterization of the chloride channel-like, *AtCLCg*, involved in chloride tolerance in *Arabidopsis thaliana*. *Plant Cell Physiol* **57**: 764–775
- Nieves-Cordones M, Alemán F, Martínez V, Rubio F** (2014) K⁺ uptake in plant roots. The systems involved, their regulation and parallels in other organisms. *J Plant Physiol* **171**: 688–695
- Nieves-Cordones M, Lara A, Ródenas R, Amo J, Rivero RM, Martínez V, Rubio F** (2019) Modulation of K⁺ translocation by *AKT1* and *AtHAK5* in *Arabidopsis* plants. *Plant Cell Environ* **42**: 2357–2371
- Nieves-Cordones M, Ródenas R, Chavanieu A, Rivero RM, Martinez V, Gaillard I, Rubio F** (2016) Uneven HAK/KUP/KT protein diversity among angiosperms: Species distribution and perspectives. *Front Plant Sci* **7**: 1–7

- O'Brien JAA, Vega A, Bouguyon E, Krouk G, Gojon A, Coruzzi G, Gutiérrez RAA** (2016) Nitrate transport, sensing, and responses in plants. *Mol Plant* **9**: 837–856
- Obrdiik P, El-Bakkoury M, Hamacher T, Cappellaro C, Vilarino C, Fleischer C, Ellerbrok H, Kamuzinzi R, Ledent V, Blaudez D, et al** (2004) K⁺ channel interactions detected by a genetic system optimized for systematic studies of membrane protein interactions. *Proc Natl Acad Sci U S A* **101**: 12242–12247
- Okamoto M, Kumar A, Li W, Wang Y, Siddiqi MY, Crawford NM, Glass ADM** (2006) High-affinity nitrate transport in roots of *Arabidopsis* depends on expression of the NAR2-Like gene *AtNRT3.1*. *Plant Physiol* **140**: 1036–1046
- Oñate-Sánchez L, Vicente-Carbajosa J** (2008) DNA-free RNA isolation protocols for *Arabidopsis thaliana*, including seeds and siliques. *BMC Res Notes* **1**: 1–7
- Oparka KJ** (1994) Plasmolysis: New insights into an old process. *New Phytol* **126**: 571–591
- Orsel M, Chopin F, Leleu O, Smith SJ, Krapp A, Daniel-Vedele F, Miller AJ** (2006) Characterization of a two-component high-affinity nitrate uptake system in *Arabidopsis*. Physiology and protein-protein interaction. *Plant Physiol* **142**: 1304–1317
- Ortiz-Ramirez C, Mora SI, Trejo J, Pantoja O** (2011) PvAMT1;1, a highly selective ammonium transporter that functions as H⁺/NH₄⁺ symporter. *J Biol Chem* **286**: 31113–31122
- Palmgren MG** (2001) Plant plasma membrane H⁺-ATPases: Powerhouses for nutrient uptake. *Annu Rev Plant Physiol Plant Mol Biol* **52**: 817–845
- Palmgren MG** (1991) Regulation of plant plasma membrane H⁺-ATPase activity. *Physiol Plant* **83**: 314–323
- Palmgren MG, Christensen G** (1993) Complementation in situ of the yeast plasma membrane H⁺-ATPase gene *pmal* by an H⁺-ATPase gene from a heterologous species. *FEBS Lett* **317**: 216–222
- Pandey GK, Cheong YH, Kim BG, Grant JJ, Li L, Luan S** (2007) CIPK9: A calcium sensor-interacting protein kinase required for low-potassium tolerance in *Arabidopsis*. *Cell Res* **17**: 411–421
- Parker JL, Newstead S** (2014) Molecular basis of nitrate uptake by the plant nitrate transporter NRT1.1. *Nature* **507**: 68–72
- Parlitz S, Kunze R, Mueller-Roeber B, Balazadeh S** (2011) Regulation of photosynthesis and transcription factor expression by leaf shading and re-illumination in *Arabidopsis thaliana*

- leaves. *J Plant Physiol* **168**: 1311–1319
- Petrezselyova S, Zahradka J, Sychrova H** (2010) *Saccharomyces cerevisiae* BY4741 and W303-1A laboratory strains differ in salt tolerance. *Fungal Biol* **114**: 144–150
- Pike S, Gao F, Kim MJ, Kim SH, Schachtman DP, Gassmann W** (2014) Members of the NPF3 transporter subfamily encode pathogen-inducible nitrate/nitrite transporters in grapevine and *Arabidopsis*. *Plant Cell Physiol* **55**: 162–170
- Pitann B, Kranz T, Mühling KH** (2009) The apoplastic pH and its significance in adaptation to salinity in maize (*Zea mays* L.): Comparison of fluorescence microscopy and pH-sensitive microelectrodes. *Plant Sci* **176**: 497–504
- Qiu J, Henderson SW, Tester M, Roy SJ, Gilliam M** (2017) SLAH1, a homologue of the slow type anion channel SLAC1, modulates shoot Cl⁻ accumulation and salt tolerance in *Arabidopsis thaliana*. *J Exp Bot* **68**: 4495–4505
- Quintero FJ, Ohta M, Shi H, Zhu J, Pardo JM** (2002) Reconstitution in yeast of the *Arabidopsis* SOS signaling pathway for Na⁺ homeostasis. *PNAS* **99**: 9061–9066
- Raddatz N, Morales de los Ríos L, Lindahl M, Quintero FJ, Pardo JM** (2020) Coordinated transport of nitrate, potassium, and sodium. *Front Plant Sci* **11**: 1–18
- Ragel P, Raddatz N, Leidi EO, Quintero FJ, Pardo JM** (2019) Regulation of K⁺ nutrition in plants. *Front Plant Sci* **10**: 1–21
- Ragel P, Ródenas R, García-Martín E, Andrés Z, Villalta I, Nieves-Cordones M, Rivero RM, Martínez V, Pardo JM, Quintero FJ, et al** (2015) CIPK23 regulates HAK5-mediated high-affinity K⁺ uptake in *Arabidopsis* roots. *Plant Physiol* **169**: pp.01401.2015
- Raggi S, Demes E, Liu S, Verger S, Robert S** (2020) Polar expedition: mechanisms for protein polar localization. *Curr Opin Plant Biol* **53**: 134–140
- Rashid M, Bera S, Banerjee M, Medvinsky AB, Sun G-Q, Li B-L, Sljoka A, Chakraborty A** (2020) Feedforward control of plant nitrate transporter NRT1.1 biphasic adaptive activity. *Biophys J* **118**: 898–908
- Reguera M, Bassil E, Tajima H, Wimmer M, Chanoca A, Otegui MS, Paris N, Blumwald E** (2015) pH regulation by NHX-type antiporters is required for receptor-mediated protein trafficking to the vacuole in *Arabidopsis*. *Plant Cell* **27**: 1200–1217
- Reintanz B, Szyroki A, Ivashikina N, Ache P, Godde M, Becker D, Palme K, Hedrich R** (2002) AtKC1, a silent *Arabidopsis* potassium channel α -subunit modulates root hair K⁺ influx. *Proc Natl Acad Sci U S A* **99**: 4079–4084

- Remans T, Nacry P, Pervent M, Filleur S, Diatloff E, Mounier E, Tillard P, Forde BG, Gojon A** (2006) The Arabidopsis NRT1.1 transporter participates in the signaling pathway triggering root colonization of nitrate-rich patches. *Proc Natl Acad Sci U S A* **103**: 19206–19211
- Rigas S, Debrosses G, Haralampidis K, Vicente-Agullo F, Feldmann KA, Grabov A, Dolan L, Hatzopoulos P** (2001) TRH1 encodes a potassium transporter required for tip growth in Arabidopsis root hairs. *Plant Cell* **13**: 139–151
- Robles-Aguilar AA, Pang J, Postma JA, Schrey SD, Lambers H, Jablonowski ND** (2019) The effect of pH on morphological and physiological root traits of *Lupinus angustifolius* treated with struvite as a recycled phosphorus source. *Plant Soil* **434**: 65–78
- Ródenas R, García-Legaz MF, López-Gómez E, Martínez V, Rubio F, Ángeles Botella M** (2017) NO₃⁻, PO₄³⁻ and SO₄²⁻ deprivation reduced LKT1-mediated low-affinity K⁺ uptake and SKOR-mediated K⁺ translocation in tomato and Arabidopsis plants. *Physiol Plant* **160**: 410–424
- Rodríguez-Navarro A** (2000) Potassium transport in fungi and plants. *Biochim Biophys Acta - Rev Biomembr* **1469**: 1–30
- Rodríguez-Navarro A, Blatt MR, Slayman CL** (1986) A potassium-proton symport in *Neurospora crassa*. *J Gen Physiol* **87**: 649–674
- Roelfsema MRG, Hedrich R, Geiger D** (2012) Anion channels: Master switches of stress responses. *Trends Plant Sci* **17**: 221–229
- Ronzier E, Corratgé-Faillie C, Sanchez F, Prado K, Brière C, Leonhardt N, Thibaud JB, Xiong TC** (2014) CPK13, a noncanonical Ca²⁺-dependent protein kinase, specifically inhibits KAT2 and KAT1 shaker K⁺ channels and reduces stomatal opening. *Plant Physiol* **166**: 314–326
- Rubin G, Tohge T, Matsuda F, Saito K, Scheible WR** (2009) Members of the LBD family of transcription factors repress anthocyanin synthesis and affect additional nitrogen responses in Arabidopsis. *Plant Cell* **21**: 3567–3584
- Rubio F, Alemán F, Nieves-Cordones M, Martínez V** (2010) Studies on Arabidopsis *athak5*, *atakt1* double mutants disclose the range of concentrations at which AtHAK5, AtAKT1 and unknown systems mediate K⁺ uptake. *Physiol Plant* **139**: 220–228
- Rubio F, Fon M, Ródenas R, Nieves-Cordones M, Alemán F, Rivero RM, Martínez V** (2014) A low K⁺ signal is required for functional high-affinity K⁺ uptake through HAK5

- transporters. *Physiol Plant* **152**: 558–570
- Rubio F, Guillermo SM, Rodríguez-Navarro A** (2000) Cloning of Arabidopsis and barley cDNAs encoding HAK potassium transporters in root and shoot cells. *Physiol Plant* **109**: 34–43
- Saito S, Hamamoto S, Moriya K, Matsuura A, Sato Y, Muto J, Noguchi H, Yamauchi S, Tozawa Y, Ueda M, et al** (2018) N-myristoylation and S-acylation are common modifications of Ca²⁺-regulated Arabidopsis kinases and are required for activation of the SLAC1 anion channel. *New Phytol* **218**: 1504–1521
- Saito S, Uozumi N** (2020) Calcium-Regulated phosphorylation systems controlling uptake and balance of plant nutrients. *Front Plant Sci* **11**: 1–11
- Sánchez-Barrena MJ, Chaves-Sanjuan A, Raddatz N, Mendoza I, Cortés Á, Gago F, González-Rubio JM, Benavente JL, Quintero FJ, Pardo JM, et al** (2020) Recognition and activation of the plant AKT1 potassium channel by the kinase CIPK23. *Plant Physiol* **182**: 2143–2153
- Santa María GE, Oliferuk S, Moriconi JI** (2018) A survey of sequences of KT-HAK-KUP transporters in green algae and basal land plants. *Data Br* **19**: 2356–2363
- Santi S, Schmidt W** (2009) Dissecting iron deficiency-induced proton extrusion in Arabidopsis roots. *New Phytol* **183**: 1072–1084
- Schachtman DP, Schroeder JI** (1994) Structure and transport mechanism of a high-affinity potassium uptake transporter from higher plants. *Nature* **370**: 655–658
- Scheible W-R, Morcuende R, Czechowski T, Fritz C, Osuna D, Palacios-Rojas N, Schindelasch D, Thimm O, Udvardi MK, Stitt M** (2004) Genome-wide reprogramming of primary and secondary metabolism, protein synthesis, cellular growth processes, and the regulatory infrastructure of Arabidopsis in response to nitrogen. *Plant Physiol* **136**: 2483–2499
- Schwacke R, Schneider A, Van Der Graaff E, Fischer K, Catoni E, Desimone M, Frommer WB, Flügge UI, Kunze R** (2003) ARAMEMNON, a novel database for Arabidopsis integral membrane proteins. *Plant Physiol* **131**: 16–26
- Sentenac H, Bonneaud N, Minet M, Lacroute F, Salmon JM, Gaymard F, Grignon C** (1992) Cloning and expression in yeast of a plant potassium ion transport system. *Science* (80-) **256**: 663–665
- Shen J, Zeng Y, Zhuang X, Sun L, Yao X, Pimpl P, Jiang L** (2013) Organelle pH in the

- Arabidopsis endomembrane system. *Mol Plant* **6**: 1419–1437
- Shin R, Schachtman DP** (2004) Hydrogen peroxide mediates plant root cell response to nutrient deprivation. *Proc Natl Acad Sci U S A* **101**: 8827–8832
- Söllner T, Whiteheart S, Brunner M, Erdjument-Bromage H, Geromanos S, Tempst P, Rothman JE** (1993) SNAP receptors implicated in vesicle targeting and fusion. *Nature* **362**: 318–324
- Song SJ, Feng QN, Li CL, Li E, Liu Q, Kang H, Zhang W, Zhang Y, Li S** (2018) A tonoplast-associated calcium-signaling module dampens ABA signaling during stomatal movement. *Plant Physiol* **177**: 1666–1678
- Steiner H -Y, Naider F, Becker JM** (1995) The PTR family: a new group of peptide transporters. *Mol Microbiol* **16**: 825–834
- Sun CH, Yu JQ, Hu DG** (2017) Nitrate: A crucial signal during lateral roots development. *Front Plant Sci* **8**: 1–9
- Sun J, Bankston JR, Payandeh J, Hinds TR, Zagotta WN, Zheng N** (2014) Crystal structure of the plant dual-affinity nitrate transporter NRT1.1. *Nature* **507**: 73–77
- Sun J, Zheng N** (2015) Molecular mechanism underlying the plant NRT1.1 dual-affinity nitrate transporter. *Front Physiol* **6**: 1–6
- Sutter JU, Campanoni P, Tyrrell M, Blatt MR** (2006) Selective mobility and sensitivity to SNAREs is exhibited by the Arabidopsis KAT1 K⁺ channel at the membrane. *Plant Cell* **18**: 935–954
- Sze H, Chanroj S** (2018) Plant endomembrane dynamics: Studies of K⁺/H⁺ antiporters provide insights on the effects of pH and ion homeostasis. *Plant Physiol* **177**: 875–895
- Sze H, Li X, Palmgren MG** (1999) Energization of plant cell membranes by H⁺-pumping ATPases: Regulation and biosynthesis. *Plant Cell* **11**: 677–689
- Taiz L, Zeiger E** (1991) *Plant Physiology*, Fifth Edit. Redwood City
- Takano J, Tanaka M, Toyoda A, Miwa K, Kasai K, Fuji K, Onouchi H, Naito S, Fujiwara T** (2010) Polar localization and degradation of Arabidopsis boron transporters through distinct trafficking pathways. *Proc Natl Acad Sci U S A* **107**: 5220–5225
- Tang RJ, Liu H, Yang Y, Yang L, Gao XS, Garcia VJ, Luan S, Zhang HX** (2012) Tonoplast calcium sensors CBL2 and CBL3 control plant growth and ion homeostasis through regulating V-ATPase activity in Arabidopsis. *Cell Res* **22**: 1650–1665
- Tang RJ, Zhao FG, Garcia VJ, Kleist TJ, Yang L, Zhang HX, Luan S** (2015) Tonoplast

- CBL-CIPK calcium signaling network regulates magnesium homeostasis in Arabidopsis. *Proc Natl Acad Sci U S A* **112**: 3134–3139
- Tang RJ, Zhao FG, Yang Y, Wang C, Li K, Kleist TJ, Lemaux PG, Luan S** (2020) A calcium signalling network activates vacuolar K⁺ remobilization to enable plant adaptation to low-K environments. *Nat Plants* **6**: 384–393
- Tsay Y-F, Schroeder JI, Feldmann KA, Crawford NM** (1993) The herbicide sensitivity gene CHL1 of Arabidopsis encodes a nitrate-inducible nitrate transporter. *Cell* **72**: 705–713
- Tsay YF, Chiu CC, Tsai CB, Ho CH, Hsu PK** (2007) Nitrate transporters and peptide transporters. *FEBS Lett* **581**: 2290–2300
- Tsujii M, Kera K, Hamamoto S, Kuromori T, Shikanai T, Uozumi N** (2019) Evidence for potassium transport activity of Arabidopsis KEA1-KEA6. *Sci Rep* **9**: 1–13
- Uemura T, Morita MT, Ebine K, Okatani Y, Yano D, Saito C, Ueda T, Nakano A** (2010) Vacuolar/pre-vacuolar compartment Qa-SNAREs VAM3/SYP22 and PEP12/SYP21 have interchangeable functions in Arabidopsis. *Plant J* **64**: 864–873
- Uemura T, Ueda T, Ohniwa RL, Nakano A, Takeyasu K, Sato MH** (2004) Systematic analysis of SNARE molecules in Arabidopsis: dissection of the post-Golgi network in plant cells. *Cell Struct Funct* **29**: 49–65
- Ueno K, Kinoshita T, Inoue SI, Emi T, Shimazaki KI** (2005) Biochemical characterization of plasma membrane H⁺-ATPase activation in guard cell protoplasts of Arabidopsis thaliana in response to blue light. *Plant Cell Physiol* **46**: 955–963
- Ulmasov T, Murfett J, Hagen G, Guilfoyle TJ** (1997) Aux/IAA proteins repress expression of reporter genes containing natural and highly active synthetic auxin response elements. *Plant Cell* **9**: 1963–1971
- Very A-A, Sentenac H** (2003) Molecular mechanisms and regulation of K⁺ transport in higher plants. *Annu Rev Plant Biol* **54**: 575–603
- Vitart V, Baxter I, Doerner P, Harper JF** (2001) Evidence for a role in growth and salt resistance of a plasma membrane H⁺-ATPase in the root endodermis. *Plant J* **27**: 191–201
- Voelker C, Gomez-Porrás JL, Becker D, Hamamoto S, Uozumi N, Gambale F, Mueller-Roeber B, Czempinski K, Dreyer I** (2010) Roles of tandem-pore K⁺ channels in plants - a puzzle still to be solved. *Plant Biol* **12**: 56–63
- Waghmare S, Lefoulon C, Zhang B, Liliakyte E, Donald N, Blatt MR** (2019) K1 channel-SEC11 binding exchange regulates SNARE assembly for secretory traffic. *Plant Physiol*

- 181: 1096–1113
- Walker DJ, Black CR, Miller AJ** (1998) The role of cytosolic potassium and pH in the growth of barley roots. *Plant Physiol* **118**: 957–964
- Walker DJ, Leigh RA, Miller AJ** (1996) Potassium homeostasis in vacuolate plant cells. *Proc Natl Acad Sci U S A* **93**: 10510–10514
- Wang MY, Glass ADM, Shaff JE, Kochian L V.** (1994) Ammonium uptake by rice roots. *Plant Physiol* **104**: 899–906
- Wang T, Hua Y, Chen M, Zhang J, Guan C, Zhang Z** (2018) Mechanism enhancing Arabidopsis resistance to cadmium: The role of NRT1.5 and proton pump. *Front Plant Sci* **871**: 1–12
- Wang Y, He L, Li HD, Xu J, Wu WH** (2010) Potassium channel α -subunit AtKC1 negatively regulates AKT1-mediated K⁺ uptake in Arabidopsis roots under low-K⁺ stress. *Cell Res* **20**: 826–837
- Wang Y, Wu W-H** (2013) Potassium transport and signaling in higher plants. *Annu Rev Plant Biol* **64**: 451–476
- Wang Y, Wu WH** (2017) Regulation of potassium transport and signaling in plants. *Curr Opin Plant Biol* **39**: 123–128
- Wang YY, Hsu PK, Tsay YF** (2012) Uptake, allocation and signaling of nitrate. *Trends Plant Sci* **17**: 458–467
- Wang YY, Tsay YF** (2011) Arabidopsis nitrate transporter NRT1.9 is important in phloem nitrate transport. *Plant Cell* **23**: 1945–1957
- Watanabe S, Takahashi N, Kanno Y, Suzuki H, Aoi Y, Takeda-Kamiya N, Toyooka K, Kasahara H, Hayashi K-I, Umeda M, et al** (2020) The Arabidopsis NRT1/PTR FAMILY Protein NPF7.3/NRT1.5 is an indole-3-butyric acid transporter involved in root gravitropism. *Proc Natl Acad Sci U S A* **202013305**: 1–10
- Wen Z, Kaiser BN** (2018) Unraveling the functional role of NPF6 transporters. *Front Plant Sci* **9**: 1–8
- Wen Z, Tyerman SD, Dechorgnat J, Ovchinnikova E, Dhugga KS, Kaiser BN** (2017) Maize NPF6 proteins are homologs of arabidopsis CHL1 that are selective for both nitrate and chloride. *Plant Cell* **29**: 2581–2596
- Weng Y, You Y, Lu Q, Zhong A, Liu S, Liu H, Du S** (2020) Graphene oxide exposure suppresses nitrate uptake by roots of wheat seedlings. *Environ Pollut* **262**: 1–11

- Wiebe CA, DiBattista ER, Fliegel L** (2001) Functional role of polar amino acid residues in Na⁺/H⁺ exchangers. *Biochem J* **357**: 1–10
- Wulff N, Ernst HA, Jørgensen ME, Lambertz S, Maierhofer T, Belew ZM, Crocoll C, Motawia MS, Geiger D, Jørgensen FS, et al** (2019) An optimized screen reduces the number of GA transporters and provides insights into Nitrate Transporter 1/Peptide transporter family substrate determinants. *Front Plant Sci* **10**: 1–18
- Xu G, Fan X, Miller AJ** (2012) Plant nitrogen assimilation and use efficiency. *Annu Rev Plant Biol* **63**: 153–182
- Xu J, Li HD, Chen LQ, Wang Y, Liu LL, He L, Wu WH** (2006) A protein kinase, interacting with two calcineurin B-like proteins, regulates K⁺ transporter AKT1 in Arabidopsis. *Cell* **125**: 1347–1360
- Yang K, Wang L, Le J, Dong J** (2020) Cell polarity: Regulators and mechanisms in plants. *J Integr Plant Biol* **62**: 132–147
- Yang T, Zhang S, Hu Y, Wu F, Hu Q, Chen G, Cai J, Wu T, Moran N, Yu L, et al** (2014) The role of a potassium transporter OsHAK5 in potassium acquisition and transport from roots to shoots in rice at low potassium supply levels. *Plant Physiol* **166**: 945–959
- Yuan W, Zhang D, Song T, Xu F, Lin S, Xu W, Li Q, Zhu Y, Liang J, Zhang J** (2017) Arabidopsis plasma membrane H⁺-ATPase genes AHA2 and AHA7 have distinct and overlapping roles in the modulation of root tip H⁺ efflux in response to low-phosphorus stress. *J Exp Bot* **68**: 1731–1741
- Yun HS, Yi C, Kwon H, Kwon C** (2013) Model for regulation of VAMP721/722-mediated secretion. *Plant Signal Behav* **8**: 721–723
- Zahrádka J, Sychrová H** (2012) Plasma-membrane hyperpolarization diminishes the cation efflux via Nha1 antiporter and Ena ATPase under potassium-limiting conditions. *FEMS Yeast Res* **12**: 439–446
- Zhang A, Ren HM, Tan YQ, Qi GN, Yao FY, Wu GL, Yang LW, Hussain J, Sun SJ, Wang YF** (2016) S-type anion channels SLAC1 and SLAH3 function as essential negative regulators of inward K⁺ channels and stomatal opening in Arabidopsis. *Plant Cell* **28**: 949–965
- Zhang B, Karnik R, Wang Y, Wallmeroth N, Blatt MR, Grefen C** (2015) The Arabidopsis R-SNARE VAMP721 interacts with KAT1 and KC1 K⁺ channels to moderate K⁺ current at the plasma membrane. *Plant Cell* **27**: 1697–1717

- Zhang F, Niu J, Zhang W, Chen X, Li C, Yuan L, Xie J** (2010) Potassium nutrition of crops under varied regimes of nitrogen supply. *Plant Soil* **335**: 21–34
- Zhang L, Zhang H, Liu P, Hao H, Jin JB, Lin J** (2011) Arabidopsis R-SNARE proteins VAMP721 and VAMP722 are required for cell plate formation. *PLoS One* **6**: 1–14
- Zhang X, Li Z, Li X, Xu Y, Xie H, Qiu Q-S** (2020) CBL3 and CIPK18 are required for the function of NHX5 and NHX6 in mediating Li⁺ homeostasis in Arabidopsis. *J Plant Physiol* **255**: 1–14
- Zhang Y, Wang X, Lu S, Liu D** (2014) A major root-associated acid phosphatase in Arabidopsis, AtPAP10, is regulated by both local and systemic signals under phosphate starvation. *J Exp Bot* **65**: 6577–6588
- Zhao J, Cheng NH, Motes CM, Blancaflor EB, Moore M, Gonzales N, Padmanaban S, Sze H, Ward JM, Hirschi KD** (2008) AtCHX13 is a plasma membrane K⁺ transporter. *Plant Physiol* **148**: 796–807
- Zhao L, Liu F, Crawford NM, Wang Y** (2018a) Molecular regulation of nitrate responses in plants. *Int J Mol Sci* **19**: 1–18
- Zhao X, Huang J, Yu H, Wang L, Xie W** (2010) Genomic survey, characterization and expression profile analysis of the peptide transporter family in rice (*Oryza sativa* L.). *BMC Plant Biol* **10**: 1–20
- Zhao X, Liu Y, Liu X, Jiang J** (2018b) Comparative transcriptome profiling of two tomato genotypes in response to potassium-deficiency stress. *Int J Mol Sci* **19**: 1–24
- Zheng X, He K, Kleist T, Chen F, Luan S** (2015) Anion channel SLAH3 functions in nitrate-dependent alleviation of ammonium toxicity in Arabidopsis. *Plant, Cell Environ* **38**: 474–486
- Zheng Y** (2018) Functional analysis of the nitrate/potassium transporter NPF7.3/NRT1.5 in Arabidopsis thaliana. Freie Universitat Berlin
- Zheng Y, Drechsler N, Rausch C, Kunze R** (2016) The Arabidopsis nitrate transporter NPF7.3/NRT1.5 is involved in lateral root development under potassium deprivation. *Plant Signal Behav* **11**: 1–5
- Zhu XF, Liu Y, Gai XT, Zhou Y, Xia ZY, Chen LJ, Duan YX, Xuan YH** (2019) SNARE proteins SYP22 and VAMP727 negatively regulate plant defense. *Plant Signal Behav* **14**: 1–3

6. Acknowledgements

I would like hearty to thanks:

To *Prof. Reinhard Kunze*, who I met luckily at an IPMB conference in the remote Iguazu falls and became an important part of my life since we decided together to embark on this big challenge to develop my PhD in his group. Thanks so much for your patience, guidance, and support during the last years, from an academic perspective, but no less important on a personal one. I am going to remember all our discussions and talks about science, traveling, and life.

To Dr. *Yue Zheng* and Dr. *Navina Drechsler*, who gave me the scientific background and skills from the NRT1.5 project.

To all my former and actual colleagues, most of them now friends, from AG. Kunze lab. They have been an incredible professional and personal support to develop my PhD and life in Germany.

To *all AG Schmuelling group* (so-called Neubau), for their generous time regarding borrowing equipments, materials, and protocols.

To MSc *Camila Garcia*, BSc *Heni Hitaj*, BSc *Melinda Kehribar* and BSc *Janine Seidal* since part of the experiments have been done by them in the context of their bachelor thesis, that I had the pleasure to orientate.

To Prof. *Nicolaus von Wiren* from IPK Gatersleben for their scientific collaboration about plant nutrient measurements.

To *Margarete Baier* to be my second supervisor and supervised yearly my project.

To DAAD (German Academic Exchange Service) not only to be the financial organization costing my studies for four and half years, but also for the enormous support in my everyday life in Germany.

To all my family and friends from all around the world, but especially the ones in my loved Uruguay. Agradecer me suena poco, pero no encuentro mejores palabras para definir el sentimiento hacia mis amigos y familia quienes me apoyaron completamente para que pueda conseguir este doctorado, pese al tenerme lejos por un gran tiempo.

finalmente, y no menos importante, a mi incondicionalismo amor, *Gaston*.

7. Appendix

Abbreviations:

ABA	Abscisic acid
ABRC	Arabidopsis biological resource center
Abs	Absorbance
ATP	Adenosine triphosphate
BiFC	Bimolecular fluorescence complementation
CaMV	Cauliflower mosaic virus
CBL	Calcineurin B-Like
cDNA	Complementary deoxyribonucleic acid
CDS	Coding DNA sequence
cfu	Colony formation units
CIPK	CBL interacting protein kinase
CLC	Chloride channel
CLSM	Confocal laser scanning microscopy
Col-0	<i>Arabidopsis thaliana</i> ecotype Columbia-0
CsCl	Cesium chloride
CTAB	N-cetyl-N,N,N-trimethyl-ammonium bromide
DEPC	Diethyl pyrocarbonate
DNA	Deoxyribonucleic acid
DNAase I	Deoxyribonuclease I
dNTP	Deoxyribonucleotide triphosphate
DPI	Days post infiltration
DW	Dry weight
EDTA	Ethylenediaminetetraacetic acid
ER	Endoplasmic reticulum
EtBr	Ethidium bromide
EtOH	Ethanol
FC	Fold change
FW	Fresh weight
GUS	β -glucuronidase
HATS	High-affinity transport system

HygB	Hygromycin B
H ₂ O	Water
ICP-OES	Inductively coupled plasma optical emission spectrometry
IPTG	Isopropyl β-D-1-thiogalactopyranoside
LATS	Low-affinity transport system
LB	Lysogeny broth media
LR	Lateral root
LRR	Leucine-rich repeat
mbSUS	Mating-based split ubiquitin system
MES	2-(N-morpholino) ethanesulfonic acid
MS	Murashige-Skoog media
NPF	Nitrate transporter 1 (NRT1)/Peptide transporter
NRT2	Nitrate transporter 2
N ₂	Liquid nitrogen
OD	Optical density
PEG	Polyethylene glycol
<i>PHO1</i>	Phosphate1 promoter
PM	Plasma membrane
PR	Primary root
qRT PCR	Quantitative real time PCR
RFP	Red fluorescent protein
RNA	Ribonucleic acid
RNAase	Ribonuclease
ROS	Reactive oxygen species
RT PCR	Reverse transcription PCR
SD	Standard deviation
SDS	Sodium dodecyl sulfate
SLAC1/SLAH	Slow-type anion channel-associated 1/homologs
TAIR	Arabidopsis information resource
T-DNA	Transfer-DNA
TF	Transcriptional factor
TM	Transmembrane domain

<i>UBQ10</i>	Polyubiquitin 10
VM	Vacuolar membrane or tonoplast
x-Gal	5-bromo-4-chloro-3-indolyl- β -D-galactopyranoside
YFP	Yellow fluorescent protein
YNB	Yeast nitrogen base
YPAD	Yeast extract-peptone-dextrose + adenine medium
3-AT	3-amino-1,2,4-triazole
<i>35Sp</i>	Cauliflower mosaic virus promoter
λ_{em}	Wavelength emission
λ_{ex}	Wavelength excitation

Table S1: The composition of fertilizer solutions used to water unfertilized soils. Fertilization solutions are based on the composition of Murashige-Skoog medium (Murashige and Skoog, 1962). All solutions were prepared freshly the same day of watering.

Solutions	0mM K ⁺	1mM K ⁺	1mM K ⁺	10mM K ⁺	1mM K ⁺	10mM K ⁺
	1mM NO ₃ ⁻	0mM NO ₃ ⁻	1mM NO ₃ ⁻	1mM NO ₃ ⁻	10mM NO ₃ ⁻	10mM NO ₃ ⁻
Macronutrientes						
KNO ₃	0mM	0mM	1mM	1mM	1mM	10mM
KCl	0mM	1mM	0mM	9mM	0mM	0mM
Ca(NO ₃) ₂ x 4H ₂ O	1mM	0mM	0mM	0mM	4.5mM	0mM
NaH ₂ PO ₄ x H ₂ O	1mM	1mM	1mM	1mM	1mM	1mM
MgSO ₄ x 7H ₂ O	1mM	1mM	1mM	1mM	1mM	1mM
CaCl ₂ x 2H ₂ O	1.5mM	1.5mM	1.5mM	1.5mM	0mM	15mM
Micronutrientes						
K ₃ BO ₄	0.05mM	0.05mM	0.05mM	0.05mM	0.05mM	0.05mM
MnSO ₄	0.05mM	0.05mM	0.05mM	0.05mM	0.05mM	0.05mM
ZnSO ₄	18.5mM	18.5mM	18.5mM	18.5mM	18.5mM	18.5mM
KI	2.5mM	2.5mM	2.5mM	2.5mM	2.5mM	2.5mM
Na ₂ MoO ₄	0.5mM	0.5mM	0.5mM	0.5mM	0.5mM	0.5mM
CuSO ₄	0.05mM	0.05mM	0.05mM	0.05mM	0.05mM	0.05mM
CoCl ₂	0.05mM	0.05mM	0.05mM	0.05mM	0.05mM	0.05mM
Fe-EDTA	0.05mM	0.05mM	0.05mM	0.05mM	0.05mM	0.05mM

7. Appendix

MES	0.5g/l	0.5g/l	0.5g/l	0.5g/l	0.5g/l	0.5g/l
pH (NaOH)	5.5	5.5	5.5	5.5	5.5	5.5